Universitat Autònoma de Barcelona

Planktonic calcifying organisms in a high CO2 Mediterranean Sea

Roberta Johnson

UNIVERSITAT AUTONOMA DE
BARCELONA

Institute of Environmental Science and Technology

Doctoral thesis

Ph.D. in Environmental Science and Technology

December 2022

Planktonic calcifying organisms in a high CO_2 Mediterranean Sea

Roberta Johnson

Tutor and thesis director:

Dr. Patrizia Ziveri

This PhD thesis was funded by the fellowship from the Ministry of Economy and Competitiveness (FPI/BES-2017-080469) granted in October 2018 to January 2023. Funding was also provided by the consolidate research group MERS - Marine and Environmental Biogeosciences Research Group (SGR 2017 – 1588) and the following research projects:

- CALMED Project (CTM2016-79547-R)
- ASSEMBLE Plus Grant Program (Project 730984_A+)

This PhD thesis contributes to the ICTA-UAB "Unit of Excellence" (Spanish Ministry of Science, Innovation and Universities, CEX2019-000940-M).

It was time,
to define,
the outline and the why,
the where and the how,
of the sea's shelled sea butterfly,
the pteropod.
With the coming and going of the tide,
sprinkled with some carbon dioxide,
the water becomes acidified.
That's ocean acidification,
ocean warming's little cousin.
And in our sea, The Mediterranean,
a body of water
that's fraughter,
and hotter,
than most,
it seems at last,
that as the seasons pass,
the ocean burns twice as fast
because as things start to heat up,
the water turns to acid,
melting shells off bodies,
and at the end of the day,
the one's that pay,
the animals,
they won't stay,
the refugees of climate change.
Cuz all species are looking for their optimum.
They all have their own space,
their own place,
and at their own pace,
they'll have to face,
this menace,
but together.
And those that don't adapt,
will feel the full impact.
And when their ranges shrink,
it makes me think,
the only thing they have left to do,
is sink.
Shells on the bottom of the sea floor
and nothing more.
And our little winged sea creature,
with its unique shell feature,
is no longer here,
they disappear.
And if they disappear,
it's pretty clear,
that the role they play,
in the marine carbon cycle today,
will too.
And so,
when we defined
the outline and the why,
the where and the how,
it seems that we may find,
in time,
the time we have,
is up,
for the sea's shelled butterfly,
the pteropod.

The Sea Butterfly - Roberta Johnson

Acknowledgements

It is hard to fully acknowledge and thank everyone that has helped me over the past four years. To capture in words the big and small helping hands along the way won't do justice to how important they were, but I shall try!

Firstly, I would like to thank my very supportive supervisor, Patrizia Ziveri. Thank you for your kind words and encouragement over my time in Spain and in Australia. Thank you for helping me get to Antarctica - I cherish that trip as one of the highlights over my PhD (and life) and for that I am very thankful. You also supported me during the pandemic while I was in Australia and with my other personal issues, and I appreciate that a lot. Hopefully this is not the end of our relationship and I wish to see you again soon in the future.

I would also like to send a special thank you to Clara Manno, who was like a second supervisor to me, and a co-author of half of my thesis. We had a very special time together on our cruise to Antarctica and I won't forget any of it!

Secondly, I would like to give thanks to my research group. Everyone has made my experience in ICTA special and unique. To the PhD students: Sven, who has been there from the beginning, is a true friend who I will miss – particularly our coffees after lunch and our very relaxed nights out. Lauraaa! You left too soon (for me). Thank you for helping me while I was in Australia, and with all the palabras del dia. I know you miss all my canciones – 'Hola a todos'. Miki, the laid back guy from Ibiza, I loved your relaxed presence in the group and I will miss your easy going approach! Stephanie – it was so nice to have this small time together and I wish we had longer! Our time at ICTA was cut too short but maybe see you when you come back to Australia? We will go to the future iteration of Hot Damn! Mouna – our time was also too short, but I appreciate the time spent getting to know each other! Arturo - you are beginning your journey while I am at the end. I wish you luck! Special mention to Griselda who was a sometimes-present group member from afar. Your positive energy was appreciated! Another special mention to Athena – it was a 'good' time with you here at ICTA and I hope you find what you are looking for in the end.

Thank you to the rest of the research group – Mika, Gerald, and Graham. It was nice to connect with you over the past few years and learn from your knowledge. It improved my thesis a lot!

To Maria Byrne, my previous Honours supervisor in Australia, thank you so much for giving me the opportunity to do a project with you while I was in Australia during the pandemic lockdowns. It was nice to be back at SIMS and back in the water! That project helped me get through those months and I'm looking forward to finishing it when I return to Australia.

Thank you to all the academic support at ICTA who helped make my PhD possible, from helping to organise my visa in Australia to every piece of administrative assistance I needed once at ICTA. Pere, who is no longer at ICTA, Maite, and Cristina – thank you so much!

To my family and friends who were there from me from afar while I was in Spain and also when I was in Australia– thank you! To my parents and sister who also supported me during those hard times, I really don't know what I would have done without you! One of the main reasons I am so looking forward to coming home is because I will get to spend more time with you and the whole family. Julio and Umbe, thank you for opening up your home to me when the world was shut down. It was a special gift and special to share that time together again, eating, chatting, and sharing a laugh.

To Bernie, who has known all the pleasure and pain of this PhD, thank you, thank you, thank you. Thank you for helping me through it all, and for coming with me on this journey. Words can't express what it, and you, mean to me. Looking forward to our next chapter together.

Abstract

Increasing CO_2 in our atmosphere is driving climate change, causing a decline in surface ocean pH (ocean acidification) and a rise in sea surface temperature (ocean warming). The Mediterranean Sea has been recognized as a global climate change hotspot whereby regional impacts are expected to be especially profound throughout the 21st century. Declines in ocean pH and increases in ocean temperature can significantly alter the physiology of marine organisms and have great effects on calcifying species. Planktic calcifying organisms play a key role in regulating ocean carbonate chemistry, atmospheric CO_2, and the marine food web, and they are particularly sensitive to ocean acidification due to their calcified skeleton. There are several knowledge gaps within the Mediterranean Sea with respect to calcifying plankton. In particular, this thesis focuses on two major calcifying planktonic groups: coccolithophores and shelled pteropods.

Coccolithophores are a major calcifying phytoplankton at the base of the marine food web. They influence seawater chemistry through photosynthesis and calcification and are major contributors to the planet's carbon cycle. As they are abundant and at the base of the food web, their nutrient content and abundance is an important predictor for the nutritional condition of their consumers. Here, the coccolithophore distribution and ecology in the Mediterranean Sea has been characterised using a systematic literature review and a meta-analysis. Coccolithophore research is mainly focused to the eastern Mediterranean Sea, in particular the Adriatic and Aegean Seas, and to the warmer seasons of spring and summer. Significant gaps in research remain, particularly during winter and autumn, and along the north coast of Africa. Using compiled data from published studies, and data available on PANGAEA, regional abundances and species contributions are estimated for heterococcolithophores and holococcolithophores. These two life cycle phases of coccolithophores exhibit opposing spatial and temporal distribution, adding further support to the theory that they fill distinct ecological niches. Using the meta-analysis data, methodological biases associated with sampling methods and microscopy were identified, indicating that phytoplankton studies utilising the Utermöhl method of sampling likely underestimate coccolithophore abundances and contribution (%) to the phytoplankton community. Heterococcolithophores are inversely correlated with temperature in the Mediterranean Sea, therefore ocean warming may negatively impact

total coccolithophore abundance, and in particular the abundance of the most common species, *Emiliania huxleyi*. Holococcolithophore abundance, however, is positively correlated with temperature, and therefore may respond favourably to temperature increases and expand their distribution.

To investigate the impact of ocean acidification and ocean warming on coccolithophore nutritional content, a culture experiment on *E. huxleyi* (a western Mediterranean strain) was performed using nine pH levels (7.6 – 8.4) and two temperatures (15℃ and 20℃). Lipid production was higher under low pH and cell growth rate increased under the warmer temperature; however, this increase was reduced under ocean acidification conditions. Using a parameter called production potential, the availability of lipids to consumers was estimated and found that it increased at 20℃ but this was mitigated by low pH. It is likely that consumers will benefit from this overall increase in lipid availability. The carbon to nitrogen ratio was higher at 20℃ and low pH, suggesting a decline in the nutritional quality for coccolithophores under climate change conditions. The structural integrity of the coccosphere was also reduced under ocean acidification conditions, which may be beneficial for consumers. Several of these responses indicate cellular stress for coccolithophores. This experiment has global implications for coccolithophores as ocean acidification and warming will be ubiquitous, however will vary regionally.

Thecosome pteropods are pelagic mollusks found in all major world oceans. Their distribution in the Mediterranean Sea is poorly documented and here, the spatial composition of pteropods across the Mediterranean Sea along a west-east transect was documented. Pteropod abundance was 5x greater in the eastern Mediterranean basin during spring, and temperature, oxygen concentration, salinity, and aragonite saturation explained 96% of the observed variations in the community structure at the time of sampling. These results indicate that pteropods may prefer environments with a lower energetic demand such as the eastern Mediterranean, which is characterised by warmer surface water, higher salinity, higher pH and carbonate saturation levels. An opposite distribution was also documented between pteropods and planktic foraminifera, another calcifying zooplankton, across the Mediterranean Sea. Additionally, for the first time, the shell length and shell mass relationship of the juvenile pteropod *H. inflatus* is presented. Shell mass is significantly related to salinity, and size normalised mass is significantly

correlated with aragonite saturation and salinity. The observed differences in shell mass and size normalised mass may be related to the biogeochemical differences between Mediterranean Sea regions, where denser/thicker shells are associated with more saline, and high pH regions.

Overall, the results in this thesis fill important knowledge gaps with respect to pteropod and coccolithophore distribution in the Mediterranean Sea and their potential responses to climate change.

Resumen

El aumento de la concentración de CO_2 en nuestra atmósfera está impulsando el cambio climático, provocando una disminución del pH (acidificación oceánica) y un aumento en la temperatura (calentamiento oceánico) de la superficie del océano. Estos cambios, en el pH y la temperatura del océano, pueden alterar significativamente la fisiología de los organismos marinos, y en particular a las especies calcificadoras. Los organismos calcificadores planctónicos son clave para la regulación de la química del carbonato oceánico, el CO_2 atmosférico y la cadena trófica marina, pero también son especialmente sensibles a la acidificación del océano debido a su esqueleto calcificado. En el Mar Mediterráneo, que ha sido reconocido como un punto crítico del cambio climático global, donde se espera que los impactos regionales sean especialmente significativos a lo largo del siglo XXI, aún existe una falta de conocimiento sobre los efectos del cambio climático en los organismos planctónicos calcificadores. Esta tesis se centra en dos grupos calcificadores planctónicos: cocolitóforos y pterópodos con caparazón.

Los cocolitóforos son fitoplancton calcificador, imprescindible en la base de la cadena trófica marina. Estos organismos influyen en la química oceánica a través de la fotosíntesis y la calcificación, también son los principales responsables del ciclo del carbono en nuestro planeta. Como son abundantes y se encuentran en la base de la cadena trófica, su contenido y abundancia de nutrientes sirve como un indicador de la condición nutricional de sus consumidores. En esta tesis, se ha caracterizado la distribución y la ecología de los cocolitóforos en el mar Mediterráneo mediante una revisión sistemática de la literatura y un metaanálisis. Hasta ahora, la investigación en los cocolitóforos se ha centrado principalmente en el mar Mediterráneo oriental, en particular en el mar Adriático y Egeo, y durante las estaciones más cálidas (primavera y verano). Por el contrario, existe una falta de estudios sobre los cocolitóforos durante el otoño e invierno, y en la costa Norte de África. Usando la información recopilada de estudios publicados y datos disponibles en PANGAEA, se han estimado las abundancias regionales y distribución de especies para heterococolitóforos y holococolitóforos. Estas dos fases del ciclo de vida de los cocolitóforos exhiben una distribución espacial y temporal opuesta, lo que apoya la teoría de que complementan nichos ecológicos distintos. Utilizando los datos del metanálisis, se han identificado diferencias metodológicas respecto a los métodos de

muestreo y la microscopía, que sugieren que los estudios de fitoplancton que utilizan el método de muestreo de Utermöhl probablemente subestiman la abundancia y la contribución (%) de los cocolitóforos a la comunidad de fitoplancton. Los resultados también muestran que los heterococolitóforos están inversamente correlacionados con la temperatura en el mar Mediterráneo, por lo que el calentamiento de los océanos puede tener un impacto negativo en la abundancia total de cocolitóforos y, en particular, en la abundancia de la especie más común, *Emiliania huxleyi*. Por el contrario, la abundancia de holococcolitóforos que está positivamente correlacionada con la temperatura, podría responder favorablemente a los aumentos de temperatura y expandir su distribución.

El impacto de la acidificación y el calentamiento de los océanos en el contenido nutricional de los cocolitóforos se investigó mediante un experimento de cultivo con *E. huxleyi* (una cepa del Mediterráneo occidental) utilizando nueve niveles de pH (7.6 - 8.4) y dos temperaturas (15 ℃ y 20 ℃). Los resultados indicaron que la producción de lípidos es mayor a menor pH y que la tasa de crecimiento celular aumenta a mayor temperatura; sin embargo, este aumento se reduce en condiciones de acidificación oceánica. La disponibilidad de lípidos para los consumidores se estimó usando un parámetro llamado potencial de producción, y se observó que a 20 ℃ aumenta el potencial de producción, pero se esto se ve limitado con un pH bajo. Probablemente, los consumidores se beneficiarían de este aumento general en la disponibilidad de lípidos. La mayor ratio entre carbono y nitrógeno se observó a 20 ℃ y a bajo pH, lo que sugiere una disminución en la calidad nutricional de los cocolitóforos en condiciones de cambio climático. La integridad estructural de la cocosfera también se vio reducida en condiciones de acidificación oceánica, lo que podría ser beneficioso para los consumidores. Aun así, se debe tener en cuenta que estas respuestas indican estrés celular para los cocolitóforos. Este experimento tiene implicaciones globales para los cocolitóforos, ya que la acidificación y el calentamiento oceánico, aunque variarán regionalmente, serán ubicuos.

Los pterópodos con caparazón son moluscos pelágicos que se encuentran en todos los océanos del mundo. Su distribución en el Mar Mediterráneo está pobremente documentada, esta tesis se describe la distribución espacial de pterópodos a lo largo del Mar Mediterráneo, cubriendo un transecto de oeste a este. La abundancia de pterópodos observada fue 5 veces mayor en la cuenca del Mediterráneo oriental durante la primavera. La temperatura, concentración de oxígeno, salinidad y saturación de aragonita explican

el 96 % de las variaciones observadas en la estructura de la comunidad en el momento del muestreo. Estos resultados sugieren que los pterópodos prefieren ambientes con una menor demanda energética como el Mediterráneo oriental, que se caracteriza por aguas superficiales más cálidas, mayor salinidad, mayor pH y niveles de saturación de carbonato. En este transecto también se observó una distribución espacial opuesta entre pterópodos y foraminíferos planctónicos, otro grupo de calcificadores (zooplancton). Además, en este estudio se describe por primera vez la relación entre la longitud y la masa de la concha del pterópodo juvenil *H. inflatus*. Las diferencias observadas en la masa de la concha y la masa normalizada por tamaño sugieren estar relacionadas con las diferencias biogeoquímicas entre las regiones del mar Mediterráneo, donde las conchas más densas/gruesas se asocian con regiones más cálidas, más salinas y con un mayor pH.

Esta tesis contribuye al conocimiento actual sobre los pterópodos y cocolitóforos en el mar Mediterráneo, así como sus posibles respuestas e impactos al cambio climático.

Table of Contents

Project significance, aims, and thesis structure

The oceans provide essential marine ecosystem services for human welfare and wellbeing, providing for example food, recreational, cultural and livelihood opportunities, as well as by regulating the global climate (Reid et al. 2009). Increasing atmospheric CO_2 emissions are causing global warming including ocean warming with cascading effects such as marine heatwaves, extreme events, and sea level rise. They are also impacting the chemistry of the surface ocean as CO_2 dissolved in surface seawater decreases seawater pH (ocean acidification). Even if greenhouse gas emissions were stopped at current levels, the warming of the oceans due to climate change would continue for generations (Blunden and Arndt 2016). The Mediterranean has been identified as a climate change 'hot-spot' and will be threatened by an increase in droughts, severe climatic events (hot waves/spells), and decreased precipitation, particularly in the western Mediterranean, southeast Europe, and the Middle East (MedECC 2020). There is an urgent need to understand the effects that climate change stressors will have on biological systems, particularly as evidence so far suggests that many marine species will be negatively affected (Pörtner 2008). Ocean acidification is predicted to have negative effects on marine organisms, in particular calcifying organisms, however the response will be taxon-specific. Coccolithophores and pteropods are abundant pelagic marine calcifying plankton that are found throughout the Mediterranean Sea. These taxa contribute significantly to ocean carbon production and play an important role in ocean carbon cycling and to the marine trophic system (Ziveri et al. 2007; Falkowski et al. 2008; Manno et al. 2010, 2019; Lefebvre et al. 2011; Bednaršek et al. 2012a; Buitenhuis et al. 2019). As individual stressors, ocean warming and acidification can have detrimental effects on the growth, morphology, and calcification of coccolithophores (Riebesell et al. 2000; Lefebvre et al. 2011; Bach et al. 2013; Schlüter et al. 2014; Rosas-Navarro et al. 2016; Feng et al. 2017; Krumhardt et al. 2017) and pteropods (Moya et al. 2016; Bednaršek et al. 2019; Engström-Öst et al. 2019). Additionally, the combined impacts of ocean warming and acidification have also been shown to have an interactive effect on coccolithophore growth (Arnold et al. 2013; Sett et al. 2014; D'Amario et al. 2017a), morphology (Milner et al. 2016; D'Amario et al. 2017a), calcification (Schlüter et al. 2014; Sett et al. 2014) and photosynthesis (Sett et al. 2014).

In the Mediterranean Sea, there is a critical lack of studies on pteropod distribution across this diverse interior basin, and globally there is limited understanding of what environmental factors drive their distribution. Similarly, for coccolithophores the Mediterranean Sea lacks a cohesive and comprehensive understanding of their distribution throughout the region. Coccolithophores are a highly abundant phytoplankton at the base of the marine food system, and little is known about how the effects of ocean warming and acidification on their nutritional content will impact their consumers. Additionally, little is known about how the distribution of this calcifying taxa will respond to ocean warming and acidification. This thesis aims to fill these research gaps through field work studies, experimental research, and a literature review on extant coccolithophore distribution in the Mediterranean Sea.

Specific Objectives

1. Spatially and temporally characterise coccolithophore distribution throughout the Mediterranean Sea and determine the main environmental drivers of their distribution.

The aim of this systematic review and meta-analysis is to characterise coccolithophore populations in the Mediterranean Sea across both spatial (regionally) and temporal scales (seasonally), and to determine the main environmental drivers of their distribution by identifying trends in the literature. Using the identified environmental parameters, we discuss the potential impacts of climate change on the distribution of coccolithophores in the Mediterranean Sea. We also identify knowledge and sampling gaps, as well as potential methodological limitations and biases.

2. Assess the effects of experimental ocean warming and ocean acidification on coccolithophore nutritional content and the potential impacts on their consumers.

This experiment investigates whether reduced pH (in line with ocean acidification) and increased temperature (ocean warming) will affect the quality of coccolithophores as a food source (Guinder and Molinero 2013) by impacting their investment in stored energy (in the form of lipids). Here, cellular lipid content and carbon and nitrogen ratios are used to measure this impact (Pond and Harris 1996). A parameter known as production

potential (which combines cellular lipid content and growth rate) is also used to investigate the availability of lipid content for coccolithophore consumers. These points have not been addressed in a combined ocean warming and acidification scenario. Other important parameters connected to coccolithophore nutritional quality are also investigated, including growth rate, chlorophyll *a* content, and coccosphere morphology.

3. Spatially characterise the community composition of pteropods throughout the Mediterranean Sea and determine the environmental factors affecting their distribution

This study explores shelled pteropod ecological preferences by investigating their distribution across the Mediterranean Sea at a large spatial scale, spanning the east-west environmental gradient, during the spring season. The results are also compared with published data on planktic foraminifera distribution, a calcifying single-celled protist with a calcite shell, from the same sample set (Mallo et al. 2016). Investigating the relationship between pteropods and foraminifera is important as the forecasted change in carbonate chemistry may cause ecosystem shifts due to altered competition between calcareous species (Kroeker et al. 2013a). Comparing these two major groups of calcifying zooplankton will improve our understanding of their ecological niches and their sensitivities to climate change.

4. Investigate pteropod shell morphological variability across the Mediterranean Sea and discuss potential environmental factors affecting this variability

This study investigates the variability in shell length, diameter, and mass of *H. inflatus* throughout the Mediterranean Sea and considers the potential environmental factors that affect the size and mass of *H. inflatus* shells in various biogeochemical regions during the spring sampling period, with a focus on the differences between the eastern and western Mediterranean Sea sub-basins. This study adds important insight to the potential environmental factors controlling pteropod mass in natural samples.

CHAPTER 1

Introduction

1. Climate change

The planet is undergoing a long-term change in climate due to the increasing level of anthropogenic greenhouse gases emitted into our atmosphere. Greenhouse gases are so named because they contribute to the planet's warming trend by trapping thermal radiation from the sun inside the earth's atmosphere. They include mainly carbon dioxide (CO_2), methane (CH_4) and nitrous oxide (N_2O). Since the industrial revolution, the increased production of greenhouse gases, particularly CO_2, has caused a rise in global mean temperature (IPCC, 2022). This rise in temperature is causing rapid change in terrestrial and marine physical, chemical and biological systems, such as geographical and ecological shifts, and altered precipitation patterns and current dynamics (Maclean and Wilson 2011; Caesar et al. 2018, 2021).

The atmospheric concentrations of CO_2 and other greenhouse gases are likely to continue to rise in the immediate future (IPCC, 2021) with the atmospheric CO_2 concentration set to rise from its current level of 414 ppm to 1020 ppm by 2100 (RCP8.5; IPCC, 2021). The Intergovernmental Panel on Climate Change (IPCC) has predicted a global mean increase in air temperature of 5.3^{o}C and a 3.4^{o}C increase in sea surface temperature by the end of this century (RCP8.5; IPCC, 2021). This anthropogenic temperature rise is occurring more quickly than any global temperature rise in the previous million years, and it might be beyond the capacity of some species to adapt (Harley et al. 2006). The inability of the biota to adapt to such rapid change has already resulted in significant ecological shifts and species loss (Dulvy et al. 2003; Sarà et al. 2014).

2. Ocean warming

The marine environment, which makes up approximately 71% of the planet's surface, is home to a wide variety of habitats and biota and is one of the most economically and ecologically significant systems on Earth. The ability of the ocean to store heat is about 1,000 times larger than that of the atmosphere, and since 1955, as a result of rising levels of greenhouse gases in the atmosphere, the ocean has absorbed thermal energy at a rate approximately 20 times greater than that of the atmosphere (Levitus et al. 2005). Most of this heat absorption occurs in the uppermost 700 m of the ocean, where a diverse range of life and ecosystems exist (Levitus et al. 2005).

As temperature influences the rate of chemical reactions, it is one of the largest factors affecting the rate of many physiological processes, including metabolism, growth, and reproduction (Somero 2012). For all biota, there is a large variation in the extent and distribution of thermal thresholds before physiological change or damage occurs, hence temperature is one of the greatest defining features of species distributions (Sunday et al. 2012; Hattab et al. 2014). From an evolutionary viewpoint, the anthropogenic rise in temperature is remarkably quick, and it may soon push many species close to, or over their physiological limitations in their natural habitats. Therefore, ocean warming has the potential to result in species loss if organisms can't migrate to cooler regions or shift their range (Doney et al. 2011).

3. Ocean acidification and reduced carbonate saturation

Approximately 25 - 30% of anthropogenic atmospheric carbon dioxide is removed by the surface ocean, where it becomes dissolved carbon (Friedlingstein et al. 2022). As a result of increaseing dissolved CO_2 in the ocean, carbonic acid (H_2CO_3) is formed, followed by an increase in bicarbonate (HCO_3^-) and hydrogen ions (H^+) and a decrease in carbonate ions ($CaCO_3$) which results in a decrease in surface ocean pH (Caldeira and Wickett 2003; IPCC, 2021). Since the industrial revolution, the accumulation of anthropogenic CO_2 in the ocean has caused a drop in surface water pH by approximately 0.1 units (Turley 2008). It is predicted that ocean surface pH will decrease by an average of 0.31 units, reaching approximately pH 7.7 by 2100 (IPCC, 2021).

A decrease in ocean pH is also accompanied by a decline in carbonate mineral saturation, which can be detrimental to calcifying organisms, as carbonate biomineralization is required for the formation of their skeletal structures (Kroeker et al. 2013a; Leung et al. 2022). Many marine organisms produce a calcium carbonate skeleton, including coccolithophores and pteropods, the taxa investigated in this thesis. A calcium carbonate structures can provides species with direct fitness benefits, such as defence from predators, structural integrity, and protection from UV damage or viral infection (Monteiro et al. 2016). Organisms that build carbonate skeletons may be especially vulnerable to the effects of decreasing ocean pH as the production of their skeletal structures is likely to be reduced in an increasingly acidifying environment (Figuerola et

al. 2021). To maintain optimum rates of skeletogenesis, organisms may be required to expend energy to pump the increase in hydrogen ions out of their internal fluids to maintain pH homeostasis (Ries 2011).

Calcite and aragonite are carbonate mineral polymorphs of calcium carbonate. These polymorphs are major constituents with different mineral structures (De Choudens-Sánchez and González 2009). Calcite, the most stable polymorph, is used in the building of solid structures and utilised by coccoltihophores, while aragonite, the less stable, is used to form filamentous and stalactite-like structures and is utilised by pteropods (De Choudens-Sánchez and González 2009).

Evidence from the fossil record indicates that high levels of CO_2 accumulation in the ocean have been associated with mass extinction events, such as the Permian and Triassic extinctions, when calcifying animals such as corals, brachiopods, and echinoderms were affected to a larger extent compared to marine animals belonging to non-calcifying phyla such as Chordata and Arthropoda (Knoll et al. 1996; Berner 2002). Calcifying taxa are, indeed, especially vulnerable to increases in seawater CO_2 (Kroeker et al., 2013) which has been identified in numerous laboratory experiments (e.g. Riebesell et al. 2000; Lefebvre et al. 2011; Lischka et al. 2011; Comeau et al. 2012; Bach et al. 2013; Schlüter et al. 2014; Busch et al. 2014; Woodworth et al. 2015; Rosas-Navarro et al. 2016; Feng et al. 2017; Krumhardt et al. 2017; Johnson et al. 2020; Mekkes et al. 2021b). Other fossil evidence shows that ocean acidification affects calcification levels in planktonic species. For instance, planktonic foraminiferal (single-celled marine eukaryotes) shell weight across glacial-interglacial periods shows a correlation with ocean carbonate levels, which corresponds to shifts in atmospheric CO_2 (Barker and Elderfield 2002; Moy et al. 2009).

The increased uptake of CO_2 by the ocean therefore results in multiple physiological stressors which include 1) reduced pH, 2) increased pCO_2, and 3) reduced calcium carbonate saturation. The effects of these stressors on taxa are varied and understanding the short and long-long responses of organisms to ocean acidification remains a challenge.

4. Study region: The Mediterranean Sea

The Mediterranean Sea is a temperate, semi-enclosed sea with an anti-estuarine circulation. It is connected to the Atlantic Ocean through the Strait of Gibraltar, where surface Atlantic waters enter, and through net evaporation, a west to east gradient of increasing sea surface temperature, nutrients, salinity, and alkalinity occurs (Schneider et al. 2007; Rohling et al. 2009; Fedele et al. 2022). The Mediterranean Sea is separated into two large sub-basins through the shallow Strait of Sicily. These basins have distinct characteristics, with the eastern basin distinguished by warmer, more saline, and ultra-oligotrophic conditions and the western basin characterised by cooler, less saline conditions. The division between the eastern and western Mediterranean Sea sub-basins is recognised as an important biogeographical boundary (Schneider et al. 2007; Rohling et al. 2009; Uitz et al. 2012; Dayan et al. 2015; Hassoun et al. 2015b). Within these sub-basins**,** the Mediterranean Sea is further divided into water masses that are largely differentiated by the basins' oceanographic setting (Fig. 1), as well as differences in temperature, salinity, nutrients, and carbonate chemistry, which persist as biogeographical boundaries over time (Schneider et al. 2007; Rohling et al. 2009; Uitz et al. 2012; Dayan et al. 2015; Hassoun et al. 2015b; Pasqueron de Fommervault et al. 2015).

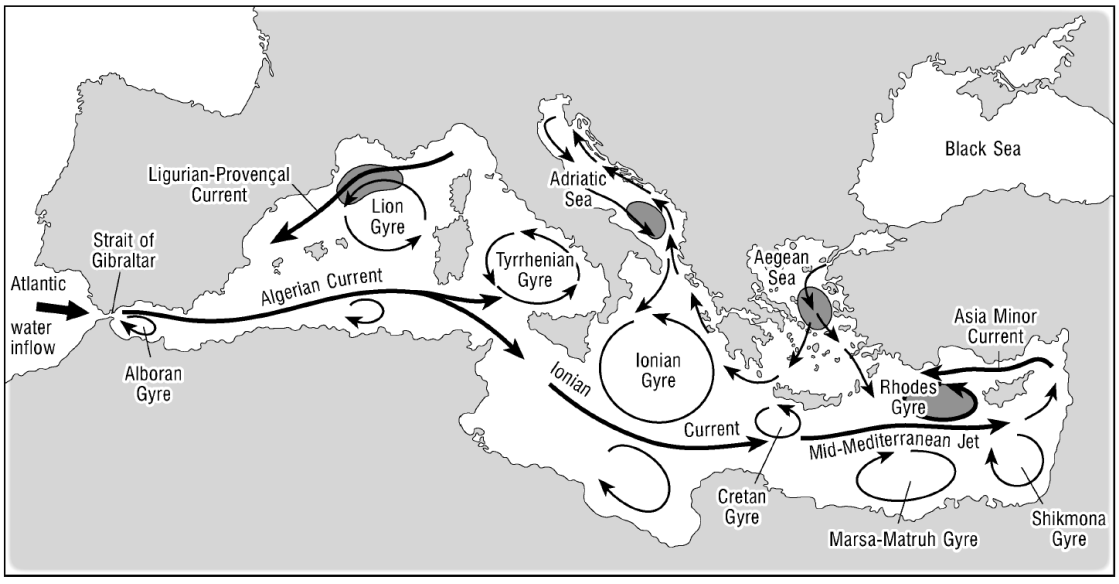

Fig. 1. Mediterranean Sea surface water circulation indicating major currents and gyres. The dark shaded areas indicate regions of deep-water formation. From Rohling et al. (2009).

5. A climate change hotspot

The Mediterranean Sea has been recognized as a global climate change 'hotspot' whereby regional impacts are expected to be especially profound throughout the 21st century (Giorgi 2006). The region is undergoing rapid changes as a result of climatic and non-climatic forcings (Fig. 2; Cramer et al. 2018; MedECC 2020) and is experiencing warming at a rate that exceeds global trends, with atmospheric temperatures rising as much as 20% faster than the global average (Lazzari et al. 2013; Lionello and Scarascia 2018). Sea surface pH in this region is projected to decrease in line with the global average (approximately 0.3 to 0.4 units by 2100) (Geri et al. 2014; Flecha et al. 2015; Kapsenberg et al. 2017), or even exceed the global average decrease (Gemayel et al. 2015; Hassoun et al. 2022). Within this scenario, it is essential to improve our knowledge of how Mediterranean marine ecosystems might respond to ocean conditions under ocean warming and acidification

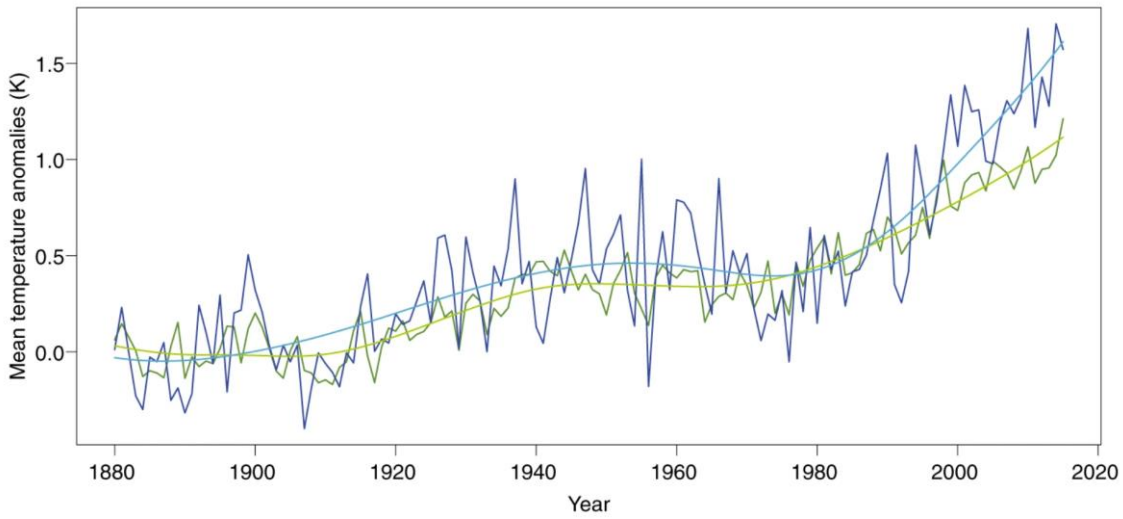

Fig. 2. Annual mean air temperature anomalies for the Mediterranean Basin (blue) and the globe (green) presented with (light curves) and without (dark curves) smoothing. From Cramer et al. (2018).

6. Coccolithophores

Coccolithophores are a marine calcifying phytoplankton that are found in all the world's oceans. Coccolithophores influence seawater chemistry and the exchange of carbon dioxide between the atmosphere and the ocean through photosynthesis and production and dissolution of their calcium carbonate skeleton. Coccolithophores are one of the

major producers of calcium carbonate in the open ocean (Iglesias-Rodríguez et al. 2002) and their calcium carbonate ballast is associated with 83% of the organic carbon flux in the oceans (Klaas and Archer 2002; Ziveri et al. 2007).

During their life cycle, coccolithophore calcification undergos two distinct phases - holococcolithophore (haploid) and heterococcolithophore (diploid). Holococcolithophores are composed of uniform calcite crystallites, while the heterococcolithophores are composed of coccoliths, which are single calcite crystals with complex shapes that are morphologically distinct (Young et al. 1999). The coccolithophore life cycle is relatively unknown as direct observations of phase changes are rare (Nöel et al. 2004) but several coccosphere specimens have been identified as having combined holo- and heter- coccoliths (both diploid and haploid phase). Holococcolithophores and heterococcolithophores are believed to inhabit distinct ecological niches, with the haplo-diplontic life-cycle expanding their niche by approximately 19% (de Vries et al. 2021).

As individual stressors, ocean warming and acidification can have significantly detrimental effects on coccolithophore growth, morphology, and calcification (Riebesell et al. 2000; Lefebvre et al. 2011; Bach et al. 2013; Schlüter et al. 2014; Rosas-Navarro et al. 2016; Feng et al. 2017; Krumhardt et al. 2017; D'Amario et al. 2020). Additionally, the combined impacts of ocean acidification and warming have also been shown to have an interactive effect on coccolithophore growth (Arnold et al. 2013; Sett et al. 2014; D'Amario et al. 2017; Johnson et al. 2022 - Chapter 1), morphology (Milner et al. 2016; D'Amario et al. 2017; Johnson et al. 2022 - Chapter 1), calcification (Schlüter et al. 2014; Sett et al. 2014) and photosynthesis (Sett et al. 2014).

7. *Emiliania huxleyi*

Emiliania huxleyi is one of the most abundant coccolithophore species in the oceans and the most abundant throughout the Mediterranean Sea (Socal et al. 1999; Caroppo et al. 1999; Totti et al. 2000; Barcena et al. 2004; Saracino and Rubino 2006; Balestra et al. 2009; Vilicic et al. 2009; Viličić et al. 2009; Moscatello et al. 2011; Godrijan et al. 2013, 2018; Ziveri et al. 2014; Oviedo et al. 2015; Supraha et al. 2016; Dimiza et al. 2016; Bonomo et al. 2017, 2021; Cerino et al. 2017, 2019; D'Amario et al. 2017a; Skejic et al.

2018; Triantaphyllou et al. 2018; Sahin and Eker-Develi 2019; Varkitzi et al. 2020; Aubry et al. 2022). It is responsible for giant seasonal algal blooms (Brown and Yoder 1994) that are visible from space (Holligan et al. 1993). These blooms can provide a substantial food source to zooplankton grazers (Pond and Harris 1996). Alkenones, alkyl alkeonates, and alkene, among other stable lipid compounds produced by *Emiliania huxleyi*, can be utilized as climatic proxies to assess the effects of a changing climate (Bendle et al. 2005; Malinverno et al. 2008). *Emiliania huxleyi* has been studied extensively and found to be sensitive to ocean acidification conditions (Riebesell et al. 2000; Beaufort et al. 2011; Lefebvre et al. 2011; Schlüter et al. 2014), however the responses can be strain-specific (Langer et al. 2009).

8. Coccolithophores and the trophic system

Coccolithophores serve as an essential source of food for zooplankton (El-Hady et al. 2016a) like copepods (Langer et al. 2007b) and dinoflagellates (Haunost et al. 2021), especially during significant bloom events (Pond and Harris 1996). Their nutritional quality—specifically, their organic carbon to nitrogen ratio and lipid content—are significant determinants of the nutritional state for consumers at higher trophic levels (Pond and Harris 1996). Lipids (total and fatty acids) in phytoplankton act as structural molecules inside cells and as energy storage units (Fuentes-Grünewald et al., 2012). These are important factors that affect food quality, and in turn affects the health of marine ecosystems (Jin et al. 2020).

Chlorophyll *a*, an indicator of photosynthetic capacity, contains a large amount of lipids, and, as such, increases in chlorophyll *a* are typically accompanied by an increase in lipids (Woodworth et al. 2015) as well as photosynthetic performance. These lipid macromolecules are a source of energy for phytoplankton consumers further up the trophic ladder (Broglio et al. 2003; Litzow 2006), and variations in the supply of critical fatty acids can have a major effect on consumer output (Fraser et al. 1989; Breteler et al. 2005). Suspension feeders and zooplankton depend on primary producers as a source of food (Sailley et al. 2013; El-Hady et al. 2016b) and the quality and availability of their food has a significant role in their ability to reproduce and survive (Gili and Coma, 1998; Broglio et al., 2003; Gori et al., 2013).

Any negative consequences of climate change on the physiology of phytoplankton may have a domino effect on other ecosystem elements (Chavez et al. 2010; Guinder and Molinero 2013). For instance, it has been demonstrated that elevated pCO_2 affects the effectiveness of trophic transfer between phytoplankton and their consumer, copepod *Acartia tonsa* (Cripps et al. 2016). The essential fatty acid content of four species of phytoplankton that were cultured at high CO_2 levels (1000 ppm) was reduced, and the copepods that consumed these phytoplankton had lower egg production, hatching success, and egg viability (Meyers et al. 2019). Under conditions of increased pCO_2, the diatom *Thalassiosira pseudonana* exhibited a decrease in fatty acid content, resulting in a ten-fold reduction in fatty acid content for their consumer, the copepod *A. tonsa*, as well as a decline in somatic growth and egg production from 34 to 5 eggs female^{-1} day^{-1} (Rossoll et al. 2012). In light of the severe effects phytoplankton nutritional content can have on their consumers, it is crucial to determine how ocean warming and acidification will affect this important marine phytoplankton and to consider the impacts this may have on the food web (Rossi et al. 2019).

9. Pteropods

Thecosome pteropods are shelled holoplanktic molluscs found in all major world oceans (Lalli and Gilmer 1989; Peijnenburg et al. 2020). These pelagic snails are passive feeders that gather food particles in large mucous webs (Lalli and Gilmer 1989) and play an important role in both the trophic system and biogeochemical cycling (Bednaršek et al., 2012; Buitenhuis et al., 2019; Manno et al., 2010, 2019). Pteropods are an important part of the marine trophic system not only as grazers of phytoplankton (Seibel and Dierssen, 2003), but also as prey for several species of fish (pink salmon *Oncorhynchus gorbuscha*, Armstrong et al., 2008; Chinook salmon sp. *Oncorhynchus tshawytscha* and Walleye pollock sp. *Gadus chalcogrammus*, Sturdevant et al., 2012), marine birds (the kittiwake *Rissa tridactyla* and the dovekie *Alle alle*, Karnovsky et al., 2008) and other pteropods (*Clione antarctica*, Seibel and Dierssen, 2003). Their mucous webs create a large surface area to maximise the rate of particle capture with the result that they filter water at high rates (Conley et al., 2018).

There are few studies that focus specifically on pteropod distribution in the Mediterranean Sea, and these are generally based in small geographically regions (e.g. Howes, 2015;

Manno et al., 2019). Pteropods, however, make up a significant amount of the zooplankton community in the region (1 – 6.6%; Fernández de Puelles et al. 2007; Mazzocchi et al. 2011; Granata et al. 2020). Further, many published studies addressing the entire zooplankton community (Batistić et al. 2004; Fernández de Puelles et al. 2007; Mazzocchi et al. 2011), or those that include both pteropods and other non-calcifying taxa (Andersen et al. 1998; Tarling et al. 2001), focus on the direct comparison of few target pteropod species only, and do not include some critical environmental parameters (e.g.; seawater carbonate chemistry data). Given the contribution of pteropods to the zooplankton community, their importance to biogeochemical cycling, and their vulnerability to changing ocean chemistry, further research is required to investigate their distribution and relationship with environmental variables, in particular, temperature and pH.

10. The pteropod shell

Thecosome pteropods shells are an essential ecological and physiological feature for defence, buoyancy control, feeding strategy (Harbison and Gilmer 1992), and reproduction (Harbison and Gilmer 1992). It is comprised of aragonite, a common rhombic and metastable polymorph of $CaCO_3$ that issignificantly more soluble than calcite (Morse et al. 1980). Their aragonitic shells are known to be very sensitive to critical changes in ocean carbonate chemistry as a result of ocean acidification (Feely et al. 2004; Mekkes et al. 2021b). Shell morphology (i.e. shell thickness and size) has been shown to be modulated by changes in pH and aragonite saturation state, as observed in laboratory experiments (i.e. Lischka et al. 2011; Comeau et al. 2012b; Busch et al. 2014) and *in situ* observations (i.e. Bednaršek et al., 2012; Manno et al., 2019; Mekkes et al., 2021; Roberts et al., 2014; Roger et al., 2011).

11. *Heliconoides inflatus*

Heliconoides inflatus (formerly *Limacina inflata*) is a coiled shelled pteropod within the super family Limacinoidae. It is a common warm-water cosmopolitan species found throughout the tropics and subtropics (Wells 1976). As is common in pteropods, this species undertakes diel vertical migration and can be found at depths greater than 200 m (Rampal 1975; Wormuth 1981), however recent studies show that this species primarily

occurs in the upper water column, particularly at night (Schiebel et al. 2002; Juranek et al. 2003; Batistić et al. 2004; Granata et al. 2020). In the Mediterranean Sea it has been recorded as the most abundant pteropod species in the Southern Adriatic (Batistić et al. 2004) and Ligurian Sea (Granata et al. 2020). This species grows at a rate of ~ 0.15 mm per month (Wells 1976), will reach the juvenile stage (from ~ 0.4 mm) after ~ 3 months, adulthood (from ~ 1.0 mm) after ~ 8 months (Wells 1976; Lalli and Wells 1978) and lives for approximately one year (Wells 1975). *Heliconoides inflatus* shells have also been found to be excellent recorders of past temperatures and carbonate ion concentrations and may be a useful species for paleoclimate reconstructions in the sedimentary record (Keul et al. 2017).

CHAPTER 2

Extant coccolithophore distribution in the Mediterranean Sea: a systematic review and meta-analysis

Abstract

This systematic review and meta-analysis provides a cohesive overview of coccolithophore distribution across the Mediterranean Sea across both spatial (regionally) and temporal scales (seasonally) and explores the main environmental drivers of their distribution by identifying trends in the literature. Using the identified environmental parameters, we discuss the potential impacts of climate change on the distribution of coccolithophores in the Mediterranean Sea. Methodological biases associated with sampling methods and microscopy were identified, indicating that phytoplankton studies utilising the Utermöhl method of sampling and inverted light microscopy likely underestimate coccolithophore abundances and contribution (%) to the phytoplankton community. Key gaps in research were also identified, such as the north coast of Africa, the western basin, the winter and spring seasons, and coccolithophore community diversity. Meta-analysis data indicated opposing geographic and temporal distributions of hetero- and holo-coccolithophores, supporting the hypothesis that the haplo-diplontic life cycle of coccolithophores widens their ecological niche. Coccolithophore abundance has been found to be negatively correlated with temperature in several studies, and additionally, abundance is higher during winter and autumn. Therefore, total coccolithophore abundance may be negatively impacted by ocean warming, however holococcolithophores, which are positively correlated with temperature, may respond positively by expanding their range.

1. Introduction

1.1 Coccolithophores

Coccolithophores are a marine calcifying phytoplankton that are found in all the world's oceans. Through photosynthesis and the formation and dissolution of their calcium carbonate skeleton, coccolithophores influence seawater chemistry and carbon dioxide exchange between the atmosphere and the ocean (Subhas et al. 2022). Coccolithophores are one the major producers of calcium carbonate in the open ocean (Iglesias-Rodríguez et al. 2002; Ziveri et al. 2007), and their calcium carbonate ballast accounts for 83% of the organic carbon flux to the sea floor (Klaas and Archer 2002). Coccolithophores reside at the base of the marine trophic web and provide an important food source to zooplankton (El-Hady et al. 2016a) such as copepods (Langer et al. 2007b) and dinoflagellates (Haunost et al. 2021), particularly during major blooms (Pond and Harris 1996).

Coccolithophores are haptophytes that utilise two distinct life-phases - holococcolithophore (haploid) and heterococcolithophore (diploid) phases. Holococcoltihs are made up of sub-micron, uniform-shaped crystallites while heterococcoliths are made up of micron-sized crystals of complex, species-specific shape (Young et al. 1999). Relatively little is still known about the coccolithophore life-cycle as direct observations of a change in phase is uncommon (Nöel et al. 2004), however several combination coccospheres have been found (both diploid and haploid phase). Hetercoccolithophores and holococcolithophores appear to inhabit distinct ecological niches and it is estimated that the haplo-diplontic life-cycle may increase their niche-space by approximately 19% (de Vries et al. 2021).

1.2 The Mediterranean Sea - physico-chemical features and climate change effects

The Mediterranean Sea has distinct biogeochemical regions that cross natural environmental gradients, with the shallow Strait of Sicily splitting the Mediterranean into the eastern and western sub-basins (Rohling et al. 2009). The eastern Mediterranean is characterised by higher temperatures and salinities than the western basin, which consists of Atlantic Ocean water entering from the Gibraltar Strait that is modified moving

eastward (Rohling et al. 2009). Surface-water circulation is mainly driven by thermohaline forcing as well as wind stress (Robinson and Golnaraghi 1994). Phosphate and nitrate have higher concentrations in the west of the Mediterranean, with a sharp decrease moving to the eastern Mediterranean, a region typified by low concentrations of phosphate and nitrate (oligotrophic system; Krom et al., 1991). These stark changes in marine environmental parameters from west to east make the Mediterranean Sea a unique region to investigate how the variability in environmental factor affects species distributions. Further details of the oceanographic settings, with respect to the eastern and western sub-basins of the Mediterranean Sea, can be found in the supplementary material.

The Mediterranean Sea has been identified as a climate change hot-spot (Giorgi 2006) that is particularly responsive and vulnerable to ecosystem changes (Lazzari et al. 2013). As a result of climatic and non-climatic forcings, this region is experiencing rapid change (Cramer et al. 2018; MedECC 2020), with atmospheric temperatures rising as much as 20% faster than the global average (Lazzari et al. 2013; Lionello and Scarascia 2018), with a current annual mean temperature of 1.4ºC above late-nineteenth-century level (as of 2018; Cramer et al., 2018). Sea surface temperatures are expected to rise by 1.5-2ºC by the end of this century, at a rate faster than the global average (Lazzari et al. 2013). Increasing temperatures have been shown to impact coccolithophore calcification (Rosas-Navarro et al. 2016; Feng et al. 2017; Krumhardt et al. 2017), growth rate (Schlüter et al. 2014; Rosas-Navarro et al. 2016; Feng et al. 2017; Krumhardt et al. 2017; Johnson et al. 2022), morphology (Harvey et al. 2015; Rosas-Navarro et al. 2016), and distribution (Hinz et al. 2012; Saavedra-Pellitero et al. 2014).

Ocean acidification is another aspect linked to global climate change. It results from the absorption of approximately 25 – 30% of the anthropogenic CO_2 produced (Friedlingstein et al. 2022). Global average sea surface pH is predicted to decrease by 0.3 to 0.4 units by 2100 (Geri et al. 2014; Flecha et al. 2015; Kapsenberg et al. 2017) however the Mediterranean Sea may exceed this decrease (Hassoun et al. 2015a, 2022). Calcifying organisms are vulnerable to ocean acidification with changes in seawater carbonate chemistry affecting calcification rate (Riebesell et al. 2000; Kroeker et al. 2010; Lefebvre et al. 2011; Schlüter et al. 2014), morphology (Lefebvre et al. 2011; Langer et al. 2011; Johnson et al. 2022) lipid content (Johnson et al. 2022), and distribution (Charalampopoulou et al. 2011). The impacts of climate change on marine systems will

be diverse and complex, with predicted disruptions to population dynamics, geographical distributions, and ecosystem functioning, as well as losses in biodiversity and species richness (Harley et al. 2006; Bulling et al. 2010; Lacoue-Labarthe et al. 2016). It is essential to improve our knowledge of key communities that are vulnerable to these changes in order to determine how organisms, communities, and ecosystems will respond to ocean conditions under climate change.

1.3 State of the art and aim of the study

Most of the Mediterranean Sea field studies that incorporate information on coccolithophores focus mainly on the whole phytoplankton community, with data collected via different strategies (i.e., collection depth) and in different regions (i.e., Ligurian, Tyrrhenian, Adriatic, Balearic, Ionian, Cretan and Levantine Seas; Table S16). There is a large review of plankton in the open Mediterranean Sea (Siokou-Frangou et al. 2010), however the inclusion of coccolithophores is very minor, likely due to the assumption that coccolithophores generally make up a small proportion of the phytoplankton community. There are also currently two atlases that identify coccolithophore species diversity, however these are focused only to the north western Mediterranean Sea (Cros and Fortuno 2002) and eastern Mediterranean Sea (Malinverno 2008), and are mainly taxonomic in nature rather than ecologically focused. The Mediterranean Sea is a highly diverse region for coccolithophores (Kleijne 1991; Malinverno 2008), and to our knowledge, there is no major review of their distribution across this unique semi-enclosed basin, limiting our understanding of this important calcifying plankton.

The aim of this systematic review and meta-analysis is to characterise coccolithophore populations in the Mediterranean Sea across both basin-wide and regional spatial scales, and to determine the main environmental drivers of their distribution by identifying trends in the literature. Using key environmental parameters, including temperature, pH, nutrients, and salinity, we aim to discuss the likely impacts of climate change drivers on the distribution of coccolithophores in the Mediterranean Sea. We will also identify knowledge and sampling gaps, as well as potential methodological limitations and biases.

2. Methods

2.1 Systematic literature review

A systematic literature review on coccolithophore distribution in the Mediterranean Sea was conducted using Web of Science and Scopus using the following terms: coccolithophor* AND Mediterranean OR Alboran OR Balearic OR Ligurian OR Tyrrhenian OR Adriatic OR Aegean OR Ionian OR Cretan OR Ligurian. Coccolithophor* was used to account for any derivatives of coccolithophore such as coccolithophorid. Web of Science produced 252 related articles and Scopus produced 202 (as of 16th October 2022). There were two duplicates which were removed each from Web of Science and Scopus. There were 165 shared documents between the results from each search engine. Web of Science had 84 unique articles and Scopus had 36 unique articles. In total 286 unique articles were identified, which were screened for eligibility (title and abstract), 96 were retrieved to determine further eligibility, and 72 were chosen to be included in the systematic revies (Fig. 1; Table S16 for article list). The documents were not included if they were: (i) palaeontological, (ii) experimental, or (iii) did not provide any new data on the distribution of extant coccolithophores. Articles were included if they collected abundance data on extant coccolithophores. This review focuses only on living coccolithophores occupying the photic layer and therefore articles on coccolithophore export fluxes were excluded. Previous reviews on coccolithophores were also removed. In general, the majority of the included studies focus on the entire phytoplankton community, rather than solely on coccolithophores.

In order to address possible relationships between environmental conditions and coccolithophore assemblages, information regarding statistically significant correlations between abundance/diversity and environmental parameters that were identified in the literature. These correlations were input into a matrix and characterised as positive, negative, or if no effect if no correlation was determined. This matrix was used to identify general trends between coccolithophore abundance and environmental conditions.

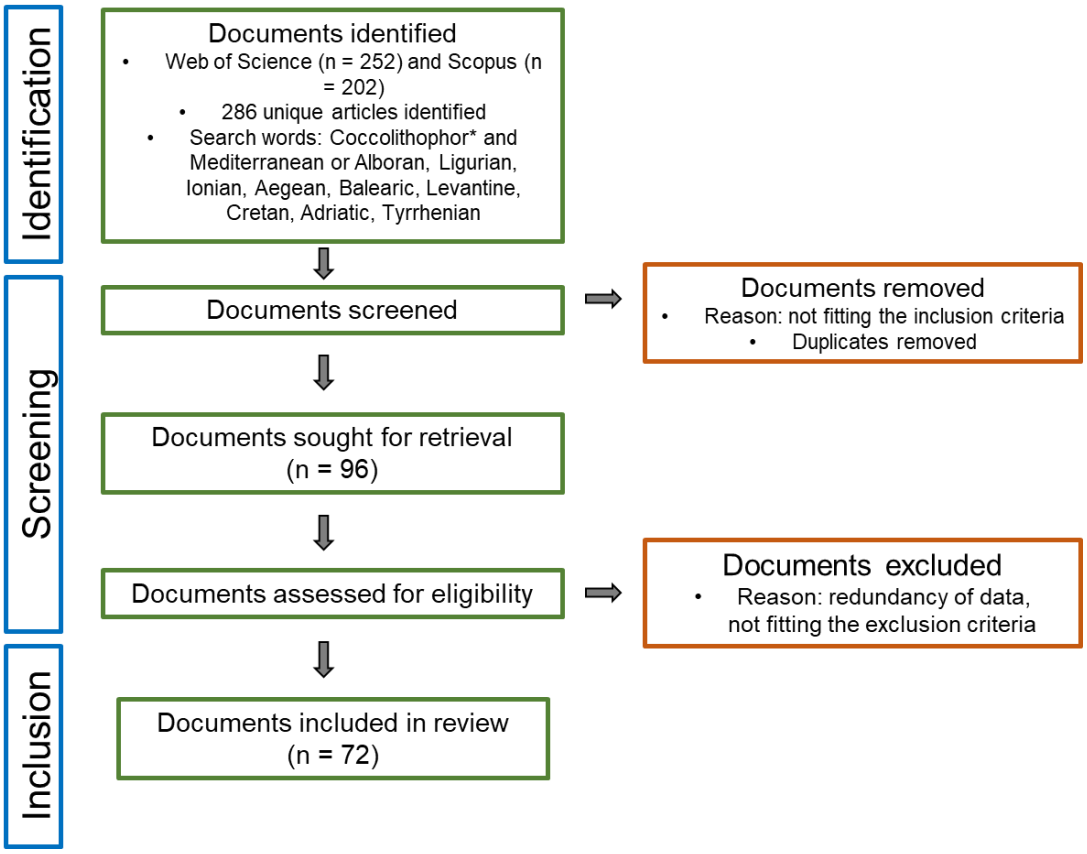

Fig 1. Flow chart outlining the systematic process of article identification and selection for the systematic review.

2.2 Dataset formulation – meta-analysis

Data on coccolithophore abundances from water samples was collected from several sources including the supplementary material/data storage facilities of the articles included in the review (16), PANGAEA (2), and the dataset of De Vries (2020) from PANGAEA (4 unique datasets and 4 already available online; dataset list in the supplementary material) to conduct a meta-analysis (MA). Each individual sample contains, at minimum, information regarding to the date of collection, the latitude and longitude of the sampling, the depth (m), and the total coccolithophore abundance (L^{-1}). This information was available in only two articles directly (Dimiza et al. 2008; Triantaphyllou et al. 2018), or as supplementary material, however many articles include information about average total abundance (coccolithophores/L^{-1}; Knappertsbusch 1993; Ignatiades et al. 1995; Aubry and Acri 2004; Mercado et al. 2005, 2007; Burić et al. 2007; Viličić et al. 2009; Bonomo et al. 2012, 2014, 2017; Valencia-Vila et al. 2016; Cerino et al. 2017, 2019; Triantaphyllou et al. 2018; Krivokapic et al. 2018; Skampa et al. 2019;

Neri et al. 2022), genus or individual species abundances (coccolithophores/L^{-1}; Carrada et al. 1981; Knappertsbusch 1993; Socal et al. 1999; Caroppo et al. 1999; Saugestad and Heimdal 2002; Malinverno et al. 2003; Mercado et al. 2005; Viličić et al. 2009, 2011; Moscatello et al. 2011; Šupraha et al. 2011; Godrijan et al. 2013; Supraha et al. 2016; Karatsolis et al. 2017; D'Amario et al. 2017; Skejic et al. 2018; Varkitzi et al. 2020; Dimiza et al. 2020) and coccolithophore contribution (%) to the phytoplankton community (Kimor et al. 1987; Ignatiades et al. 1995; Gotsis-Skretas et al. 1999; Socal et al. 1999; Caroppo et al. 1999; Totti et al. 2000, 2019; Boldrin et al. 2002; Aubry and Acri 2004; Saracino and Rubino 2006; Mercado et al. 2007; Bouza and Aboal 2008; Aktan 2011; Hernández-Almeida et al. 2011; Moscatello et al. 2011; Cabrini et al. 2012; Valencia-Vila et al. 2016; Dimiza et al. 2016; Rekik et al. 2017; Cerino et al. 2017, 2019; Drakulović et al. 2017; Triantaphyllou et al. 2018; Varkitzi et al. 2020) which are analysed separately from the MA as they only contribute one datapoint. Furthermore, several studies report average total abundances in the article as well as provide the supplementary material (Bonomo et al. 2012, 2014, 2017; Valencia-Vila et al. 2016; Cerino et al. 2017). Some datasets provide additional data including bottom depth (m), temperature (°C), salinity (PSU), chlorophyll (mg/m^3), fluorescence (µg L^{-1}), oxygen (µmol kg^{-1}), pH, NO_2 (µmol L^{-1}), NO_3 (µmol L^{-1}), NO_4 (µmol L^{-1}), PO_4 (µmol L^{-1}), DIN (dissolved inorganic nitrogen; µmol L^{-1}), pCO_2 (µmol L^{-1}), SiO_2 (µmol L^{-1}),, NH_4 (µmol L^{-1}), CO_3^2 (µmol kg^{-1}), aragonite saturation (µmol kg^{-1}), PAR (*µmol photons* m^{-2} s^{-1}), heterococcolithophore abundance (L^{-1}), holococcolithophore abundance (L^{-1}), and the abundance of a genus or individual species (L^{-1}; datasets provided different units of measurement for several environmental variables). There are 5739 rows of data from 27 sets of data included in the MA formulated here (Fig. S17). If the data analysed in each study was not available, each corresponding author was contacted (if possible) regarding data availability. Fifty-four corresponding authors were contacted to request the coccolithophore abundance data. Four authors were not able to be contacted due to the lack of current contact information. Most authors did not respond to the data request (40), some authors were unable to share the data as it was not open access, and often, due to the age of several studies, the data was not able to be retrieved due to obsolete methods of storage (e.g., floppy disks, software that requires former operating systems). An additional five datasets were obtained through contacting the corresponding author via email. In total, data from 24 studies are included in the dataset and data from 49 studies are not included in the dataset (Table S17). There are three sets of data included here that

are not connected to any article in the review (Table S17). While not all the data from the articles was obtained, the dataset reflects the general nature of the articles in the review, in that spring and summer are more heavily represented and it is more heavily biased to the eastern Mediterranean, in particular, the Aegean and Adriatic Seas (Fig. 2). The northern Adriatic Sea includes a large long-term dataset comprised of 3070 samples (53% of the total dataset) collected over 38 years (Acri et al. 2019).

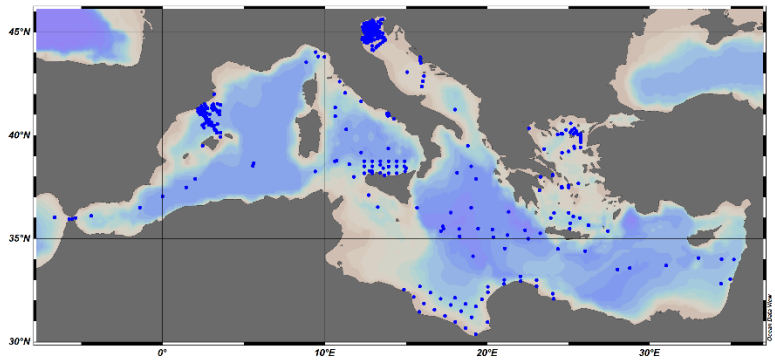

Fig 2. Distribution of datapoints in dataset. Each blue spot signifies an individual site which have either been sampled once or several times. Map by Ocean Data View.

Due to the uneven distribution of collected environmental parameters within the dataset, statistical correlations between abundances and environmental variables are not included here. Discussion regarding the relationship of abundance with these parameters are included based on reported findings in the literature.

Using the position (latitude and longitude coordinates) included in the MA, abundance and composition estimates for several regions in the Mediterranean Sea could be made. To determine differences in spatial (reginal and depth) and temporal (seasonal) coccolithophore distribution, average abundances were calculated within the following depth brackets (0 – 25 m, 25 – 50 m, 50 – 100 m, 100 – 215 m) for each individual sampling (not averaged if there was only one sample within the depth bracket) and separated by season. These are presented using maps created in Ocean Data View v3.1 (Figure S3A, B, C). Diversity estimates were also calculated using Shannon's Diversity Index (H'):

$$H' = -\Sigma [p_i * \ln(p_i)]$$

Where H' is Shannon's Diversity Index and p_i is the proportion of species in a population. Total coccolithophore, hetero- and holo-coccolithophore diversity at 0 – 25 m, 25 – 50 m, 50 – 100 m and 100 – 215 m are also presented using maps created in Ocean Data View v3.1 (Figure S4). Species composition and diversity estimates are only calculated using SEM data for reasons discussed below (Section 3.3). Species abundance and contribution (%) to the coccolithophore community are calculated for the entire Mediterranean Sea and individual regions. The most abundant species across the Mediterranean Sea (Table S10) and regionally (Table S11) are also calculated.

2.3 Statistical methods

To determine significant differences between total abundances and hetero- and holo-coccolithophore abundances (seasonally and regionally) a Kruskal-Wallis non-parametric test was used. As the data was not normally distributed in nearly all groups, and due to the high presence of outliers (often related to bloom events), a non-parametric test was used as it is robust toward outliers and suitable for non-normal data distribution. Reported significance values have been adjusted by the Bonferroni correction for multiple tests. The Kruskal-Wallis tests were conducted using IBM SPSS v. 29. The results of all statistical analyses can be found in the supplementary material.

3. Results and Discussion

3.1. Characterisation of the studies

The majority of studies (84%) investigating coccolithophore distribution in the Mediterranean Sea were published after the year 2002 (Fig. 3). There were eight studies produced in the 1990s (four of those in 1999) and there were very few studies before this period. There was a slight increase in published articles in the late 2010s, but this increase tapered off. The increase in studies during the 2010s are characterised by some notable projects including the "European Mediterranean Sea Acidification in a changing climate" funded by the European Commission (MedSeA; Bonomo et al. 2012; Ziveri et al. 2014; Oviedo et al. 2015; Cerino et al. 2017; D'Amario et al. 2017), the global program "Long-Term Ecological Research" (LTER; Zingone et al. 2010; Cabrini et al. 2012; Cerino et al. 2017, 2019; Totti et al. 2019; Acri et al. 2019; Aubry et al. 2021; Bernardi Aubry et al.

2022; Neri et al. 2022), and "Assessment and Monitoring of the Fishery Resources and the Ecosystems in the Straits of Sicily" (MEDSUDMED; Bonomo et al. 2012, 2017, 2018b) funded by the Italian Ministry of Agricultural, Food and Forestry Policies. Information regarding the country of the first author and the origin of funding bodies can be found in the supplementary material (Fig. S2A and S2B).

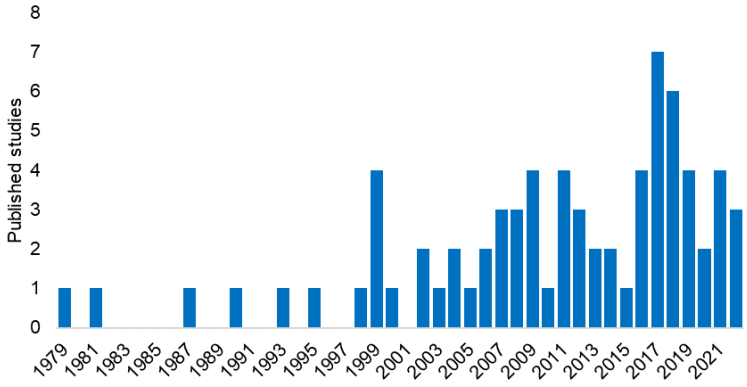

Fig 3. Published studies per year that incorporate coccolithophore abundance data in the Mediterranean region.

The majority of articles in this review focus on the phytoplankton community as a whole (44 articles) rather than solely on the coccolithophore community (29). The western Mediterranean is underrepresented compared to the eastern Mediterranean, with 15 studies compared to the eastern Mediterranean's 52. The majority of studies in the Eastern Mediterranean are phytoplankton studies (35 compared to 17), while there is a more even spread in the western Mediterranean (8 phytoplankton studies compared to 7 coccolithophore studies). There are five trans-Mediterranean cruises included here that transect both the eastern and western sub-basins of the Mediterranean Sea (Fig. 4A). Four of these cruises sample solely coccolithophores and one samples the entire phytoplankton community.

Most studies are based in the northern Adriatic Sea, and a large proportion of those are phytoplankton studies (24 out of 30; Fig. 4A). The Aegean Sea is the next most represented region with 12 articles, which is split evenly between phytoplankton and coccolithophore studies. The Tyrrhenian Sea is the most represented region in the western Mediterranean, with six coccolithophore studies and two phytoplankton studies. Most studies focus on one region (63), while very few focus on either two (2) or three (2) regions.

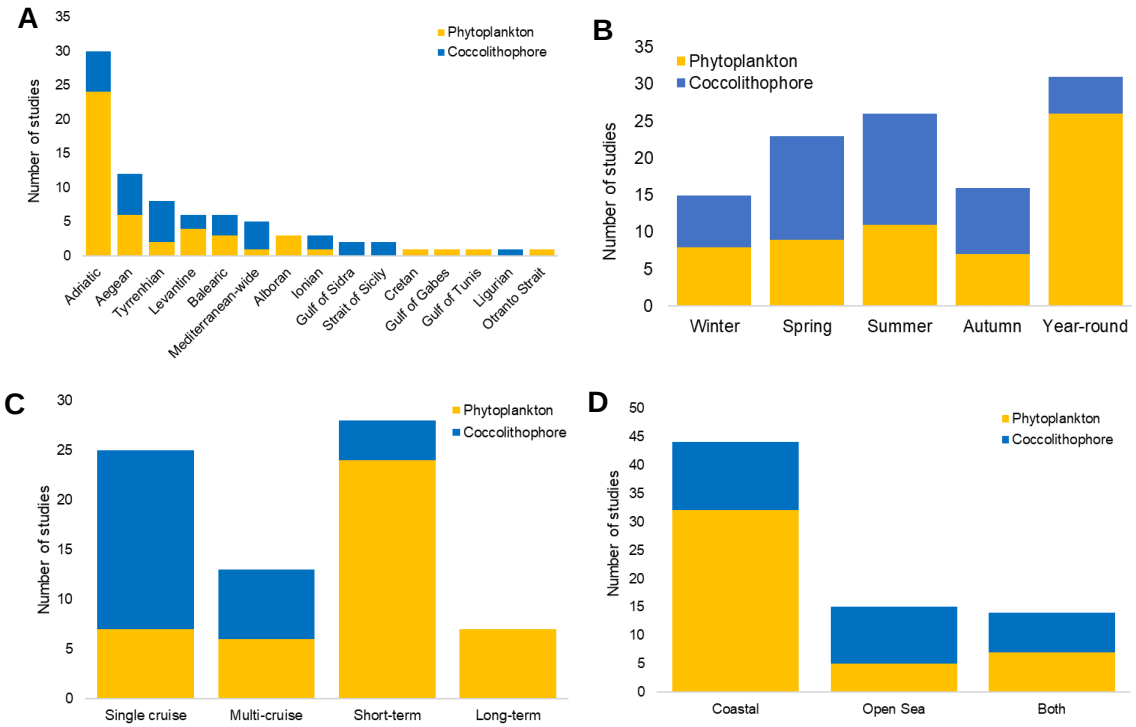

Fig. 4. A The number of studies by region **B** Number of studies by season or year-round **C** Study length or single/multi-cruise studies, and **D** Number of coastal, open-sea, or combination of coastal and open-sea studies. The total number in Fig. **A** and **B** here exceeds the number of studies included in the review as some articles target more than one season and region.

The north of African Mediterranean region is understudied with respect to phytoplankton and coccolithophore research. There are only three studies that are based on the north coast of Africa (Fig. 4A)– two off the coast of Tunisia (Challouf et al. 2017; Rekik et al. 2017) and one off the coast of Libya (Bonomo et al. 2018b).

Most studies included in the review are year-round to account for the seasonality of phytoplankton communities (Fig. 4B). There are 15 studies that occur during winter and 16 in autumn (Fig. 4B). Winter is the most underrepresented season, while spring and summer have 22 and 25 studies, respectively (Fig. 4B). Nineteen studies focus on a single season, 11 on two seasons and 7 on three seasons.

Most coccolithophore studies are based on data collected from a single cruise, whereas most phytoplankton studies are short-term studies (Fig. 4C). Short-term studies (1 – 10 years) accounted for most of the studies included in this review (28 studies), followed by single cruise studies (25), and then multi-cruise studies (12) which sometimes spanned

several years but with irregular sampling (Fig. 4C). There are 7 long-term studies included in this review which are phytoplankton studies (Fig 4C), and they range in span from 11 to 25 years, with sampling normally conducted bi-weekly or monthly.

Most research is conducted in coastal regions (44), and a large proportion of these studies are based in the Adriatic Sea (23; Fig. 4D). There are 15 open sea studies, 4 of which include trans-Mediterranean cruises (Fig. 4D). There are 13 studies that include a combination of coastal and open sea stations (Fig. 4D).

3.2 The northern Adriatic Sea long-term time-series

The dataset from the Adriatic Sea is one of the longest running phytoplankton studies in the Mediterranean region. Due to the regular sampling, it was able to capture data on the seasonality of coccolithophore and phytoplankton communities, as well as detect significant and irregular algal bloom events. The northern Adriatic Sea is characterised by high productivity due to the riverine input (Zavatarelli et al. 1998), therefore we expect that the coccolithophore abundances here will be higher than the majority of the oligotrophic Mediterranean Sea. As this long-term study makes up 53% of the total dataset, it shifts average abundance estimates toward its average. Overall, this time-series increases the average total abundance for the Mediterranean, the Eastern Mediterranean, the Adriatic Sea, and the ILM calculations (it does not provide any data on individual species abundances), therefore, abundance calculations do not include the long-term dataset.

3.3 Methodological biases

Inverted light microscopy has been traditionally used in phytoplankton studies for calculating abundance and identifying species and species groups. The Utermöhl (1958) method is the most broadly used in phytoplankton studies to enable the counting and identification of the whole phytoplankton community. This method uses unfiltered seawater laced with Lugol's iodine for organism preservation, followed by a period of at least 24 hrs to allow for sedimentation of the specimens (Paxinos and Mitchell 2000). The specimens are then enumerated using inverted light microscopy (ILM). A common method used to count and identify coccolithophores is polarised light microscopy (PLM).

This method is often used to identify calcareous nannofossils as it highlights the calcified components of coccolithophores (Fuertes et al. 2014). Scanning electron microscopy (SEM) is often used in coccolithophore research and is the benchmark for identifying species level as it provides clear imagery of distinct morphological characteristics. This method, however, is more costly than using ILM or PLM.

It has been suggested that cell density estimates of small coccospheres using ILM are potentially unreliable due to an underestimation of standing stock (Reid 1980). In a study investigating techniques used for quantifying calcareous phytoplankton, the Utermöhl method consistently provided lower density estimates than SEM (Bollmann et al. 2002) which the author's contributed to its low resolution and difficulty with identifying small species compared to SEM (Bollmann et al. 2002). In cases where there is a diversity of size classes, small coccolithophores such as *E. huxleyi* and several Syracosphaera species, may be underestimated using ILM (Bollmann et al. 2002).

To investigate how these methods affect abundances across the Mediterranean Sea, we calculated average total abundances using ILM, PLM, and SEM at different depths using the MA dataset. There is a clear trend of increasing abundances, irrespective of region, from ILM to PLM and SEM across three depth brackets 25 – 50 m, 50 – 100 m, and 100 > 200 m (Fig. 5A; Table S6). The comparatively high average abundance for ILM in the 0 – 25 m bracket is driven by very high abundances recorded in the northern Adriatic Sea (n = 21), which is a highly productive region (Zavatarelli et al. 1998). If this dataset is removed from the calculation, average ILM abundance drops to 18913 cells/L^{-1}, following the trend in other depth brackets. The abundances derived from the PLM do not appear to follow a general trend in relation to the other microscopy methods, but abundances are higher than those of ILM and are generally of the same order of magnitude as the SEM abundances. These results suggest that abundance estimates using ILM are underestimations (between 5.9 – 83.7%). Shannon's diversity index follows a clear and expected trend, with diversity increasing from ILM to PLM, then further from PLM to SEM (Fig. 5B; Table S2).

The assemblage composition between ILM and SEM can also be very different. This is likely the result of using a higher volume of water used for counting using ILM, increasing the probability of coming across larger species, while SEM analyses a smaller

volume of water but has a greater chance of identifying smaller species (Bollmann et al. 2002). Bollmann et al. (2002) also suggested that selective dissolution may occur for smaller coccolithophores

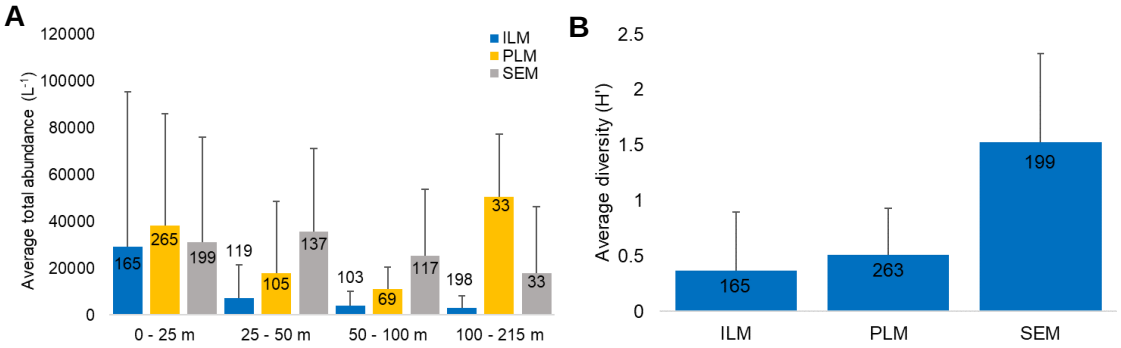

Fig. 5. A Average total abundance averages for each sampling between 0 – 25m, 25 – 50m, 50 – 100m, and 100 – 200m, and **B** Average diversity (H') using different methods of microscopy (0 – 25 m depth bracket). ILM = Inverted Light Microscope; PLM = Polarised Light Microscope; SEM = Scanning Electron Microscope. Not including the long-term dataset from the north Adriatic Sea. Error Bars indicate standard deviation. The number of samples included in the calculation is provided on the column.

during the settling process with the Utermöhl method. When considering species assemblage data determined using ILM and the Utermöhl method compared to SEM, it is important to consider that the assemblage will likely reflect the microscopy method.

While the data that used the Utermöhl method and ILM makes up the greatest proportion of the dataset (69.6%), the clear discrepancy between methods requires a more conservative approach, and therefore only PLM and SEM data are included in calculations of regional abundance. As SEM is the only method that can provide accurate identification of coccolithophores to species level, particularly for smaller coccolithophores and holococcolithophores, comparisons between hetero- and holo-coccolithophores, calculations of species diversity, and species compositions are only calculated using SEM data.

3.4 Coccolithophore contribution to phytoplankton communities

Phytoplankton studies generally provide estimates of the abundance contribution of individual groups or species to the phytoplankton community. Using estimates provided by phytoplankton and coccolithophore studies in the literature, coccolithophores

contribute a year-round average of 8.7% to phytoplankton community abundance (cells/L^{-1}; Fig. 6). This varies depending on the season, with higher contributions of coccolithophores during autumn (29.1%) and winter (14.8%). Using the MA dataset, within the upper 25 m, estimates of coccolithophore abundance contributions to the phytoplankton community are distinctly higher, with the average contribution reaching 71.2% in spring, 39.4% in winter, 26.3% in autumn, and 20.6% in summer (using ILM only; not including the long-term time-series from the Adriatic Sea; Fig. 6; Table S5).

There are no studies using SEM or PLM that calculate the coccolithophore contribution to the phytoplankton community included in the MA. Based on the MA results presented here (Fig. 5A) and previous conclusions regarding underestimates using ILM and the Utermöhl method (Reid 1980; Bollmann et al. 2002), it is likely that these studies that use the Utermöhl method and ILM underestimate coccolithophore abundances and their contribution to phytoplankton communities. Studies that use PLM and SEM will likely provide more accurate estimates of coccolithophore contribution.

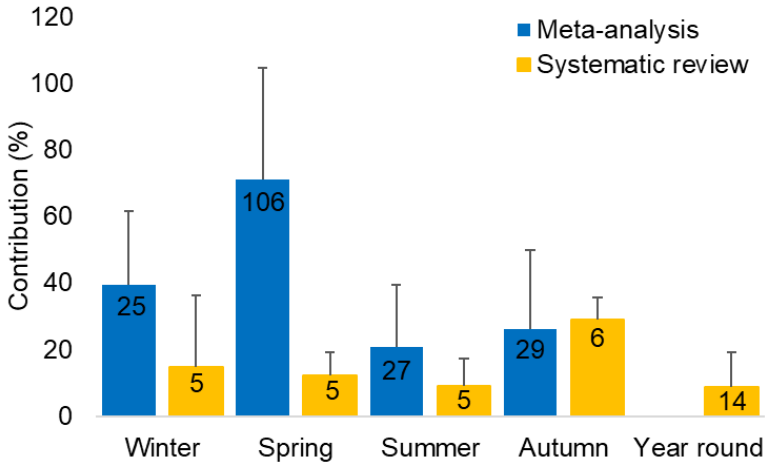

Fig. 6. Seasonal contribution (%) of coccolithophores to the phytoplankton community using values collected from the systematic review (yellow) and from the meta-analysis (blue – ILM data from 0 – 25 m; not including the long-term time-series from the Adriatic Sea). Error Bars indicate standard deviation. The number of samples included in the calculation is provided on the column.

3.5 General trends and abundance

The dataset compiled for this meta-analysis identified 158 heterococcolithophore species, 57 holococcolithophore species, 8 combination coccospheres, and 3 polycrater phase coccospheres (Table S1). Average total abundance is greater in the western

Mediterranean than the eastern Mediterranean (31918 cells/L^{-1} and 25552 cells/L^{-1}, respectively; PLM and SEM data; H(1) = 24.8, p = 0.00). Total abundance in the western Mediterranean was also greater than in the eastern Mediterranean during two spring Mediterranean-wide transects in 2013 (D'Amario et al. 2017) and two Mediterranean wide cruises during the 1980s (Knappertsbusch 1993). Heterococcolithophores make up the majority of coccolithophores in the Mediterranean Sea (84%; Fig. 7A using SEM data; Table S3). Abundance declines with depth in both the eastern and western Mediterranean, however abundances between 50 – 100 m and 100 – 215 m in the eastern Mediterranean remains stable (Fig. 7B; Table S7). Between 0 – 100 m depth, average abundance is greater in the western Mediterranean, however from 100 – 200 m, abundance is greater in the eastern Mediterranean (Table S7), which likely reflects the deeper chlorophyll maxima of the eastern basin (Teruzzi et al. 2021). Highly abundant regions include the Alboran (average 132169 cells/L^{-1}) and Adriatic Seas (average 63346 cells/L^{-1}; SEM data; Fig. 7C; Table S4). Detailed discussion regarding coccolithophore distribution and abundance within biogeographic regions in the Mediterranean Sea can be found in the supplementary material.

3.6 Hetero- and holo-coccolithophores – opposing spatial and temporal distributions

Heterococcolithophores and holococcolithophores have opposing spatial distribution in the Mediterranean Sea, with higher abundances for heterococcolithophores in the western Mediterranean and higher abundances for holococcolithophores in the eastern Mediterranean (Fig. 7A), as seen in several trans-Mediterranean cruises (Kleijne 1991; Knappertsbusch 1993; D'Amario et al. 2017a). Furthermore, there are also depth related spatial differences between hetero- and holo-coccolithophores. For holococcolithophores, abundance is also highest in the upper <50 m (Fig. S3C) as previously reported by D'Amario et al. (2017), while for heterococcolithophore abundance is higher at greater depths (Fig. S3B).

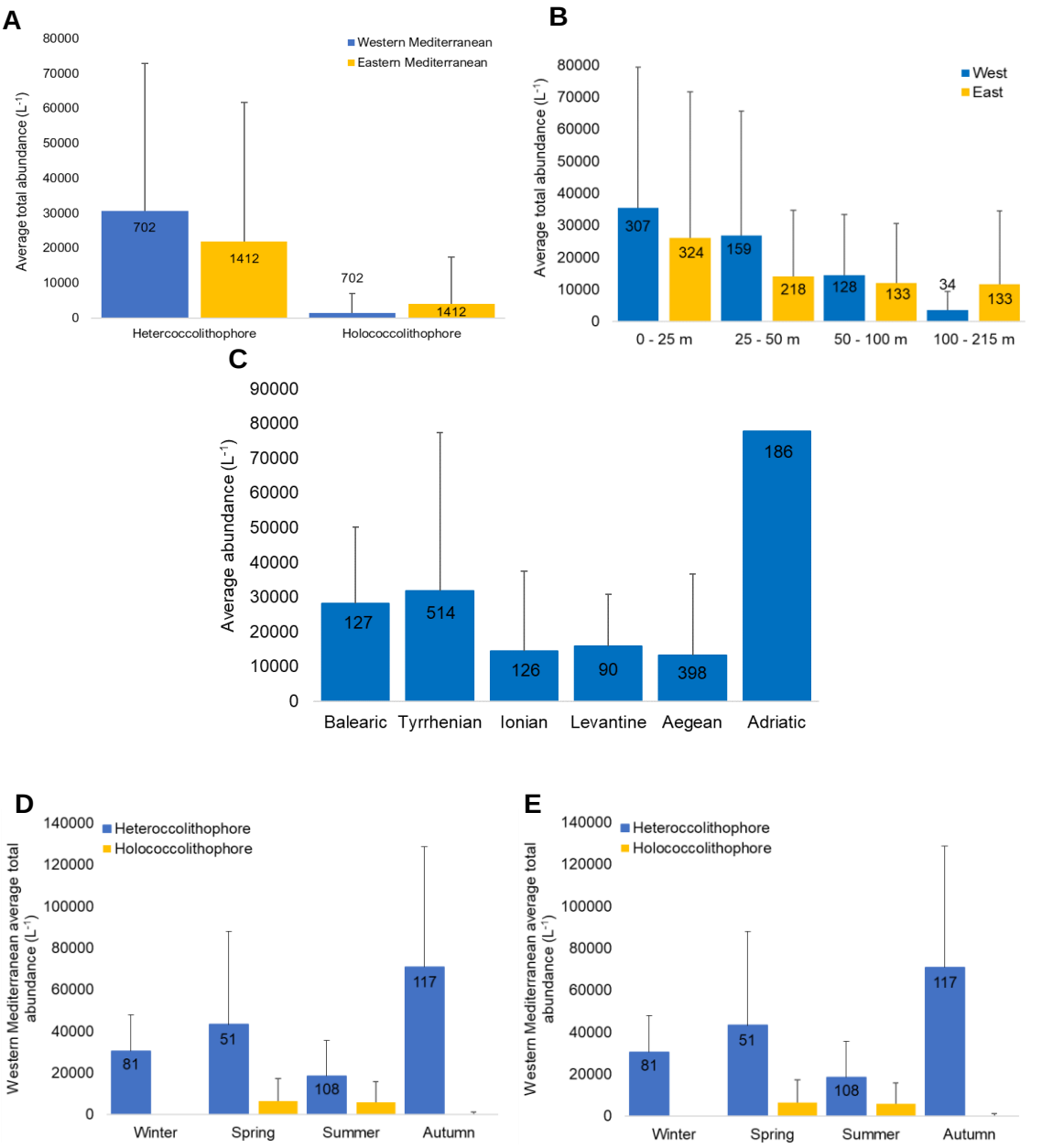

Fig 7. **A** Average total abundances (L^{-1}) for heterococcolithophores and holococcolithophores in Eastern and western Mediterranean (SEM data only); **B** Average total abundance (L^{-1}) in the eastern and western Mediterranean within depth brackets 0 - 25 m, 25 - 50 m, 50 - 100 m, and 100 - 215 m (using all types of microscopy data; not including the long-term time-series from the Adriatic Sea); **C** Average total abundance (L^{-1}) for Mediterranean regions (PLM and SEM data only). There was no PLM or SEM data for the Alboran Sea therefore it is not included here. The standard deviation for the Adriatic Sea is not included here for ease of comparison with other regions (SD = 536335); **D** Average total seasonal abundance (L^{-1}) of heterococcolithophores and holococcolithophores in the western Mediterranean, and **E** Average total seasonal abundance (L^{-1}) of heterococcolithophores and holococcolithophores in the eastern Mediterranean for the entire water column using only PLM and SEM. Error Bars indicate standard deviation. The number of samples included in the calculation is provided on the column.

There are also differences in the temporal distribution of hetero- and holo-coccolithophores. Heterococcolithophore abundance is highest in spring and autumn and lower in winter and summer in the western Mediterranean (Fig. 7D; Table S8), however in the eastern Mediterranean abundance is higher in winter and spring and lower in autumn and summer (Fig. 7E; Table S8). This may be related to the general ecological preference of heterococcolithophore for cooler waters (Supraha et al. 2016; Krivokapic et al. 2018; Neri et al. 2022), where abundances follow a west-east gradient of temperature and nutrients. For holococcolithophores, abundance is greater in spring and summer in both the western and eastern Mediterranean (Fig. 7D, E). They are barely present in autumn and absent in winter in the western Mediterranean, which may reflect their preference for warmer conditions (Supraha et al. 2016; D'Amario et al. 2017a; Bonomo et al. 2018a).

These spatial and temporal differences in distribution between hetero- and holo-coccolithophores add support to the hypothesis that the haploid-diploid lifecycle allow coccolithophores to expand their ecological niche (D'Amario et al. 2017a; de Vries et al. 2021).

3.7 Hetero- and holo-coccolithophore diversity

The Mediterranean Sea is known to be a highly diverse coccolithophore region (O'Brien et al. 2016) for both hetero- and holo-coccolithophores (Kleijne 1991; Cros and Fortuno 2002; Malinverno 2008). Overall, heterococcolithophore diversity is greater than holococcolithophore diversity (H' = 1.02 and 0.70, respectively), and diversity in slightly higher in the eastern basin than the western basin (H' = 0.89 and 0.77, respectively), however this differs seasonally (Fig. 8A, B; Table S9). For the eastern basin, diversity remains stable throughout the year for both hetero- and holo-coccolithophores (Fig. 8B), while for the western basin, diversity peaks in spring and then declines throughout the year to winter (Fig. 8A). Diversity generally declines with depth in all seasons excluding spring (Fig. S4). While holococcolithophores have been previously shown to have greater diversity in the western Mediterranean (Kleijne 1991), the dataset indicates that both hetero- and holo-coccolithophore diversity is higher in the eastern Mediterranean (H' = 0.65 and 0.43, respectively).

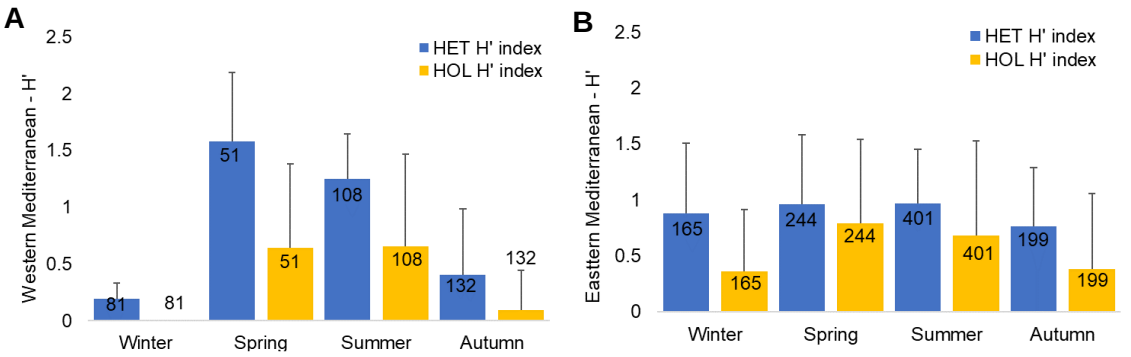

Fig. 8. Seasonal hetero- and holo-coccolithophore diversity (H`) in **A** the western and **B** the eastern Mediterranean Sea (SEM data only). Error Bars indicate standard deviation. The number of samples included in the calculation is provided on the column.

3.8 General species trends

We focus here on the 20 most common identified species across the Mediterranean Sea (contribution above 0.62% to coccolithophore abundance and abundances higher than 350 cells/L^{-1}). As is noted throughout the literature, *E. huxleyi* is generally named as the most common species (Fig. 9; Table S10 and Table S11; Socal et al. 1999; Caroppo et al. 1999; Totti et al. 2000; Barcena et al. 2004; Saracino and Rubino 2006; Balestra et al. 2009; Vilicic et al. 2009; Viličić et al. 2009; Moscatello et al. 2011; Godrijan et al. 2013, 2018; Ziveri et al. 2014; Oviedo et al. 2015; Supraha et al. 2016; Dimiza et al. 2016; Bonomo et al. 2017, 2021; Cerino et al. 2017, 2019; D'Amario et al. 2017; Skejic et al. 2018; Triantaphyllou et al. 2018; Sahin and Eker-Develi 2019; Varkitzi et al. 2020; Bernardi Aubry et al. 2022). *Emiliania huxleyi* makes up on average 46.3% of the coccolithophore population across the Mediterranean Sea (Fig. 9), with an average Mediterranean wide abundance of 17071 cells L^{-1} (Table S10). Other common species include *F. profunda*, a dominant deep dwelling species, that is common in central Mediterranean regions (Fig. 9; Table S11). Syracosphaera species are common throughout the Mediterranean, particularly *S. molischii* and the hetero- and holo-coccolithophore forms *of S. pulchra* (Fig. 9; Table S11 and Table S11). Rhabdosphaera species, both *R. xiphos* and *R. clavigera*, are very common (Fig. 9; Table S10). *Rhabdosphaera clavigera* is the greatest contributor to coccolithophore community abundance in the Mediterranean Sea (5.5%; Fig. 9) after *E. huxleyi* and is the third most abundant species, with higher abundances in the eastern than western Mediterranean sub-basins (1219 cells L^{-1}; Table S10). In general, *S. halldalli* makes up a small proportion of

total abundances (Fig. 9), however due to several bloom events, its average abundance is high (1536 cells/L^{-3}; Table S10). *Gephyrocapsa* species, *G. oceanica, G. erisconii*, and *G. muellera*, common in the Atlantic Ocean, are abundant in the Alboran and Balearic Seas (Table S11), likely entering the Mediterranean Sea via the Atlantic Ocean influx waters. The most common species are heterococcolithophores, though *S. arethesae* (HOL), *A. robusta* (HOL), *S. histrica* (HOL), S. *pulchra* (HOL), *and H. cornifera* (HOL) are also common (Fig 9).

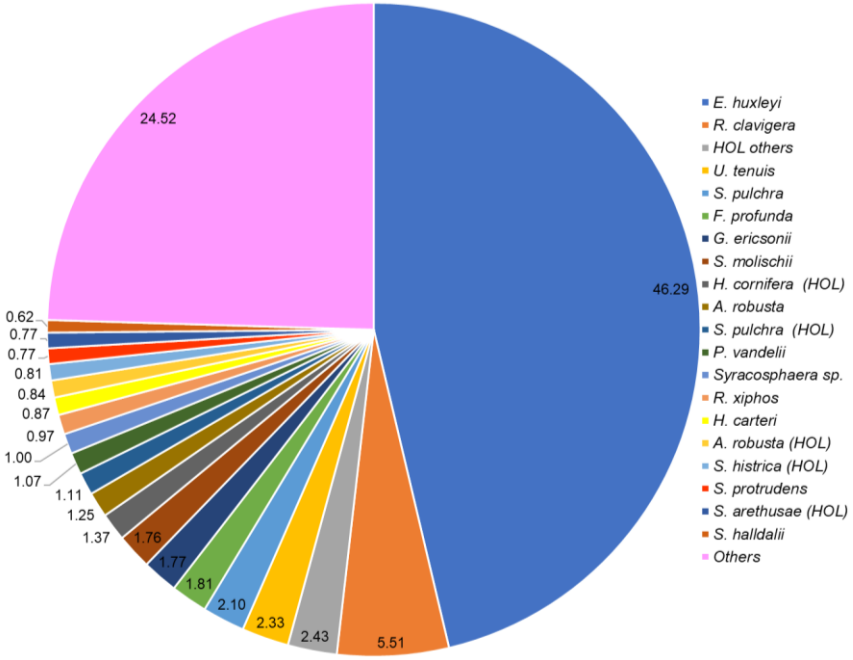

Fig 9. Species or species groups with relative abundance (%) higher than 0.62% in the Mediterranean Sea (SEM data). All other species are included in 'Others'.

3.9 Relationships with environmental parameters

Coccolithophore abundances: Information regarding the statistical correlation between environmental variables and coccolithophore total abundance is often not provided in publications, and each article investigates its own suite of parameters, reporting the results in different formats. Several publications identified trends however many were not statistically significant and therefore not included in the matrix. Additionally, many phytoplankton studies identified statistically significant correlations for the whole community, rather than solely for coccolithophores. Temperature, nitrate, and salinity were the most commonly measured variables, followed by phosphate, silicate, and pH (Table 1). Several parameters included only three or less correlations, therefore there are

not enough data points to make concrete assumptions regarding the relationship between coccolithophore abundance and the environmental variables. Total abundance will generally reflect heterococcolithophore abundance, as heterococcolithophores makes up the majority of the coccolithophore assemblages, however most studies did not differentiate between heterococcolithophore and holococcolithophore abundance.

Several negative correlations between temperature and total abundance were identified, however more commonly there was no effect of temperature detected on total abundance (Table 1). Similarly with nitrate, an equal number of articles identified a positive trend and a negative trend, although most did not identify a trend at all (Table 1). Few positive correlations were identified between total abundance and salinity, however most articles did not detect a relationship (Table 1). pH is the only parameter where three out of four studies identified a positive relationship with total abundance, and the other study did not identify an effect. This may be related to the observed impact of reduced pH on coccolithophores, which has been shown to negatively affect their calcification and morphology (Lefebvre et al. 2011; Langer et al. 2011; Kottmeier et al. 2022; Johnson et al. 2022), lipid content (Johnson et al. 2022), and impact their distribution (Charalampopoulou et al. 2011). The correlations included here were made irrespective of season or region, which may be contributing to the lack of cohesion between the identified trends.

Ultimately, there is a clear species-specific and group-specific preference for environmental conditions. For instance, *F. profunda*, which resides mostly in the deeper photo layer, is correlated with salinity (Bonomo et al. 2018), while holococcolithophores usually occupy the upper photic layer and prefer warmer conditions (Bonomo et al. 2018). This may explain the several conflicting correlations, as species abundances and distribution change seasonally.

Table 1. Relationship with environmental variables and total coccolithophore abundance outlined in 16 published articles. Publications and their contributions to the matrix can be found in Table S12.

Relationship	Temp	Depth	Nutrients	NO_3	PO_4	SiO_4	pH	pCO_2	CO^3_2	Salinity	O_2
Positive	**2**	**1**	**0**	**2**	**1**	**2**	**3**	**0**	**1**	**3**	**1**
Negative	**3**	**1**	**1**	**2**	**2**	**2**	**0**	**1**	**0**	**1**	**0**
No effect	**4**	**0**	**0**	**4**	**2**	**1**	**1**	**0**	**0**	**5**	**1**

Holococcolithophores: There was limited information regarding holococcolithophores and associated environmental parameters in the literature, however contrary to total coccolithophore abundance, several clear trends were identified considering the existing information (Table 2). Several positive correlations between temperature and holococcolithophores were identified, which may explain their preference for the warmer eastern Mediterranean Sea. There was also a negative correlation between total abundance and depth, and it has been shown in several studies as well as in the MA that holococcolithophores prefer the upper 50 m of the water column (Fig. S3C). There were also negative trends identified between pH (two out of three), nitrate, and phosphate. These relationships contrast with the relationships between total coccolithophore abundance and the environmental parameters (which largely reflect heterococcolithophore abundance), adding further support to the hypothesis that the haploid and diploid life stages are ecologically distinct and fill different ecological niches. A study investigating the relationships between environmental parameters and hetero- and holo-coccolithophore abundances in the Mediterranean Sea similarly showed that the two different life cycle phases of the same species had opposing relationships with environmental parameters (D'Amario et al. 2017).

Table 2. Relationship with environmental variables and holococcolithophore abundance outlined in seven published articles. Publications and their contributions to the matrix can be found in Table S13.

Relationship	Temp	Depth	NO_3	PO_4	pH	pCO_2	CO^3_2	Salinity	PAR
Positive	**3**	**0**	**0**	**0**	**1**	**1**	**0**	**0**	**1**
Negative	**0**	**2**	**2**	**2**	**2**	**1**	**1**	**0**	**0**
No effect	**1**	**0**	**0**	**0**	**0**	**0**	**0**	**2**	**0**

Diversity: The relationship between diversity and environmental parameters was only investigated in two studies (Table 3). There are not enough clear trends to identify any concrete relationships between diversity and the environmental parameters, however the limited information so far suggests that diversity is negatively correlated with several environmental parameters (Dimiza et al. 2020; Oviedo et al. 2015). Diversity is a key indicator of marine ecosystem health (Tett et al. 2013) as it provides systems with increased resilience and adaptability to changes in the environment (McCann 2000). For phytoplankton in particular, increased taxonomic diversity has been positively correlated

with phytoplankton biomass (Otero et al. 2020). With increasing impacts associated with ocean warming and acidification, more studies should focus on species diversity as this will be an important element of ecosystem resilience under climate change.

Table 3. Relationship with environmental variables and coccolithophore diversity outlined in published two articles. Publications and their contributions to the matrix can be found in Table S14.

Relationship	Temp	Depth	PO_4	pH	CO^3_2	Salinity
Positive	**0**	**0**	**0**	**0**	**0**	**0**
Negative	**1**	**1**	**1**	**1**	**1**	**1**
No effect	**0**	**0**	**0**	**0**	**0**	**0**

Emiliania huxleyi: As the most common coccolithophore species in the Mediterranean, several articles included specific correlations between *E. huxleyi* abundance and environmental parameters (Table 4). Temperature shows a clear negative correlation with *E. huxleyi* abundance, and nitrate and phosphate show clear positive correlations. As *E. huxleyi* is the greatest contributor to species abundance, correlations between coccolithophore total abundance and environmental parameters are likely to reflect, to varying degrees, the environmental preferences of *E. huxleyi*. This is reflected in the correlations between total abundance and several environmental parameters such as temperature and salinity, which similarly show general negative correlations, and the positive relationship with nutrients (Table 1 and 4). The negative relationship with temperature and salinity and positive relationship with nutrients follows the west-east gradient of increasing temperature and salinity and decreasing nutrients, reflecting their preference for the western sub-basin.

Table 4. Relationship with environmental variables and *E. huxleyi* abundance outlined in five published articles. Publications and their contributions to the matrix can be found in Table S15.

Relationship	Temp	Depth	NO_3	PO_4	SiO_4	Salinity	O_2
Positive	**0**	**0**	**3**	**2**	**0**	**2**	**1**
Negative	**3**	**0**	**0**	**0**	**0**	**0**	**0**
No effect	**2**	**1**	**1**	**1**	**1**	**3**	**0**

3.10 Potential impacts of climate change on coccolithophores in the Mediterranean Sea

The impacts of climate change on phytoplankton communities will be diverse, with each taxonomic group and species responding differently (Seifert et al. 2020). There is a clear negative relationship between coccolithophore abundance and pH, suggesting coccolithophores may be negatively impacted by ocean acidification. This may be the result of disturbed proton homeostasis which is enhanced via the process of calcification (Kottmeier et al 2022). The negative correlation between total abundance and temperature, in particular for the most common species *E. huxleyi*, suggests that we may see Mediterranean wide reductions in total abundance under ocean warming. We may also see increases in abundance deeper in the photic zone as coccolithophores shifts to more favourable conditions. These shifts may be greater during warmer seasons. In general, however, this will differ by species as well as life cycle phase.

As heterococcolithophores and holococcolithophores have several opposing environmental preferences, we may see specific effects of climate change related to their life cycle phase. For instance, we may see reductions in heterococcolithophore abundance throughout all regions as this life stage is negatively correlated with temperature. Holococcolithophores however are positively correlated with temperature and therefore they may increase in abundance and expand their distribution. For holococcolithophores, they could increase their abundance in the western Mediterranean as temperatures in that region will increase under ocean warming. While the positive correlation between total abundance and pH (Table 1) suggests that ocean acidification may negatively affect coccolithophore total abundance, holococcolithophore abundance is negatively associated with pH, and therefore may not be as adversely affected by ocean acidification. The negative correlation between holococcolithophores and pH might be explained by the relatively small proton load generated in holococcolith production versus heterococcolithophore coccolith production (Kottmeier et al 2022).

3.11 Gaps in research

The MA generated for this study has shown that many species, including the ubiquitous *E. huxleyi*, are more abundant during the cooler seasons (fall and winter) of the western Mediterranean Sea when surface mixing is enhanced. However, the sampling effort to monitor these specific periods and regions are distinctly lower than in the eastern Mediterranean, as shown by both the systemic review and MA. A research focus on these cooler seasons will provide important information regarding the seasonality of coccolithophores across the Mediterranean Sea. Notable gaps in the literature, as well as the MA dataset, include the north coast of Africa, and this reflects a European bias of research. This coast spans large biogeographical boundaries and is composed of several major currents and gyres, therefore it is likely this region contains valuable material about coccolithophore communities and dynamics in the Mediterranean Sea.

Sampling between 100 - 200 m is underrepresented in all seasons, particularly in summer and autumn in the western and far eastern Mediterranean, and the Adriatic and Aegean Seas (Fig. S3A). While sampling between 100 and 200 m is not always possible, particularly in shallow coastal regions, coccolithophores are present at depth, particularly deep dwelling species such as *F. profunda*, and much of the knowledge of these deeper dwelling communities is minimal in the Mediterranean Sea due to the limited sampling at these depths.

Diversity is an understudied but highly important element of ecosystem health, and in coccolithophore research, this biological feature deserves more attention. In studies where species abundances are collected, diversity should also be addressed. This will provide important information regarding the resilience and adaptive potential of coccolithophore communities to a changing climate.

Further coccolithophore research efforts should aim to focus on these gaps in data to provide a more holistic picture of coccolithophores communities in the Mediterranean Sea. Specifically, cooler seasons, the north coast of Africa, deeper sampling and species diversity should be targeted in future research efforts.

3.12 Conclusions

- The Utermöhl method and ILM, the most utilised sampling and enumeration method in phytoplankton community studies, likely underestimates (between 5.9 – 83.7%) coccolithophore abundance and their contribution to the phytoplankton community. Phytoplankton studies should aim to employ a different method, such as PLM or SEM, to more accurately quantify coccolithophore abundances.
- The north coast of Africa remains a large gap in coccolithophore research, and collaborations between north African countries and European countries bordering the Mediterranean Sea should be fostered.
- The western Mediterranean, along with winter and spring, are underrepresented in coccolithophore research, and future research efforts should aim to focus in these areas.
- Diversity, a highly important measure of ecosystem resilience and health, requires more attention
- *Emiliania huxleyi* is the most abundant species in all regions of the Mediterranean Sea and shares several environmental relationships with total coccolithophore abundance
- Hetero- and holo-coccolithophores exhibit opposing spatial and temporal distribution, as well as opposing relationships to environmental parameters. This adds support to the hypothesis that the haplo-diplontic life cycle of coccolithophores allows them to expand their ecological niche
- Hetero and holo-coccolithophores have several opposing environmental preferences and therefore will likely respond differently to climate change stressors. For instance, ocean acidification may have a negative effect on total coccolithophore abundance, however holococcolithophores may respond positively to a drop in ocean pH. Additionally, ocean warming may negatively impact total coccolithophore abundance, in particular *E. huxleyi* abundance, however holococcolithophores may respond favourably to temperature increases and expand their distribution

CHAPTER 3

Nutritional response of a coccolithophore to changing pH and temperature

Abstract

Coccolithophores are a calcifying unicellular phytoplankton group that are at the base of the marine food web, and their lipid content provides a source of energy to consumers. Coccolithophores are vulnerable to ocean acidification and warming, therefore it is critical to establish the effects of climate change on these significant marine primary producers and determine potential consequences that these changes can have on their consumers. Here, we quantified the impact of changes in pH and temperature on the nutritional condition (lipid content, particulate organic carbon/nitrogen), growth rate, and morphology of the most abundant living coccolithophore species, *Emiliania huxleyi*. We used a regression type approach with nine pH levels (ranging from 7.66–8.44) and two temperatures (15°C and 20°C). Lipid production was greater under reduced pH, and growth rates were distinctly lower at 15°C than at 20°C. The production potential of lipids, which estimates the availability of lipids to consumers, increased under 20°C, but decreased under low pH. The results indicate that, while consumers will benefit energetically under ocean warming, this benefit will be mitigated by ocean acidification. The carbon to nitrogen ratio was higher at 20°C and low pH, indicating that the nutritional quality of coccolithophores for consumers will decline under climate change. The impact of low pH on the structural integrity of the coccosphere may also mean that coccolithophores are easier to digest for consumers. Many responses suggest cellular stress, indicating that increases in temperature and reductions in pH may have a negative impact on the ecophysiology of coccolithophores.

Chapter based on: Johnson, R., G. Langer, S. Rossi, I. Probert, M. Mammone, and P. Ziveri. 2022. Nutritional response of a coccolithophore to changing pH and temperature. Limnol. Oceanogr. **67**. doi:https://doi.org/10.1002/lno.12204

1. Introduction

Coccolithophores are unicellular calcifying phytoplankton found in all of the world's oceans. They influence seawater chemistry and the exchange of carbon dioxide between the atmosphere and the ocean via photosynthesis and the formation and dissolution of their calcium carbonate skeleton. An estimated 83% of the organic carbon flux to the seafloor is associated with their calcium carbonate ballast (Klaas and Archer 2002), establishing coccolithophores as major contributors to the carbon cycle in the oceans (Ziveri et al. 2007; Falkowski et al. 2008; Lefebvre et al. 2011).

Coccolithophores form part of the base of the food web and their nutritional quality, particularly in terms of their organic carbon to nitrogen ratio and lipid content, are important predictors of the nutritional condition for consumers at higher trophic levels (Pond and Harris 1996; Mitra and Flynn 2005; Schlüter et al. 2014). In phytoplankton, lipids (total and fatty acids) serve as structural molecules within cells and as energy storage units (Fuentes-Grünewald et al., 2012). These are key determinants of food quality, and, in turn, the health and functioning of marine ecosystems (Jin et al. 2020). Chlorophyll *a*, an indicator of photosynthetic capacity, contains a large amount of lipids, and, as such, increases in chlorophyll *a* are usually associated with an increase in lipids (Woodworth et al. 2015) as well as photosynthetic performance. These lipid macromolecules provide a source of energy to phytoplankton consumers higher on the trophic ladder (Broglio et al. 2003; Litzow 2006), and changes in the availability of essential fatty acids can have a significant impact on consumer productivity (Fraser et al. 1989; Breteler et al. 2005). Suspension feeders and zooplankton depend on primary producers as a food source (Sailley et al. 2013; El-Hady et al. 2016b), and food quality and availability is a major factor affecting reproduction and survival in these organisms (Gili and Coma, 1998; Broglio et al., 2003; Gori et al., 2013).

Any detrimental effects of climate change on phytoplankton physiology may have cascading effects on other components of the ecosystem (Chavez et al. 2010; Guinder and Molinero 2013). For instance, increased pCO_2 has been shown to effect trophic transfer efficiency between phytoplankton and their consumer, copepod *Acartia tonsa* (Cripps et al. 2016). Additionally, four species of phytoplankton grown under high CO_2 conditions (1000 ppm) showed reduced essential fatty acid content, and the copepods consuming

this plankton experienced reduced egg production, hatching success, and egg viability (Meyers et al. 2019). The diatom *Thalassiosira pseudonana* experienced reduced fatty acid content under elevated pCO_2, which translated to a ten-fold decrease in fatty acids for the consumer, copepod *A. tonsa*, including a decrease in somatic growth and egg production from 34 to 5 eggs female^{-1} day^{-1} (Rossoll et al. 2012). When considering such drastic impacts that changes in phytoplankton nutritional status can have on consumers, it is critical to establish the effects of climate change stressors on this significant marine phytoplankton, and the consequences that they may have on the food web (Rossi et al. 2019).

Emiliania huxleyi is one of the most abundant coccolithophores in the oceans and is responsible for giant seasonal algal blooms (Brown and Yoder 1994) that are visible from space (Holligan et al. 1993). Such blooms can provide a substantial food source to zooplankton grazers (Pond and Harris 1996). *Emiliania huxleyi* is known to produce stable lipid compounds, including alkenones, alkyl alkeonates, and alkene, which can be used as climatic proxies to evaluate the impacts of a changing climate (Bendle et al. 2005; Malinverno et al. 2008). *Emiliania huxleyi* has been studied extensively and found to be sensitive to ocean acidification conditions (Riebesell et al. 2000; Beaufort et al. 2011; Lefebvre et al. 2011; Schlüter et al. 2014). The most relevant climate change impacts for coccolithophores are ocean acidification and ocean warming.

Ocean acidification is the result of increasing atmospheric CO_2, which is absorbed by the ocean, resulting in an increase in $[H^+]$ and a decrease in ocean pH, as well as a decrease in the concentration of carbonate ions (Fabry et al. 2008; Doney et al. 2009). Global open ocean surface seawater pH is projected to decrease by approximately 0.3 units by 2100 under RCP 8.5 (business as usual scenario; IPCC, 2019). The reduction in seawater pH has been shown to impact *E. huxleyi* calcification (Riebesell et al. 2000; Lefebvre et al. 2011; Schlüter et al. 2014), morphology (Langer et al. 2009; Lefebvre et al. 2011), photosynthetic ability (Bach et al. 2013; Fukuda et al. 2014), and growth rate (Lefebvre et al. 2011; Bach et al. 2013; Schlüter et al. 2014).

Global sea surface temperature is expected to increase by approximately 3°C on average by the end of this century, though this will vary by region (RCP 8.5; IPCC, 2019). Ocean warming has been shown to impact coccolithophore growth (Schlüter et al. 2014; Rosas-

Navarro et al. 2016; Feng et al. 2017; Krumhardt et al. 2017), calcification (Rosas-Navarro et al. 2016; Feng et al. 2017; Krumhardt et al. 2017) and morphology (Rosas-Navarro et al. 2016). The combined impacts of ocean acidification and warming have also been shown to have an interactive effect on coccolithophore growth (Arnold et al. 2013; Sett et al. 2014; D'Amario et al. 2017a), morphology (Milner et al. 2016; D'Amario et al. 2017a), calcification (Schlüter et al. 2014; Sett et al. 2014) and photosynthesis (Sett et al. 2014).

While there has been some focus on the effects of climate change stressors on the quality of some primary producers as a food source (Klauschies et al. 2012; Guinder and Molinero 2013), there has been no published work that investigates how ocean acidification combined with ocean warming conditions will alter the quality and quantity (in terms of food availability) of coccolithophores as a source of nutrition for higher trophic levels. This study aims to fill this gap. We focus on *E. huxleyi* here due to its extensive use in previous studies, making this an ideal species for comparison. The hypothesis tested here is that reduced pH (in line with ocean acidification) and increased temperature (ocean warming) will likely affect the quality of coccolithophores as a food source (Guinder and Molinero 2013) by impacting their investment in stored energy (in the form of lipids). This is investigated here by measuring cellular lipid content (Pond and Harris 1996), as well as carbon and nitrogen ratios. We also explore the impact of pH and temperature on food quantity through a parameter known as production potential, which combines cell growth with cellular lipid content. Production potential translates cellular lipid production to community production and estimates the availability of lipids in a coccolithophore community (Gafar et al. 2018; Klintzsch et al. 2019). These points have rarely been addressed, particularly in a combined ocean acidification and warming scenario. In addition, we investigate the impacts of pH and temperature on important parameters related to coccolithophore nutritional quality, including growth rate, particulate organic and inorganic content, and coccosphere morphology (Table 1).

Table 1. Information on how each response variable relates to nutritional quantity or quality, and other parameters indicating fitness and cellular function for *E. huxleyi*. The response variables include: Lipids (pg cell^{-1}), POC (pg cell^{-1}), PIC (pg cell^{-1}), Chlorophyll *a* (pg cell^{-1}), growth rate (day^{-1}), Lipid production (pg cell^{-1} day^{-1}), POC production (pg cell^{-1} day^{-1}), PIC production (pg cell^{-1} day^{-1}), Chlorophyll *a* production (pg cell^{-1} day^{-1}), Production Potential - Lipids (ng), POC:N, PIC:N, PIC:POC, Lipid:POC (Cellular lipid content:Cellular POC content), coccosphere diameter (µm), coccolith distal shield length (µm), coccolith distal shield width (µm), inner circle diameter (µm), tube width (µm), collapsed coccosphere (%).

Response variable	Parameter relevance
Cellular quotas	
Lipid quota	High energy carbon source Increase indicates higher associated energy to catabolize (food quantity)
POC quota	Organically digestible carbon – comprised of both low and high energy (i.e. lipids) compounds
PIC quota	Increase might indicate lower food quality
Chlorophyll *a* quota	Increase can indicate higher capability of photosynthesis – effect on food quality uncertain
Production rates	
Growth rate	Main driver of food production (quantity)
Lipid production	Food quantity (energy) production Note that this is cellular level and less important for consumers (see also production potential)
POC production	Food quantity (see also production potential) Alone insufficient to indicate food quality
PIC production	Increase tends to lower food quality but ratios more informative
Chlorophyll *a* production	Effect on food quality/quantity uncertain
Production potential - Lipids	Best indication of food quantity for coccolithophore consumers Amount of lipids available to consumers after a given period of growth
Carbon ratios	
POC:N	High quality food (low ratio) i.e. less nitrogen Nitrogen is involved in the production of amino acids and proteins, including chlorophyll, and is essential for cellular function
PIC:N	High food quality (low ratio) PIC has no nutritional value but might hamper digestion
PIC:POC	High food quality (low ratio) i.e. less PIC
Lipid:POC	High food quality (high ratio) i.e. more lipids
Morphological characteristics	
Coccosphere diameter	Reduced size may mean the coccosphere is more easily digestible for non-selective grazers
Distal Shield length	General coccolith morphological parameter – differences indicate change in growth and/or calcification
Distal Shield Width	General coccolith morphological parameter – differences indicate change in growth and/or calcification

Inner Circle diameter	General coccolith morphological parameter – differences indicate change in growth and/or calcification
Tube width	General coccolith morphological parameter – differences indicate change in growth and/or calcification
Collapsed coccospheres	Weak coccospheres may mean cell contents are more readily digestible for selective grazers

2. Materials and methods

2.1 Culture medium preparation

Seawater collected from 3 km off the coast of Roscoff (Brittany, France) on the 3rd and 10th of June 2019 was mixed homogenously, pre-filtered using 0.7 µm nominal pore size glass fibre filters (Whatman GF/F) and 0.2 µm mixed cellulose ester membrane filters (Millipore), heated to 80°C for 10 minutes, and then cooled overnight. The seawater was enriched with 100 µmol L^{-1} nitrate, 6.25 µmol L^{-1} phosphate, trace metals and vitamins as in K/2 medium (Keller et al. 1987). The culture medium was then filter sterilized using 0.2 µm Fast Flow Polyethersulfone (PES) Express PLUS filter modules (Millipore).

Cultures of *Emiliania huxleyi* RCC 1832 (Western Mediterranean strain collected from latitude 39°10"N and longitude 5°35"E; Type A morphotype) from the Roscoff Culture Collection (www.roscoff-culture-collection.org) were initially grown for one week at a light intensity of 150 µmol m^{-2} s^{-1} in a 16/8 h light/dark cycle in culture cabinets set to either 15°C or 20°C. Using these initial temperature acclimated pre-cultures, acclimation cultures were inoculated with 500 cells/mL in culture flasks (300 mL) and held in experimental conditions (two temperatures: 15°C and 20°C, 9 pH levels targeted to approximately: 8.4, 8.3, 8.2, 8.1, 8.0, 7.9, 7.8, 7.7, 7.6, light regime as above) until cell concentrations reached between 50,000-100,000 cells/mL. For the experimental cultures, polycarbonate Nalgene bottles (2.95 L) completely filled with sterile culture medium with target pH levels (Refer to section 2.7) were then inoculated with either 500, 1000, or 2000 cells/mL from the corresponding acclimation culture, and incubated in the same temperature and light conditions as the acclimation cultures (without replication). Experimental cultures were sampled for the response variables once cell counts reached approximately 50,000-100,000 cells/mL. This so called dilute batch approach ensures a quasi-constant seawater carbonate chemistry (Langer et al. 2009).

As a western Mediterranean Sea strain of *E. huxleyi* was used here, the temperature levels were chosen to reflect current and future projected temperatures for this region. The optimum growth temperature for this strain is likely within the range of 22°C - 25°C based on other strains of *E. huxleyi* collected from the western Mediterranean Sea. The higher temperature of 20°C was chosen to ensure that thermal damage to lipids and proteins did not occur, and that the cultures did not crash, particularly as the combined, and possible synergistic, effect of temperature and pH was not known. This is particularly important when investigating the impact of multiple stressors, as reduced pH and increased temperature are known to have negative interactive effects on multiple physiological parameters for coccolithophores (Arnold et al. 2013; Sett et al. 2014; D'Amario et al. 2017a). In the Algerian Basin, where this culture originated from, recorded sea surface temperatures range from 14°C - 16°C in winter, 18°C – 18.4°C in spring (for 80% of the basin), 19.5°C – 19.9°C in autumn (for 50% of the basin), and 24.5°C – 24.9°C in summer (for 70% of the basin; Shaltout and Omstedt, 2014). Anticipating a 3°C warming of sea surface temperatures by 2100, 20°C is a useful temperature to investigate the potential impacts of ocean warming, as by 2100, average temperatures in the region that this strain of *E. huxleyi* was collected will be closer to 20°C for most of the year. A 5°C difference between temperatures was chosen to ensure a clear, observable effect (if there was one) of temperature on the response variables.

We utilised a large range of pH levels (ranging from 7.66 – 8.44) and two temperatures (15°C and 20°C) to create a response curve for the dependent variables over the two temperature levels. The lower end of the pH range is in line with, and exceeds, future predictions of ocean acidification over the next century, the middle range is in line with current ocean pH levels, and the upper range includes pre-industrial pH levels and above. A higher number of treatment levels for pH were used at the expense of replication and a generalised linear model (GLM) including linear and non-linear terms was used to analyse the data (Cottingham et al. 2005).

2.2 Growth rates

Cell counts were conducted using a Guava easyCyte HT flow cytometer (software guavaSoft 3.1.1 – detected via chlorophyll fluorescence) at the same time each day (after cell counts were estimated to be above 4000 cells/ml). Cells were suspended in the

Nalgene bottles to ensure cell concentrations were homogenous by inverting the bottle 5-10 times. Cells counts were conducted in duplicate (200 µl). The Nalgene bottle lids were covered in parafilm between each sampling to minimise gas exchange. Cell growth rates were determined using the equation *growth rate* = [Ln(D_f)-Ln(D_0)]/t where D_f is the final concentration, D_0 is the initial concentration and *t* is the time in days. At the end of the experiment, all samples were taken within 3 hours of conducting cell counts.

2.3 Lipids

For total lipid extraction, triplicate 0.15 L samples were filtered onto pre-combusted (8 h, 450ºC) GF/F Whatman glass-fibre filters, immediately frozen in liquid N_2 and then stored at -20°C until analysis. Lipids were extracted in chloroform:methanol (2:1) following Barnes and Blackstock (1973) (colorimetry). Samples were evaporated and sulfuric acid was added; the final reaction was performed using vanillin. Cholesterol was used as a standard, and measurements were read using a spectrophotometer (UV mini1240, Shimadzu). Lipid cellular quotas are reported as pg cell^{-1}. The production rate for lipids (pg cell^{-1} day^{-1}) was calculated as:

$$Lipid\ production = growth\ rate\ \times cellular\ lipid\ content\ pg\ cell^{-1}$$

Production potential is a parameter that extrapolates the cellular lipid production of a community of coccolithophores. This parameter assumes exponential growth and starts from a known cell density (1 cell). The corresponding lipid production of the community can be calculated using the growth rate (μ) and cellular lipid content (pg cell^{-1}) to determine the amount of lipids available to consumers after one week of growth (Gafar et al. 2018; Klintzsch et al. 2019). The following equation was used to calculate the production potential of lipids:

$$PP_{lipids} = N_0 \times e^{\mu \times t} \times \frac{m(lipids)}{cell}$$

Where PP_{lipids} is the production potential of lipids after 7 days, N_0 is the assumed cell density of the community (using a starting cell density of 1), *e* is the exponential growth factor, μ is the growth rate, *t* is the time in days (here we use 7 days), *m* (lipids) is the

cellular lipid content (pg cell^{-1}) of each experimental culture, and *cell* is the final cell concentration.

2.4 Particulate inorganic/organic carbon and nitrogen ratios

For the determination of total particulate carbon (TPC includes both inorganic and organic carbon; duplicates) and particulate organic carbon (POC; duplicates), 0.25 L of water was filtered onto pre-combusted (8 h, 450°C) 0.7 µm nominal pore size glass fibre filters (Whatman GF/F) and stored at -20°C. The filters for POC analysis were dried at 60°C for 24 h, then exposed to HCl vapours for 48 h to dissolve the calcite and convert all particulate inorganic carbon (PIC) to CO_2, leaving only POC to be measured (Rossi and Gili 2007). These filters were then re-dried at 60°C for 24 h. The analyses were performed with an elemental analyser (Elementar Vario Pyro Cube EA CNS; Elementar Analysensysteme GmbH, Hanau, Germany). To calculate PIC, which represents the calcite shell of the coccolithophore, POC was subtracted from TPC. PIC and POC (pg cell^{-1}) were calculated as well as C:N ratios (particulate inorganic or organic carbon:nitrogen).

Rates of production for particulate inorganic carbon (pg cell^{-1} day^{-1}) and particulate organic carbon (pg cell^{-1} day^{-1}) were calculated as:

$$PIC\ production = growth\ rate\ \times PIC\ content\ pg\ cell^{-1}$$

and

$$POC\ production = growth\ rate\ \times POC\ content\ pg\ cell^{-1}$$

The ratio between lipids (pg cell^{-1}) and POC (pg cell^{-1}) was used to explore the relationship between cellular lipids and POC content (Lipid:POC*100).

2.5 Chlorophyll *a*

To determine the chlorophyll *a* concentration, 3 x 100 mL replicates were filtered through GF/F pre-combusted glass fibre filters and stored at -20°C. Chlorophyll was extracted in 8 mL 90% acetone and left for 24 h covered with aluminium foil at +4˚C. Samples were then centrifuged for 15 minutes at 10,000 g and 4˚C, and then analysed using a

spectrophotometer (UV mini1240, Shimadzu). The absorbance was read at 630, 663, 750nm. Chlorophyll *a* concentration was calculated according to the spectrometric equations reported in Jeffrey and Humphrey (1975). Chlorophyll *a* cellular quotas are reported as pg cell^{-1}. The production rate for chlorophyll *a* (pg cell^{-1} day^{-1}) was calculated as:

$$Chlorophyll\ a\ production = growth\ rate\ \times cellular\ chlorophyll\ a\ content\ pg\ cell^{-1}$$

2.6 Morphology

Malformations in coccolith formation might lead to unstable coccospheres, which in turn may lead to impaired protection (Monteiro et al. 2016; Kottmeier et al. 2022). To investigate potential malformation, 1 ml samples for scanning electron microscopy were filtered onto 0.8 µm pore size polycarbonate filters (Millipore) and dried in a drying cabinet at 55°C for 24 – 48 h. A desktop Phenom G2 pro scanning electron microscope was used to take images for subsequent analysis (using ImageJ software) of coccosphere diameter (along the longest axis) and coccolith morphological features (distal shield length, distal shield width, inner circle diameter, tube width; SFig. 1).

To determine whether the integrity of the coccolithophore cell was maintained, cell counts of collapsed (4 or more interlocked coccoliths; Fig. 1) and intact coccospheres (Fig. 1) were conducted using a scanning electron microscope (Merlin, Zeiss). The results are reported as a percentage of the total cell count.

2.7 Carbonate system

The pH of experimental cultures was adjusted through calculated additions of either HCl or NaOH. Samples for total alkalinity (TA) were collected from the filtrate of the TPC/POC filters and stored at 4°C for a maximum of 7 days before processing. The TA was measured in duplicates via titration with Metrohm 877 Titrino plus (software tiBase 1.1) at 25°C using Dickson Certified Standards (Batch #100).

Samples for pH were collected using unfiltered experimental medium and stored in gas tight bottles, without air bubbles. All samples were measured spectrophotometrically in

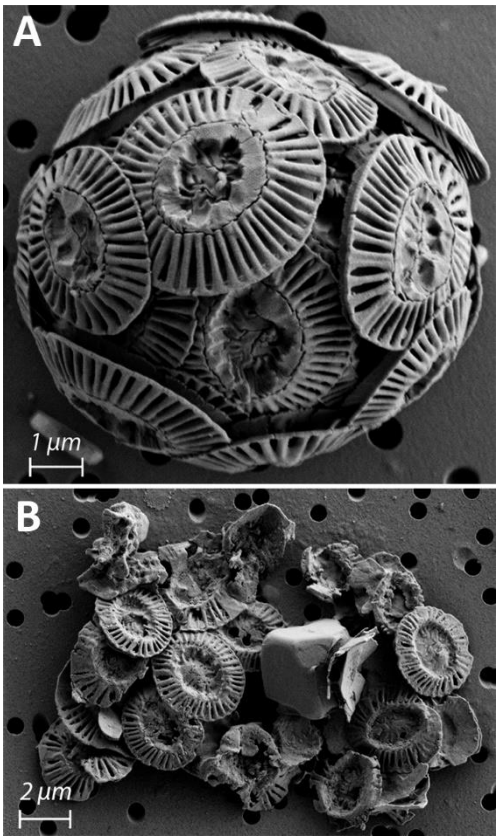

Fig. 1. (A) An intact coccosphere and (**B)** a collapsed coccosphere of *Emiliania huxleyi*. Images taken using a desktop Phenom G2 pro scanning electron microscope.

triplicate within 3 hours of collection in the method of Liu et al. (2011) at 25°C (PerkinElmner UV/VIS Lambda 365).

The carbonate system was calculated with TA and pH using CO2SYS (Pierrot et al. 2011). The TA and pH were measured at 25°C and used to calculate DIC. Following this, TA and DIC were used to calculate the system at the target temperature (either 15°C or 20°C; Table S1).

2.8 Statistics

Data were analysed using a GLM (Nelder and Wedderburn, 1972; Zuur et al., 2009a). Each model was run using a gamma distribution with log link (continuous response variable *Y* that has a positive values > 0; (Zuur et al. 2009b), and chosen following a backward selection criteria and based on the lowest Akaike Information Criterion (AIC) score (Aho et al. 2014). In the model, temperature was selected as the fixed factor and pH as the co-variate, including their interaction and possible non-linear responses (with

a maximum nonlinearity of a cubic term - pH^3). Significant variables ($P < 0.05$) for the chosen models were included. Only significant terms were kept in the model except in instances where models including non-significant variables had lower AIC scores. The following linear and non-linear predictors were tested in the GLM:

1. Response variable ~ Temperature + pH + pH^2 + pH^3 + temperature*pH

The model was run with 100 iterations and Wald chi-squared statistics and confidence intervals were used. For the covariance matrix, the robust estimate was used which provides a more conservative model. A Type III analysis was chosen as it holds all the variables constant relative to each other. Data from each sample was averaged to create a single data point for each treatment. Assumptions of normality were satisfied for each dependent variable (Shapiro-Wilk Test). Outliers were defined as any data point outside of the following ranges – 3^{rd} quartile + 1.5*interquartile range or 1^{st} quartile – 1.5*interquartile range, and were removed from the dataset for the statistical analysis. The reference category is included for comparison against the other predictors. The models were run using IBM SPSS v22. The GLM results are reported in detail in the supplementary material (Table S2).

3. Results

3.1 Cellular quotas

The average cellular lipid content for both temperatures across all pH levels was 44.75 pg $cell^{-1}$ (SD = 9.25; range = 29.42 – 61.34 pg $cell^{-1}$). The average cellular lipid content at 15°C (47.66 pg $cell^{-1}$; SD = 6.61) was slightly higher than at 20°C (41.85 pg $cell^{-1}$; SD = 10.92). Cellular lipid content increased as pH decreased and this trend appeared to be similar across both temperatures (Fig. 2A). The quadratic term for pH was significant in the selected model (Table S2). Temperature, pH, and their interaction were significant predictors for cellular lipid content (Table S2).

Cellular POC content (pg $cell^{-1}$) followed a parabolic trend at 20°C (Fig. 2B), with a higher average of 27.50 pg $cell^{-1}$ (SD = 7.25) than at 15°C (25.64 pg $cell^{-1}$; SD = 3.10).

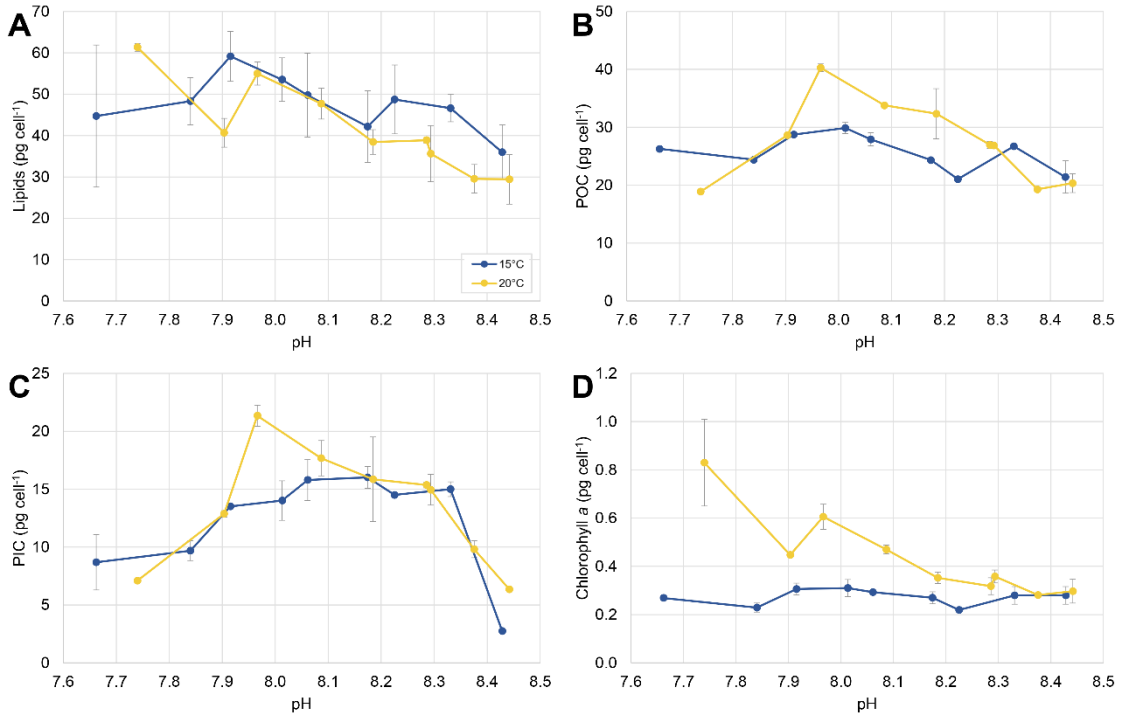

Fig. 2. Cellular quotas in response to pH levels and temperatures. (**A**) Lipids (pg cell^{-1}), (**B**) POC (pg cell^{-1}), (**C**) PIC (pg cell^{-1}), and (**D**) Chlorophyll *a* (pg cell^{-1}). Error bars indicate data standard deviation within each treatment, not between replicates.

At 15°C, cellular POC content had a linear trend, which slightly decreased toward higher pH (Fig. 2B). The selected model includes a significant quadratic term for pH (Table S2). Temperature was not a significant predictor yet is still included in the model (lowest AIC value).

Cellular PIC content (pg cell^{-1}) followed a similar parabolic trend at both temperatures (Fig. 2C). Average cellular PIC content at 20°C (13.48 pg cell^{-1}; SD = 4.95) was slightly higher than at 20°C (12.22 pg cell^{-1}; SD = 4.38), both similar to the overall average of 12.85 pg cell^{-1} (SD = 4.58). The highest cellular PIC content was 21.34 pg cell^{-1} at 20°C and pH 7.97 (Fig. 2C). PIC content responded in a cubic relationship with pH, which was the only significant predictor (Table S2). Temperature and the interaction between temperature and pH are still included in the model (lowest AIC score).

Cellular chlorophyll *a* content followed distinctly different trends at 15°C and 20°C, and was stable across the pH range at 15°C, while 20°C exhibited a clear negative trend from low to high pH (Fig. 2D). Average cellular chlorophyll *a* content at 15°C was 0.27 pg cell^{-1} (SD = 0.03) and 0.44 pg cell^{-1} (SD = 0.18) at 20°C. A linear term for pH was

significant in the selected model. Temperature, pH, and their interaction were significant predictors for cellular chlorophyll *a* content (Table S2).

3.2 Production rates

The average growth rate (day^{-1}) over both temperatures was 0.74 (day^{-1}; SD=0.13) with a range of 0.55 – 0.98 (day^{-1}). The growth rate at 20°C was distinctly higher with an average rate of 0.86 (day^{-1}; SD = 0.07; range = 0.75 – 0.98) compared with 0.62 (day^{-1}; SD = 0.04; range = 0.55 – 0.67) at 15°C. Growth rate showed no clear trend from low to high pH (Fig. 3A). The growth rate at 20°C was overall higher than at 15°C, with a visible trend of decreasing growth rate with decreasing pH. Temperature, pH (quadratic), and the interaction between temperature and pH were significant predictors of the growth rate response for *E. huxleyi* (Table S2).

The average lipid production for both temperatures was 32.68 pg $cell^{-1}$ day^{-1} (SD = 6.95; range = 20.19 – 46.31 pg $cell^{-1}$ day^{-1}), with each temperature group having similar average values (15°C = 29.86 and 20°C = 35.49 pg $cell^{-1}$ day^{-1}; Table S2). Lipid production increased as pH decreased, however this response varied between temperatures, particularly at the lower range of pH (Fig. 3B). Temperature and pH (quadratic) were significant predictors for lipid production in *E. huxleyi* (Table S2).

The average POC production at 20°C (23.62 pg $cell^{-1}$ day^{-1}; SD = 6.34) was higher than at 15°C (16.01 pg $cell^{-1}$ day^{-1}; SD = 2.44). There was a bell curve trend at 20°C, with a higher POC production within the middle of the pH range, while there was no clear trend at 15°C (Fig. 3C). The selected model included a significant quadratic term for pH, which was the only significant predictor of POC production for *E. huxleyi* (Table S2).

The average PIC production (pg $cell^{-1}$ day^{-1}) was higher at 20°C (11.57 pg $cell^{-1}$ day^{-1}; SD = 4.29) than at 15°C (7.71 pg $cell^{-1}$ day^{-1}; SD = 2.94), with a bell curve trend across the pH range, which was more pronounced at the higher temperature (Fig. 3D). The selected model included a significant cubic term for pH, and temperature and pH were both significant predictors for POC production (Table S2).

Chlorophyll *a* production (pg cell^{-1} day^{-1}) remained stable across all pH levels at 15°C (average = 0.15 pg cell^{-1}; SD = 0.04), while it gradually declined from low to high pH at 20°C (average = 0.32 pg cell^{-1}; SD = 0.15; Fig. 3E). Temperature and pH (quadratic) were significant predictors for chlorophyll a production (Table S2).

The production potential of lipids showed a clear difference between 15°C and 20°C, and there was a trend of increasing production potential as pH increased, but only at 20°C (Fig. 3F). This largely followed the pattern of growth rate (Fig. 3A), showing that growth rate was the major factor driving the production potential for *E. huxleyi* here. Similar to

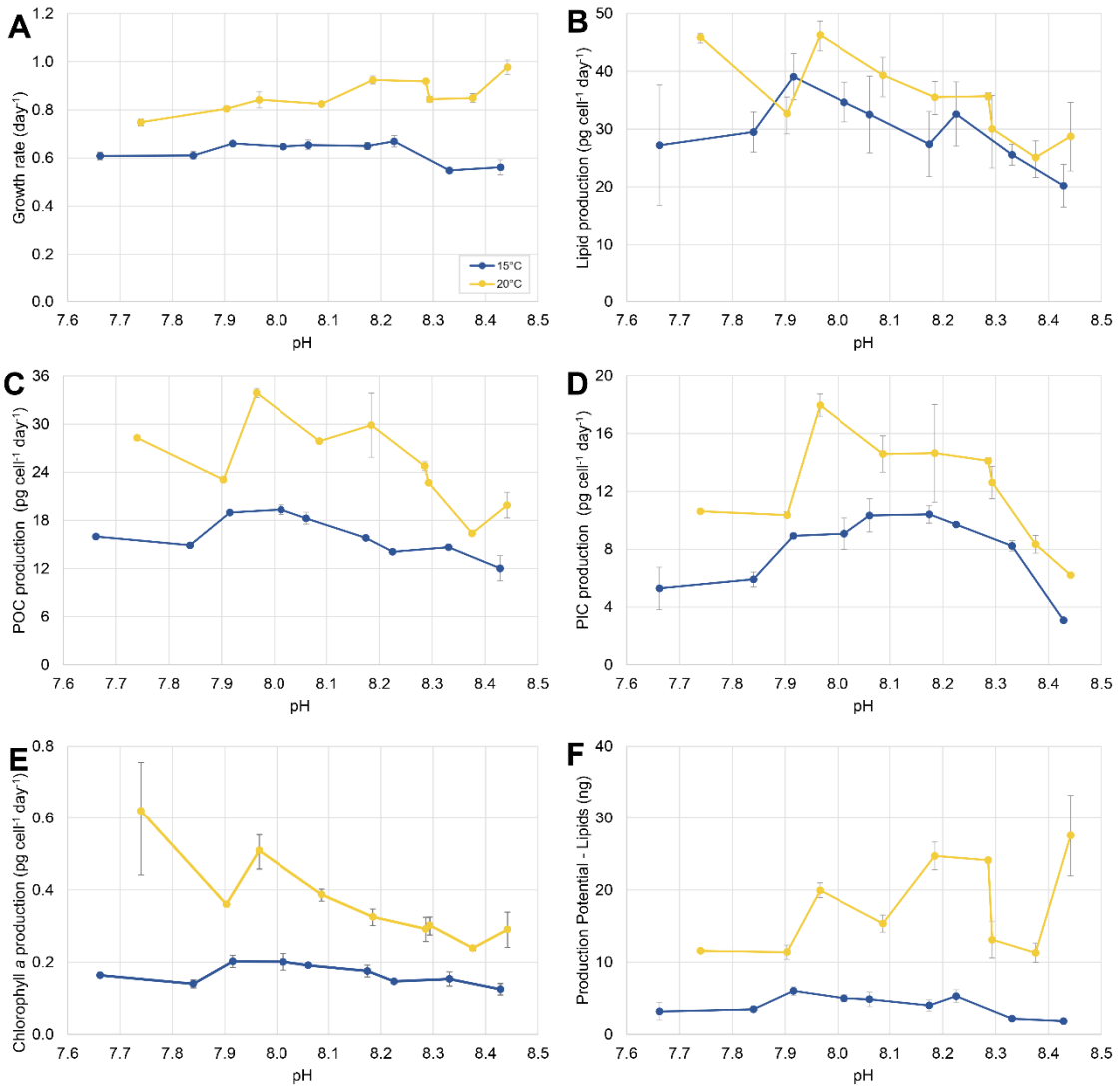

Fig. 3. Production rates in response to pH levels and temperatures. (**A**) growth rate (day^{-1}), (**B**) Lipid production (pg cell^{-1} day^{-1}), (**C**) POC production (pg cell^{-1} day^{-1}), (**D**) PIC production (pg cell^{-1} day^{-1}), (**E**) Chlorophyll *a* production (pg cell^{-1} day^{-1}), and (**F**) Production Potential – lipids (ng). Error bars indicate data standard deviation within each treatment, not between replicates.

growth rate, the quadratic term for pH was significant in the selected model. Temperature, pH, and their interaction were significant predictors of the production potential of lipids (Table S2).

3.2 Carbon ratios

Mean POC:N ratio for all treatments was 6.28 (range 4.9 – 9.2). POC:N ratios were higher at 20°C (6.74; SD = 1.35) than at 15°C (6.74; SD = 1.35). Both temperatures followed a similar trend of decreasing POC:N with increasing pH (Fig. 4A). This trend was stronger at 20°C. The cubic term for pH was significant in the selected model and pH, temperature, and their interaction, were significant predictors of the POC:N response in *E. huxleyi* (Table S2).

Similar to POC:N, PIC:N ratios were higher at 20°C ($\overline{x}$ = 3.77; SD = 0.52) than at 15°C ($\overline{x}$ = 3.15; SD = 0.55), however this difference was not as distinct. At low pH, PIC:N showed similar values for both temperatures, however at approximately pH 8.0 and above, the response curves started to diverge, with PIC:N values higher at 20°C than at 15°C (Fig. 4B). Temperature and the interaction between temperature and pH were significant predictors of the PIC:N response of *E. huxleyi* (Table S2). For PIC:N, pH in still included in the selected model and was minorly significant ($p < 0.1$).

The average PIC:POC ratio was similar across both temperatures (15°C = 0.49, SD = 0.14; 20°C = 0.48, SD = 0.09), however PIC:POC had a parabolic relationship with pH, with the highest ratios in the middle range of the pH range, where it reached a maximum of 0.69 at pH 8.23 before declining toward low and high pH (Fig. 4C). Both temperatures followed this relationship curve, and the results of the GLM indicate that pH (cubic term) was a significant predictor of the PIC:POC response of *E. huxleyi* (Table S2).

The Lipid:POC ratio overall was higher at 15°C (average = 1.87, SD = 0.21) than at 20°C (average = 1.6, SD = 0.63), except at pH 7.74, where the ratio distinctly increases at 20°C (Fig. 4D). Temperature was a significant predictor for Lipid:POC (Table S2).

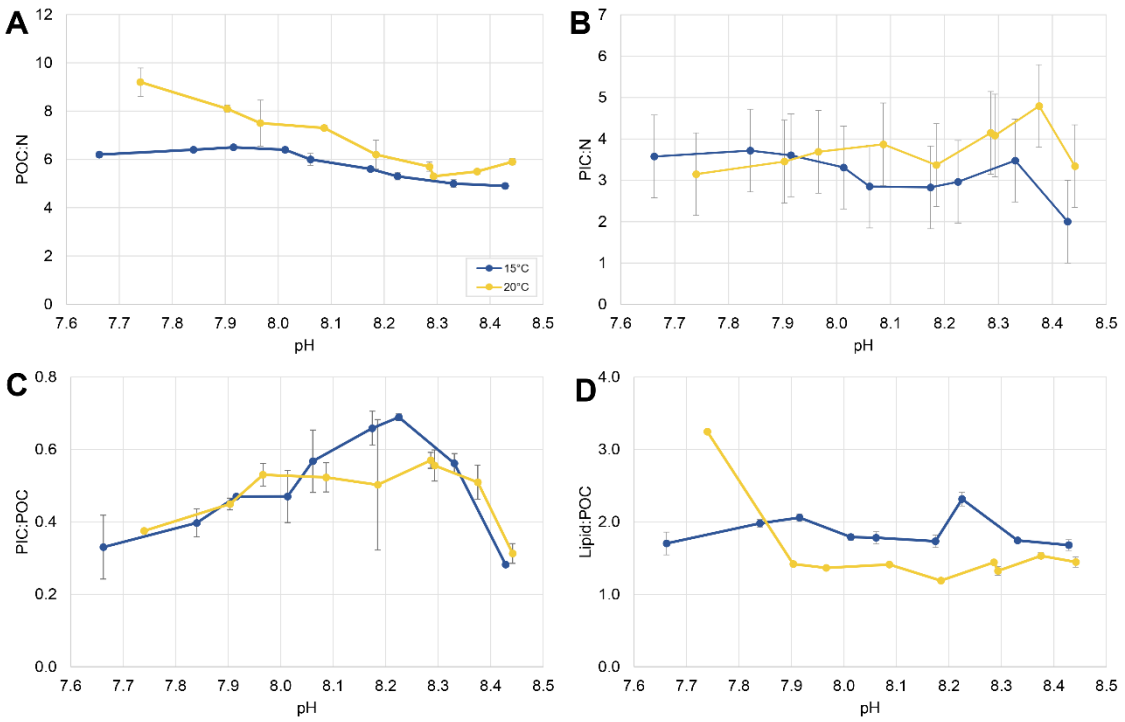

Fig. 4. Carbon ratios in response to pH levels and temperatures. (**A**) Particulate organic carbon:Nitrogen ratio (POC:N), (**B**) Particulate inorganic carbon:Nitrogen ratio (PIC:N) (**C**) Particulate organic carbon:Particulate inorganic carbon (PIC:POC), and (**D**) Cellular Lipid quota:Cellular particulate organic carbon quota (Lipid:POC). Error bars indicate data standard deviation within each treatment, not between replicates.

3.3 Morphology

Coccosphere diameter (µm) followed similar trends for both temperatures in the higher pH range, however at low pH, coccosphere diameter was smaller at 20°C (Fig. 5A). The selected model includes a significant quadratic term for pH and temperature, and their interaction was significant predictors of coccosphere diameter for *E. huxleyi* (Table S2).

Distal shield length (µm) was greater at 15°C than 20°C. It also exhibited slight bell curve response at 15°C (Fig. 5B). A quadratic term for pH was significant in the selected model and temperature and pH were significant predictors for distal shield length (Table S2). Distal shield width (µm) followed a similar pattern to distal shield length, however here only temperature and the interaction between temperature and pH were significant predictors (Fig.

5C; Table S2). Although pH was a non-significant term for the model, it was retained as it is included in the interaction. It may be the effect of high variability associated with distal shield length that may explain why pH was not a significant predictor here.

Average inner circle diameter (µm) remained largely stable across pH at both temperatures, however was highly variable. Inner circle diameter had no significant predictors (Fig. 5D; Table S2). Coccolith tube width increased with increasing pH for both temperatures, and pH was a significant predictor (Fig. 5E; Table S2).

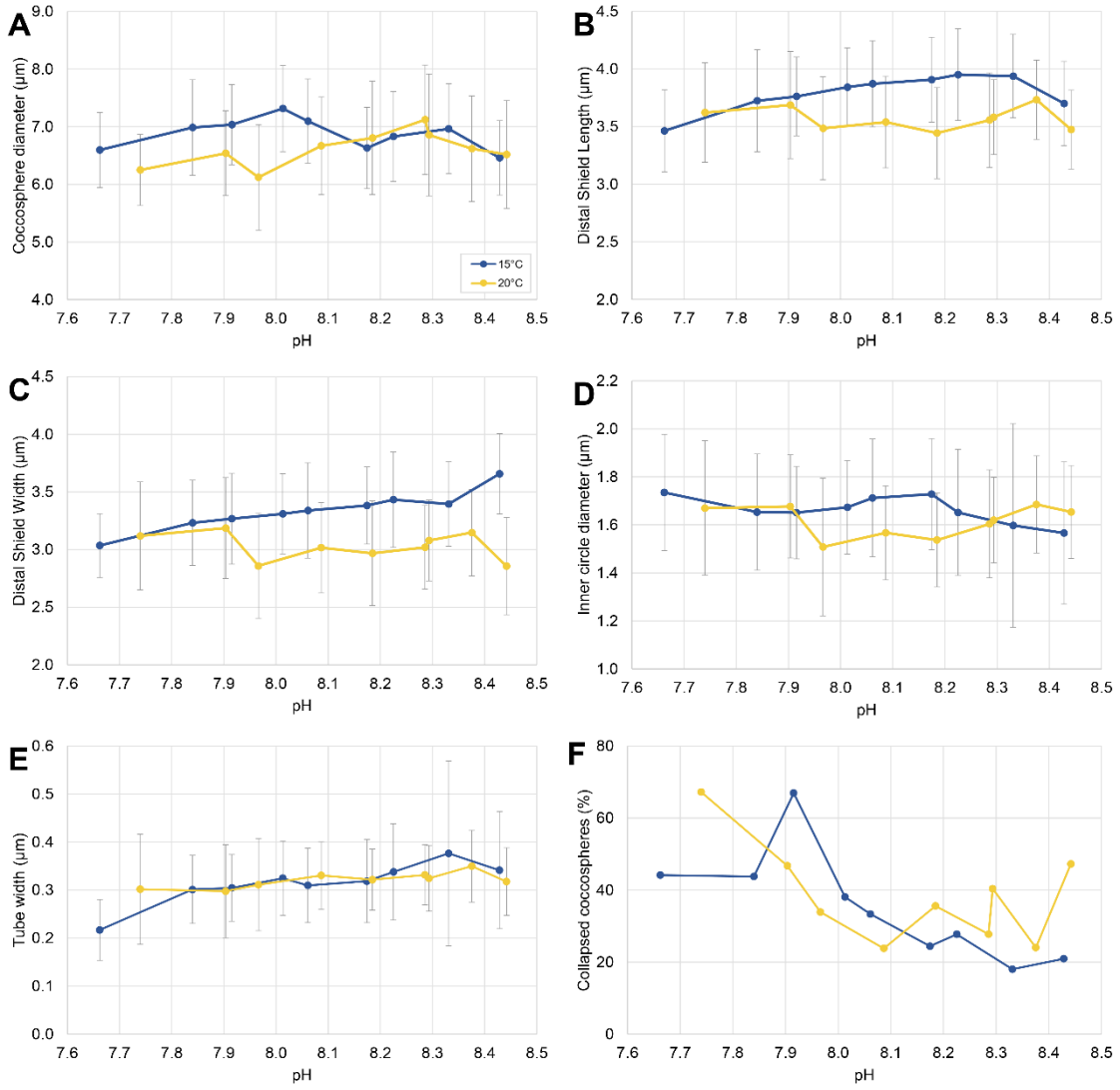

Fig. 5. Coccosphere morphological characteristics in response to pH levels and temperatures. (**A**) Coccosphere diameter (µm), (**B**) Distal Shield Length (µm), (**C**) Distal Shield Width (µm), (**D**) Inner circle diameter (µm), (**E**) Tube width (µm), and (**F**) Collapsed coccospheres (%). Error bars indicate data standard deviation within each treatment, not between replicates (not applicable for collapsed coccospheres as percentage was calculated from a single filter).

Overall, collapsed coccospheres (%) made up approximately 37% of the cells. This differed with temperature, with an average of 35% at 15°C, and 39% at 20°C. A cubic term for pH was significant in the selected model and is the only significant predictor for collapsed coccospheres (Table S2), with the percentage of collapsed coccospheres increasing toward the lower pH range (Fig. 5F). Temperature and the interaction between temperature and pH were not significant, however they were included in the selected model (lowest AIC score).

4. Discussion

4.1 Consumer impacts

4.1.1 Food quantity

In this study we show that temperature is an important predictor for the production potential of lipids, indicating increases in lipid availability under ocean warming. This increase will likely be energetically favourable for consumers. pH is also a significant predictor of the production potential of lipids, and the results suggest that this increase in availability will be mitigated by ocean acidification. The availability of lipids in coccolithophores for their consumers is important when investigating potential energy transfer between trophic levels and to understand how this may change under ocean acidification and warming. The production potential of lipids is strongly influenced by the growth rate, and it is distinctly higher under the warmer temperature (Fig. 3F). The decrease in production potential under low pH was mostly related to the impact of pH on growth rate, rather than the impact of pH on cellular lipid quota, which increased under lower pH (Fig. 2A). At any rate, this suggests that consumers may be positively affected by the increased quantity of available cells, and in warmer conditions, there will be greater lipid availability, which is likely to be energetically beneficial for coccolithophore consumers.

4.1.2 Food quality

The interaction between pH and temperature was an important driver for POC:N which was higher at low pH (~7.9 – 7.7) and 20°C (Fig. 4A), indicating that the availability of nitrogen for coccolithophore consumers will be reduced under ocean acidification and warming. Nitrogen is essential for cellular function and is involved in the production of macromolecules, such as proteins or amino acids, including chlorophyll (Riegman et al. 2000). A higher POC:N suggests a lower quality food as a higher ratio of carbon can indicate nitrogen limitation. The mean POC:N ratio across all treatments is similar to the Redfield ratio of 6.3 (Martiny et al. 2014), however this average differs with temperature. The range of POC:N is similar to what is expected in natural populations of phytoplankton (Geider and La Roche 2002) and experimental work with coccolithophores (Fiorini et al. 2010). Contrary to our results, there was no significant effect of elevated pCO_2 (760 µatm corresponding to pH 7.81) on POC:N for *E. huxleyi* strain (AC472) from the South Pacific (Fiorini et al. 2010). However, the difference in pH levels was not as pronounced as they are in this experiment. For instance, an increase in POC:N was also reported under elevated pCO_2 for *E. huxleyi* using a wider range of pH levels (6.8-8.3; Iglesias-Rodriguez et al., 2008 - morphotype R). Under ocean acidification conditions, the reduced nitrogen availability might have negative impacts on micrograzers that have issues with nitrogen limitation.

Lipid content is also an important indicator of the nutritional quality of coccolithophores for secondary consumers (Pond and Harris 1996), as also seen for diatoms in particular, and plankton in general (Rossoll et al. 2012; Meyers et al. 2019). While we see greater availability of *E. huxleyi* in terms of the production potential of lipids (Fig. 3F), given that the availability of nitrogen under both ocean acidification and warming will be reduced (Fig. 4A), the quality of coccolithophores as a food source will likely be negatively impacted (Conde-Porcuna et al. 2002; Mitra and Flynn 2005; Iglesias-Rodriguez et al. 2008). However, as cellular lipid content is predicted to either be unaffected (Fiorini et al. 2010) or increase under ocean acidification conditions, as is the case here (Fig. 2A), the nutritional impacts on coccolithophore consumers will likely be varied. From the perspective of lipid:POC, however, food quality appears unaltered (Kharbush et al. 2020) except under the lowest pH at 20°C, which is exceptionally high (Fig. 4D). This increase might indicate a crossed threshold under ocean acidification

conditions at 20°C involving a carbon storage strategy related to extreme stress which has been previously reported for both micro- and macro-algae (Kuwata et al. 1993; Fuentes-Grünewald et al. 2012; Prabhu et al. 2019).

4.1.3 Coccosphere integrity and PIC:POC ratio

Coccoliths can diminish the nutritional value of coccolithophores in three ways. Firstly, through mechanical protection, making it more difficult for grazers to access the protoplast (Haunost et al. 2021). Secondly, through the need to counteract the increase in the pH of guts or food vacuoles due to carbonate dissolution (Harvey et al. 2015). Thirdly, through reduction in the percentage of digestible material (Haunost et al. 2021). While the first point hinges on morphology, the last two points centre on the amount of calcite relative to organic material. To assess the first point, we focus on the percentage of collapsed coccospheres, which indicates reduced mechanical stability (Jaya et al. 2016), and to assess the last two points, we analysed the PIC:POC ratio.

The percentage of collapsed coccospheres increased with decreasing pH at both temperatures, indicating reduced structural integrity of the coccosphere (Fig. 5F). Copepods do not need to destroy the coccosphere as they have to in the case of the diatom frustule (Langer et al. 2007a; Jansen 2008), however dinoflagellates need to penetrate the coccosphere to digest the cell contents, and then egest the remaining indigestible calcium carbonate (Haunost et al. 2021). This means that if the interlocking between coccoliths is reduced, dinoflagellates may be able to more readily access coccolithophore cell contents, potentially aiding in digestion.

The PIC:POC ratio was unaffected by temperature, however we observed a distinct bell-curve in response to pH under both temperatures (Fig. 2H). Although PIC:POC response patterns are strain specific (Langer et al. 2009; Rosas-Navarro et al. 2016), a meta-analysis suggests a negative correlation between PIC:POC and pH (Meyer and Riebesell 2015). Taken together, the PIC:POC ratio and the coccosphere integrity response suggest that ocean acidification will make it easier for grazers to digest coccolithophores and access cell contents. Therefore, macrograzers such as copepods will likely benefit from the higher percentage of digestible material, and less so from both the reduced structural integrity of the coccosphere and the potentially negligible gut pH change (Harris 1994;

Nejstgaard et al. 1997; Langer et al. 2007b; White et al. 2018; Mayers et al. 2020). Micrograzers such as dinoflagellates will likely benefit from all three aspects of coccolith-related nutritional value change (Harvey et al. 2015; Jaya et al. 2016; Haunost et al. 2021).

4.2 Individual response

4.2.1 Physiological rates

The response to ocean acidification conditions in terms of physiological rates generally shows high inter- and intra-species variability (Langer et al. 2009, Hoppe et al. 2011). After initial uncertainty as to the interpretation of this variability, the work of L. Bach and co-authors has produced a plausible and now widely accepted interpretation using substrate-inhibitor concept (Bach et al. 2011, 2013, 2015; Paul and Bach 2020) which states that with increasing substrate (CO_2) concentration, POC production increases up to the point when the inhibitory effect of increasing H+ concentration then causes a decrease in POC production (ca. pH 8 in our data, Fig. 3C). In these studies, it was shown that the response of coccolithophores to seawater carbonate chemistry changes is best thought of as a bell curve, with different strains featuring different optima. In our case, we can see the bell curve in the PIC and POC production, while other rates display only part of the full bell curve (Fig 4A, B, F, E). Growth rate for instance, shows a somewhat atypical increase at 20°C (Iglesias-Rodriguez et al. 2008; Langer et al. 2009 - morphotypes A, B, R; Mackey et al. 2015), however the dependence of growth rate on temperature has been seen in several coccolithophorid strains (Buitenhuis et al. 2008; Fielding 2013). The response patterns over the pH range tested here do not appear to be related to morphotype or other easily identifiable strain features (see also Krumhardt et al. 2017).

4.2.2 Morphological parameters as PIC production proxy

The decrease in PIC production does not correlate with changes in any morphological characteristics at both temperatures or across the pH range. Coccosphere size and coccolith weight (usually correlated with coccolith size) have been proposed as proxies for PIC production (Beaufort et al. 2011; Bach et al. 2012; Gibbs et al. 2013). In contrast to our study, Rosas-Navarro et al. (2016) described a positive correlation of coccolith size and PIC production in three *E. huxleyi* strains. This discrepancy could stem from strain

specificity but seems unrelated to morphotype because all strains considered here are morphotype A. A widespread strain specificity in the relationship between coccolith size and PIC production would make the application of this proxy difficult.

4.3 Future ramifications

Future coccolithophore consumers will likely benefit from an energetic standpoint, due to the increase in lipid availability under ocean warming, however this increase will be mitigated by ocean acidification. As this experiment was done under nutrient replete exponential growth, concurrent changes in nutrient availability may alter these impacts on the nutritional condition of *E. huxleyi* (Müller et al. 2017). From a functional point of view, a higher POC:N will not contribute as much to cell function for consumers, and as such, the capacity of coccolithophores to provide a healthy food source may be reduced. The nutritional quality of coccolithophores as indicated by POC:N, lipid:POC and PIC:POC will likely have varied impacts, depending on an organism's specific requirements. For example, organisms with limited nutrient supplies could be affected by increases in POC:N under future conditions, while organisms that have difficulty digesting calcite may benefit from decreases in PIC:POC under ocean acidification.

Phytoplankton biomass is predicted to have a varied response to ocean acidification and warming, and this response will largely vary depending on latitude and taxonomic group (Seifert et al. 2020). Due to the calcifying nature of coccolithophores, they will have the additional stress of reduced seawater pH (Guinder and Molinero 2013), affecting their ability to calcify (Riebesell et al. 2000; Engel et al. 2005; Hoppe et al. 2011; Lefebvre et al. 2011; Schlüter et al. 2014) and potentially pushing them closer to a stress response than non-calcifying plankton. Although adaptation to ocean acidification and warming has been shown to occur relatively rapidly in *E. huxleyi* (1 year for PIC and POC to return to present-day levels; growth 16% higher than non-adapted controls after 1 year; Schlüter et al., 2014), for the coccolithophore *Gephyrocapsa oceanica*, growth rate (after an initial increase), POC production, and nitrogen production all decreased over 2000 generations (approximately 1400 days) under high CO_2 conditions, indicating that resilience to ocean acidification conditions can reduce over time (Jin and Gao 2016). In another experiment, *E. huxleyi* cells adjusted their chlorophyll content more rapidly than other coccolithophore species (Lewis et al. 1984), potentially as an adaptive photosynthetic trait

to changing ocean conditions (Feng et al. 2008). This suggests that the ability to adapt to ocean acidification conditions will likely vary depending on the species and physiological parameter in question.

We may see future shifts in *E. huxleyi* ranges as they shift to warmer areas where they achieve a more favourable growth rate (Neukermans et al. 2018), and this may further affect other organisms that rely on coccolithophores as a food source. Despite inter- and intra-species variability in response patterns (Langer et al. 2006, 2009), our results suggest that combined low pH and an increased temperature has the potential to increase coccolithophore lipid standing stock, but decrease food quality, as inferred from an increased POC:N ratio.

The short-term experiment presented here provides us with important information about the immediate response of coccolithophores to changes in temperature and pH, and this can be decisive in field scenarios, particularly in cases where populations are not given the opportunity to adapt. Further work investigating the long-term impact of ocean acidification and warming on the nutritional content (in terms of both quality and quantity) of coccolithophores, a globally important phytoplankton at the base of the marine food web, will be a key part of understanding the impacts of climate change on ocean trophic dynamics.

CHAPTER 4

Shelled pteropod abundance and distribution across the Mediterranean Sea during spring

Abstract

Thecosome pteropods are a dominant group of calcifying pelagic molluscs and an important component of the food web. In this study, we characterise spring pteropod distribution throughout the Mediterranean Sea, an understudied region for this common group of marine calcifying organisms. This semi-enclosed sea is rapidly changing under climatic and anthropogenic forcings. The presence of surface water biogeochemical gradients from the Atlantic Ocean/Gibraltar Strait to the Eastern Mediterranean Sea allowed us to investigate pteropod distribution and their ecological preferences. In the ultra-oligotrophic Eastern Mediterranean Sea, we found the mean upper 200 m pteropod standing stock of 2.13 ind. m^{-3} was approximately 5x greater than the Western basin (mean 0.42 ind. m^{-3}). Where standing stocks were high, pteropods appeared largely in the same family grouping belonging to Limacinidae. Temperature, O_2 concentration, salinity, and aragonite saturation (Ω_{ar}) explain 96% of the observed variations in the community structure at the time of sampling, suggesting that pteropods might show a preference for environmental conditions with a lower energetic physiological demand. We also document that pteropods and planktonic foraminifera have an opposite geographical distribution in the Mediterranean Sea. Our findings indicate that in specific pelagic ultra-oligotrophic conditions, such as the Eastern Mediterranean Sea, different feeding strategies could play an important role in regulating calcifying zooplankton distribution.

Chapter based on: Johnson, R., C. Manno, and P. Ziveri. 2023. Shelled pteropod abundance and distribution across the Mediterranean Sea during spring. Prog. Oceanogr. **210**: 102930. doi:https://doi.org/10.1016/j.pocean.2022.102930.

1. Introduction

The Mediterranean region is undergoing rapid changes as a result of climatic and non-climatic forcings (Cramer et al. 2018; MedECC 2020) and is experiencing warming at a rate that exceeds global trends, with atmospheric temperatures rising as much as 20% faster than the global average (Lazzari et al. 2013; Lionello and Scarascia 2018). Sea surface pH is projected to decrease in line with the global average (approximately 0.3 to 0.4 units by 2100) (Geri et al. 2014; Flecha et al. 2015; Kapsenberg et al. 2017), or to exceed the global rate of decline (Gemayel et al., 2015; Hassoun et al., in review). Within this scenario, it is essential to improve our knowledge of how Mediterranean marine ecosystems might respond to ocean conditions under climate change and ocean acidification.

Ocean acidification is a direct consequence of the surface ocean uptake of carbon dioxide from the atmosphere, resulting in a reduction of seawater pH, carbonate ion concentrations, and carbonate saturation state (Caldeira and Wickett, 2003; Gattuso et al., 2015). Calcifying zooplankton, such as pteropods and foraminifera, are sensitive to changes in seawater carbonate chemistry as they biomineralise their $CaCO_3$ exoskeleton (Bednaršek et al. 2016, 2019; Davis et al. 2017; Kuroyanagi et al. 2021). Pteropods in particular are known for their sensitivity to ocean acidification (e.g. Bednaršek et al., 2019; Bednaršek et al., 2016; Comeau et al., 2012; Lischka et al., 2011; Maas et al., 2017; Manno et al., 2012), mainly due to their aragonite shell, which is a more soluble form of calcium carbonate compared to other mineral forms such as calcite (Mucci et al. 1989). As there are notorious difficulties associated with maintaining pteropods in captivity through a full life cycle (Howes et al. 2014; Thabet et al. 2015), field observations are fundamental to improve the current knowledge on their vulnerability to climate change and to provide key data on their ecological preferences.

Thecosome pteropods are shelled holoplanktic molluscs found in all major world oceans (Lalli and Gilmer 1989; Peijnenburg et al. 2020). These pelagic snails are passive feeders, utilising large mucous webs to collect food particles (Lalli and Gilmer 1989). Pteropods play an important role in both the trophic system and biogeochemical cycling (Bednaršek et al., 2012; Buitenhuis et al., 2019; Manno et al., 2010, 2019), linking phytoplankton and larger pelagic predators, such as carnivorous zooplankton, cephalopods (Lalli and

Gilmer 1989; Fabry 1989), fish (Armstrong et al., 2008; Sturdevant et al., 2012), marine birds (Karnovsky et al., 2008) as well as other gymnosomes (Seibel and Dierssen, 2003).

Pteropods make up 1 - 6.6% of the total zooplankton community in the Mediterranean Sea (Fernández de Puelles et al. 2007; Mazzocchi et al. 2011; Granata et al. 2020), yet there are few studies within this region that focus solely on detailed pteropod community distribution (e.g. Howes, 2015; Manno et al., 2019) and those that do are limited to restricted geographical and/or coastal regions. Further, many published studies addressing the entire zooplankton community (Batistić et al. 2004; Fernández de Puelles et al. 2007; Mazzocchi et al. 2011), or those that include both pteropods and other non-calcifying taxa (Andersen et al. 1998; Tarling et al. 2001), focus on the direct comparison of few target pteropod species only, and do not include seawater carbonate chemistry data. The thesis manuscript of Rampal (1975) was the first study investigating pteropod distribution and ecology across the Mediterranean Sea, combining samples collected with different methods and within different seasons and regions. More recently, Bednaršek et al. (2012), Buitenhuis et al. (2013), and Buitenhuis et al. (2019) estimated the global distribution of pteropods and their importance as $CaCO_3$ producers by merging a large number of existing and diverse datasets collected globally, as well as in several Mediterranean regions (Bednaršek et al., 2012). To our knowledge, there is no published peer reviewed study on pteropod abundance and distribution across the whole Mediterranean basin, covering relatively large biogeochemical gradients and using a consistent sampling and processing methodology.

We explore shelled pteropod ecological preferences by investigating their distribution across the Mediterranean Sea at a large spatial scale, spanning the east-west environmental gradient from the Atlantic surface water influx in the Gibraltar Strait, to the Levantine basin in the Eastern Mediterranean Sea, and to the North-western Mediterranean Sea during the spring season. We also compare our results with a previous study by Mallo et al. (2017) which presented the distribution of planktic foraminifera collected during the same research cruise and in the same sampling nets as the pteropods of this study. Planktic foraminifera are calcifying single-celled protists with a calcite shell, and together with shelled pteropods, constitute the main marine calcifying zooplankton groups. They generally reside in the upper 100 m of the water column (Kemle-von Mücke and Oberhänsli 1999; Lessa et al. 2020) and feed on bacteria,

phytoplankton, and small zooplankton using their many, thin pseudopodia which extend out from apertures in their test (Anderson et al. 1979). Investigating the relationship between pteropods and foraminifera is important as the forecasted change in carbonate chemistry, due to increasing surface ocean uptake of atmospheric CO_2 and ocean acidification, has been shown to trigger ecosystem shifts due to altered competition between calcareous species (Kroeker et al. 2013a). The direct comparison of these two major groups of calcifying zooplankton allows us to improve our understanding of their ecological niches and their sensitivities to environmental change.

2. Materials and methods

Samples were collected from the Mediterranean Sea during the MedSeA research cruise on R/V Angeles Alvariño from May 2nd to June 3rd, 2013 (Fig. 1; Ziveri and Grelaud, 2015). The sampling covered the majority of the Mediterranean Sea sub-basins (Fig. 1) and was part of the European project "Mediterranean Sea Acidification in a changing climate - MedSeA". The main aim of the research cruise was to characterise the Mediterranean Sea biogeochemistry at the basin scale, focussing on the marine $CaCO_3$ system, and to investigate target calcifying organisms due to their known vulnerability to increasing CO_2 conditions (Kroeker et al. 2013a; Busch et al. 2014; Goyet et al. 2015; Ziveri and Grelaud 2015; Fox et al. 2020).

2.1 Study Region

The Mediterranean Sea has distinct biogeochemical regions (Reygondeau et al. 2017), with the sill system of the Strait of Sicily connecting the Eastern and Western sub-basins (Rohling et al. 2009). It's anti-estuarine circulation is characterised by surface Atlantic waters entering the Western basin through the Strait of Gibraltar, and by a net evaporation, that results in eastward increases in sea surface temperature, salinity, and alkalinity (Schneider et al. 2007; Rohling et al. 2009; Fedele et al. 2022). In general, the Western basin has higher concentrations and production of surface phosphate and nitrate compared to the Eastern basin. The Eastern basin is characterised by ultra-oligotrophic surface water conditions,

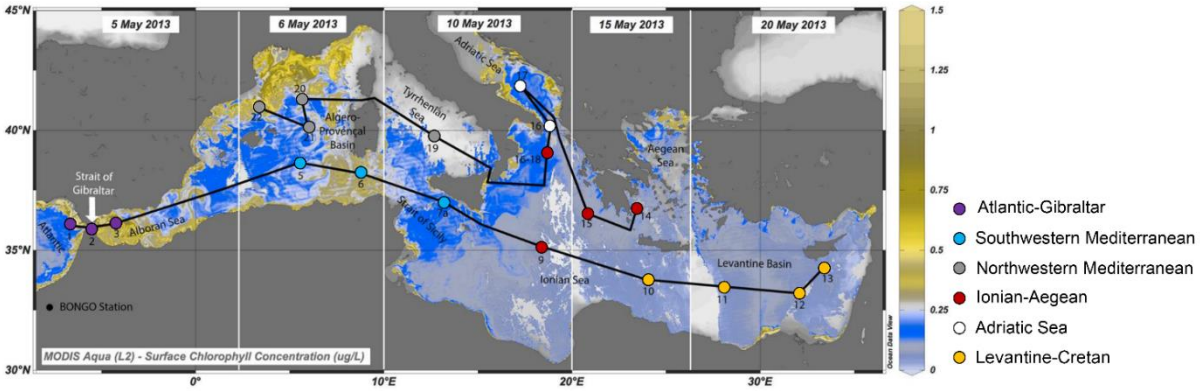

Figure 1. Location map of sampled stations are indicated by dots. The numbers represent the station codes. Research cruise Leg 1: stations 1 to 13, Leg 2: stations 14 to 22. The colour scale corresponds to the satellite-derived surface chlorophyll *a* concentration (in µg/l), retrieved from *MODIS Aqua (L2)* (NASA OB.DAAC 2018), closest day to the start of each new sector, as indicated by each date. Stations: **1** – Atlantic; **2** – Strait of Gibraltar; **3** – Alboran Sea; **5** – Southern Alguero-Balear; **6** – Strait of Sardinia; **7a** – Strait of Sicily; **9** – Ionian Sea; **10** – Southern Crete; **11** – Eastern basin; **12** – Nile Delta; **13** – Lebanon; **14** – Antikythera Strait; **15** – Eastern Ionian Sea; **16** – Otronto Strait; **17** – Adriatic Sea; **"16-18"** – Between Otronto Strait and Central Ionian; **19** – Tyrrhenian Sea; **20** – Northern Alguero-Balear; **21** - Central Alguero-Balear; **22** – Catalano-Balear (Schlitzer, Reiner, Ocean Data View, odv.awi.de, 2021). Coloured points at each station correspond to different biogeochemical regions (Reygondeau et al. 2017).

including phosphorus limitation (Krom et al., 1991) and deep chlorophyll maxima. The Atlantic-Gibraltar region connects the Mediterranean Sea with the Atlantic Ocean through the Strait of Gibraltar (Fig. 1), which is comprised of cooler, less saline waters and relatively higher levels of chlorophyll *a* due to the influx of water from the Atlantic and Alboran gyre dynamics (Oguz et al. 2014). The northwest Mediterranean region combines the Central and Northern Alguero-Balear basin and Tyrrhenian Sea, and is comprised of warmer and more saline modified Atlantic surface waters compared to the Atlantic-Gibraltar region. The southwest Mediterranean, made up of the Southern Alguero-Balear basin and the shallow Strait of Sicily, is comprised of modified Atlantic surface water moving eastward along the weakening Algerian current (Rohling et al. 2009), resulting in a lower chlorophyll *a* content than other regions in the Western basin, as well as warmer and more saline waters. The Ionian-Adriatic waters in the Eastern Mediterranean basin are 3-4°C warmer here than the southwest Mediterranean and are distinctly ultra-oligotrophic. The eastern Mediterranean regions, including the Levantine and Cretan basins, remain ultra-oligotrophic throughout, with waters gradually increasing in temperature and salinity moving further east. The Adriatic Sea stands apart and is characterized by cooler surface waters than the southern Mediterranean Sea and has a

higher chlorophyll *a* content. It is connected to the eastern Mediterranean through the Strait of Otranto into the Ionian Sea.

2.2 Hydrological and chemical collection analyses

Temperature, salinity, oxygen and fluorescence (proxy for phytoplankton biomass and therefore food availability) for the upper 200 m of the plankton tow stations were obtained from the corresponding conductivity-temperature-depth (CTD) stations using an ITS-90 and an oxygen sensor SBE 43. The overall accuracy for temperature was ± 0.001ºC and ± 0.0003 for salinity. Oxygen concentrations were measured using Winkler iodometric titration (Hansen 1999) with a Mettler-Toledo with a Platinum ring redox electrode, with an overall accuracy of ± 1.5 µmol kg-1. Samples for phosphate (PO_4) and nitrate (NO_3) were filtered using a Whatman glass fibre filter (0.7 µm) after collection, then stored at -20°C. The final nutrient concentrations were obtained using a Bran+Luebbe3 AutoAnalyzer (detection limits were 0.01 and 0.02 µM for PO_4 and NO_3 respectively; see Grasshoff and Kremling, 1999 and D'Amario et al., 2017 for a detailed methodology of the nutrient analysis). Methods for the analysis of water chemistry (based on collected samples for total alkalinity and dissolved inorganic carbon) have been described in Goyet et al. (2015) and Gemayel et al. (2015). Ocean chemistry data were input into the software CO2sys v2.1 (van Heuven et al. 2009) for carbonate system calculation of pH_{Total}, aragonite saturation (Ω_{ar}) and [CO_3^{2-}] using dissolved inorganic carbon (DIC) and total alkalinity (TA) and applying the equilibrium constants of Mehrbach et al. (1973) refitted by Dickson and Millero (1987). Satellite-derived surface chlorophyll *a* concentration during the sampling period was obtained from Moderate Resolution Imaging Spectroradiometer (MODIS) Aqua L2. We used these data to illustrate the Mediterranean-wide surface distribution of primary production (NASA OB.DAAC, 2018; Fig. 1).

2.3 Pteropod sample collection and analyses

Oblique plankton tow sampling for this pteropod study was conducted using BONGO nets (mesh size 150 µm, 40 cm diameter), integrating the upper 200 m water depth. The net mesh size in this study targets the majority of the pteropod community in the upper 200 m of the water column (Bednaršek et al. 2012a), including different life stages

(Howes et al. 2014) and therefore allowed for the quantification of most of the pteropod community standing stock. Based on a study investigating the global distribution of pteropods, which utilised a very large dataset (25939 data points) that included 41 scientific studies (Bednaršek et al. 2012a), it was found that most of the species live in the photic zone. In the Mediterranean Sea specifically, Bednaršek et al. (2012) showed that pteropod abundance from depths deeper than 200 m is one order of magnitude lower (mean 0.07 ± 0.89 ind. m^{-3}) compared to the upper 200 m community (mean 0.98 ± 2.77 ind. m^{-3}). Using the dataset in Bednaršek et al. (2012), we calculated that our sampling allows us to characterise approximately 93% of the total pteropod abundance (Table S1 and Fig. S1). However, a small number of species with deeper distribution might be underestimated in this study and this limitation is considered (see below).

The plankton towing was performed while the vessel was moving at approximately 1 nautical knot. A flow meter attached to the ring of the net was used to determine the volume filtered through the net. Please refer to Appendix Table 1 for information pertaining to the date, time, location, environmental parameters and water volume per plankton sample. From these samples, pteropod standing stocks were determined for each station. Plankton samples were preserved on board in a 4% formaldehyde solution that was buffered with hexamethylenetetramine at pH 8.2 and were stored in 500 ml polycarbonate bottles at 4ºC in the dark. The pH of all samples was measured at the beginning, middle, and end of the storing period to ensure that the state of the pteropod shells were not affected by the preservation technique. The samples were processed within one month of collection. Pteropod standing stocks were determined for each station and species were identified and counted using a Leica z16 APO binocular light microscope. Standing stocks were calculated as absolute abundance (ind. m^{-3}) and integrated abundance 0-200 m (ind. m^2; Table A2). Here, findings are reported as ind. m^{-3} (unless for the purpose of comparison with other studies). We identified four target families (Limacinidae, Heliconoididae [both in the limacinid super family Limacinoidea], Cavoliniidae and Cresidae) and seven species (*Heliconoides inflatus, Limacina trochiformis, Limacina bulimoides, Cavolina inflexa, Creseis acicula, Creseis conica* and *Styliola subula*). The online plankton portal (www.planktonportal.org) was used to aid in the identification of pteropods to species level.

Limacina bulimoides, L. trochiformis, C. acicula and *C. conica* are classified as surface and subsurface species (Rampal, 1975). *Heliconoides inflatus* and *S. subula* can be found at depths larger than 200 m and are classified as mesopelagic by Rampal (1975), however recent studies show that *H. inflatus* primarily occurs in the upper water column (Schiebel et al. 2002; Juranek et al. 2003; Batistić et al. 2004; Granata et al. 2020) while *S. subula* is more abundant below 150 m (Andersen et al. 1998). *Cavolina inflexa* is classified by Rampal (1975) as a bathypelagic species with a distribution extending below 1000 m, and this preference for deeper water has been corroborated by more recent studies in the Ligurian Sea (Sardou et al. 1996; Tarling et al. 2001; Granata et al. 2020). Due to the strong diel and seasonal variations in the depth distribution habitat of some species (Rampal 1975; Andersen et al. 1998; Tarling et al. 2001), we do not incorporate *S. subula* and *C. inflexa* into our statistical analyses of species distribution to discuss their ecological preferences. This conservative methodological approach is to prevent any artefact related to species depth preferences versus sampling depth.

2.4 Statistical methods

Heliconoides inflatus, L. trochiformis, L. bulimoides, C. acicula and *C. conica* were investigated in relation to the environmental conditions at the time of sampling. All environmental parameters used in the analyses were averaged from 5 – 200 m. A parsimonious Canonical Correspondence Analysis (CCA) was used to explore the species environmental preferences using the standing stock data. It should be noted that due to the high collinearity among several environmental variables (Fig. S2), the variability of the coefficients could be overestimated (Alves et al., 2017). However, to prevent bias to individual parameters, we have included all parameters in the statistical analysis to widen our power of explanation and to provide as much information as possible about the relationship of species with all the measured environmental variables.

To investigate species groupings across all stations, a K-means cluster analysis was conducted until all species significantly contributed to the cluster formation (ANOVA; < $p = 0.5$; standing stock values standardised between -3 to 3; 10 iterations). The CCA and correlation matrix were analysed using R version 3.6.0 (R Core Team, 2020) and the K-means cluster analysis was performed using IBM SPSS v23. To run the environmental

parsimonious CCA, the functions *cca* and *ordistep* from the "vegan" package were used for the CCA and the permutation test, respectively (Oksanen et al. 2019).

3. Results and Discussion

3.1 Mediterranean Sea pteropod distribution

In our Mediterranean basin-wide study, we found the mean standing stock was 1.27 ± 1.62 (SD) ind. m^{-3} (Table S2) which was approximately five times greater in the Eastern basin (2.13 ind. m^{-3}; SD = 0.4 ind. m^{-3}) compared to the Western basin (0.42 ind. m^{-3}; SD = 2.0 ind. m^{-3}). Mean pteropod standing stocks are comparable to reported records in studies investigating pteropod communities in different Mediterranean Sea regions (e.g. Ligurian Sea, Balearic Sea, Adriatic Sea, Tyrrhenian Sea; Batistić et al., 2004; Fernández de Puelles et al., 2007; Howes et al., 2015, Fernández de Puelles et al., 2007; Manno et al., 2019; Table 1). However, all the previous investigations mentioned here (Table 1) differed in sampling methodology (including different net sizes and sampling depths), in sampling seasons and in oceanographic settings (mainly from coastal systems rather than open sea), making a direct comparison between the studies and regions difficult.

The highest standing stock was recorded in the Otranto Straight (station 16) toward the southern end of the Adriatic Sea with 5.21 ind. m^{-3}/1041.04 ind. m^2 (Table S2, Fig. 2). High pteropod abundances have previously been reported in the Adriatic Sea (2412 ind. m^2 0-50m; Batistić et al., 2004; Table 1). The lowest standing stock of 0.02 ind. m^{-3} was at the Catalan-Balearic Station (station 22) off the coast of Spain (Table S2, Fig. 2). A long-term zooplankton study reported average pteropod abundances of 5.9 ind. m^{-3} in the Balearic Sea, however this was for a coastal site with a relatively shallow water depth of 78 – 200 m (Fernández de Puelles et al., 2007; Table 1). Coastal systems are complex and highly dynamic, and likely not representative of the open sea where the samples from this study were collected. A low standing stock was also recorded in the Strait of Sicily (0.11 ind. m^2), however a very high density (120 ind. m^{-3}) has been previously noted (Mazzocchi et al. 1997). In terms of biogeochemical regions (as identified by Reygondeau et al., 2017, Fig. 1), the Ionian-Aegean region had the highest average abundance in the Eastern basin (3.05 ind. m^{-3}; SD = 1.98 ind. m^{-3}), followed by the Adriatic Sea (2.74 ind.

m^{-3}; SD = 3.49 ind. m^{-3}), which also has the greatest variance between stations, and then the Levantine-Cretan basins (0.90 ind. m^{-3}; SD = 0.83 ind. m^{-3}). A large range in abundance has previously been noted in the Adriatic Sea (Batistić et al., 2004; Table 1).

The Western basin had consistently lower standing stocks when compared to the Eastern basin, with an average of 0.63 ind. m^{-3} (SD = 0.49 ind. m^{-3}) in the Atlantic-Gibraltar region, 0.25 ind. m^{-3} (SD = 0.19 ind. m^{-3}) in the south western Mediterranean, and 0.51 ind. m^{-3} (SD = 0.47 ind. m^{-3}) in the north western Mediterranean (Fig. 2). Similar average abundances were recorded in the Tyrrhenian Sea (*C. acicula* – 1.48 ind. m^{-3}; *C. conica* – 1.11 ind. m^{-3}; *H. inflatus* – 1.03 ind. m^{-3}; *L. trochiformis* – 0.64 ind. m^{-3}; *L. bulimoides* – 0.33 ind. m^{-3}), albeit in shallower waters (73 – 185 m; Manno et al., 2019; Table 1).

The super family Limacinoidea made up 76.4% of the total pteropod abundance. Limacinidae was the most abundant family (47.0%), which dominated the eastern part of the Mediterranean Sea, followed by Heliconoididae (29.4%), Creseidae (15.4 %) and then Cavoliniidae (6.8%). Specimens within the target families that were unidentifiable to species level made up 1.4% of the total abundance. A previous study based on pteropod distribution is the seminal work of Rampal (1975) who performed a comparative analysis of abundances within the different Mediterranean sectors. Unfortunately, the heterogeneity of the presented studies (no standardized sampling strategy; samples collected using different methods) limited the quantitative approach of this work and the results are not presented in terms of pteropod concentration. Howes et al. (2015) is the only study investigating pteropod abundance in the Mediterranean Sea from a time-series over a long-term scale (1957-2003).

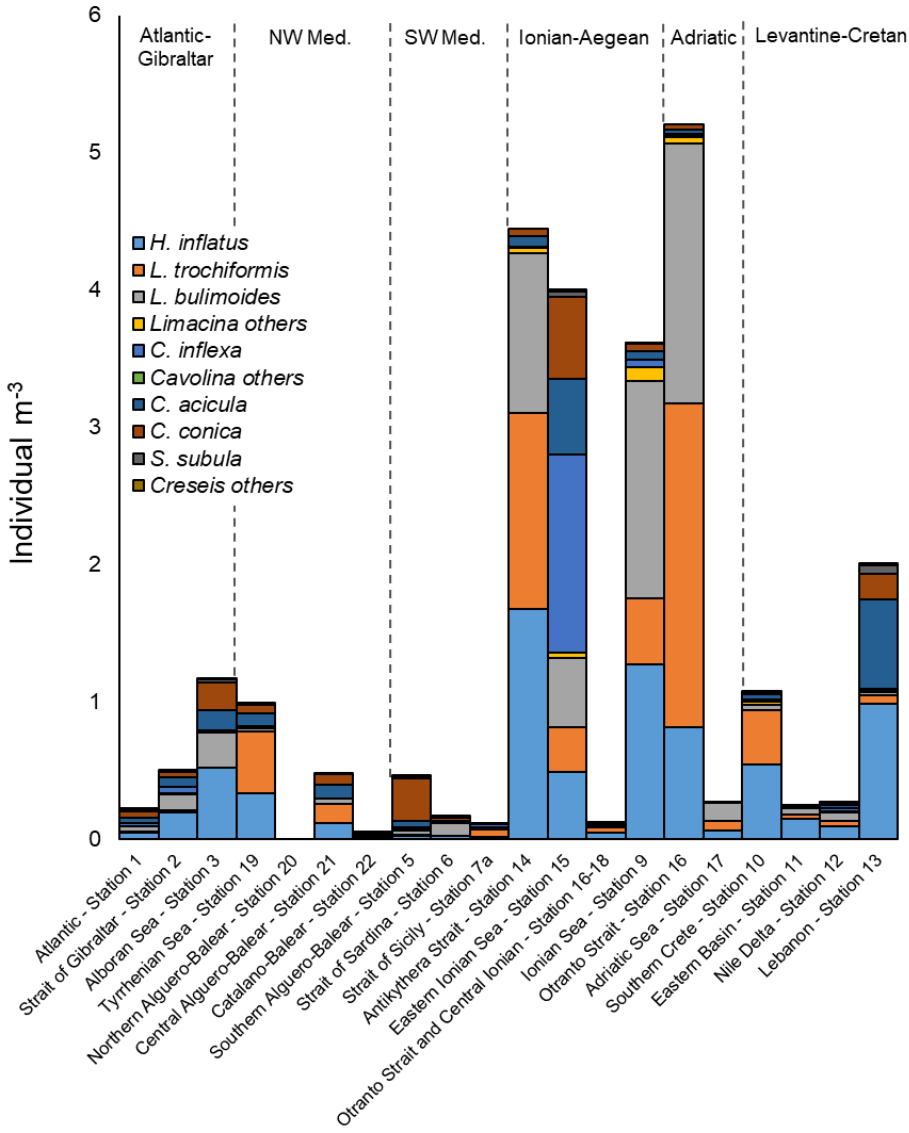

Figure 2. Pteropod standing stocks from stations 1-22 from the western to the eastern Mediterranean Sea. Stations are organized according to their respective biogeochemical region: Atlantic Gibraltar; North-western Mediterranean; South-western Mediterranean; Ionian-Aegean; Adriatic; Levantine-Cretan.

This study is solely focused on a shallow water coastal site of the Ligurian Sea (water depth approximately 80 m), and contrary to our results, Limacinidae was the least abundant family, which the authors attributed to a sampling bias. In our study, *H. inflatus* was the most abundant species in the Mediterranean Sea (29.4%) and recorded at all stations, followed by *L. bulimoides* (23.8%) and *L. trochiformis* (23.2%). *H. inflatus* has previously been reported as the most common species in specific regions in the Mediterranean Sea (Batistić et al., 2004 – Southern Adriatic Sea; Granata et al., 2020 - Ligurian Sea). Species belonging to the super family Limacinodea, included *H. inflatus*, *L. bulimoides* and *L. trochiformis*, and followed a similar distribution pattern with high

standing stocks in the Ionian Sea (station 9) and the Antikythera Strait (station 14) and the Otranto Strait (station 16), while there were lower standing stocks in the southwest Mediterranean. *C. inflexa* (6.8%), *C. acicula* (7.7%) and *C. conica* (6.8%) all presented the highest standing stocks in the Eastern Ionian Sea (station 15), while *S. subula* (0.63%) was most abundant at the easternmost station of the Levantine basin (Station 13; Table S2). Howes et al. (2015), indicated that the dominant species in each family were *C. acicula* and *H. inflatus* (previously *Limacina inflata*), corroborating our overall findings.

A global study showed that pteropod biomass generally peak in the spring in both hemispheres (Bednaršek et al. 2012a), suggesting that total pteropod community abundances reported here may be at their peak. This seasonal pattern has also been reported from a long-term (1994 – 2003) zooplankton time-series study in the Balearic Sea, where pteropod abundance was highest during late spring (Fernández de Puelles et al. 2007). In addition, in a coastal region of the Ligurian Sea, a distinct Mediterranean biogeochemical region (Reygondeau et al. 2017), Howes et al. (2015) observed a species-specific seasonal pattern, with blooms for Limacinid pteropods in both the spring and early autumn, while Cresidae bloomed during summer and winter, suggesting that different species groups could experience different peaks throughout the year. In contrast, an inter-comparison of long-term zooplankton studies in the Mediterranean Sea shows that peaks in abundance during spring may not be uniform across the region, and that overall, late summer to autumn experience the highest annual maxima (Berline et al. 2012; Skjoldal et al. 2013). Pteropod biomass also experiences seasonal oscillations corresponding to their various life-history stages, therefore further Mediterranean-wide investigations over different seasons would be important in determining temporal differences in pteropod abundance and distribution.

3.2 Species groupings in the Mediterranean

We found that mean pteropod standing stocks were not only greater in the Eastern Mediterranean, but this basin also presented high variability in pteropod distribution between, and within, the distinct biogeochemical regions. The pteropod populations, when abundant, were generally made up of family groups. The Western basin was typified by low standing stocks of both the super family Limacinoidea and family Cresidae, as was the central Levantine basin in the easternmost Mediterranean Sea (stations 10-12).

High numbers of the super family Limacinoidea were associated with lower standing stocks of Cresidae (Fig. 3). Where Cresidae was more abundant however, *H. inflatus* was also present in higher numbers (Fig. 3). Notably, the pteropod communities in the Western Mediterranean Sea were more homogenous, while there was more variability in community groupings in the Eastern Mediterranean Sea. Cluster analysis on species standing stocks (Fig. 3) shows that cluster 1 makes up the entirety of the Western basin and the central Levantine basin, with overall lower species standing stocks. Cluster 2 is comprised of only 2 stations (stations 13 and 15) and dominated by family Cresidae. The dominant taxa in cluster 3 belong to the super family Limacinodea, and is mainly found in the Ionian Sea (stations 9, 14 and 16).

A recent study investigating pteropod trophic dynamics in the Southern Ocean suggested that the niche partitioning for groups of species (between thecosomes and gymnosomes) was likely associated with anatomical differences, particularly those used for feeding (Weldrick et al. 2019). The super family Limacinodea (*H. inflatus* and *Limacina* species) and the super family Cavoliniidae (*Creseis* species) are evolutionarily and anatomically distinct (Burridge et al., 2017). Limacinodea are characterised by a coiled shell and Cavoliniidae are characterised by a bilaterally symmetrical conical shell. While these taxa have similar feeding structures, their anatomical differences may lead to one group being more successful or favouring a particular environment over another, which may in part explain some of the taxonomic clustering that we see in the Eastern Mediterranean Sea. While we did not investigate what specific taxonomic differences have led to the clustering in this study, taxonomic clustering was also observed in the Atlantic Ocean between uncoiled and coiled pteropods in Burridge et al. (2017).

3.3 Environmental drivers of pteropod distribution

The CCA that includes all variables explains 90.8% (CCA1 – 67.6%; CCA2 – 23.2%) of the observed community structure at the time of sampling. CCA1 exhibits positive loadings for O_2, pH, salinity and Ω_{ar}, and negative loadings for fluorescence, PO_4 and NO_3 (Fig. 4). CCA2 exhibits positive loadings for O_2 and negative loadings for temperature (Fig. 4). Temperature, O_2, salinity and Ω_{ar} are significantly affecting 96.0% (CCA1 – 73.6%; CCA2 – 22.4%) of the structure of the observed community at the time of sampling (adj. $r^2 = 0.51$, $F = 4.14$, $p = <0.001$; Fig 4).

Table 1. An overview of published pteropod studies in the Mediterranean Sea.

Region of Collection	Min-max conc. of pteropods community (ind. m^{-2} or m^{-3})	$\bar{x}$ conc. (ind. m^{-2} or m^{3})	Period of sampling	Sampling depth (m)	Water column depth (m)	Most abundant species/taxa	Net/mesh size	Reference
Ligurian and Tyrrhenian Seas (NW Mediterranean)	**Ind. m^{-2}** Study focuses on *C. inflexa*, *C. pyramidata* and *S. subula*). Min-max not provided	**Ind. m^{-2}** Day: *Cavolina inflexa*: 4.0 ± 3.1 *Clio pyramidata*: 2.1 ± 2.6 *Styliola subula*: 0.3 ± 0.8 Night: *Cavolina inflexa*: 1.7 ± 2.7 *Clio pyrimidata*: 1.6 ± 0.9 *Styliola subula*: 0.4 ± 1.5	April, 1994	Various 0-350 0-450 0-550 0-700 Oblique haul	Various 700-2700	*Cavolina inflexa*	BIONESS 1 m^2 mouth 500 µm mesh	Andersen et al., 1998
Southern Adriatic	**Ind. m^{-2}** Min: 1 Max: 2412 (0-50m)	Not provided	April, 1993 September November February June, 1994	0-50 50-100 100-200 200-300 300-400 400-600 600-1000 Vertical haul	1242	*Heliconoides inflatus*	Nansen opening-closing net 113 cm diameter 380 cm length 250 µm mesh	Batistić et al., 2004
Balearic Sea	**Ind. m^{-3}** Only monthly $\bar{x}$ provided. Min: 4 ± 6 Max: 11 ± 6	**Ind. m^{-3}** 5.9	1994-2003 (all year round)	75 Oblique haul	Various 78-200	*Creseis acicula*	Bongo-20 Plankton net 100 µm and 120 µm meshes	Fernández de Puelles et al., 2007
Ligurian Sea	Not provided	**Ind. m^{-2}** Day: *C. inflexa:* 41.2 *C. pyramidata:* 9 *H. inflatus:* 340 Night: *C. inflexa:* 31.5 *C. pyramidata:* 1.4 *H. inflatus:* 9.6	April-May, 2013	0-60 60-100 100-600 600-1300 Oblique haul	Various 1400-1639	*Heliconoides inflatus*	BIONESS multinet 1 m^2 mouth 230 µm mesh	Granata et al., 2020
NW Ligurian Sea	**Ind. m^{-3}** Creseidae: ~630 Cavoliniidae: ~790 Limacinidae (incl. *H. inflatus*): max 60.8	**Ind. m^{-3}** Creseidae: 15.7 Cavoliniidae: 13.8 Limacinidae: 5.5	1967-2003 (all year round)	0-75 Vertical haul	~80	Creseidae	Juday Bogorov net 330 µm mesh 50 cmdiameter	Howes et al. (2015)
Tyrrhenian Sea	**Ind. m^{-3}** Min: 0.00 Max: 4.02	**Ind. m^{-3}** *C. acicula*: 1.48 *C. conica*: 1.11 *H. inflatus:* 1.03 *L. trochiformis:* 0.64 *L. bulimoides:* 0.33	August, 2015	Various 0-65 to 0-170	Various (73-185)	*Creseis acicula*	Bongo-40 200 µm mesh	(Manno et al. 2019)
Eastern Mediterranean	**Ind. m^{-3}** Sicilian Channel: Max. 120 ind. m^{-3}	Not provided	October - November 1991	0-50 50-100 100-200 200-300 Vertical haul	Various: 449-4359	N/A	WP-3 net 113 cm diameter 200 µm mesh	Mazzocchi et al., 1997
Ligurian Sea	**Ind. m^{-3}** Study focuses solely on *Cavolina inflexa* Max: $\bar{x}$ 1.64 (0-200 m)	Not provided	September, 1997	0-25 25-50 50-75 75-100 100-125 125-150 150-200 Oblique haul	Not provided	*Cavolina inflexa*	MOCNESS 1 m^2 mouth 300 µm and 2000 µm meshes	Tarling et al., 2001

The CCA indicates that in the Mediterranean Sea, the distribution of the super family Limacinodea is predominately driven by specific environmental parameters. In particular, *H. inflatus* is mainly linked to temperature, and *L. trochiformis* and *L. bulimoides* more strongly to O_2 (Fig. 4). *C. acicula* is not driven by any significant parameter, but is negatively associated with salinity, Ω_{ar}, and O_2. *Creseis conica* does not exhibit a clear pattern, which may be because the standing stock of this species is too low to statistically identify any solid relationship with the environmental parameters. The inverse distribution of family Creseidae, and the super family Limacinodea, as indicated by the

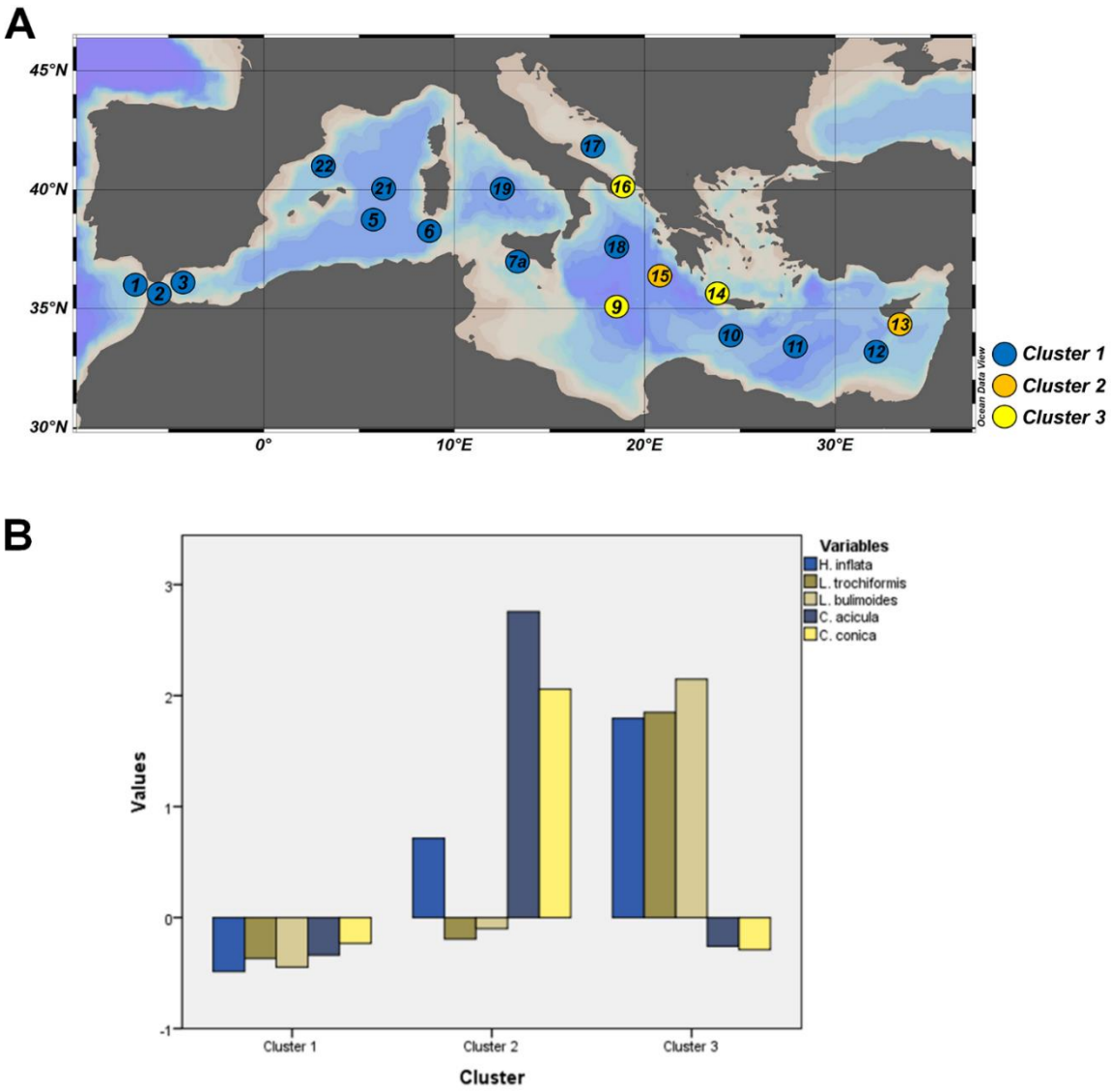

Figure 3. The results of a K-means cluster based on species standing stocks split the 20 stations within the Mediterranean into 3 clusters. **A** Cluster distribution according to the sampling stations, each cluster is characterized by a colour. In this figure, we can see more homogenous communities in the Western Mediterranean and more heterogeneity in the Eastern Mediterranean. Blue circles = cluster 1; orange circles = cluster 2; yellow circles = cluster 3. **B** Column graph indicating the relative contribution of each species to each cluster.

cluster analysis (Fig. 3), is reflected in the opposite relationship these groups have with the environmental variables in the Mediterranean Sea (Fig. 4).

The results indicate that temperature is one of the main factors modulating shelled pteropod distribution in the Mediterranean Sea, as observed in previous studies (Beaugrand et al., 2012, North Atlantic; Howes et al., 2015, Ligurian Sea; Kacprzak et al., 2017, Barents Sea; Thibodeau et al., 2019, Southern Ocean). Indeed, a positive

correlation between pteropod respiration rates and temperature have been observed in eastern tropical North Pacific, Arctic, and Antarctic pteropods under experimental conditions (Comeau et al. 2010; Maas et al. 2012b; Thibodeau et al. 2020). For instance, in the Mediterranean, sea surface temperatures (SST) vary by about 10°C over the course of a year, with winter-summer averages of 12-21°C and 18-28°C in the Northwest and Southwest Mediterranean, respectively. Therefore, the temperature variability of this springtime study is by comparison relatively small (14.08 – 18.18°C) and are temperatures that will likely be experienced at some point over the course of the year for all pteropod populations (Rohling et al. 2009). Given the ongoing rapid warming of the Mediterranean Sea, further studies should address the potential impacts of sustained warming on pteropod distribution in this region.

We found that pteropod standing stocks are positively related to Ω_{ar}, even in waters above critical values of aragonite saturation state for pteropods (Ω_{ar} <1 - Bednaršek et al., 2019). The pteropod shell is made of aragonite and therefore changes in Ω_{ar} might modulate the net calcification process (Bednaršek et al. 2014; Mekkes et al. 2021a). Further, pteropod distribution is predicted to decline as a result of the projected global decrease in Ω_{ar} (Comeau et al., 2012). A study in the Mediterranean Sea at CO_2 vents in the Gulf of Naples investigated pteropod abundance along an Ω_{ar} gradient (1.9-2.7; Manno et al., 2019) and found a positive correlation between pteropod abundance and Ω_{ar} in oversaturated conditions, similar to our study. Howes et al. (2017; Ligurian Sea) showed that shells of *S. subula* were thicker and shells of *C. inflexa* were denser under higher Ω_{ar} conditions when comparing samples collected from 1910 (Ω_{ar} – 3.97) to 2012 (Ω_{ar} – 3.4).

Similarly, a 50 year long-term Australian study (tropical waters) revealed a significant decrease in shell thickness of *C. acicula* and *Diacavolinia longirostris*, coinciding with a decrease in 0.4 Ω_{ar} in waters greater than 3.0 Ω_{ar} (averaged over 7 sites; Roger et al. 2011). An experiment using oversaturated aragonite conditions showed that with a reduction of Ω_{ar} (control - 2.8; reduced - 2.1 Ω_{ar}), *H. inflatus* calcification rate decreased, and metabolic rate increased (Moya et al., 2016). Overall, these studies suggest a high level of sensitivity to carbonate saturation for pteropods, and even in oversaturated conditions such as the Mediterranean Sea, variability in Ω_{ar} (2.68 – 3.61 here) can generate physiological stress.

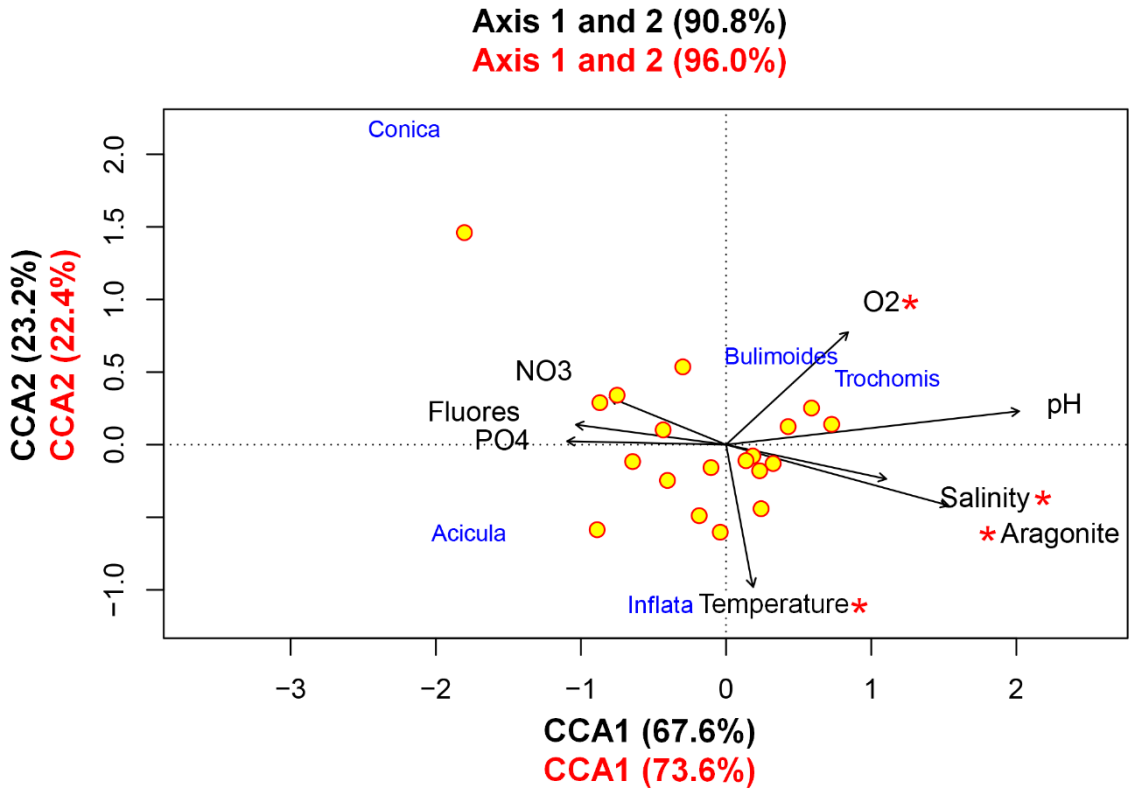

Figure 4. Triplot of the CCA indicating the relationship between pteropod species (as indicated by species name only) in the Mediterranean Sea and the environmental variables. The first CCA (black) shows that NO_3 (NO3), PO_4 (PO4), fluorescence (Fluores), temperature, salinity, pH, O_2 (O2), and Ω_{ar} (Aragonite) are affecting 90.8% (CCA1 – 67.6%; CCA2 – 23.2%) of the structure of the observed community at the time of sampling (adj. r^2 = 0.32, F = 1.99, p = <0.06). The red text and asterisks indicate the results of parsimonious CCA showing the relationship between pteropod species in the Mediterranean and the significant environmental variables. Temperature, O_2, salinity and Ω_{ar} are significantly affecting 96.0% (CCA1 – 73.6%; CCA2 – 22.4%) of the structure of the observed community at the time of sampling (adj. r^2 = 0.51, F = 4.14, p = <0.001).

While pH, another key parameter of the carbonate system that was not significant here, has also been shown to induce a response in pteropods to reduced pH conditions (from pH 8.1 – 7.9_T; Moya et al., 2016). Increased gene expression involved in acid-base regulation in pteropods demonstrates that this is an important mechanism for many physiological processes, including calcification (Moya et al. 2016), and shows that impacts on internal pH homeostasis can be costly. Due to the collinearity of carbonate chemistry parameters, including both pH and Ω_{ar}, it is difficult to disentangle their individual effects on pteropod physiology. Nevertheless, pteropods in the Mediterranean Sea may show an ecological preference for areas (i.e., the Eastern Mediterranean Sea)

with relatively high pH and Ω_{ar}, where they will likely devote less energy to maintaining physiological processes.

We observed a positive correlation between O_2 concentration and *L. bulimoides* and *L. trochiformis* distribution. Oxygen is an important driver of pteropod biology and ecology (Bednaršek et al. 2016). The Mediterranean is in general a well oxygenated sea (Powley et al. 2016), and the O_2 measurements collected in this study are within the normal range for pteropods (191-233 µmol O_2 kg^{-1} – well above hypoxic conditions for pteropods characterised as <20 µmol O_2 kg^{-1} in Manno et al., 2017). However, different pteropod species have different O_2 requirements (Maas et al. 2012b), and the positive correlation between *L. bulimoides* and *L. trochiformis*, both shallow water species, could reflect higher oxygen requirements for these limacinid species, and therefore an ecological preference for areas with higher O_2 concentration compared to other species, such as *Clio pyramidata* and *Creseis virgula* (Maas et al. 2012a), which may be better adapted to experience lower O_2 levels during their vertical migration.

The results indicate that salinity significantly affected pteropod distribution in the Mediterranean Sea. Only relatively low salinities (<33 PSU) have been shown to negatively impact pteropod abundance (Pasternak et al. 2020) and the range of salinity in this study (36.2 – 39.1 PSU) is within the normal range for most pteropods. For *C. acicula* however, their preferred salinity is between 28 to 33 ppt based on physiological responses such as oxygen consumption and calcification rate (Han et al. 2022), and here this species does exhibit a negative relationship with salinity. However, a study investigating the impacts of ocean acidification and sea water freshening on *Limacina retroversa* found that mortality significantly increased only with a combined decrease in pH and salinity, and it was suggested that high salinities may be energetically favourable to pteropods as they are benefited by increased buoyancy (Manno et al. 2012b).

Fluorescence (as indicative of food availability) was not a significant parameter affecting pteropod distribution in this study. Fluorescence has a weak and slightly negative relationship with the super family Limacinodea (76.4% of total pteropod abundance), which is unexpected as pteropod distribution has been previously correlated with high productivity (Bednaršek et al., 2012a; Burridge et al., 2017; Figure 4). There is an east-

west gradient of oligotrophy in the Mediterranean Sea that does not have much seasonal variability (Pasqueron de Fommervault et al., 2015) and in our study, pteropod abundance was higher in the ultra-oligotrophic eastern Mediterranean, which accounts for the weak negative correlation to fluorescence. An intercomparison of long-term studies in the Mediterranean also showed an overall negative correlation between abundance and chlorophyll *a* (Berline et al. 2012). However, the quality of food (in terms of energy), rather than quantity, might be an important factor driving distribution, and further analysis of gut contents would be required to investigate this aspect. Further, the majority of shelled pteropods have a unique feeding behaviour involving the production of a large mucous web that is suspended in the water column, which passively entraps organic particles and motile organisms, enabling them to filter water at high rates (Conley et al. 2018). This feeding method may allow them to overcome low food conditions due to their ability to capture and filter through relatively large amounts of organic matter (Hamner et al. 1975).

Other factors outside of those measured in this study may affect pteropod community composition. For instance, lateral advection is one of the major physical forcings experienced by marine life and plankton. In the Mediterranean Sea, however, the large-scale surface circulation in the Mediterranean has been described as sub-basin-scale, with mesoscale gyres interconnected and bounded by currents and jets (Rohling et al. 2009; Millot and Taupier-Letage 2012). The general circulation flow can impact coastal regions and heavily influence local current dynamics. Mediterranean shelf areas are relatively small and are separated from deeper regions by steep continental shelf breaks. While lateral advection may play a role in pteropod distribution, it is more likely that the coastal pteropod populations in the Mediterranean Sea are influenced by coastal currents and local dynamics rather than the deeper, ocean-like stations of this study. We also investigated the effect of day/night on pteropod standing stocks (ANOVA – day/night fixed factor; IBM SPSS v23) and found there was no significant effect of day/night on total and individual species abundances (Table S2). Given that these species primarily occur in the upper water column (above 200 m depth), we suggest that the time of day did not play a major role in pteropod species distribution here.

3.4 Pteropod and foraminiferal interaction

Planktic foraminiferal standing stocks and distribution data presented in Mallo et al. (2017) were compared to the pteropod data from this study. Pteropod samples from this study and foraminiferal samples from Mallo et al. (2017) came from the same plankton tow samples and stations and were preserved using the same methodology. For a more detailed description of the foraminiferal collection, preservation and taxonomic identification methods, please refer to Mallo et al. (2017). To compare the standing stocks of pteropods and foraminifera within specific regions of the Mediterranean Sea, we used a generalized linear mixed model (GLMM) with a gamma distribution. As the magnitude of the count data is very different between pteropods and foraminifera (almost one order of magnitude), it was transformed to logarithmic scale to make standing stocks from both groups comparable. For this analysis, the Mediterranean Sea was split into two main sub-basins: "Western" stations (1, 2, 3, 5, 6, 7, 19, 20, 21, 22) and "Eastern" stations (11, 12, 13, 14, 15, 16, 17, 16-18). The GLMM was conducted with R version 3.6.0 (R Core Team, 2020) using functions "glm" in the glmmTMB package (Brooks et al. 2017).

The results from the GLMM, comparing the standing stocks of pteropods and foraminifera between the two basins (Eastern and Western basins), indicates that there are significant differences between the abundance of both taxa ($chisq = 29.27$, $p < 0.05$) between the Eastern and Western Mediterranean basins ($chisq = 5.57$, $p < 0.05$), and also in their interaction ($chisq = 4.97$, $p < 0.05$). These results indicate that an inverse relationship between taxa distribution and the Mediterranean Sea sub-basins is present (Fig. 5). Pteropod abundance is distinctly greater in the Eastern Mediterranean Sea than in the Western Mediterranean Sea. Foraminifera showed a contrasting abundance distribution (Fig. 5) with higher abundances in the Western Mediterranean Sea than in the Eastern Mediterranean Sea.

There have been only a handful of studies that investigate the relationship between pteropod and foraminiferal distribution. In the Western Arabian Sea (January – September, 1993), the ratio between pteropod and foraminifera abundance shifted throughout the year, indicating an opposing temporal distribution (Mohan et al. 2006). A

multi-decadal study at two sites off the coast of Southern California and Central California showed no relationship between foraminifera or pteropod abundances (Ohman et al. 2009). In the Gulf Stream, Sargasso Sea and the Gulf of Mexico, pteropod and foraminifera distribution followed a similar pattern, with abundance decreasing closer to oligotrophic conditions (Casey et al. 1979). In Schiebel et al. (2001), foraminiferal and pteropod abundance in the North Atlantic was positively correlated with chlorophyll-*a*. In the Arctic Ocean, there was no clear trend between foraminifera and pteropod abundances along a longitudinal transect (Zamelczyk et al. 2021). The results of these studies indicate that the environmental factors that impact pteropod and foraminiferal abundance and distribution might be distinct.

In the Mediterranean Sea, Mallo et al. (2017) found that foraminiferal distribution is not strongly linked to carbonate saturation levels as observed for pteropod distribution in this study (see section 3.3), but instead links more to trophic complexity. Mallo et al. (2017) found that foraminifera distribution was strongly dependent on food availability and suggested that the lower foraminiferal abundance in the Eastern Mediterranean Sea (ultra-oligotrophic sector) results from reduced reproduction due to limiting resources. Planktic foraminifera have lifespans on the scale of weeks to months, and their production is often seasonal, thus peaks and troughs in foraminiferal abundance are often in line with peaks and troughs in phytoplankton biomass (Hernández-Almeida et al. 2011), their main food source. In contrast to foraminifera, pteropod feeding behaviour allows them to capture large amounts of organic matter (see prg.3.3) and they are also able to actively swim (Hamner et al. 1975; Lalli and Gilmer 1989) and potentially search for more favourable food conditions. These different feeding strategies indicate that foraminifera are more reliant on sustenance in their immediate surroundings, whereas pteropods may not be as restricted. Holocene downcore samples from the North Aegean Sea also indicated that pteropod and foraminifera distribution did not respond similarly to changes in productivity (Giamali et al. 2021). Further, results from incubation experiments show that the survival of pteropods does not appear to be affected when experiencing prolonged starvation (i.e. Busch et al., 2014; Lischka et al., 2011).

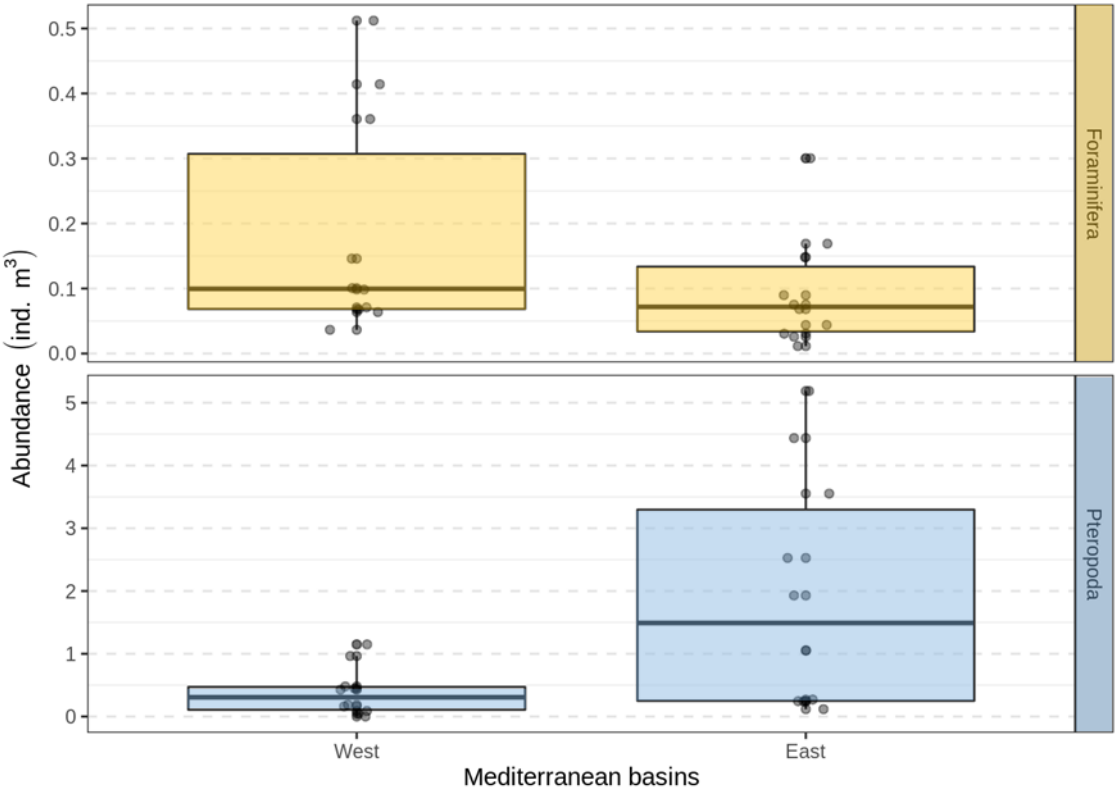

Figure 5. Box plot comparing the abundance distribution of pteropods (blue) and foraminifera (orange) (ind. m^{-3}) between the east and west of the Mediterranean Sea. Pteropods and foraminifera are inversely distributed within the two major sub-basins of the Mediterranean Sea. The results of the Generalized Linear Mixed Model indicate that there are significant differences between the abundance of both taxa (chisq = 29.27, $p < 0.05$) including between the Eastern and Western Mediterranean basins (chisq = 5.57, $p < 0.05$), and also in their interaction (chisq = 4.97, $p < 0.05$). Note that the scale of foraminiferal abundance is distinctly lower than pteropod abundance.

Our results show a relationship between pteropod distribution and several environmental parameters, however it is difficult to determine if there is a single main driver or a combination of drivers. Overall, we suggest that the Eastern Mediterranean basin is more energetically favourable for pteropods due to more favourable environmental conditions (i.e., low energetic physiological demand due to higher Ω_{ar}), and that pteropods may be able to adapt better to the low food availability than foraminifera, which could be due to a combination of both their feeding behaviour, a greater capability to actively move along the water column, and their ability to withstand starvation.

4. Conclusions

Our results provide new insights into pteropod distribution during spring across diverse biogeochemical regions of the Mediterranean Sea, with particular focus on the two largest Mediterranean basins (Western and Eastern). Spring pteropod standing stocks in the Eastern, and largely ultra-oligotrophic sector of the Mediterranean Sea, were 5x greater than in the Western basin. The natural environmental longitudinal gradient across the Mediterranean Sea influences pteropod distribution, and they may be exhibiting a preference for environments with a lower energy demand, such as regions with higher aragonite saturation levels. During the sampling period, foraminifera and pteropods were inversely distributed in the Mediterranean, with greater foraminiferal abundance in the Western Mediterranean Sea, a region of greater nutrients and surface food availability. We speculate that feeding behaviour, alongside swimming capability, may be factors promoting the observed inverse distribution. While our findings provide only a snapshot during the spring season, the paucity of pteropod studies in the Mediterranean Sea makes this work important in providing ecological data on pteropod distribution across this entire region. Future studies covering other seasons, depths, and additional sites would further help to characterise the pteropod distribution across the Mediterranean Sea over large temporal scales as a function of environmental forcings, with implications for their global ecological preferences, life cycle, and impacts on ocean biogeochemistry.

CHAPTER 5

Heliconoides inflatus shell size and mass change across the Mediterranean Sea

Abstract

Thecosome pteropods are a common marine group of calcifying gastropods and an important component of the pelagic carbonate system. In this study we focus on the shell mass and morphometric distribution of an abundant pteropod, *Heliconoides inflatus*, across the Mediterranean Sea. Pteropod mass changes are still poorly addressed and can be related to different factors both physiological (e.g., life cycle) and/or environmental. These data are important for understanding the dynamics of biocalcification and the carbonate cycle. The Mediterranean Sea offers the possibility of sampling across a broad gradient of environmental variables, and here we collected basin-wide data from distinct biogeochemical regions and quantified the mass, length, and diameter of individual specimens. We also present size normalised mass (SNM) to gauge differences in shell density and/or shell wall thickness. Shell mass is significantly related to salinity, and size normalised mass is significantly correlated with aragonite saturation and salinity. The results indicate greater shell mass and thickness/density in the eastern basin regions, which may be driven by differences in temperature, salinity, and carbonate chemistry parameters. Pteropod distribution in the Mediterranean Sea is associated with higher carbonate saturation, pH, and salinity, and here we suggest that the observed differences in mass and SNM across the Mediterranean Sea might similarly be related to the general biogeochemical differences between Mediterranean Sea regions, where the Eastern basin provides more favourable conditions for pteropod calcification.

1. Introduction

Thecosome pteropods are free-swimming, shelled pelagic molluscs that can be found in high numbers in all of the world's upper oceans (Lalli and Gilmer 1989). Their shell is a critical ecological and physiological feature for defence, buoyancy control, feeding methodology (Harbison and Gilmer 1992) and reproduction (Gilmer and Harbison 1986). It is made of aragonite, the rhombic and metastable form of $CaCO_3$, which is considerably more soluble than calcite, the other common polymorph of $CaCO_3$ (Morse et al. 1980). Their aragonitic shells are known to be very sensitive to critical changes in ocean carbonate chemistry as a result of ocean acidification (Feely et al. 2004; Mekkes et al. 2021b), consequently, pteropod shell morphology (i.e. shell thickness and size) is modulated by critical changes such as pH and aragonite saturation state (Ω_{ar}), as observed in laboratory experiments (i.e. Lischka et al. 2011; Comeau et al. 2012b; Busch et al. 2014) and *in situ* observations (i.e. Bednaršek et al., 2012; Manno et al., 2019; Mekkes et al., 2021; Roberts et al., 2014; Roger et al., 2011)

Pteropods are also an important component of the pelagic carbonate system (Bednaršek et al. 2012a; Buitenhuis et al. 2019) and play a role in regulating seawater carbonate chemistry and the partitioning of carbon between the ocean and atmosphere (Broecker et al. 1979; Berelson 2001; Feely et al. 2004; Buitenhuis et al. 2019). Considering the importance of their shell to the marine carbonate system, there is a paucity of studies that focus on pteropod shell mass distribution (Bednaršek et al. 2012a).

The Mediterranean Sea is particularly sensitive to climate change and anthropogenic pressure (Cramer et al. 2018; MedECC 2020; Hassoun et al., 2022). In the Mediterranean Sea, pteropod abundance can be high, with over 700 ind. m^{-3} in the upper water column (0 – 50 m) in some regions (Mazzocchi et al., 1996; Sicily Channel), and average abundances ranging from 0.3 ind. m^{-3} and up to 15.7 ind. m^{-3} throughout the basin (Batistić et al., 2004, Southern Adriatic; Granata et al., 2020, Lugurian Sea; Howes et al., 2015, Ligurian Sea; Manno et al., 2019, Northern Tyrrhenian Sea and the Gulf of Naples).

Heliconoides inflatus (formerly *Limacina inflata*) is a coiled shelled pteropod within the super family Limacinoidae. In the Mediterranean Sea it has been recorded as the most abundant species in the Southern Adriatic (Batistić et al. 2004) and Ligurian Sea (Granata

et al. 2020) and in a trans-Mediterranean cruise (Johnson et al. 2023). This species grows at a rate of ~ 0.15 mm per month (Wells 1976), and will reach the juvenile stage (from ~ 0.4 mm) after ~ 3 months, and adulthood (from ~ 1.0 mm) after ~ 8 months (Wells 1976; Lalli et al. 1978).

Here, we focus on *H. inflatus* and its morphological variability (shell length, diameter, mass and size normalised mass) across the Mediterranean Sea. As this basin is characterised by large biogeochemical gradients and distinct upper water masses (Schneider et al. 2007; Rohling et al. 2009; Uitz et al. 2012; Dayan et al. 2015; Hassoun et al. 2015b), we consider the potential environmental factors that may influence *H. inflatus* shell features in different biogeochemical regions in the Mediterranean Sea during the spring sampling period, with a particular focus on the differences between the eastern and western Mediterranean basins. Our previous study showed that pteropod standing stocks were higher in the eastern Mediterranean, indicating a preference for environmental conditions with a lower energetic physiological demand (Johnson et al. 2023). We present shell length and mass and shell diameter and mass relationships for juvenile *H. infaltus* for the first time. This paper contributes to the limited body of published studies aiming to provide new insights on the factors controlling pteropod mass in natural environments. Understanding this variability contributes to the body of knowledge addressing shelled pteropods as an important pelagic calcium carbonate producer (Bednaršek et al. 2012a; Buitenhuis et al. 2019; Anglada-Ortiz et al. 2021).

2. Materials and methods

2.1 Pteropod collection and processing

Pteropod samples were collected during the MedSeA (Mediterranean Sea Acidification in a Changing Climate) cruise from May 2nd to May 31st 2013. This cruise spanned the majority of the Mediterranean Basin, with the first west to east leg running from the Atlantic Ocean to the Levantine Basin, and the second leg beginning in the north-eastern Ionian Sea and ending in the Alguero-Provençal basin in the north-western region in the Balearic Sea (Fig. 1). The depth-integrated sampling was undertaken using BONGO nets (mesh size 150 µm, 40 cm) from ~ 0 – 200 m depth (oblique towing with the vessel

moving at 1 nautical knot). The mesh size used here provides a good estimate of most of the pteropod community, especially the superfamily Limacinidae, which can be easily lost when using a large mesh size (Howes et al. 2014). Information regarding collection data, time, location, bottom depth and environmental parameters can be found in Table S1. The target depth of 200 m ensured that the majority of the pteropod population could be sampled. Based on a large global dataset (Bednaršek et al. 2012), in the Mediterranean Sea 93% of pteropods are found in the upper 200 m (Johnson et al. 2022).

The plankton samples were stored in 4% formaldehyde solution buffered with hexamethylenetetramine at pH 8.2 and stored in 500 ml polycarbonate bottles kept in the dark at 4ºC. To ensure that the pteropod shells were not affected by this storing technique, the pH of each sample was measured at the beginning, during, and the end of the preservation period. Samples were processed within a month of collection. The pteropod samples were sorted and counted for abundance using a Leica z16 APO binocular light microscope. *Heliconoides inflatus* was identified to species level using a manual for identifying Mediterranean Sea plankton (Trégouboff and Rose 1957) and with the aid of the online plankton portal (www.planktonportal.org). Specimen were measured across the shell for length from the end of the outer whorl across the operculum, through the

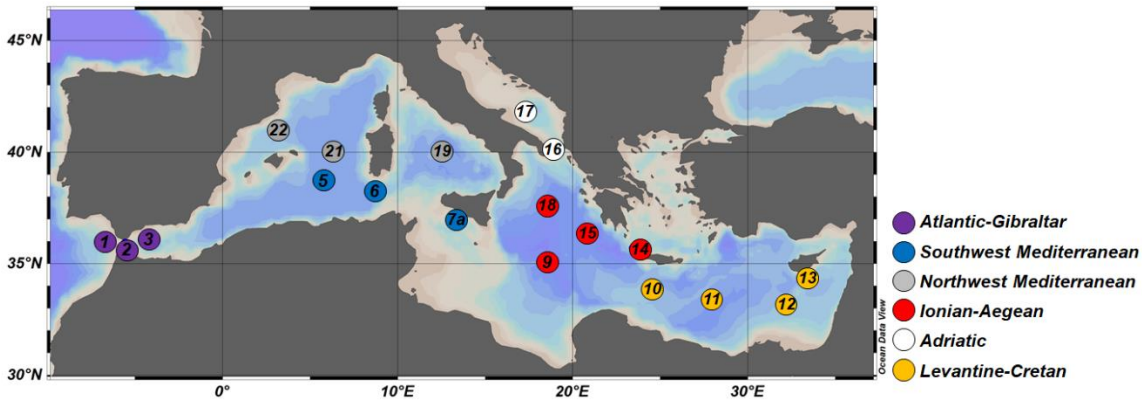

Fig. 1. Map of the Mediterranean Sea with the location of sampled stations. The numbers represent the station codes: **1** – Atlantic; **2** – Strait of Gibraltar; **3** – Alboran Sea; **5** – Southern Alguero-Balear; **6** – Strait of Sardinia; **7a** – Strait of Sicily; **9** – Ionian Sea; **10** – Southern Crete; **11** – Eastern basin; **12** – Nile Delta; **13** – Lebanon; **14** – Antikythera Strait; **15** – Eastern Ionian Sea; **16** – Otronto Strait; **17** – Adriatic Sea; **"16-18"** – Between Otronto Strait and Central Ionian; **19** – Tyrrhenian Sea; **20** – Nothern Alguero-Balear; **21** - Central Alguero-Balear; **22** – Catalano-Balear (Schlitzer, Reiner, Ocean Data View, odv.awi.de, 2021). The coloured points at each station correspond to different biogeochemical regions as presented in (Reygondeau et al. 2017).

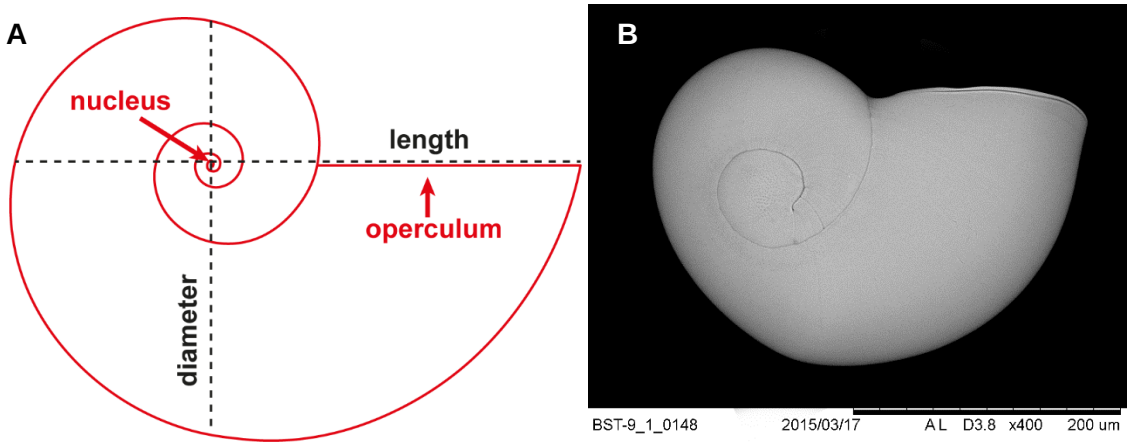

Fig. 2A Schematic shell diagram of *H. inflatus* indicating the metrics used for size in this study. Length, also known as the line of aperture, represents the straight line across the shell from the edge of the shell aperture through the nucleus (centre) to the other side of the shell. Perpendicular to length is shell diameter, which moves through the central nucleus to the edge of the shell on both sides. **B** A scanning electron micrograph of the *H. inflatus* shell using a Zeiss EVO MA 10.

centre of the shell (nucleus), to the other side of the shell (maximum shell length), and then perpendicularly for shell diameter through the centre of the shell (Gardner 2019; Fig. 1). Shell length and diameter were measured with a Leica M165 stereomicroscope using a micrometre on the microscope stage.

2.2 Aragonite mass

To obtain individual aragonite shell mass (as µg $CaCO_3$), *H. inflatus* specimens were transferred to pre-weighed aluminium containers for ashing in a muffle furnace. Pteropod samples were heated to 550ºC for 5 h as for Manno et al. (2018), and then weighed to determine the weight lost due to the burning of organic carbon (Heiri et al. 2001; Kreeger and Padeletti 2020). The remaining ashes are considered a direct estimate of aragonite $CaCO_3$ content as carbonate decomposes at ignition temperatures above 600°C (decarbonisation; Kasozi *et al.* 2009). The ashes were transferred into a desiccator and were then weighed using a Metter Toledo, XPR Ultra-Microbalance (precision = 0.0001 mg).

2.3 Relationships between shell mass, length and diameter

In order to obtain size-normalised *H. inflatus* mass, we consider common morphological metrics such as shell length (also known as the line of aperture) and diameter (Fig. 2). Size-normalised weight or mass (SNM) is a common metric used to normalise mass in relation to size for planktic foraminifera (Beer et al. 2010; Henehan et al. 2017). In essence, techniques used to establish SNM attempt to gauge changes in shell density or test wall thickness (Beer et al. 2010). However, there is no analogous metric for pteropods.

Here, we apply a simple factor to investigate differences in the relationship between shell mass and length by dividing mass by length (SNM). This is a straightforward method and provides information about the specimen-specific relationship between mass and size. A difficulty with plankton samples is that it is assumed that the measured specimens all represent an equivalent ontogenetic stage, because calcification increases with ontogeny (Bé and Lott 1964). During our sampling the *H. inflatus* specimens were within the juvenile stage (observed class size ranging from 395 – 699 µm), and therefore we assume that they all calcify with similar intensity. Further, to reduce the potential bias due to the ontogenetic stage within this class size (i.e., early versus late juveniles), we also present SNM on a sub sample of specimens within a small length size class between 525 – 575 µm. This size class was chosen due to the high number of specimens within that range and as it was close to the average shell length for all specimens of 538 µm; SNM_{SC}).

2.4 Statistics

As the morphometric and mass data are not normally distributed, the non-parametric Kruskal-Wallis test is used to compare shell mass, shell diameter, shell length, SNM, and SNM_{SC} of *H. inflatus* across the Mediterranean Sea and between the 6 target biogeochemical regions in the Mediterranean Sea: the Atlantic-Gibraltar (stations 1, 2, and 3), the Southwest Mediterranean (stations 5-7a), the Northwest Mediterranean (stations 19, 21 and 22), the Ionian-Aegean Seas (stations 9, 14, 15 and 18), the Adriatic Sea (stations 16 and 17), and the Levantine-Cretan Seas (stations 10-13). Due to the small number of samples in the small size class in some biogeochemical regions (e.g. <10), we combine the Eastern and Western Mediterranean regions (Brunner et al. 2018) and

investigate differences in mass between these two basins using a Kruskall-Wallis test. Reported significance values have been adjusted by the Bonferroni correction for multiple tests. Pearson's correlation coefficients were calculated to determine if there were any significant relationships between the environmental parameters and all *H. inflatus* shell parameters with the caveat the environmental data is only a reflection of the conditions at the time of sampling and may not reflect the environmental conditions experienced by the pteropods over their lifespan. All analyses were conducted using IBM SPSS Statistics v23. Using Microsoft Excel, power regression curves and equations were calculated to indicate differences between the mass and diameter relationship between the biogeochemical regions.

2.5 Oceanographic sampling setting

The present study focuses on the Mediterranean Sea which is a semi-enclosed marginal basin characterised by distinct biogeochemical water masses largely differentiated by the basins' oceanographic settings. The Atlantic surface water inflow to the Mediterranean from the Gibraltar Strait is transformed by warming and evaporation when moving eastwards. In addition, the shallow sills of the Strait of Gibraltar (average depth of 365 m) and the Strait of Sicily (average depth of 330 m), combined with the main anti-estuarine circulation, partly limit the Mediterranean Sea water deep circulation. The large-scale basin circulation is generally characterized in the northern regions by cyclonic gyres and in its southern parts by anticyclonic gyres and eddy-dominated flow fields, with the exception of the Tyrrhenian and the northern Ionian Sea (Pinardi et al. 2015).

Different surface water masses are characterised by specific ranges in environmental parameters (e.g. temperature, salinity, nutrients, carbonate chemistry) resulting in biogeographical boundaries throughout the year (Dayan et al., 2015; Hassoun et al., 2015; Pasqueron de Fommervault et al., 2015; Rohling et al., 2009; Schneider et al., 2007; Uitz et al., 2012; Table 1, Fig. 1). Using the biogeochemical regions of the Mediterranean Sea indicated in Reygondeau et al. (2017), we distinguish six water masses in the upper 200 m (Fig. 1) as related to our sampling stations (Figure S5): The Atlantic-Gibraltar, the Southwest Mediterranean, the Northwest Mediterranean, the Ionian-Aegean, the Adriatic, and the Levantine-Cretan region. There are some general characteristic differences between the Eastern and Western sub-basins of the Mediterranean Sea. In general, the

Eastern Mediterranean is warmer, more saline, oligotrophic, and has higher carbonate saturation and pH than the Western Mediterranean.

Table 1. Average and standard deviation of environmental parameters from the 200 m integrated sampling depth from the individual regions in the Mediterranean Sea (Fig. 1 and 2) from data collected at the time of sampling during the MedSeA research cruise 2013. Atlantic-Gibraltar (A-G); Southwest Mediterranean (SW); Northwest Mediterranean (NW); Ionian-Aegean (I-Ag); Adriatic (Ad); Levantine-Cretan (L-C).

	Ind. m^{-3}	**Temp (°C)**	**Salinity (PSU)**	**pH**	**Fluores (µg/L)**	**Ω_{ar}**	**NO_3 (µmol/L)**	**PO_4 (µmol/L)**	**O_2 (µmol/kg)**	***p*CO_2 (µatm)**
A-G	0.63	15.50	36.79	8.07	0.31	2.75	2.73	0.16	212.48	390.08
St. dev.	1.67	1.26	0.81	0.02	0.10	0.30	1.20	0.07	9.57	17.03
SW	0.25	16.49	38.74	8.10	0.16	3.32	1.28	0.07	217.44	375.57
St. dev.	0.19	1.80	0.53	0.01	0.04	0.32	0.93	0.07	7.29	12.08
NW	0.51	16.33	38.50	8.11	0.14	3.34	0.74	0.03	227.38	361.26
St. dev.	0.47	1.59	0.53	0.01	0.04	0.33	0.42	0.02	3.12	6.99
I-Ag	3.05	16.18	38.95	8.12	0.15	3.40	1.28	0.04	228.73	359.75
St. dev.	1.98	0.76	0.13	0.01	0.03	0.14	0.71	0.01	3.56	13.88
Ad	2.74	17.07	38.89	8.12	0.16	3.52	0.65	0.03	226.98	359.48
St. dev.	3.49	1.03	0.10	0.02	0.00	0.02	0.36	0.00	4.71	14.91
L-C	0.90	14.56	38.24	8.12	0.24	3.18	2.49	0.12	221.48	352.27
St. dev.	0.83	0.40	0.24	0.01	0.09	0.10	1.53	0.08	11.05	8.36

3. Results

Overall, there is a strong positive relationship between shell mass (M) and length (L) (r^2 = 0.96; M= 2E-05$L^{2.21}$; power regression) as well as between shell diameter and mass within the studied size range (r^2 = 0.86; M = 7E-05$L^{2.07}$; power regression). Shell mass and length have a similar relationship between the western Mediterranean biogeochemical regions (Fig. 4), and the eastern biogeochemical regions also have a similar shell mass and length relationship (Fig. 4).

Across the Mediterranean Sea *H. inflatus* presents a shell length, shell diameter and shell mass ranging between 699 µm – 395 µm, 581 µm – 271 µm, and 31.5 µg and 7.1 µg, respectively (Figure A, B, C, respectively). The average *H. inflatus* length, diameter and

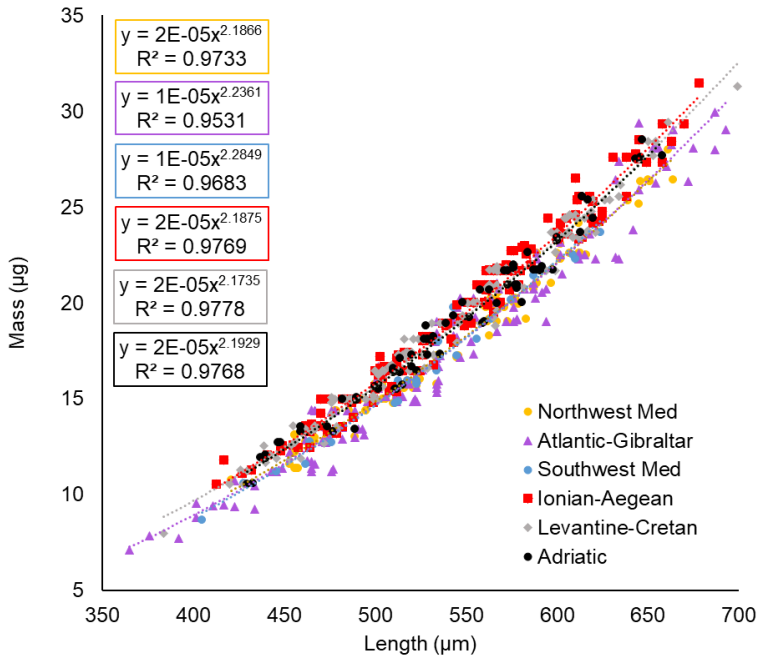

Fig. 4. Relationship between *H. inflatus* shell length and mass in the Mediterranean Sea regions: Atlantic-Gibraltar (n = 140; purple); Southwest Mediterranean (n = 29; blue); Northwest Mediterranean (n = 98; yellow); Ionian-Aegean (n = 169; red); Adriatic (n = 75; black); Levantine-Cretan (n = 177; gray). The slopes for Western Mediterranean regions are overlaid onto each other and the slopes from the Eastern Mediterranean regions are overlaid onto each other and are therefore difficult to discern individually.

mass was 539 µm (SD = 61); 540.6 µm (SD = 49) and 18.4 µg (SD = 4.6), respectively, with the highest values recorded for the Catalano-Balear region in the northwest Mediterranean (station 22; Table S2; Fig. S1, S2, S3) and the lowest in Southern Alguero-Balear region in the southwest Mediterranean (station 5; Table S2; Fig. S1, S2, S3). The shell length and diameter were not significantly different across the Mediterranean regions (Table 2; Fig. 5). Average values at each station for each parameter can be found in Table S2.

Mass was significantly greater in the Levantine-Cretan region than in the Atlantic-Gibraltar (Table 2; Fig. 5). The SNM was significantly higher in the Levantine-Cretan region compared with the Atlantic Gibraltar (<0.01), the Northwest Mediterranean (<0.05), and the Southwest Mediterranean (<0.05) in the western basin (Table 2; Fig. 5). The Adriatic Sea also has a higher SNM compared with the Atlantic Gibraltar (<0.01), the Northwest Mediterranean (<0.05), and the Southwest Mediterranean (<0.05) (Table 2; Fig. 5). SNM_{SC} was significantly higher in the Levantine-Cretan and Ionian-Aegean

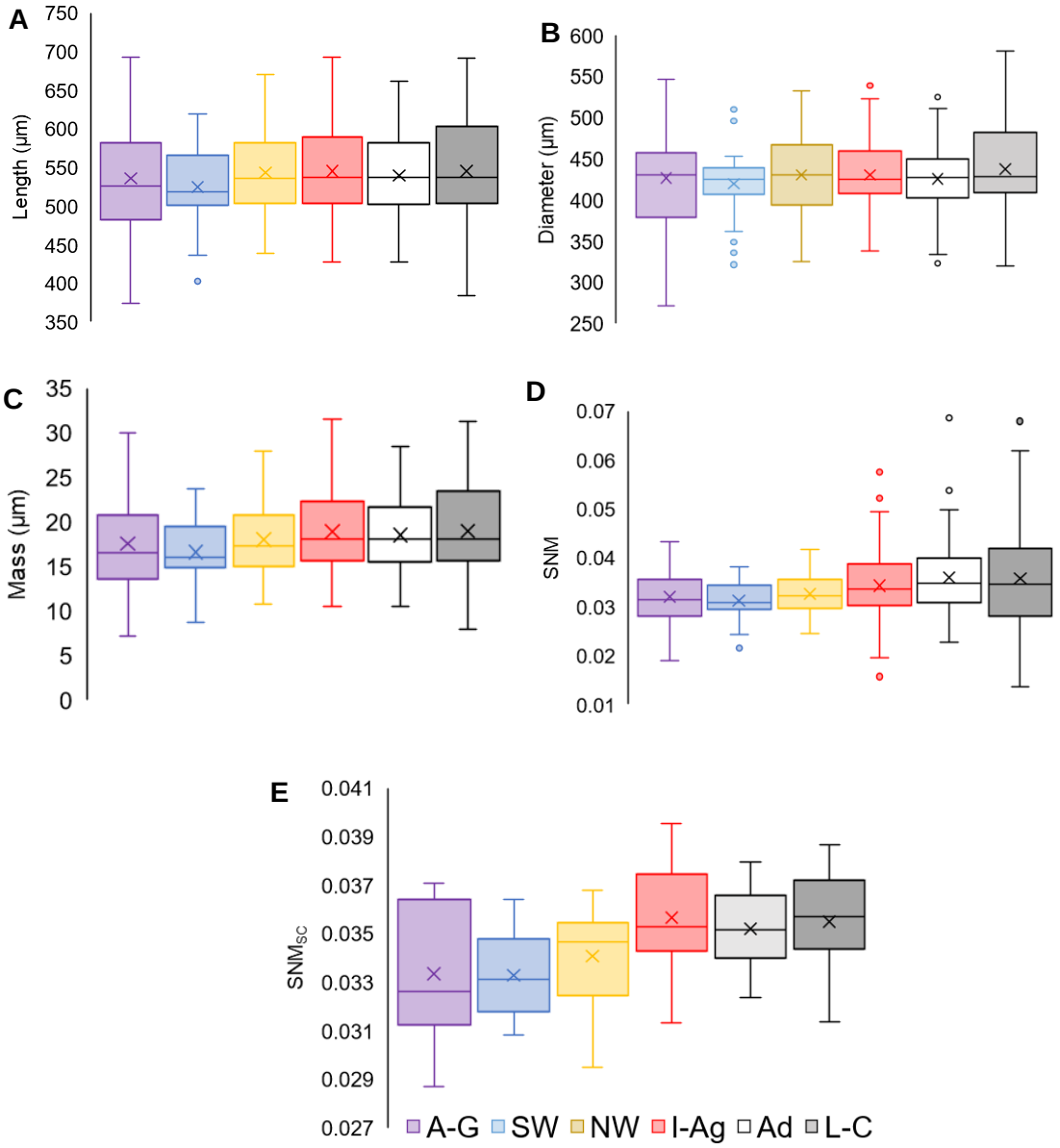

Fig. 3. The distribution of *H. inflatus* shell length, diameter, mass, since normalized mass (SNM). Atlantic-Gibraltar (A-G – purple; n = 137); Southwest Mediterranean (SW – blue; n = 29); Northwest Mediterranean (NW – yellow; n = 177); Ionian-Aegean (I-Ag – red; n = 1733); Adriatic (Ad – white; n = 850); Levantine-Cretan (L-C – gray; n = 1336) of *H. inflatus* **(A)** shell length (µm), **(B)** shell diameter (µm), **(C)** Shell mass (µg), **(D)** SNM for the size class 365 – 699 µm, and **(E)** SNM_{SC} - size class 525 – 575 µm.

Table 2. Significant results ($p < 0.5$) of the Kruskal-Wallis tests comparing the individual Mediterranean regions for *H. inflatus* shell length, diameter, and mass, as well as the calculated factors SNM, SNM_{SC} (mass length factor for the size class 525 – 575 µm), and L:D. Regions: Atlantic-Gibraltar (A-G); Southwest Mediterranean (SW); Northwest Mediterranean (NW); Ionian-Aegean (I-Ag); Adriatic (Ad); Levantine-Cretan (L-C).

Region	Test Statistic	Std. Error	Adj. Significance
Length	No significant differences between regions		
Diameter	No significant differences between regions		
Mass		-	
A-G – L-C	-68.79	22.48	.033
SNM		-	
SW – Ad	-132.40	39.95	.014
SW – L-C	-132.82	39.82	.013
A-G – Ad	-96.95	22.71	.000
A-G – L-C	-97.38	22.48	.000
NW – Ad	-77.41	25.24	.032
NW – L-C	77.84	25.03	.028
SNM_{SC}		-	
A-G – L-C	-38.59	12.42	.028
A-G – I-Ag	39.87	12.27	.017

regions than the Atlantic-Gibraltar (Table 2; Fig. 5). Overall, mass is greater in eastern Mediterranean Sea regions (18.9 µm compared to 17.6 µm) as well as SNM (7.5 %).

The results of the Pearson's correlation show that *H. inflatus* shell mass was minorly significantly positively correlated with salinity and negatively correlated with fluorescence (Table 3). The SNM was significantly positively correlated with salinity and Ω_{ar}, and negatively correlated with fluorescence (Table 3). The SNM_{sc} was significantly positively correlated with salinity, pH, and Ω_{ar} (Table 3).

Table 3. Pearson's correlation results highlighting the significant correlations between the environmental parameters and *H. inflatus* shell length, diameter, and mass, as well as the calculated factors SNM, SNM_{SC} (mass length factor for the size class 525 – 575 µm). Significant is 2-tailed. *p* = *0.1, **0.05, ***0.001.

Shell characteristics		Temp. (^{O}C)	Salinity PSU	Fluor. (µg L^{1})	pH	Ω_{ar} (µmol kg^{-1})	NO_3 (µmol L^{-1})	PO_4 (µmol L^{-1})	O_2 (µmol kg^{-1})
Length (µm)	**Correlation**	-0.060	-0.073	0.130	-0.028	-0.057	-0.028	0.000	-0.070
	p	0.800	0.761	0.586	0.906	0.811	0.907	1.000	0.769
	N	20	20	20	20	20	20	20	20
Diameter (µm)	**Correlation**	-0.193	0.093	-0.032	0.228	0.056	0.270	0.223	-0.172
	p	0.414	0.696	0.894	0.335	0.816	0.249	0.345	0.469
	N	20	20	20	20	20	20	20	20
Mass (µm)	**Correlation**	0.204	0.394*	-0.436*	0.235	0.368	-0.241	-0.299	0.114
	p	0.387	0.086	0.055	0.318	0.110	0.306	0.200	0.632
	N	20	20	20	20	20	20	20	20
SNM	**Correlation**	0.286	.567**	-.535**	0.312	.512**	-0.299	-0.401	0.230
	p	0.221	0.009	0.015	0.181	0.021	0.201	0.080	0.329
	N	20	20	20	20	20	20	20	20
SNMsc	**Correlation**	0.154	.459***	-0.055	.483**	.445**	-0.159	-0.260	0.283
	p	0.516	0.042	0.818	0.031	0.049	0.502	0.269	0.227
	N	20	20	20	20	20	20	20	20

4. Discussion

The first data presented here on the relationship between shell size and mass for the juvenile phase of the pteropod *H. inflatus* demonstrates an expected strong relationship that varies between the eastern and western Mediterranean sub-basins (Fig. 4). A similar relationship between shell diameter and mass has been observed in other limacinid species and has been modelled for *Limacina helicina* also using a power regression curve (1972; ash free dry weight as aragonite [ng]; Conover & Lalli 1972).

Our sampling was conducted during a period of relatively high productivity (Howes et al. 2015) during the Limacinidae juvenile stage of their life cycle (Johnson et al., in press), the most dominant life-cycle phase for Limacinidae globally (Hofmann Elizondo and Vogt 2022). A long-term study (1967 - 2003) in the Ligurian Sea (Western Mediterranean) indicates that limacinid pteropods have a peak in abundance during spring (Howes et al. 2015), and as most *H. inflatus* specimens collected during sampling were juveniles (395 – 699 µm, Lalli & Wells 1978 - juvenile shell length from 0.4 - 1.0 mm), this suggests that this organism was in a production/bloom phase. In pteropods, shell mass and diameter vary depending on the life stage, and the relationship between these shell characteristics can differ depending on the season, with growth generally higher in the

warmer summer period and lower during winter (Bednaršek et al., 2012b). As all specimens of *H. inflatus* were collected during the spring season and are within the juvenile stage (Lalli & Wells 1978), this makes the population an ideal starting point from which to determine potential differences in shell characteristics based on factors outside of ontogeny.

A main striking feature of the results is that *H. inflatus* shell mass was significantly greater (Table 2) in the Levantine-Cretan region in the far eastern Mediterranean than in the Atlantic-Gibraltar region in the far western Mediterranean. This result correlates well with the significant positive relationship between shell mass and salinity, which is higher in the Levantine-Cretan region, and the significant negative relationship between mass and fluorescence, which is higher in the Atlantic-Gibraltar region (Table 3). Despite the difference in mass, there were no significant differences in shell length or diameter across the Mediterranean Sea. Furthermore, the results show that SNM is higher in the eastern Mediterranean than the western Mediterranean (Table 2), specifically in the southern Adriatic Sea compared to all the western Mediterranean regions, and in the Levantine-Cretan region compared to the western Mediterranean regions. The SNM is significantly positively correlated with salinity and Ω_{ar}, both of which are higher in the Adriatic Sea and Levantine-Cretan regions, and significantly negatively correlated with fluorescence, which is greater in the western Mediterranean basin (Table 3). When focusing on the SNM_{sc}, there is a similar significant positive relationship between salinity, pH, and Ω_{ar}, all of which are higher in the eastern Mediterranean. The difference in shell mass and SNM without an accompanied change in length or diameter suggests that the difference in mass and SNM are related to other shell features such as shell density/thickness. Similarly for foraminifera, changes in SNM are assumed to be indicative of changes in shell density/thickness (Beer et al. 2010), and here we follow the same assumption that the higher SNM indicates that *H. inflatus* in the Levantine-Cretan region and Adriatic Sea regions have thicker or denser shells than in the western Mediterranean. General characteristics of eastern Mediterranean regions is that they are warmer, more saline, and have higher pH and carbonate saturation levels when compared to the Western Mediterranean. These general differences in environmental parameters may be driving the differences we see in shell mass and SNM (including for the similar size class of *H. inflatus* juveniles) between the eastern and western sub-basins.

Several environmental factors can drive changes in pteropod shell mass or SNM (shell density/thickness). Variability in nutrient concentration (Oakes and Sessa 2020) and aragonite saturation ($\Omega_{ar;}$ Roger et al., 2011; Howes et al., 2017) in over saturated conditions have been shown to affect pteropod shell mass and thickness *in situ*. Oakes & Sessa (2020) found that in the Cariaco Basin (2.3 – 3.6 Ω_{ar}) the shell of *H. inflatus* (from sediment traps) was 40 % thicker during nutrient-rich upwelling periods, coinciding with diatom blooms, a major food source for pteropods. This is contrary to our observations, which indicate significant negative relationships between shell mass and SNM (Table 3), where thicker/denser shells are associated with ultra-oligotrophic conditions in the eastern Mediterranean. However, the peaks of nutrients (PO_4 – 0.52 µm L^{-1}; NO_3 and NO_2 – 8.84 µm L^{-1}) during the upwelling period in Oakes and Sessa (2020) far surpass the values recorded in the Mediterranean Sea in our stations (Table 1), and year-round for NO_3 across the Mediterranean Sea (below 0.5 µm L^{-1}, except in the north-west Mediterranean when it peaks at 2.3 µm L^{-1} in January; Pasqueron de Fommervault *et al.* 2015). This suggests that nutrient concentration may not be the main driver of the observed change in mass and SNM here as the Mediterranean Sea is in general oligotrophic, with the exception of high productivity regions such as the Gulf of Lion and the northern Adriatic Sea which were not sampled in this study.

We observed greater mass SNM in regions with higher Ω_{ar} (Table 2) and significant positive correlations between SNM and SNM_{sc} with Ω_{ar} (Table 3). High Ω_{ar} has previously been shown to have positive effects on calcification (Moya et al. 2016) and increase shell thickness and density (Roger et al. 2011; Howes et al. 2017). A 50 year long-term Australian (tropical waters) revealed a significant decrease in shell thickness (–4 to –5µm) of *Creseis acicula* and *Diacavolinia longirostris*, coinciding with a decrease in 0.4 Ω_{ar} in waters greater than 3.0 Ω_{ar} (averaged over 7 sites; Roger *et al.* 2011). Similarly, Howes et al. (2017; Ligurian Sea) showed that shells of *Styliola subula* were thicker and shells *of Cavolina inflexa* were denser under higher Ω_{ar} conditions when comparing samples collected from 1910 (Ω_{ar} – 3.97) to 2012 (Ω_{ar} – 3.4). Calcification for *H. inflatus* has also been shown to decrease when Ω_{ar} is reduced, even in oversaturated conditions (control – 2.1; reduced – 1.9 Ω_{ar}; Moya et al. 2016). The studies mentioned above indicate that even a relatively small variability in oversaturated conditions of Ω_{ar} (such as the variability observed here across the Mediterranean Sea water masses - 2.7 to 3.6 Ω_{ar}) might have an influence on pteropod shell mass and SNM, with mass and

density/thickness increasing towards a higher Ω_{ar}. It is important to note, however, that while many studies focus on Ω_{ar} as aragonite is the building block of pteropod shells, it is unlikely that Ω_{ar} has a direct impact on calcification (Cyronak et al. 2016). Rather, it is likely the associated change in pH that affects calcification due to the impact of H^+ in coelomic fluid which can influence internal acid/base balance (Cyronak et al. 2016).

Salinity is positively correlated with *H. inflatus* mass, SNM, and SNM_{sc} (Table 3) and changes in shell mass or density may be an adaptive strategy related to buoyancy in different seawater densities. This has been proposed as a strategy influencing calcification in planktic foraminifera which have greater mass and SNM (referred to as size-normalised weight) during glacial periods (Zarkogiannis et al. 2019) and may be another explanation for the greater *H. inflatus* mass in the eastern basin in response to the higher density (27.05 – 28.1 Kg/m^{-3}). In a study focusing on sapropels (sapropel S5; 126 – 121 ka) from the Levantine Basin, it was shown that calcification increased for four species of planktic foraminifera in high salinity conditions and then reduced after an influx of fresh water to the region (Weinkauf et al. 2013). In the Mediterranean Sea, sea surface density increases eastward from 26 – 26.5 Kg/m^{-3} in the Atlantic/Gibraltar region to 27.5 – 28.0 Kg/m^{-3} in the Levantine/Cretan region. While there are no studies investigating the impact of seawater density on pteropod mass or shell density/thickness, the increases observed here may be an adaptation strategy to a more buoyant environment, whereby greater shell mass/density allows the organism to sink to their desired conditions, as suggested for planktic foraminifera (Zarkogiannis et al. 2019).

While greater shell mass and SNM are associated with regions with higher temperature, no significant positive correlations were identified (Table 3). Studies investigating the impact of temperature on pteropod shell growth are uncommon (Hofmann Elizondo and Vogt 2022). There is some effect of temperature on growth, given the slowing of growth during the cooler seasons such as winter (Wang et al. 2017; Thibodeau et al. 2020; Hofmann Elizondo and Vogt 2022), and Limacinid pteropods are known to be metabolically sensitive temperature (Comeau et al. 2010; Maas et al. 2011; Thibodeau et al. 2020). For *L. helicina* juveniles, temperature did not affect shell diameter, increment, and degradation in an experimental setting (Lischka et al. 2011). A study along a north – south transect in the Atlantic Ocean noted that *H. inflatus* shells from cooler temperate waters were thicker than shells from warmer conditions (Burridge et al. 2017b), however

it was hypothesised that they may represent a distinct population (*H. inflatus* S). Importantly, Burridge et al. (2017b) did not collect data on carbonate chemistry parameters which may also impact shell growth. As such, it is difficult to determine the direct impact that temperature may have on shell mass and density/thickness.

Distinguishing the impact of individual environmental and/or physiological parameters on shell morphology *in situ* is expectedly challenging. Recently, Mekkes et al. (2021) found a significant decrease in the shell thickness of *L. helicina* along the onshore-offshore coastal upwelling gradient of the California coast. The decrease in shell thickness was associated with decreasing carbonate chemistry parameters (Ω_{ar} and pH), temperature, and O_2 (Ω_{ar}: 1.08 – 1.79; temperature: 8.84 – 10.77°C; O_2: 154.70 – 164.60 µmol/kg) and the authors concluded that as these environmental parameters strongly covary, a single environmental variable could not be determined to explain the observed differences in shell thickness as these variables may either be working together or independently to impact shell calcification. The authors pointed out however, that O_2 was unlikely to impact calcification given that concentrations were above physiologically compromising levels (Vaquer-Sunyer and Duarte 2008).

The samples collected here were mainly juveniles, therefore the differences we see across the Mediterranean basin may reflect this early life stage. For many marine calcifiers, the impact of temperature and carbonate chemistry parameters have been found to be more keenly experienced by juveniles than by adults (Dupont and Thorndyke 2008; Cripps et al. 2014), and therefore the impact of environmental factors on morphology are potentially more visible during than juvenile life stage than the adult life stage. The differences in shell morphology in response to environmental parameters may not only be life stage-specific but also species-specific, reflecting an individual species' physiology. This was shown in Roberts et al. (2014), where changes in the shell weight/mass of three polar pteropod species either increased (*L. retroversa australis*), decreased (*L. helicina antarctica* forma *Antarctic*), or remained the same (*H. antarctica* forma *rangi*) in response to the variability in environmental conditions over a 10 year period (1997 – 2007). Therefore, the difference in shell mass and SNM we see here across the Mediterranean Sea may be specific to *H. inflatus* during the juvenile life stage.

Pteropod distribution has been shown to be positively related to pH, Ω_{ar}, salinity and temperature in the Mediterranean Sea (Johnson et al. 2023), and it has been suggested that the eastern basin is a preferred region for pteropods in the Mediterranean as it is more energetically favourable for processes such as calcification. Overall, greater salinities, and carbonate chemistry parameters, including pH and Ω_{ar}, can contribute to favourable conditions for pteropod calcification, and may explain the significant relationships between these environmental parameters and *H. inflatus* shell mass and SNM across the Mediterranean Sea. Further research is required to investigate pteropod ecology and calcification, and the impact that individual environmental factors might have on modulating shell mass changes. Tools such as micro-computed tomography or nanoindentation could be utilised in future studies as they can provide detailed information about changes in calcified shell microstructure in response to environmental variables (Johnson et al. 2020; Ofstad et al. 2021). While there are known difficulties associated with maintaining pteropods in captivity through a full life cycle (Howes et al. 2014; Thabet et al. 2015), a useful approach is to conduct both multi-stressor experiments and *in situ* observations (Doo et al. 2020). By combining these two methods of investigation, the impact of individual variables or synergistic effects of multiple variables can inform *in situ* observations.

CHAPTER 6

Conclusions, synthesis, and future research

The marine environment is changing rapidly due to anthropogenic pressures. Ocean warming and acidification are major global issues that threaten marine organisms and ecosystem functioning. An example of a sea under climate change and direct human pressure is the Mediterranean Basin, home to diverse flora and fauna and recognised as a biodiversity hotspot (Valavanidis and Vlachogianni 2013). This semi-enclosed basin is identified as a climate change hotspot, with many associated processes disrupting the marine ecosystem (Giorgi 2006). This region also contains a high diversity of calcifying plankton, including coccolithophores, a ubiquitous phytoplankton, and pteropods, a unique pelagic shelled gastropod. Though microscopic, the importance of these organisms to the marine trophic system, plankton dynamics, and the carbon cycle cannot be understated (Ziveri et al. 2007; Falkowski et al. 2008; Manno et al. 2010, 2019; Lefebvre et al. 2011; Bednaršek et al. 2012a; Buitenhuis et al. 2019). Their calcified components suggest they will be particularly vulnerable to ocean acidification (Riebesell et al. 2000; Lefebvre et al. 2011; Bach et al. 2013; Schlüter et al. 2014; Rosas-Navarro et al. 2016; Moya et al. 2016; Feng et al. 2017; Krumhardt et al. 2017; Bednaršek et al. 2019; Engström-Öst et al. 2019). This thesis focuses on the pressing question – how will marine calcifying plankton, in particular coccolithophores and pteropods, respond to ocean acidification and warming in the Mediterranean Sea? The Mediterranean Sea is characterized by distinct biogeochemical regions that cross natural environmental gradients (Schneider et al. 2007; Rohling et al. 2009; Fedele et al. 2022), and the stark changes in marine environmental parameters across this semi-enclosed sea make it a natural laboratory to investigate how the variability in environmental factors affects species distributions. While significant efforts have been undertaken to characterise the distribution and coccolithophores in the Mediterranean Sea and to investigate their response to marine climate change stressors, there is still a considerable number of gaps in research, including how the impacts of ocean warming and acidification on this important food source will affect the marine trophic system. The distribution of pteropods in the Mediterranean Sea is considerably less known and this dissertation published the first Mediterranean-wide pteropod field study. This work assesses their abundance and community composition, as well as the environmental drivers affecting their distribution in the Mediterranean Sea, contributing to a significant gap in research for this vulnerable species in a climate change hotspot region. Additionally, many experimental studies have investigated the impacts of ocean warming and acidification on pteropod calcification,

but less is known about the drivers of shell growth *in situ*. This thesis has filled many of these research gaps.

6.1 Conclusions

- The systematic review of extant coccolithophore distribution in the Mediterranean Sea (Chapter 2) provides a cohesive overview of coccolithophore distribution across the entire basin, and specifically identifies key gaps in research areas, such as the north coast of Africa, the western basin, and the winter and spring seasons (Fig. 1; Chapter 2). Methodological biases associated with sampling methods and microscopy were identified, indicating that phytoplankton studies utilising the Utermöhl method of sampling likely underestimate coccolithophore abundances and contribution (%) to the phytoplankton community. Using the meta-analysis data, opposing geographical and temporal distribution of hetero and holococcolithophores were identified, supporting the hypothesis that the haplo-diplontic life cycle of coccolithophores widens their ecological niche. Several studies indicate a negative correlation between coccolithophore abundance and temperature, and additionally, abundance is highest during the cooler seasons of winter and autumn. As such, coccolithophore abundance in the Mediterranean Sea may be negatively impacted by ocean warming, however holococcolithophores, which are positively associated with temperature, may respond favourably to warming conditions by widening their distribution.

- The experiment on the nutritional content of coccolithophores in response to changing pH and temperature indicated that coccolithophore growth will likely increase under ocean warming which will increase the availability of lipids for their consumers (Chapter 3). Their nutritional content, however, will likely be reduced under ocean warming and acidification conditions, which is expected to impact their consumers, such as copepods and other zooplankton, whose nutritional situation

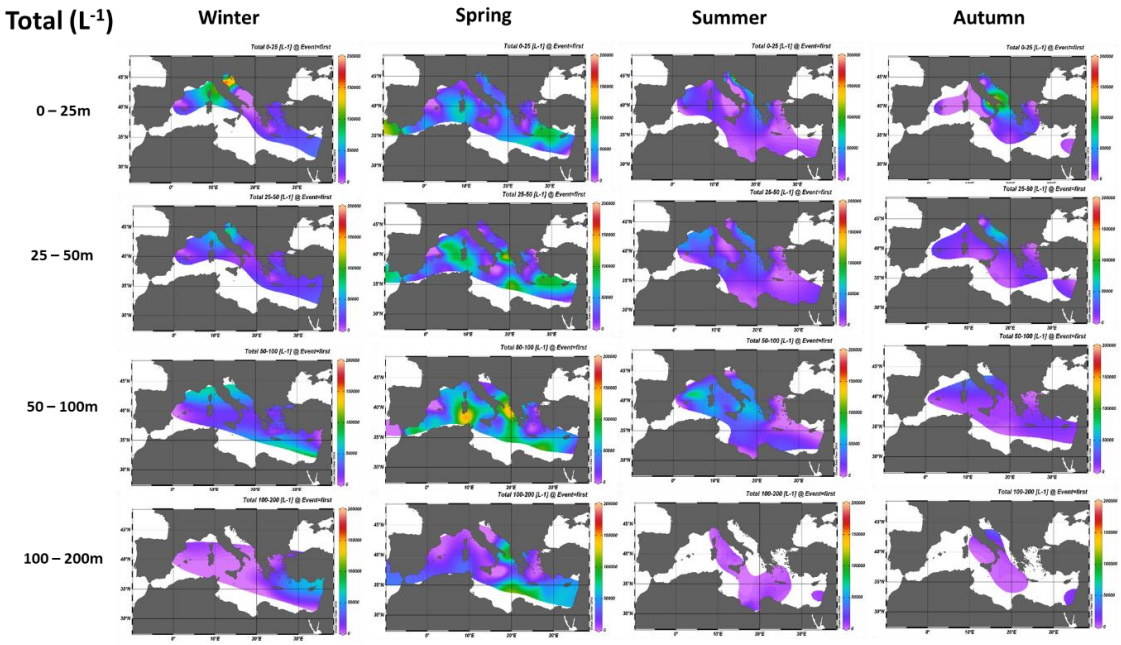

Fig. 1. Total coccolithophore abundance (L^{-1}) based on a systematic literature review across the Mediterranean Sea during winter, spring, summer, and autumn at different depth profiles including 0 – 25m, 25 – 50 m, 50 – 100m, and 100 – 215m. Maximum abundances for total and heterococcolithophores are capped at 200,000 coccolithophores L^{-1}. Note that abundances indicated outside of the Mediterranean, for instance in the Atlantic Ocean, are an artefact of the Data-Interpolating Variational Analysis (DIVA) gridding tool by ODV and do not reflect the data. White regions indicate a lack of data (Chapter 1).

depends on the nutritional quality and quantity of their prey. Additionally, the capacity of coccolithophores to defend against predation may be reduced due to theweakened integrity of their coccosphere under ocean acidification conditions. The impact on the consumers will vary depending on the requirements of each individual taxa. For instance, organisms with limited nutrient supplies could be affected by increases in cellular POC:N under future conditions, while organisms that have difficulty digesting calcite may benefit from decreases in PIC:POC under ocean acidification. As this experiment was done under nutrient replete exponential growth, concurrent changes in nutrient availability may also alter these impacts on the nutritional status of *E. huxleyi* (Müller et al. 2017). These impacts have the potential to disrupt the marine food web.

- The first dataset on thecosome pteropod distribution across the entire Mediterranean Sea using the same sampling methodology was generated in this dissertation (Chapter 4). Pteropod abundance was 5x greater in the ultra-oligotrophic eastern Mediterranean basin than in the western basin. The natural

environmental longitudinal gradient across the Mediterranean Sea influences pteropod distribution, and they may be exhibiting a preference for environments with a lower energy demand. Temperature, oxygen, salinity, and aragonite saturation were shown to significantly affect 96.0% of the structure of the observed community at the time of sampling. As temperature, salinity, oxygen, and the saturation of aragonite, a highly soluble form of calcite, are greater in the western basin, pteropods may show a preference for this region due to a lower energetic demand on physiological functioning and calcification. For foraminifera, another important group of calcifying plankton, their abundance does not appear to be related to higher calcite saturation, but rather food availability, which is greater in the western Mediterranean. As such, foraminifera and pteropods exhibit an inverse distribution in the Mediterranean Sea. We speculate that feeding behaviour, alongside swimming capability, may be factors promoting the observed inverse distribution of these taxa.

- The distribution of pteropod shell length, diameter, and mass, across the Mediterranean Sea were presented in this dissertation (Chapter 5). The results show that pteropod shells have a greater mass to length ratio, or size normalised mass, in the eastern basin, indicating they have thicker or denser shells. The observed difference in size normalised mass may be related to the biogeochemical conditions between Mediterranean Sea sub-basins, where higher carbonate saturation, temperature, and salinity (or a combination of these factors) in the eastern basin promotes greater calcification.

6.2 Synthesis

The response of calcifying plankton to ocean acidification and warming will be group- and taxon- specific and modulated by synergistic local drivers. It is likely that we will see shifts in the distribution of species to regions that are more physiologically and energetically favourable for growth and calcification (Neukermans et al. 2018). Phytoplankton are expected to have a varied response to ocean acidification and warming (Seifert et al. 2020), and due to the calcifying nature of coccolithophores and pteropods, they will have the additional stress of reduced seawater pH (Guinder and Molinero 2013; Bednaršek et al. 2016) which can affect their ability to calcify (Riebesell et al. 2000;

Engel et al. 2005; Hoppe et al. 2011; Lefebvre et al. 2011; Schlüter et al. 2014; Bednaršek et al. 2016).

The combination of potential shifts in distribution, lower abundances, and reduced nutritional quality of coccolithophores in the Mediterranean Sea under ocean warming and acidification may have drastic impacts on the zooplankton community that utilise coccolithophores as a food source, however the impacts will vary regionally. While coccolithophore growth from culture experiments is enhanced under relative ocean warming (Johnson et al. 2022), total abundance is negatively correlated with temperature *in situ*. Furthermore, temperature increases in the Mediterranean Sea may pass critical thresholds for coccolithophores over the coming century (D'Amario et al. 2020). Coccolithophore distribution in the Mediterranean Sea reflects a preference for cooler regions, particularly for the most abundant coccolithophore species in the region, *E. huxleyi* (Chapter 1). As such, it is likely that increasing temperatures will impact coccolithophore distribution by having a detrimental effect on abundance. Additionally, the two distinct life-cycle phases of coccolithophores, the diploid heterococcolithophore and the haploid holococcolithophore, have several opposing environmental preferences, therefore we may see specific effects related to their lifecycle phase in response to ocean warming and acidification. As the Mediterranean Sea is warming fast under climate change (Lazzari et al. 2013; Lionello and Scarascia 2018), we may see reductions in heterococcolithophore abundance throughout all regions as this life stage is negatively correlated with temperature, while holococcolithophore abundance shows a preference for warmer conditions, therefore their abundance may increase under ocean warming. If there is a beneficial increase in growth rate under ocean warming, ocean acidification conditions may reduce that increase (D'Amario et al. 2020; Johnson et al. 2022), and as the western basin has lower carbonate saturation and pH levels than the eastern basin, coccolithophores in this region may experience impacts to abundance sooner than coccolithophores in the eastern basin. The rapid warming of the Mediterranean Sea will also negatively impact the nutritional content of coccolithophores, in terms of the PIC:POC ratio (Johnson et al. 2022), and this impact may be heightened in the eastern basin given the initial conditions of higher temperatures and ultra-oligotrophic surface waters. Although adaptation to ocean acidification and warming has been shown in experimental cultures to occur relatively quickly in *E. huxleyi* (~460 generations - 1 year; Schlüter et al. 2014), for the coccolithophore *Gephyrocapsa oceanica*, growth rate (after

an initial increase), POC production, and nitrogen production all decreased over 2000 generations (roughly 1400 days) under high CO_2 conditions (Jin and Gao 2016), which suggests that resilience to ocean acidification conditions can diminish over time and will vary by taxa.

The higher abundance of thecosome pteropods in the eastern Mediterranean Sea, and the greater thickness/density of the shells in this region, suggests that the conditions of in the eastern Mediterranean Sea, such as warm sea water temperatures and high pH and carbonate saturation, might be favourable for pteropod growth and calcification (Johnson et al., 2022). Mediterranean waters are already affected by acidification, especially the western Mediterranean basin (Hassoun et al. 2019; 2022), and acidification over this century is expected to affect the western basin more than the eastern basin (Goyet et al. 2016), suggesting that the eastern basin may continue to be the preferred region for pteropods. Well after the end of this century, pH will decrease similarly for both basins (Goyet et al. 2016), which will likely reduce the advantageous aspect of the eastern Mediterranean for pteropods. Temperature, however, will remain higher in the eastern basin, and as the ocean continues to warm, the increasing temperature may pass critical thresholds for pteropods (Han et al. 2022) before the reduction in carbonate saturation and pH crosses physiological thresholds. The positive association with pteropod community composition and aragonite saturation in the Mediterranean Sea suggests there may be a general decline in abundance and impacts to community composition over the coming century due to ocean acidification. These changes to carbonate chemistry may also impact pteropod calcification and shell morphology.

Coccolithophores (phytoplankton) and pteropods (zooplankton, pelagic gastropod) have clearly very distinct physiologies and life cycles, as well as distinct ecological requirements, however both are cosmopolitan marine plankton groups united by their ability to calcify. Calcification leaves them susceptible to changes in ocean carbonate chemistry, in particular to increasing ocean acidification, with each taxa experiencing different thresholds. Calcite is utilised by coccolithophores and is the most stable calcium carbonate polymorph, while aragonite, the rhombic and metastable form of calcium carbonate, is considerably more soluble than calcite (Morse et al. 1980). This suggests that pteropods may be especially vulnerable to ocean acidification due to their aragonite shell. Indeed, pteropod shells are known to be very sensitive to critical changes in ocean

carbonate chemistry associated with ocean acidification (Feely et al. 2004; Mekkes et al. 2021b). Like pteropods and foraminifera, pteropods and coccolithophores also have an opposite geographical distribution in the Mediterranean Sea, where abundance of pteropods is greater in the eastern basin and abundance of coccolithophores is greater in the wester basin. In the Mediterranean Sea, pteropod distribution is positively correlated with temperature and coccolithophore distribution is negatively correlated with temperature. In the case of pH and carbonate saturation, pteropods appear more susceptible to variations in the aragonite saturation state, whereas coccolithophore distribution does not appear to be as affected by the calcite saturation state. This may be related to the different calcite morphs that both taxa utilise. As aragonite is a highly soluble form of calcium carbonate, it may be driving their increased sensitivity, whereas coccolithophores are made of calcite and may not be as sensitive to changes in carbonate chemistry as pteropods are. Coccolithophores are autotrophic and require both sunlight and nutrients for growth, and in environments where carbonate saturation remains relatively high, such as the Mediterranean Sea (Hassoun et al. 2019), they are likely more reliant on nutrient availability. They are however, common in oligotrophic conditions (Winter et al. 2002), and it has been hypothesized that calcification may increase their access to phosphate and carbon dioxide in such environments (Pomar et al. 2022). Nitrogen limitation has also been shown to enhance calcification in *Gephyrocapsa oceanica* (Jiang et al. 2022). As such, their distribution in the Mediterranean is likely driven by other environmental variables such as temperature, rather than nutrients or carbonate saturation, which suggests that under ocean warming, coccolithophores in the eastern Mediterranean may move deeper into the photic zone to achieve a temperature closer to their optimum, and that in general, the cooler western Mediterranean will remain their preferred region. Pteropods may also not be reliant on food availability in their direct surroundings. Their unique feeding method involves the production of a mucous web that creates a large surface area, allowing them to filter water and maximise particle capture at high rates (Conley et al., 2018). Additionally, pteropods appear able to withstand periods of prolonged starvation (i.e. Busch et al., 2014; Lischka et al., 2011), therefore it is likely that nutrients are not a driver of pteropod abundance in the Mediterranean Sea, but rather other parameters such as carbonate chemistry and temperature.

Although not specifically investigated here, coccolithophores (e.g. Ziveri et al. 2000; Rigual-Hernández et al. 2020) and pteropods (e.g. Bednarsek et al. 2012; Buitenhuis et

al. 2019) provide significant contributions to carbonate production and organic carbon export in the oceans (Ziveri et al., 2007). Negative impacts on abundance and calcification in the Mediterranean basin for coccolithophores and pteropods will likely result in a regional reduction of carbonate production and export (Loubere et al. 2007).

6.2 Future research

There are significant gaps in knowledge for coccolithophores in the Mediterranean Sea that need to be addressed. Further research should be focused to the western Mediterranean basin, as well as winter and autumn, given that several abundant coccolithophore species are associated with cooler seasons and conditions. The entire north coast of Africa is understudied, representing a substantial geographical area. This coast spans large biogeographical boundaries, diverse local conditions, and is composed of several major currents and gyres, therefore it is likely this region contains valuable material regarding coccolithophore communities and dynamics in the Mediterranean Sea. Collaborative efforts need to be encouraged and fostered between European countries and north African countries that border the Mediterranean Sea. These research targets will provide a more holistic understanding of coccolithophore communities in the Mediterranean basin.

Multi-stressor experiments (which more closely simulate real-world scenarios) are the means by which we can make considered conclusions regarding the effects of climate change on species. While the short-term experiment presented here provides important information about the immediate response of coccolithophores to changes in temperature and pH, which can be decisive in field scenarios, further work investigating the long-term impact of ocean acidification and warming on the nutritional content (in terms of both quality and quantity) of coccolithophores is essential and will be a key part of understanding the impacts of climate change on ocean trophic dynamics. As there will likely be shifts in interactions and competition between calcareous species (Kroeker et al. 2013b), experiments involving multiple calcifying taxa will be crucial to accurately project changes to species compositions and interactions. As the physiological response of organisms will determine their biogeography, utilising a multi-stressor and multi-species approach will enable these experimental responses to be scaled up to the ecological level.

Despite the limited number of pteropod studies in the Mediterranean Sea, our findings provide essential ecological information on pteropod distribution across the whole region. As there are notorious difficulties associated with maintaining pteropods in captivity through a full life cycle (Howes et al. 2014; Thabet et al. 2015), field observations are fundamental to improve the current knowledge on their ecology and vulnerability to climate change. The study here provides a snapshot during the spring season, and further research should target different depths, seasons, and regions. This will ultimately contribute to an improved understanding of how environmental forcings affect pteropod distribution over a broad spatial and temporal scale in the Mediterranean Sea, with implications for their global ecological preferences, life cycles, and effects on ocean biogeochemistry. In this thesis a first interesting comparison between pteropods and foraminifera distribution is shown, however, the interaction of pteropod and other plankton groups remains poorly known, and research in this area will improve our understanding of plankton community and trophic system dynamics. Additionally, many details remain unknown about their life-cycle, feeding method, and reproduction, and the focus so far has mainly been confined to limacinid species (Lalli and Wells 1973, 1978; Thabet et al. 2015). Very few studies investigate these aspects of pteropod biology in-depth, yet a diversity of breeding strategies have already been identified. Within family Limacinoidea, various reproductive strategies have been observed, including internal fertilization and egg laying (*L. bulimoides*, *L. helicina*, *L. lesueruri*, *L. retroversa* and *L. trochiformis*), brooding small numbers of young in the mucous gland until they are juveniles (*L. helicoides*), and one unique strategy in which the shell mantle is used as a brood chamber for embryos and young veligers (*H. inflatus*; Lalli and Wells 1978). Research in these areas that focuses on different taxonomic groups within Pteropoda will improve our basic biological understanding of their life cycle.

Further research is required to investigate pteropod morphology and mass distribution across the Mediterranean Sea, and to determine the impact that environmental factors might have on the observed variability in calcification. Regular sampling will also capture seasonal developments in pteropod growth and calcification. Furthermore, utilising techniques that investigate the density or porosity of calcified skeletons, such as micro-computed tomography or nanoindentation, can provide detailed information about skeletal components and microstructure (Johnson et al. 2020; Ofstad et al. 2021).

There is an urgent need to understand the effects that climate change forcings will have on biological systems, particularly as evidence so far suggests that many marine species and ecosystems will be negatively affected (Pörtner 2008). Additionally, competition between calcareous species is predicted to change under ocean acidification (Kroeker et al. 2013a). Calcifying plankton are significant marine organisms that are an important component of the marine trophic system and also play a substantial role in carbon flux systems in the ocean. To determine how marine biological and carbon flux systems will be impacted under ocean warming and acidification, there is need to understand the current state of ecosystems, and to determine the impact that environmental variables and anthropogenic stressors have on the physiology and distribution of organisms.

References

Acri, Bastianini, B. Aubry, and others. 2019. LTER Northern Adriatic Sea (Italy) marine data from 1965 to 2015.doi:10.5281/ZENODO.3465097

Aho, K., D. Derryberry, and T. Peterson. 2014. Model selection for ecologists: the worldviews of AIC and BIC. Ecology **95**: 631–636. doi:https://doi.org/10.1890/13-1452.1

Aktan, Y. 2011. Large-scale patterns in summer surface water phytoplankton (except picophytoplankton) in the Eastern Mediterranean. Estuar. Coast. Shelf Sci. **91**: 551–558. doi:10.1016/j.ecss.2010.12.010

Alhammoud, B., K. Béranger, L. Mortier, M. Crépon, and I. Dekeyser. 2005. Surface circulation of the Levantine Basin: Comparison of model results with observations. Prog. Oceanogr. **66**: 299–320. doi:https://doi.org/10.1016/j.pocean.2004.07.015

Amores, A., S. Monserrat, and M. Marcos. 2013. Vertical structure and temporal evolution of an anticyclonic eddy in the Balearic Sea (western Mediterranean). J. Geophys. Res. Ocean. **118**: 2097–2106. doi:https://doi.org/10.1002/jgrc.20150

Andersen, V., F. François, J. Sardou, and others. 1998. Vertical distributions of macroplankton and micronekton in the Ligurian and Tyrrhenian seas (northwestern Mediterranean). Oceanol. Acta **21**: 655–676. doi:10.1016/s0399-1784(98)90007-x

Anderson, O. R., M. Spindler, A. W. H. Bé, and C. Hemleben. 1979. Trophic activity of planktonic foraminifera. J. Mar. Biol. Assoc. United Kingdom **59**: 791–799. doi:DOI: 10.1017/S002531540004577X

Anglada-Ortiz, G., K. Zamelczyk, J. Meilland, P. Ziveri, M. Chierici, A. Fransson, and T. L. Rasmussen. 2021. Planktic Foraminiferal and Pteropod Contributions to Carbon Dynamics in the Arctic Ocean (North Svalbard Margin) . Front. Mar. Sci. **8**.

Armstrong, J. L., K. W. Myers, D. A. Beauchamp, and others. 2008. Interannual and Spatial Feeding Patterns of Hatchery and Wild Juvenile Pink Salmon in the Gulf of Alaska in Years of Low and High Survival. Trans. Am. Fish. Soc. **137**: 1299–1316. doi:10.1577/t07-196.1

Arnold, H. E., P. Kerrison, and M. Steinke. 2013. Interacting effects of ocean acidification and warming on growth and DMS-production in the haptophyte coccolithophore Emiliania huxleyi. Glob. Chang. Biol. **19**: 1007–1016.

doi:10.1111/gcb.12105

Astraldi, M., and G. P. Gasparini. 1994. The Seasonal Characteristics of the Circulation in the Tyrrhenian Sea. Seas. Interannual Var. West. Mediterr. Sea 115–134. doi:https://doi.org/10.1029/CE046p0115

Aubry, F., and F. Acri. 2004. Phytoplankton seasonality and exchange at the inlets of the Lagoon of Venice (July 2001–June 2002). J. Mar. Syst. **51**: 65–76. doi:https://doi.org/10.1016/j.jmarsys.2004.05.008

Aubry, F., F. Acri, M. Bastianini, S. Finotto, and A. Pugnetti. 2022. Differences and similarities in the phytoplankton communities of two coupled transitional and marine ecosystems (the Lagoon of Venice and the Gulf of Venice - Northern Adriatic Sea). Front. Mar. Sci. **9**.

Aubry, F. B., F. Acri, S. Finotto, and A. Pugnetti. 2021. Phytoplankton Dynamics and Water Quality in the Venice Lagoon. Water **13**. doi:10.3390/w13192780

Bach, L. T., C. Bauke, K. J. S. Meier, U. Riebesell, and K. G. Schulz. 2012. Influence of changing carbonate chemistry on morphology and weight of coccoliths formed by *Emiliania huxleyi*. Biogeosciences **9**: 3449–3463. doi:10.5194/bg-9-3449-2012

Bach, L. T., L. C. M. Mackinder, K. G. Schulz, G. Wheeler, D. C. Schroeder, C. Brownlee, and U. Riebesell. 2013. Dissecting the impact of CO2 and pH on the mechanisms of photosynthesis and calcification in the coccolithophore Emiliania huxleyi. New Phytol. **199**: 121–134. doi:10.1111/nph.12225

Bach, L. T., U. Riebesell, M. A. Gutowska, L. Federwisch, and K. G. Schulz. 2015. A unifying concept of coccolithophore sensitivity to changing carbonate chemistry embedded in an ecological framework. Prog. Oceanogr. **135**: 125–138. doi:https://doi.org/10.1016/j.pocean.2015.04.012

Bach, L. T., U. Riebesell, and K. G. Schulz. 2011. Distinguishing between the effects of ocean acidification and ocean carbonation in the coccolithophore Emiliania huxleyi. Limnol. Oceanogr. **56**: 2040–2050. doi:https://doi.org/10.4319/lo.2011.56.6.2040

Balestra, B., M. Marino, S. Monechi, C. Marano, and F. Locaiono. 2009. Coccolithophore communities in the Gulf of Manfredonia (Southern Adriatic Sea): data from water and surface sediments. Micropaleontology **54**: 377–396.

Barcena, M. A., J. A. Flores, F. J. Sierro, M. Perez-Folgado, J. Fabres, A. Calafat, and M. Canals. 2004. Planktonic response to main oceanographic changes in the Alboran Sea (Western Mediterranean) as documented in sediment traps and surface

sediments. Mar. Micropaleontol. **53**: 423–445. doi:10.1016/j.marmicro.2004.09.009

Barker, S., and H. Elderfield. 2002. Foraminiferal calcification response to glacial-interglacial changes in atmospheric CO2. Science (80-.). **297**: 833–836.

Batistić, M., F. Kršinić, N. Jasprica, M. Carić, D. Viličić, and D. Lučić. 2004. Gelatinous invertebrate zooplankton of the South Adriatic: Species composition and vertical distribution. J. Plankton Res. **26**: 459–474. doi:10.1093/plankt/fbh043

Bé, A. W. H., and L. Lott. 1964. Shell Growth and Structure of Planktonic Foraminifera. Science (80-.). **145**: 823 LP – 824. doi:10.1126/science.145.3634.823

Beaufort, L., I. Probert, T. de Garidel-Thoron, and others. 2011. Sensitivity of coccolithophores to carbonate chemistry and ocean acidification. Nature **476**: 80–83. doi:10.1038/nature10295

Beaugrand, G., A. Mcquatters-Gollop, M. Edwards, and E. Goberville. 2012. Long-term responses of North Atlantic calcifying plankton to climate change. Nat. Clim. Chang. **3**: 263–267. doi:10.1038/nclimate1753

Bednaršek, N., R. A. Feely, E. L. Howes, and others. 2019. Systematic Review and Meta-Analysis Toward Synthesis of Thresholds of Ocean Acidification Impacts on Calcifying Pteropods and Interactions With Warming. Front. Mar. Sci. **6**: 227. doi:10.3389/fmars.2019.00227

Bednaršek, N., C. J. Harvey, I. C. Kaplan, R. A. Feely, and J. Možina. 2016. Pteropods on the edge: Cumulative effects of ocean acidification, warming, and deoxygenation. Prog. Oceanogr. **145**: 1–24. doi:10.1016/j.pocean.2016.04.002

Bednaršek, N., J. Možina, M. Vogt, C. Brien, and G. A. Tarling. 2012a. The global distribution of pteropods and their contribution to carbonate and carbon biomass in the modern ocean. Earth Syst. Sci. Data **4**: 167–186. doi:10.5194/essd-4-167-2012

Bednarsek, N., J. Mozina, M. Vogt, C. J. J. O'Brien, and G. A. A. Tarling. 2012. Global distributions of pteropods (Gymnosomata, Thecosomata, Pseudothecosomata) abundance and biomass - Gridded data product (NetCDF) - Contribution to the MAREDAT World Ocean Atlas of Plankton Functional Types.doi:10.1594/PANGAEA.777387

Bednaršek, N., G. A. Tarling, D. C. Bakker, and others. 2012b. Description and quantification of pteropod shell dissolution: a sensitive bioindicator of ocean acidification. Glob. Chang. Biol. **18**: 2378–2388. doi:10.1111/j.1365-

2486.2012.02668.x

Bednaršek, N., G. A. Tarling, D. C. E. Bakker, S. Fielding, and R. A. Feely. 2014. Dissolution Dominating Calcification Process in Polar Pteropods Close to the Point of Aragonite Undersaturation P. Ross [ed.]. PLoS One **9**: e109183. doi:10.1371/journal.pone.0109183

Bednaršek, N., G. A. Tarling, S. Fielding, and D. C. E. Bakker. 2012c. Population dynamics and biogeochemical significance of Limacina helicina antarctica in the Scotia Sea (Southern Ocean). Deep Sea Res. Part II Top. Stud. Oceanogr. **59**–**60**: 105–116. doi:10.1016/j.dsr2.2011.08.003

Beer, C., R. Schiebel, and P. Wilson. 2010. Technical Note: Determining the size-normalised weight of planktic foraminifera. Biogeosciences Discuss. **7**. doi:10.5194/bgd-7-905-2010

Bendle, J., A. Rosell-Melé, and P. Ziveri. 2005. Variability of unusual distributions of alkenones in the surface waters of the Nordic seas. Paleoceanography **20**. doi:https://doi.org/10.1029/2004PA001025

Berelson, W. M. 2001. Particle settling rates increase with depth in the ocean. Deep. Res. Part II Top. Stud. Oceanogr. **49**: 237–251. doi:10.1016/S0967-0645(01)00102-3

Berline, L., I. Siokou-Frangou, I. Marasović, and others. 2012. Intercomparison of six Mediterranean zooplankton time series. Prog. Oceanogr. **97**–**100**: 76–91. doi:https://doi.org/10.1016/j.pocean.2011.11.011

Berner, R. A. 2002. Examination of hypotheses for the Permo–Triassic boundary extinction by carbon cycle modeling. Proc. Natl. Acad. Sci. **99**: 4172–4177. doi:10.1073/pnas.032095199

Blunden, J., and D. S. Arndt. 2016. State of the Climate in 2015. Bull. Am. Meteorol. Soc. **97**: Si-S275. doi:10.1175/2016BAMSStateoftheClimate.1

Boldrin, A., S. Miserocchi, S. Rabitti, M. M. Turchetto, V. Balboni, and G. Socal. 2002. Particulate matter in the southern Adriatic and Ionian Sea: characterisation and downward fluxes. J. Mar. Syst. **33**: 389–410. doi:10.1016/S0924-7963(02)00068-4

Bollmann, J., M. Y. Cortés, A. T. Haidar, and others. 2002. Techniques for quantitative analyses of calcareous marine phytoplankton. Mar. Micropaleontol. **44**: 163–185. doi:https://doi.org/10.1016/S0377-8398(01)00040-8

Bonomo, S., A. Cascella, I. Alberico, L. Ferraro, L. Giordano, F. Lirer, M. Vallefuoco, and E. Marsella. 2014. Coccolithophores from near the Volturno estuary (central

Tyrrhenian Sea). Mar. Micropaleontol. **111**: 26–37. doi:10.1016/j.marmicro.2014.06.001

Bonomo, S., A. Cascella, I. Alberico, F. Lirer, M. Vallefuoco, E. Marsella, and L. Ferraro. 2018a. Living and thanatocoenosis coccolithophore communities in a neritic area of the central Tyrrhenian Sea. Mar. Micropaleontol. **142**: 67–91. doi:10.1016/j.marmicro.2018.06.003

Bonomo, S., M. Grelaud, A. Incarbona, and others. 2012. Living Coccolithophores from the Gulf of Sirte (Southern Mediterranean Sea) during the summer of 2008. MICROPALEONTOLOGY **58**: 487–503.

Bonomo, S., F. Placenti, E. M. Quinci, A. Cuttitta, S. Genovese, S. Mazzola, and A. Bonanno. 2017. Living coccolithophores community from Southern Tyrrhenian Sea (Central Mediterranean - Summer 2009). Mar. Micropaleontol. **131**: 10–24. doi:10.1016/j.marmicro.2017.02.002

Bonomo, S., F. Placenti, S. Zgozi, and others. 2018b. Relationship between coccolithophores and the physical and chemical oceanography of eastern Libyan coastal waters. Hydrobiologia **821**: 215–234. doi:10.1007/s10750-017-3227-y

Bonomo, S., K. Schroeder, A. Cascella, I. Alberico, and F. Lirer. 2021. Living coccolithophore communities in the central Mediterranean Sea (Summer 2016): Relations between ecology and oceanography. Mar. Micropaleontol. **165**. doi:10.1016/j.marmicro.2021.101995

Bouza, N., and M. Aboal. 2008. Checklist of phytoplankton on the south coast of Murcia (SE Spain, SW Mediterranean Sea) V. Evangelista, L. Barsanti, A.M. Frassanito, V. Passarelli, and P. Gualtieri [eds.]. ALGAL TOXINS NATURE, Occur. Eff. Detect. 179–196. doi:10.1007/978-1-4020-8480-5_6

Breteler, W. C. M., N. Schogt, and S. Rampen. 2005. Effect of diatom nutrient limitation on copepod development: Role of essential lipids. Mar.Ecol-Prog.Ser. **291**: 125–133. doi:10.3354/meps291125

Broecker, W. S., T. Takahashi, H. J. Simpson, and T.-H. Peng. 1979. Fate of Fossil Fuel Carbon Dioxide and the Global Carbon Budget. Science (80-.). **206**: 409–418. doi:10.1126/science.206.4417.409

Broglio, E., S. Jonasdottir, A. Calbet, H. Jakobsen, and E. Saiz. 2003. Effect of heterotrophic versus autotrophic food on feeding and reproduction of the calanoid copepod Acartia tonsa: relationship with prey fatty acid composition. Aquat. Microb. Ecol. **31**: 267–278.

Brooks, M. E., K. Kristensen, K. J. van Benthem, and others. 2017. {glmmTMB} Balances Speed and Flexibility Among Packages for Zero-inflated Generalized Linear Mixed Modeling. R J. **9**: 378–400. doi:10.32614/rj-2017-066

Brown, C. W., and J. A. Yoder. 1994. Coccolithophorid blooms in the global ocean. J. Geophys. Res. Ocean. **99**: 7467–7482. doi:https://doi.org/10.1029/93JC02156

Brunner, E., F. Konietschke, A. C. Bathke, and M. Pauly. 2018. Ranks and Pseudo-Ranks - Paradoxical Results of Rank Tests -.doi:10.48550/arxiv.1802.05650

Buitenhuis, E. T., T. Pangerc, D. J. Franklin, C. Le Quéré, and G. Malin. 2008. Growth rates of six coccolithophorid strains as a function of temperature. Limnol. Oceanogr. **53**: 1181–1185. doi:https://doi.org/10.4319/lo.2008.53.3.1181

Buitenhuis, E. T., C. Le Quéré, N. Bednaršek, and R. Schiebel. 2019. Large Contribution of Pteropods to Shallow CaCO3 Export. Global Biogeochem. Cycles **33**: 458–468. doi:10.1029/2018GB006110

Buitenhuis, E. T. T., M. Vogt, R. Moriarty, and others. 2013. MAREDAT: towards a world atlas of MARine Ecosystem DATa. Earth Syst. Sci. Data **5**: 227–239. doi:10.5194/essd-5-227-2013

Bulling, M. T., N. Hicks, L. Murray, D. M. Paterson, D. Raffaelli, P. C. L. White, and M. Solan. 2010. Marine biodiversity–ecosystem functions under uncertain environmental futures. Philos. Trans. R. Soc. B Biol. Sci. **365**: 2107–2116. doi:10.1098/rstb.2010.0022

Burić, Z., I. Cetinić, D. Viličić, K. C. Mihalić, M. Carić, and G. Olujić. 2007. Spatial and temporal distribution of phytoplankton in a highly stratified estuary (Zrmanja, Adriatic Sea). Mar. Ecol. **28**: 169–177. doi:https://doi.org/10.1111/j.1439-0485.2007.00180.x

Burridge, A. K., C. Hörnlein, A. W. Janssen, and others. 2017a. Time-calibrated molecular phylogeny of pteropods. PLoS One **12(6)**: e0177325. doi:10.1371/journal.pone.0177325

Burridge, A. K., M. Tump, R. Vonk, E. Goetze, D. Wall-Palmer, S. L. Le Double, J. Huisman, and K. T. C. A. C. A. Peijnenburg. 2017b. Diversity and abundance of pteropods and heteropods along a latitudinal gradient across the Atlantic Ocean. Prog. Oceanogr. **158**: 213–223. doi:10.1016/j.pocean.2016.10.001

Busch, S. D., M. Maher, P. Thibodeau, and others. 2014. Shell condition and survival of Puget Sound pteropods are impaired by ocean acidification conditions G.E. Hofmann [ed.]. PLoS One **9**: e105884. doi:10.1371/journal.pone.0105884

Cabrini, M., D. Fornasaro, G. Cossarini, M. Lipizer, and D. Virgilio. 2012. Phytoplankton temporal changes in a coastal northern Adriatic site during the last 25 years. Estuar. Coast. SHELF Sci. **115**: 113–124. doi:10.1016/j.ecss.2012.07.007

Caesar, L., G. D. McCarthy, D. J. R. Thornalley, N. Cahill, and S. Rahmstorf. 2021. Current Atlantic Meridional Overturning Circulation weakest in last millennium. Nat. Geosci. **14**: 118–120. doi:10.1038/s41561-021-00699-z

Caesar, L., S. Rahmstorf, A. Robinson, G. Feulner, and V. Saba. 2018. Observed fingerprint of a weakening Atlantic Ocean overturning circulation. Nature **556**: 191–196. doi:10.1038/s41586-018-0006-5

Caldeira, K., and M. E. Wickett. 2003. Anthropogenic carbon and ocean pH. Nature **425**: 365–365. doi:10.1038/425365a

Caroppo, C., A. Fiocca, P. Sammarco, and G. Magazzu. 1999. Seasonal Variations of Nutrients and Phytoplankton in the Coastal SW Adriatic Sea (1995–1997). Bot. Mar. - BOT MAR **42**: 389–400. doi:10.1515/BOT.1999.045

Carrada, G., E. Fresi, D. Marino, M. Modigh, and M. Ribera d'Alcala. 1981. Structural analysis of winter phytoplankton in the Gulf of Naples. J. Plankton Res. **3**. doi:10.1093/plankt/3.2.291

Casey, R., L. Gust, A. Leavesley, D. Williams, R. Reynolds, T. Duis, and J. M. Spaw. 1979. Ecological Niches of Radiolarians, Planktonic Foraminiferans and Pteropods Inferred from Studies on Living Forms in the Gulf of Mexico and Adjacent Waters. Gulf Coast Assoc. Geol. Soc. Trans. **29**: 216–223.

Cerino, F., D. Fornasaro, M. Kralj, M. Giani, and M. Cabrini. 2019. Phytoplankton temporal dynamics in the coastal waters of the north-eastern Adriatic Sea (Mediterranean Sea) from 2010 to 2017. Nat. Conserv. 343–372. doi:10.3897/natureconservation.34.30720

Cerino, F., E. Malinverno, D. Fornasaro, M. Kralj, and M. Cabrini. 2017. Coccolithophore diversity and dynamics at a coastal site in the Gulf of Trieste (northern Adriatic Sea). Estuar. Coast. Shelf Sci. **196**: 331–345. doi:10.1016/j.ecss.2017.07.013

Challouf, R., A. Hamza, M. Mahfoudhi, K. Ghozzi, and M. N. Bradai. 2017. Environmental assessment of the impact of cage fish farming on water quality and phytoplankton status in Monastir Bay (eastern coast of Tunisia). Aquac. Int. **25**: 2275–2292. doi:10.1007/s10499-017-0187-1

Charalampopoulou, A., P. AJ, and T. Tyrrell. 2011. Irradiance and pH affect

coccolithophore community composition on a transect between the North Sea and the Arctic Ocean . Mar. Ecol. Prog. Ser. **431**: 25–43.

Chavez, F. P., M. Messié, and J. T. Pennington. 2010. Marine Primary Production in Relation to Climate Variability and Change. Ann. Rev. Mar. Sci. **3**: 227–260. doi:10.1146/annurev.marine.010908.163917

De Choudens-Sánchez, V., and L. A. González. 2009. Calcite and Aragonite Precipitation Under Controlled Instantaneous Supersaturation: Elucidating the Role of CaCO3 Saturation State and Mg/Ca Ratio on Calcium Carbonate Polymorphism. J. Sediment. Res. **79**: 363–376. doi:10.2110/jsr.2009.043

Comeau, S., S. Alliouane, and J. P. Gattuso. 2012a. Effects of ocean acidification on overwintering juvenile Arctic pteropods Limacina helicina. Mar. Ecol. Prog. Ser. **456**: 279–284. doi:10.3354/meps09696

Comeau, S., J.-P. Gattuso, A.-M. Nisumaa, and J. Orr. 2012b. Impact of aragonite saturation state changes on migratory pteropods. Proc. R. Soc. B Biol. Sci. **279**: 732. doi:10.1098/RSPB.2011.0910

Comeau, S., R. Jeffree, J.-L. Teyssié, and J.-P. Gattuso. 2010. Response of the Arctic Pteropod Limacina helicina to Projected Future Environmental Conditions A. Stepanova [ed.]. PLoS One **5**: e11362. doi:10.1371/journal.pone.0011362

Conde-Porcuna, J. M., E. Ramos-Rodriguez, and C. Perez-Martinez. 2002. Correlations between nutrient concentrations and zooplankton populations in a mesotrophic reservoir. Freshw. Biol. **47**: 1463–1473. doi:https://doi.org/10.1046/j.1365-2427.2002.00882.x

Conley, K. R., F. Lombard, and K. R. Sutherland. 2018. Mammoth grazers on the ocean's minuteness: A review of selective feeding using mucous meshes. Proc. R. Soc. B Biol. Sci. **285**. doi:10.1098/rspb.2018.0056

Conover, R. J., and C. M. Lalli. 1972. Feeding and growth in Clione limacina (Phipps), a pteropod mollusc. J. Exp. Mar. Bio. Ecol. **9**: 279–302. doi:10.1016/0022-0981(72)90038-X

Core Team, R. C. 2020. R: A language and environment for statistical computing.

Cottingham, K. L., J. T. Lennon, and B. L. Brown. 2005. Knowing when to draw the line: designing more informative ecological experiments. Front. Ecol. Environ. **3**: 145–152. doi:https://doi.org/10.1890/1540-9295(2005)003[0145:KWTDTL]2.0.CO;2

Cramer, W., J. Guiot, M. Fader, and others. 2018. Climate change and interconnected

risks to sustainable development in the Mediterranean. Nat. Clim. Chang. **8**: 972–980. doi:10.1038/s41558-018-0299-2

Cripps, G., K. J. J. Flynn, and P. K. K. Lindeque. 2016. Ocean Acidification Affects the Phyto-Zoo Plankton Trophic Transfer Efficiency. PLoS One **11**: e0151739.

Cripps, G., P. Lindeque, and K. J. Flynn. 2014. Have we been underestimating the effects of ocean acidification in zooplankton? Glob. Chang. Biol. **20**: 3377–3385. doi:https://doi.org/10.1111/gcb.12582

Cros, L., and J. M. Fortuno. 2002. Atlas of Northwestern Mediterranean coccolithophores. Sci. Mar. **66**: 5-+.

Cushman-Roisin, B., M. Gacic, P.-M. Poulain, and A. Artegiani. 2013. Physical oceanography of the Adriatic Sea: past, present and future, Springer Science & Business Media.

Cyronak, T., K. G. Schulz, and P. L. Jokiel. 2016. The Omega myth: what really drives lower calcification rates in an acidifying ocean. ICES J. Mar. Sci. **73**: 558–562. doi:10.1093/icesjms/fsv075

D'Amario, B., C. Perez, M. Grelaud, and others. 2020. Coccolithophore community response to ocean acidification and warming in the Eastern Mediterranean Sea: results from a mesocosm experiment. Sci. Rep. **10**: 12637. doi:10.1038/s41598-020-69519-5

D'Amario, B., P. Ziveri, M. Grelaud, A. Oviedo, and M. Kralj. 2017a. Coccolithophore haploid and diploid distribution patterns in the Mediterranean Sea: can a haplo-diploid life cycle be advantageous under climate change? J. Plankton Res. **39**: 781–794. doi:10.1093/plankt/fbx044

D'Amario, B., P. Ziveri, M. Grelaud, A. M. Oviedo, and M. Kralj. 2017b. Hydrology and geochemistry in the Mediterranean Sea during the MedSeA and Meteor M84/3 cruises (May 2013, April 2011). Suppl. to D'Amario, B al. Coccolithophore haploid diploid Distrib. patterns Mediterr. Sea can a haplo-diploid life cycle be advantageous under Clim. Chang. J. Plankt. Res. 1-14, https//doi.org/10.10. doi:10.1594/PANGAEA.875923

Davis, C. V., E. B. Rivest, T. M. Hill, B. Gaylord, A. D. Russell, and E. Sanford. 2017. Ocean acidification compromises a planktic calcifier with implications for global carbon cycling. Sci. Rep. **7**: 1–8. doi:10.1038/s41598-017-01530-9

Dayan, U., K. Nissen, and U. Ulbrich. 2015. Review Article: Atmospheric conditions inducing extreme precipitation over the eastern and western Mediterranean. Nat.

Hazards Earth Syst. Sci. **15**: 2525–2544. doi:10.5194/nhess-15-2525-2015

Dickson, A. G., and F. J. Millero. 1987. A comparison of the equilibrium constants for the dissociation of carbonic acid in seawater media. Deep Sea Res. Part A, Oceanogr. Res. Pap. **34**: 1733–1743. doi:10.1016/0198-0149(87)90021-5

Dimiza, D., O. Koukousioura, I. Michailidis, V.-G. Dimou, V. Navrozidou, K. Aligizaki, and M. Seferlis. 2020. Seasonal living coccolithophore distribution in the enclosed coastal environments of the Thessaloniki Bay (Thermaikos Gulf, NW Aegean Sea). Rev. Micropaléontologie **69**: 100449. doi:https://doi.org/10.1016/j.revmic.2020.100449

Dimiza, M. D., M. V Triantaphyllou, and M. D. Dermitzakis. 2008. Seasonality and ecology of living coccolithophores in Eastern Mediterranean coastal environments (Andros Island, Middle Aegean Sea). Micropalontology **54**: 159–175.

Dimiza, M., M. V Triantaphyllou, E. Malinverno, S. Psarra, B. T. Karatsolis, P. Mara, A. Lagaria, and A. Gogou. 2016. The composition and distribution of living coccolithophores in the Aegean Sea (NE Mediterranean). Micropaleontology **61**: 521–540.

Doney, S. C., V. J. Fabry, R. A. Feely, and J. A. Kleypas. 2009. Ocean Acidification: The Other CO2 Problem. Ann. Rev. Mar. Sci. **1**: 169–192. doi:10.1146/annurev.marine.010908.163834

Doney, S. C., M. Ruckelshaus, J. Emmett Duffy, and others. 2011. Climate Change Impacts on Marine Ecosystems. Ann. Rev. Mar. Sci. **4**: 11–37. doi:10.1146/annurev-marine-041911-111611

Doo, S. S., A. Kealoha, A. Andersson, and others. 2020. The challenges of detecting and attributing ocean acidification impacts on marine ecosystems. ICES J. Mar. Sci. **77**: 2411–2422. doi:10.1093/icesjms/fsaa094

Drakulović, D., B. Pestorić, and A. Huter. 2021. Distribution of Phytoplankton in Montenegrin Open Waters BT - The Montenegrin Adriatic Coast: Marine Biology, p. 73–105. *In* A. Joksimović, M. Đurović, I.S. Zonn, A.G. Kostianoy, and A. V Semenov [eds.]. Springer International Publishing.

Drakulović, D., B. Pestorić, R. Kraus, S. Ljubimir, and S. Krivokapić. 2017. Phytoplankton Community and Trophic State in Boka Kotorska Bay BT - The Boka Kotorska Bay Environment, p. 169–201. *In* A. Joksimović, M. Djurović, A. V Semenov, I.S. Zonn, and A.G. Kostianoy [eds.]. Springer International Publishing.

Dulvy, N., Y. Sadovy, and J. Reynolds. 2003. Extinction vulnerability in marine populations. Fish Fish. **4**: 25–64. doi:10.1046/j.1467-2979.2003.00105.x

Dupont, S., and M. Thorndyke. 2008. Ocean acidification and its impact on the early life-history stages of marine animals. Impacts Acidif. Biol. Chem. Phys. Syst. Mediterr. Black Seas 89–97.

Eker-Develi, E., A. E. Kideys, and S. Tugrul. 2006. Role of Saharan dust on phytoplankton dynamics in the northeastern Mediterranean. Mar. Ecol. Prog. Ser. **314**: 61–75. doi:10.3354/meps314061

El-Hady, H., S. A. Fathey, G. H. Ali, Y. G. Gabr, H. H. Abd El-Hady, S. A. Fathey, G. H. Ali, and Y. G. Gabr. 2016a. Biochemical profile of phytoplankton and its nutritional aspects in some khors of Lake Nasser, Egypt. Egypt. J. Basic Appl. Sci. **3**: 187–193. doi:10.1016/j.ejbas.2016.03.002

El-Hady, H., S. Fathey, G. Ali, and Y. Gabr. 2016b. Biochemical profile of phytoplankton and its nutritional aspects in some khors of Lake Nasser, Egypt. Egypt. J. Basic Appl. Sci. doi:10.1016/j.ejbas.2016.03.002

Engel, A., I. Zondervan, K. Aerts, and others. 2005. Testing the direct effect of CO2 concentration on a bloom of the coccolithophorid Emiliania huxleyi in mesocosm experiments. Limnol. Oceanogr. **50**: 493–507. doi:https://doi.org/10.4319/lo.2005.50.2.0493

Engström-Öst, J., O. Glippa, R. A. Feely, and others. 2019. Eco-physiological responses of copepods and pteropods to ocean warming and acidification. Sci. Rep. **9**: 1–13. doi:10.1038/s41598-019-41213-1

Estrada, M., and R. Margalef. 1988. Supply of nutrients to the Mediterranean photic zone along a persistent front. Ocean. Acta **0399**.

Estrada, M., and J. Salat. 1989. Phytoplankton assemblages of deep and surface water layers in a Mediterranean frontal zone. Sci. Mar. **53**: 203–214.

Estrada, M., R. A. Varela, J. Salat, A. Cruzado, and E. Arias. 1999. Spatio-temporal variability of the winter phytoplankton distribution across the Catalan and North Balearic fronts (NW Mediterranean). J. Plankton Res. **21**: 1–20. doi:10.1093/plankt/21.1.1

Fabry, V. J. 1989. Aragonite production by pteropod molluscs in the subarctic Pacific. Deep Sea Res. Part A, Oceanogr. Res. Pap. **36**: 1735–1751. doi:10.1016/0198-0149(89)90069-1

Fabry, V. J., B. A. Seibel, R. A. Feely, and J. C. Orr. 2008. Impacts of ocean

acidification on marine fauna and ecosystem processes. ICES J. Mar. Sci. **65**: 414–432. doi:10.1093/icesjms/fsn048

Falkowski, P. G., T. Fenchel, and E. F. Delong. 2008. The Microbial Engines That Drive Earth's Biogeochemical Cycles. Science (80-.). **320**: 1034–1039. doi:10.1126/science.1153213

Fedele, G., E. Mauri, G. Notarstefano, and P. M. Poulain. 2022. Characterization of the Atlantic Water and Levantine Intermediate Water in the Mediterranean Sea using 20 years of Argo data. Ocean Sci. **18**: 129–142. doi:10.5194/os-18-129-2022

Feely, R. A., C. L. Sabine, K. Lee, W. Berelson, J. Kleypas, V. J. Fabry, and F. J. Millero. 2004. Impact of anthropogenic CO2 on the CaCO3 system in the oceans. Science (80-.). **305**: 362–366. doi:10.1126/science.1097329

Feng, Y., M. Y. Roleda, E. Armstrong, P. W. Boyd, and C. L. Hurd. 2017. Environmental controls on the growth, photosynthetic and calcification rates of a Southern Hemisphere strain of the coccolithophore Emiliania huxleyi. Limnol. Oceanogr. **62**: 519–540. doi:10.1002/lno.10442

Feng, Y., M. E. Warner, Y. Zhan, J. Sun, F. Fu, J. M. Rose, and D. A. Hutchins. 2008. Interactive effects of increased pCO2, temperature and irradiance on the marine coccolithophore Emiliania huxleyi (Prymnesiophyceae). Eur. J. Phycol. **43**: 87–98. doi:10.1080/09670260701664674

Fernández de Puelles, M. L., F. Alemany, and J. Jansá. 2007. Zooplankton time-series in the Balearic Sea (Western Mediterranean): Variability during the decade 1994–2003. Prog. Oceanogr. **74**: 329–354. doi:10.1016/j.pocean.2007.04.009

Fielding, S. R. R. 2013. Emiliania huxleyi specific growth rate dependence on temperature. Limnol. Oceanogr. **58**: 663–666. doi:https://doi.org/10.4319/lo.2013.58.2.0663

Figuerola, B., A. M. Hancock, N. Bax, V. J. Cummings, R. Downey, H. J. Griffiths, J. Smith, and J. S. Stark. 2021. A Review and Meta-Analysis of Potential Impacts of Ocean Acidification on Marine Calcifiers From the Southern Ocean . Front. Mar. Sci. **8**.

Fiorini, S., J.-P. Gattuso, P. van Rijswijk, and J. J. Middelburg. 2010. Coccolithophores lipid and carbon isotope composition and their variability related to changes in seawater carbonate chemistry. J. Exp. Mar. Bio. Ecol. **394**: 74–85. doi:10.1016/j.jembe.2010.07.020

Flecha, S., F. F. Pérez, J. García-Lafuente, S. Sammartino, A. F. Ríos, and I. E. Huertas.

2015. Trends of pH decrease in the Mediterranean Sea through high frequency observational data: indication of ocean acidification in the basin. Sci. Rep. **5**: 16770. doi:10.1038/srep16770

Font, J., J. Salat, and J. Tintore. 1988. Permanent features of the circulation in the Catalan Sea. Oceanol. Acta **9**: 51–57.

Fox, L., S. Stukins, T. Hill, and C. G. Miller. 2020. Quantifying the Effect of Anthropogenic Climate Change on Calcifying Plankton. Sci. Rep. **10**: 1620. doi:10.1038/s41598-020-58501-w

Fraser, A. J., J. R. Sargent, J. C. Gamble, and D. D. Seaton. 1989. Formation and transfer of fatty acids in an enclosed marine food chain comprising phytoplankton, zooplankton and herring (Clupea harengus L.) larvae. Mar. Chem. **27**: 1–18. doi:https://doi.org/10.1016/0304-4203(89)90024-8

Friedlingstein, P., M. O'Sullivan, M. W. Jones, and others. 2022. Global Carbon Budget 2022. Earth Syst. Sci. Data **14**: 4811–4900. doi:10.5194/essd-14-4811-2022

Fuentes-Grünewald, C., E. Garcés, E. Alacid, N. Sampedro, S. Rossi, and J. Camp. 2012. Improvement of lipid production in the marine strains Alexandrium minutum and Heterosigma akashiwo by utilizing abiotic parameters. J. Ind. Microbiol. Biotechnol. **39**: 207–216. doi:10.1007/s10295-011-1016-6

Fuertes, M.-Á., J.-A. Flores, and F. J. Sierro. 2014. The use of circularly polarized light for biometry, identification and estimation of mass of coccoliths. Mar. Micropaleontol. **113**: 44–55. doi:https://doi.org/10.1016/j.marmicro.2014.08.007

Fukuda, S. Y., Y. Suzuki, and Y. Shiraiwa. 2014. Difference in physiological responses of growth, photosynthesis and calcification of the coccolithophore Emiliania huxleyi to acidification by acid and CO2 enrichment. Photosynth. Res. **121**: 299–309. doi:10.1007/s11120-014-9976-9

Gafar, N. A., B. D. Eyre, and K. G. Schulz. 2018. A Conceptual Model for Projecting Coccolithophorid Growth, Calcification and Photosynthetic Carbon Fixation Rates in Response to Global Ocean Change . Front. Mar. Sci. **4**: 433.

Garcia-Gorriz, E., and M.-E. Carr. 1999. The climatological annual cycle of satellite-derived phytoplankton pigments in the Alboran Sea. Geophys. Res. Lett. **26**: 2985–2988. doi:https://doi.org/10.1029/1999GL900529

Gardner, J. 2019. Winners and losers in a changing ocean: Impact on the physiology and life history of pteropods in the Scotia Sea; Southern Ocean. University of East Anglia.

Gattuso, J.-P., A. Magnan, R. Billé, and others. 2015. Contrasting futures for ocean and society from different anthropogenic CO2 emissions scenarios. Science (80-.). **349**: aac4722. doi:10.1126/science.aac4722

Geider, R., and J. La Roche. 2002. Redfield revisited: variability of C:N:P in marine microalgae and its biochemical basis. Eur. J. Phycol. **37**: 1–17. doi:10.1017/S0967026201003456

Gemayel, E., A. E. R Hassoun, M. A. Benallal, and others. 2015. Climatological variations of total alkalinity and total dissolved inorganic carbon in the Mediterranean Sea surface waters. Earth Syst. Dyn. **6**: 789–800. doi:10.5194/esd-6-789-2015

Geri, P., S. El Yacoubi, and C. Goyet. 2014. Forecast of Sea Surface Acidification in the Northwestern Mediterranean Sea. J. Comput. Environ. Sci. **2014**: 1–7. doi:10.1155/2014/201819

Giamali, C., G. Kontakiotis, A. Antonarakou, and E. Koskeridou. 2021. Ecological Constraints of Plankton Bio-Indicators for Water Column Stratification and Productivity: A Case Study of the Holocene North Aegean Sedimentary Record. J. Mar. Sci. Eng. **9**. doi:10.3390/jmse9111249

Gibbs, S. J., A. J. Poulton, P. R. Bown, and others. 2013. Species-specific growth response of coccolithophores to Palaeocene–Eocene environmental change. Nat. Geosci. **6**: 218–222. doi:10.1038/ngeo1719

Gili, J.-M., and R. Coma. 1998. Benthic suspension feeders: their paramount role in littoral marine food webs. Trends Ecol. Evol. **13**: 316–321. doi:https://doi.org/10.1016/S0169-5347(98)01365-2

Gilmer, R. W., and G. R. Harbison. 1986. Morphology and field behavior of pteropod molluscs: feeding methods in the families Cavoliniidae, Limacinidae and Peraclididae (Gastropoda: Thecosomata). Mar. Biol. **91**: 47–57. doi:10.1007/BF00397570

Giorgi, F. 2006. Climate change hot-spots. Geophys. Res. Lett. **33**: L08707. doi:10.1029/2006GL025734

Godrijan, J., D. Marić, I. Tomažić, R. Precali, and M. Pfannkuchen. 2013. Seasonal phytoplankton dynamics in the coastal waters of the north-eastern Adriatic Sea. J. Sea Res. **77**: 32–44. doi:https://doi.org/10.1016/j.seares.2012.09.009

Godrijan, J., J. R. Young, D. M. Pfannkuchen, R. Precali, and M. Pfannkuchen. 2018. Coastal zones as important habitats of coccolithophores: A study of species

diversity, succession, and life-cycle phases. Limnol. Oceanogr. **63**: 1692–1710. doi:10.1002/lno.10801

Gori, A., C. Linares, N. Viladrich, and others. 2013. Effects of food availability on the sexual reproduction and biochemical composition of the Mediterranean gorgonian Paramuricea clavata. J. Exp. Mar. Bio. Ecol. **444**: 38–45. doi:https://doi.org/10.1016/j.jembe.2013.03.009

Gotsis-Skretas, O., K. Pagou, M. Moraitou-Apostolopoulou, and L. Ignatiades. 1999. Seasonal horizontal and vertical variability in primary production and standing stocks of phytoplankton and zooplankton in the Cretan Sea and the Straits of the Cretan Arc (March 1994-Jannuary 1995). Prog. Oceanogr. **44**: 625–649. doi:10.1016/S0079-6611(99)00048-8

Goyet, C., A. E. R. R. Hassoun, E. Gemayel, F. Touratier, M. Abboud-Abi Saab, V. Guglielmi, M. Abbous-Abi Saab, and V. Guglielmi. 2016. Thermodynamic forecasts of the Mediterranean Sea acidification. Mediterr. Mar. Sci. **17**: 508–518. doi:10.12681/mms.1487

Goyet, C., A. El Rahman Hassoun, and E. Gemayel. 2015. Carbonate system during the May 2013 MedSeA cruise. PANGAEA. doi:10.1594/PANGAEA.841933

Granata, A., A. Bergamasco, P. Battaglia, and others. 2020. Vertical distribution and diel migration of zooplankton and micronekton in Polcevera submarine canyon of the Ligurian mesopelagic zone (NW Mediterranean Sea). Prog. Oceanogr. **183**: 102298. doi:https://doi.org/10.1016/j.pocean.2020.102298

Grandjacquet, C., and G. Mascle. 1978. The Structure of the Ionian Sea, Sicily, and Calabria-Lucania BT - The Ocean Basins and Margins, p. 257–329. *In* A.E.M. Nairn, W.H. Kanes, and F.G. Stehli [eds.]. Springer US.

Grasshoff, K., and K. Kremling. 1999. Methods of seawater analysis, 3rd ed. K. Grasshoff, M. Ehrhardt, and K. Kremling [eds.]. Wiley-VCH.

Guinder, V., and J. Molinero. 2013. Climate Change Effects on Marine Phytoplankton, p. 68–90. *In* Marine Ecology in a Changing World. CRC Press.

Hamner, W. M., L. P. Madin, A. L. Alldrege, R. W. Gilmer, and P. P. Hamner. 1975. Underwater observations of gelatinous zooplankton: sampling problems, feeding biology, and behavior. Limnol. Oceanogr. **20**: 907–917.

Han, T., Z. Qi, R. Shi, Q. Liu, M. Dai, and H. Huang. 2022. Effects of Seawater Temperature and Salinity on Physiological Performances of Swimming Shelled Pteropod Creseis acicula During a Bloom Period . Front. Mar. Sci. **9**.

Hansen, H. P. 1999. Determination of oxygen. Methods Seawater Anal. 75–89. doi:https://doi.org/10.1002/9783527613984.ch4

Harbison, G. R., and R. W. Gilmer. 1992. Swimming, buoyancy and feeding in shelled pteropods: a comparison of field and laboratory observations. J. Molluscan Stud. **58**: 337–339. doi:10.1093/mollus/58.3.337

Harley, C. D. G. G., A. R. Hughes, K. M. Hultgren, and others. 2006. The impacts of climate change in coastal marine systems. Ecol. Lett. **9**: 228–241. doi:10.1111/j.1461-0248.2005.00871.x

Harris, R. P. 1994. Zooplankton grazing on the coccolithophore Emiliania huxleyi and its role in inorganic carbon flux. Mar. Biol. **119**: 431–439. doi:10.1007/BF00347540

Harvey, E. L., K. D. Bidle, and M. D. Johnson. 2015. Consequences of strain variability and calcification in Emiliania huxleyi on microzooplankton grazing. J. Plankton Res. **37**: 1137–1148. doi:10.1093/plankt/fbv081

Hassoun, A. E. R., A. Bantelman, D. M. Canu, and others. 2022. Ocean acidification research in the Mediterranean Sea: Status, trends and next steps. Front. Mar. Sci. **9**. doi:org/10.3389/fmars.2022.892670

Hassoun, A. E. R., M. Fakhri, N. Raad, M. Abboud-Abi Saab, E. Gemayel, and E. H. De Carlo. 2019. The carbonate system of the Eastern-most Mediterranean Sea, Levantine Sub-basin: Variations and drivers. Deep. Res. Part II Top. Stud. Oceanogr. **164**: 54–73. doi:10.1016/j.dsr2.2019.03.008

Hassoun, A. E. R., E. Gemayel, E. Krasakopoulou, C. Goyet, M. Abboud-Abi Saab, V. Guglielmi, F. Touratier, and C. Falco. 2015a. Acidification of the Mediterranean Sea from anthropogenic carbon penetration. Deep Sea Res. Part I Oceanogr. Res. Pap. **102**: 1–15. doi:10.1016/J.DSR.2015.04.005

Hassoun, A. E. R., V. Guglielmi, E. Gemayel, and others. 2015b. Is the Mediterranean Sea Circulation in a Steady State. J. Water Resour. Ocean Sci. **4**: 6. doi:10.11648/j.wros.20150401.12

Hattab, T., C. Albouy, F. B. R. Lasram, S. Somot, F. Le Loc'h, and F. Leprieur. 2014. Towards a better understanding of potential impacts of climate change on marine species distribution: a multiscale modelling approach. Glob. Ecol. Biogeogr. **23**: 1417–1429. doi:https://doi.org/10.1111/geb.12217

Haunost, M., U. Riebesell, F. D'Amore, O. Kelting, and L. T. T. Bach. 2021. Influence of the Calcium Carbonate Shell of Coccolithophores on Ingestion and Growth of a

Dinoflagellate Predator . Front. Mar. Sci. **8**.

Heburn, G. W., and P. E. La Violette. 1990. Variations in the structure of the anticyclonic gyres found in the Alboran Sea. J. Geophys. Res. Ocean. **95**: 1599–1613. doi:https://doi.org/10.1029/JC095iC02p01599

Heiri, O., A. F. Lotter, and G. Lemcke. 2001. Loss on ignition as a method for estimating organic and carbonate content in sediments: reproducibility and comparability of results. J. Paleolimnol. **25**: 101–110. doi:10.1023/A:1008119611481

Henehan, M. J., D. Evans, M. Shankle, and others. 2017. Size-dependent response of foraminiferal calcification to seawater carbonate chemistry. Biogeosciences **14**: 3287–3308. doi:10.5194/bg-14-3287-2017

Hernández-Almeida, I., M. A. Bárcena, J. A. Flores, F. J. Sierro, A. Sanchez-Vidal, and A. Calafat. 2011. Microplankton response to environmental conditions in the Alboran Sea (Western Mediterranean): One year sediment trap record. Mar. Micropaleontol. **78**: 14–24. doi:https://doi.org/10.1016/j.marmicro.2010.09.005

van Heuven, S., D. Pierrot, E. Lewis, and E. W. R. Wallace. 2009. MATLAB Program Developed for CO2 System Calculations. ORNL/CDIAC-105b.

Hinz, D. J., A. J. Poulton, M. C. Nielsdóttir, S. Steigenberger, R. E. Korb, E. P. Achterberg, and T. S. Bibby. 2012. Comparative seasonal biogeography of mineralising nannoplankton in the Scotia Sea: Emiliania huxleyi, Fragilariopsis spp. and Tetraparma pelagica. Deep Sea Res. Part II Top. Stud. Oceanogr. **59**–**60**: 57–66. doi:https://doi.org/10.1016/j.dsr2.2011.09.002

Hofmann Elizondo, U., and M. Vogt. 2022. Individual-based modeling of shelled pteropods. Ecol. Modell. **468**: 109944. doi:https://doi.org/10.1016/j.ecolmodel.2022.109944

Holligan, P. M., E. Fernández, J. Aiken, and others. 1993. A biogeochemical study of the coccolithophore, Emiliania huxleyi, in the North Atlantic. Global Biogeochem. Cycles **7**: 879–900. doi:https://doi.org/10.1029/93GB01731

Hoppe, C. J. M., G. Langer, and B. Rost. 2011. Emiliania huxleyi shows identical responses to elevated pCO2 in TA and DIC manipulations. J. Exp. Mar. Bio. Ecol. **406**: 54–62. doi:https://doi.org/10.1016/j.jembe.2011.06.008

Howes, E. 2015. The effects of ocean acidification on calcification and incorporation of isotopes in Mediterranean pteropods and foraminifers To cite this version : HAL Id : tel-01127368.

Howes, E. L., N. Bednaršek, J. Büdenbender, and others. 2014. Sink and swim: a status review of thecosome pteropod culture techniques. J. Plankton Res. **36**: 299–315. doi:10.1093/plankt/fbu002

Howes, E. L., R. A. Eagle, J.-P. Gattuso, and J. Bijma. 2017. Comparison of Mediterranean pteropod shell biometrics and ultrastructure from historical (1910 and 1921) and present day (2012) samples provides baseline for monitoring effects of global change F. Melzner [ed.]. PLoS One **12(1)**: e0167891. doi:10.1371/journal.pone.0167891.s008

Howes, E. L., L. Stemmann, C. Assailly, J. O. Irisson, M. Dima, J. Bijma, and J. P. Gattuso. 2015. Pteropod time series from the North Western Mediterranean (1967-2003): Impacts of pH and climate variability. Mar. Ecol. Prog. Ser. **531**: 193–206. doi:10.3354/meps11322

Iglesias-Rodríguez, M. D., C. W. Brown, S. C. Doney, J. Kleypas, D. Kolber, Z. Kolber, P. K. Hayes, and P. G. Falkowski. 2002. Representing key phytoplankton functional groups in ocean carbon cycle models: Coccolithophorids. Global Biogeochem. Cycles **16**: 20–47. doi:https://doi.org/10.1029/2001GB001454

Iglesias-Rodriguez, M. D., P. R. Halloran, R. E. M. Rickaby, and others. 2008. Phytoplankton Calcification in a High-CO2 World. Science (80-.). **320**: 336 LP – 340. doi:10.1126/science.1154122

Ignatiades, L., D. Georgopoulos, and M. Karydis. 1995. Description of the phytoplankton community of the oligotrophic waters of the SE Aegean Sea (Mediterranean). Mar. Ecol. Publicazioni Della Stn. Cool. Di Napolo I **16**: 13–26. doi:10.1111/j.1439-0485.1995.tb00391.x

IPCC. 2019. IPCC, 2019: IPCC Special Report on the Ocean and Cryosphere in a Changing Climate.

IPCC 2022. Climate Change 2022: Impacts, Adaptation, and Vulnerability. Pörtner, H.-O. Roberts, D.C. Tignor, M. Poloczanska, E.S. Mintenbeck, K. Alegría, A.ç Craig, M. Langsdorf, S. Löschke, S. Möller, V. Okem, A. Rama, B.

Jansen, S. 2008. Copepods grazing on Coscinodiscus wailesii: a question of size? Helgol. Mar. Res. **62**: 251–255. doi:10.1007/s10152-008-0113-z

Jaya, B. N., R. Hoffmann, C. Kirchlechner, G. Dehm, C. Scheu, and G. Langer. 2016. Coccospheres confer mechanical protection: New evidence for an old hypothesis. Acta Biomater. **42**: 258–264. doi:https://doi.org/10.1016/j.actbio.2016.07.036

Jeffrey, S. W., and G. F. Humphrey. 1975. New spectrophotometric equations for

determining chlorophylls a, b, c1 and c2 in higher plants, algae and natural phytoplankton. Biochem. und Physiol. der Pflanz. **167**: 191–194. doi:https://doi.org/10.1016/S0015-3796(17)30778-3

Jiang, X., H. Li, S. Tong, and K. Gao. 2022. Nitrogen Limitation Enhanced Calcification and Sinking Rate in the Coccolithophorid Gephyrocapsa oceanica Along With Its Growth Being Reduced. Front. Mar. Sci. **9**. doi:10.3389/fmars.2022.834358

Jin, P., and K. Gao. 2016. Reduced resilience of a globally distributed coccolithophore to ocean acidification: Confirmed up to 2000 generations. Mar. Pollut. Bull. **103**: 101–108. doi:https://doi.org/10.1016/j.marpolbul.2015.12.039

Jin, P., D. A. A. Hutchins, and K. Gao. 2020. The Impacts of Ocean Acidification on Marine Food Quality and Its Potential Food Chain Consequences . Front. Mar. Sci. **7**.

Johnson, R., J. Harianto, M. Thomson, and M. Byrne. 2020. The effects of long-term exposure to low pH on the skeletal microstructure of the sea urchin Heliocidaris erythrogramma. J. Exp. Mar. Bio. Ecol. **523**: 151250. doi:10.1016/j.jembe.2019.151250

Johnson, R., G. Langer, S. Rossi, I. Probert, M. Mammone, and P. Ziveri. 2022. Nutritional response of a coccolithophore to changing pH and temperature. Limnol. Oceanogr. **67**. doi:https://doi.org/10.1002/lno.12204

Johnson, R., C. Manno, and P. Ziveri. 2023. Shelled pteropod abundance and distribution across the Mediterranean Sea during spring. Prog. Oceanogr. **210**: 102930. doi:https://doi.org/10.1016/j.pocean.2022.102930

Juranek, L. W., A. D. Russell, and H. J. Spero. 2003. Seasonal oxygen and carbon isotope variability in euthecosomatous pteropods from the Sargasso Sea. Deep. Res. Part I Oceanogr. Res. Pap. **50**: 231–245. doi:10.1016/S0967-0637(02)00164-4

Kacprzak, P., A. Panasiuk, J. Wawrzynek, and A. Weydmann. 2017. No Title. Oceanol. Hydrobiol. Stud. **46**: 393–404. doi:10.1515/ohs-2017-0039

Kapsenberg, L., S. Alliouane, F. Gazeau, L. Mousseau, and J.-P. Gattuso. 2017. Coastal ocean acidification and increasing total alkalinity in the northwestern Mediterranean Sea. Ocean Sci **13**: 411–426. doi:10.5194/os-13-411-2017

Karatsolis, B. T., M. V Triantaphyllou, M. D. Dimiza, E. Malinverno, A. Lagaria, P. Mara, O. Archontikis, and S. Psarra. 2017. Coccolithophore assemblage response to Black Sea Water inflow into the North Aegean Sea (NE Mediterranean). Cont.

Shelf Res. **149**: 138–150. doi:10.1016/j.csr.2016.12.005

Karnovsky, N., K. Hobson, S. Iverson, and H. G. L. Jr. 2008. Seasonal changes in diets of seabirds in the North Water Polynya: a multiple-indicator approach. Mar. Ecol. Prog. Ser. **357**: 291–299.

Kasozi, G. N., P. Nkedi-Kizza, and W. G. Harris. 2009. Varied Carbon Content of Organic Matter in Histosols, Spodosols, and Carbonatic Soils. Soil Sci. Soc. Am. J. **73**: 1313–1318. doi:https://doi.org/10.2136/sssaj2008.0070

Kemle-von Mücke, S., and H. Oberhänsli. 1999. The Distribution of Living Planktic Foraminifera in Relation to Southeast Atlantic Oceanography BT - Use of Proxies in Paleoceanography: Examples from the South Atlantic, p. 91–115. *In* G. Fischer and G. Wefer [eds.]. Springer Berlin Heidelberg.

Keul, N., K. T. C. A. C. A. Peijnenburg, N. Andersen, V. Kitidis, E. Goetze, and R. R. Schneider. 2017. Pteropods are excellent recorders of surface temperature and carbonate ion concentration. Sci. Rep. **7**: 12645. doi:10.1038/s41598-017-11708-w

Keuter, S., J. Silverman, M. D. Krom, and others. 2022. Seasonal patterns of coccolithophores in the ultra-oligotrophic South-East Levantine Basin, Eastern Mediterranean Sea. Mar. Micropaleontol. **175**: 102153. doi:https://doi.org/10.1016/j.marmicro.2022.102153

Kharbush, J. J., H. G. Close, B. A. S. Van Mooy, and others. 2020. Particulate Organic Carbon Deconstructed: Molecular and Chemical Composition of Particulate Organic Carbon in the Ocean. Front. Mar. Sci. **7**: 518.

Kimor, B., T. Berman, and A. Schneller. 1987. Phytoplankton assemblages in the deep chlorophyll maximum layers off the Mediterranean coast of Israel. J. Plankton Res. **9**: 433–443. doi:10.1093/plankt/9.3.433

Klaas, C., and D. E. Archer. 2002. Association of sinking organic matter with various types of mineral ballast in the deep sea: Implications for the rain ratio. Global Biogeochem. Cycles **16**: 63-1-63–14. doi:10.1029/2001GB001765

Klauschies, T., B. Bauer, N. Aberle-Malzahn, U. Sommer, and U. Gaedke. 2012. Climate change effects on phytoplankton depend on cell size and food web structure. Mar. Biol. **159**: 2455–2478. doi:10.1007/s00227-012-1904-y

Kleijne, A. 1991. Holococcolithophorids from the Indian-Ocean, Red-Sea, Mediterranean-Sea and north-Atlantic Ocean. Mar. Micropaleontol. **17**: 1–76. doi:10.1016/0377-8398(91)90023-Y

Klintzsch, T., G. Langer, G. Nehrke, A. Wieland, K. Lenhart, and F. Keppler. 2019.

Methane production by three widespread marine phytoplankton species: Release rates, precursor compounds, and potential relevance for the environment. Biogeosciences **16**: 4129–4144. doi:10.5194/bg-16-4129-2019

Knappertsbusch, M. 1993. Geographic distribution of living and holocene coccolithophores in the Mediterranean Sea. Mar. Micropaleontol. **21**: 219–247. doi:10.1016/0377-8398(93)90016-Q

Knoll, A. H., R. K. Bambach, D. E. Canfield, and J. P. Grotzinger. 1996. Comparative Earth History and Late Permian Mass Extinction. Science (80-.). **273**: 452–457. doi:10.1126/science.273.5274.452

Kottmeier, D. M., A. Chrachri, G. Langer, K. E. Helliwell, G. L. Wheeler, and C. Brownlee. 2022. Reduced H+ channel activity disrupts pH homeostasis and calcification in coccolithophores at low ocean pH. Proc. Natl. Acad. Sci. **119**: e2118009119. doi:10.1073/pnas.2118009119

Kourafalou, V. H., and K. Barbopoulos. 2003. High resolution simulations on the North Aegean Sea seasonal circulation. Ann. Geophys. **21**: 251–265. doi:10.5194/angeo-21-251-2003

Kreeger, D., and A. Padeletti. 2020. Loss-On-Ignition (LOI) Weight Analyses. Partnership for the Delaware Estuary. PDE Method No. 33.

Krivokapic, S., S. Bosak, D. Vilicic, G. Kuspilic, D. Drakulovic, and B. Pestoric. 2018. Algal pigments distribution and phytoplankton group assemblages in coastal transitional environment - Boka Kotorska Bay (South eastern Adriatic Sea). ACTA Adriat. **59**: 35–50. doi:10.32582/aa.59.1.3

Kroeker, K. J., R. L. Kordas, R. Crim, I. E. Hendriks, L. Ramajo, G. S. Singh, C. M. Duarte, and J.-P. Gattuso. 2013a. Impacts of ocean acidification on marine organisms: quantifying sensitivities and interaction with warming. Glob. Chang. Biol. **19**: 1884–1896. doi:10.1111/gcb.12179

Kroeker, K. J., R. L. Kordas, R. N. Crim, and G. G. Singh. 2010. Meta-analysis reveals negative yet variable effects of ocean acidification on marine organisms. Ecol. Lett. **13**: 1419–1434. doi:https://doi.org/10.1111/j.1461-0248.2010.01518.x

Kroeker, K. J., F. Micheli, and M. C. Gambi. 2013b. Ocean acidification causes ecosystem shifts via altered competitive interactions. Nat. Clim. Chang. **3**: 156–159. doi:10.1038/nclimate1680

Krom, M. D., N. Kress, S. Brenner, and L. I. Gordon. 1991. Phosphorus limitation of primary productivity in the eastern Mediterranean Sea. Limnol. Oceanogr. **36**:

424–432. doi:10.4319/lo.1991.36.3.0424

Krumhardt, K. M., N. S. Lovenduski, M. D. Iglesias-Rodriguez, and J. A. Kleypas. 2017. Coccolithophore growth and calcification in a changing ocean. Prog. Oceanogr. **159**: 276–295. doi:10.1016/j.pocean.2017.10.007

Kuroyanagi, A., T. Irie, S. Kinoshita, and others. 2021. Decrease in volume and density of foraminiferal shells with progressing ocean acidification. Sci. Rep. **11**: 19988. doi:10.1038/s41598-021-99427-1

Kuwata, A., T. Hama, and M. Takahashi. 1993. Ecophysiological characterization of two life forms, resting spores and resting cells, of a marine planktonic diatom, Chaetoceros pseudocun/isetus, formed under nutrient depletion. Mar. Ecol. Prog. Ser. **102**: 245–255. doi:10.3354/meps102245

Lacoue-Labarthe, T., P. A. L. D. Nunes, P. Ziveri, and others. 2016. Impacts of ocean acidification in a warming Mediterranean Sea: An overview. Reg. Stud. Mar. Sci. **5**: 1–11.

Lalli, C. M., and R. W. Gilmer. 1989. Pelagic snails : the biology of holoplanktonic gastropod mollusks, Stanford University Press.

Lalli, C. M., and F. E. Wells. 1973. Brood protection in an epipelagic thecosomatous pteropod, Spiratella ("Limacina") Inflata (D'Orbigny). Bull. Mar. Sci. **23**: 933–941.

Lalli, C. M., and F. E. Wells. 1978. Reproduction in the genus Limacina (Opisthobranchia: Thecosomata). J. Zool. **186**: 95–108. doi:https://doi.org/10.1111/j.1469-7998.1978.tb03359.x

Lalli, C. M., F. E. Wells, M. Lalli, F. E. Wells, C. M. Lalli, F. E. Wells, M. Lalli, and F. E. Wells. 1978. Reproduction in the genus Limacina (Opisthobranchia: Thecosomata). J. Zool. **186**: 95–108. doi:https://doi.org/10.1111/j.1469-7998.1978.tb03359.x

Langer, G., M. Geisen, K. H. Baumann, J. Klas, U. Riebesell, S. Thoms, and J. R. Young. 2006. Species-specific responses of calcifying algae to changing seawater carbonate chemistry. Geochemistry, Geophys. Geosystems **7**: Q09006. doi:10.1029/2005GC001227

Langer, G., N. Gussone, G. Nehrke, U. Riebesell, A. Eisenhauer, and S. Thoms. 2007a. Calcium isotope fractionation during coccolith formation in Emiliania huxleyi: Independence of growth and calcification rate. Geochemistry, Geophys. Geosystems **8**. doi:https://doi.org/10.1029/2006GC001422

Langer, G., G. Nehrke, and S. Jansen. 2007b. Dissolution of Calcidiscus leptoporus coccoliths in copepod guts? A morphological study. Mar. Ecol. Ser. - MAR ECOL-PROGR SER **331**: 139–146. doi:10.3354/meps331139

Langer, G., G. Nehrke, I. Probert, J. Ly, and P. Ziveri. 2009. Strain-specific responses of Emiliania huxleyi to changing seawater carbonate chemistry. Biogeosciences **6**: 2637–2646. doi:10.5194/bg-6-2637-2009

Langer, G., I. Probert, G. Nehrke, and P. Ziveri. 2011. The morphological response of Emiliania huxleyi to seawater carbonate chemistry changes: An inter-strain comparison. J. Nannoplankt. Res. **32**: 29–34.

Lascaratos, A., and K. Nittis. 1998. A high-resolution three-dimensional numerical study of intermediate water formation in the Levantine Sea. J. Geophys. Res. Ocean. **103**: 18497–18511. doi:https://doi.org/10.1029/98JC01196

Lazzari, P., G. Mattia, C. Solidoro, S. Salon, A. Crise, M. Zavatarelli, P. Oddo, and M. Vichi. 2013. The impacts of climate change and environmental management policies on the trophic regimes in the Mediterranean Sea: Scenario analyses. J. Mar. Syst. **135**: 137–149. doi:10.1016/j.jmarsys.2013.06.005

Lee, J.-Y., J. Marotzke, G. Bala, and others. 2021. Climate Change 2021: The Physical Science Basis. Contribution of Working Group I to the Sixth Assessment Report of the Intergovernmental Panel on Climate Change, *In* V. Masson-Delmotte, P. Zhai, A. Pirani, et al. [eds.]. Cambridge University Press.

Lefebvre, S. C., I. Benner, J. H. Stillman, and others. 2011. Nitrogen source and pCO2 synergistically affect carbon allocation, growth and morphology of the coccolithophore Emiliania huxleyi: potential implications of ocean acidification for the carbon cycle. Glob. Chang. Biol. **18**: 493–503. doi:10.1111/j.1365-2486.2011.02575.x

Lessa, D., R. Morard, L. Jonkers, I. M. Venancio, R. Reuter, A. Baumeister, A. L. Albuquerque, and M. Kucera. 2020. Distribution of planktonic foraminifera in the subtropical South Atlantic: depth hierarchy of controlling factors. Biogeosciences **17**: 4313–4342. doi:10.5194/bg-17-4313-2020

Leung, J. Y. S., S. Zhang, and S. D. Connell. 2022. Is Ocean Acidification Really a Threat to Marine Calcifiers? A Systematic Review and Meta-Analysis of 980+ Studies Spanning Two Decades. Small **18**: 2107407. doi:https://doi.org/10.1002/smll.202107407

Levitus, S., J. Antonov, and T. Boyer. 2005. Warming of the world ocean, 1955–2003.

Geophys. Res. Lett. **32**. doi:https://doi.org/10.1029/2004GL021592

Lewis, M. R., J. J. Cullen, and T. Platt. 1984. Relationships between vertical mixing and photoadaptation of phytoplankton: Similarity criteria. Mar. Ecol. Prog. Ser. **15**: 141–149. doi:10.3354/meps015141

Lionello, P., and L. Scarascia. 2018. The relation between climate change in the Mediterranean region and global warming. Reg. Environ. Chang. **18**: 1481–1493. doi:10.1007/s10113-018-1290-1

Lischka, S., J. Büdenbender, T. Boxhammer, and U. Riebesell. 2011. Impact of ocean acidification and elevated temperatures on early juveniles of the polar shelled pteropod Limacina helicina: Mortality, shell degradation, and shell growth. Biogeosciences **8**: 919–932. doi:10.5194/bg-8-919-2011

Litzow, M. 2006. Climate regime shifts and community reorganization in the Gulf of Alaska: how do recent shifts compare with 1976/1977? Ices J. Mar. Sci. **63**: 1386–1396. doi:10.1016/j.icesjms.2006.06.003

Liu, X., M. C. Patsavas, and R. H. Byrne. 2011. Purification and Characterization of meta-Cresol Purple for Spectrophotometric Seawater pH Measurements. Environ. Sci. Technol. **45**: 4862–4868. doi:10.1021/es200665d

Loubere, P., S. A. Siedlecki, and L. I. Bradtmiller. 2007. Organic carbon and carbonate fluxes: Links to climate change. Deep Sea Res. Part II Top. Stud. Oceanogr. **54**: 437–446. doi:https://doi.org/10.1016/j.dsr2.2007.02.001

Maas, A. E., G. L. Lawson, A. J. Bergan, and A. M. Tarrant. 2017. Exposure to CO 2 influences metabolism, calcification and gene expression of the thecosome pteropod Limacina retroversa. J. Exp. Biol. **221**: jeb164400. doi:10.1242/jeb.164400

Maas, A. E., K. F. Wishner, and B. A. Seibel. 2012a. The metabolic response of pteropods to acidification reflects natural CO2-exposure in oxygen minimum zones. Biogeosciences **9**: 747–757. doi:10.5194/bg-9-747-2012

Maas, A. E., K. F. Wishner, and B. A. Seibel. 2012b. Metabolic suppression in thecosomatous pteropods as an effect of low temperature and hypoxia in the eastern tropical North Pacific. Mar. Biol. **159**: 1955–1967. doi:10.1007/s00227-012-1982-x

Maas, A., L. Elder, H. Dierssen, and B. Seibel. 2011. Metabolic response of Antarctic pteropods (Mollusca: Gastropoda) to food deprivation and regional productivity. Mar. Ecol. Prog. Ser. **441**: 129–139. doi:10.3354/meps09358

Mackey, K. R. M., J. J. Morris, F. M. M. Morel, and S. A. Kranz. 2015. Response of photosynthesis to ocean acidification. Oceanography **28**: 74–91. doi:10.5670/oceanog.2015.33

Maclean, I. M. D., and R. J. Wilson. 2011. Recent ecological responses to climate change support predictions of high extinction risk. Proc. Natl. Acad. Sci. **108**: 12337–12342. doi:10.1073/pnas.1017352108

Malinverno, E. 2008. Coccolithophores of the Eastern Mediterranean Sea: a look into the marine microworld,.

Malinverno, E., F. G. Prahl, B. N. Popp, and P. Ziveri. 2008. Alkenone abundance and its relationship to the coccolithophore assemblage in Gulf of California surface waters. Deep Sea Res. Part I Oceanogr. Res. Pap. **55**: 1118–1130. doi:https://doi.org/10.1016/j.dsr.2008.04.007

Malinverno, E., P. Ziveri, and C. Corselli. 2003. Coccolithophorid distribution in the Ionian Sea and its relationship to eastern Mediterranean circulation during late fall to early winter 1997. J. Geophys. Res. **108**. doi:10.1029/2002JC001346

Mallo, M., P. Ziveri, P. G. Mortyn, R. Schiebel, and M. Grelaud. 2017. Low planktic foraminiferal diversity and abundance observed in a 2013 West-East Mediterranean Sea transect. Biogeosciences Discuss. 1–31. doi:10.5194/bg-2016-266

Manno, C., N. Bednaršek, G. A. Tarling, and others. 2017. Shelled pteropods in peril: Assessing vulnerability in a high CO2 ocean. Earth-Science Rev. **169**: 132–145. doi:10.1016/j.earscirev.2017.04.005

Manno, C., N. Morata, and R. Bellerby. 2012a. Effect of ocean acidification and temperature increase on the planktonic foraminifer Neogloboquadrina pachyderma (sinistral). Polar Biol. **35**: 1311–1319. doi:10.1007/s00300-012-1174-7

Manno, C., N. Morata, and R. Primicerio. 2012b. Limacina retroversa's response to combined effects of ocean acidification and sea water freshening. Estuar. Coast. Shelf Sci. **113**: 163–171. doi:https://doi.org/10.1016/j.ecss.2012.07.019

Manno, C., P. Rumolo, M. Barra, S. d'Albero, G. Basilone, S. Genovese, S. Mazzola, and A. Bonanno. 2019. Condition of pteropod shells near a volcanic CO2 vent region. Mar. Environ. Res. **143**: 39–48. doi:10.1016/j.marenvres.2018.11.003

Manno, C., V. Tirelli, A. Accornero, and S. Fonda Umani. 2010. Importance of the contribution of Limacina helicina faecal pellets to the carbon pump in Terra Nova Bay (Antarctica). J. Plankton Res. **32**: 145–152. doi:10.1093/plankt/fbp108

Mara, P., S. Psarra, A. Tselepides, A. Eleftheriou, and N. Mihalopoulos. 2016. Influence of phytoplankton taxonomic proile on the distribution of total and dissolved dimethylated sulphur (DMSx) species in the North Aegean Sea (Eastern Mediterranean). Mediterr. Mar. Sci. **17**: 65–79.

Martiny, A. C., J. A. Vrugt, and M. W. Lomas. 2014. Concentrations and ratios of particulate organic carbon, nitrogen, and phosphorus in the global ocean. Sci. Data **1**: 140048. doi:10.1038/sdata.2014.48

Mayers, K. M. J. M. J., A. J. J. Poulton, K. Bidle, and others. 2020. The Possession of Coccoliths Fails to Deter Microzooplankton Grazers . Front. Mar. Sci. **7**.

Mazzocchi, M., E. Christou, N. Fragopoulu, and I. Siokoufrangou. 1997. Mesozooplankton distribution from Sicily to Cyprus (Eastern Mediterranean) .1. General aspects. Oceanol. Acta **20**: 521–535.

Mazzocchi, M. G., P. Licandro, L. Dubroca, I. Di Capua, and V. Saggiomo. 2011. Zooplankton associations in a Mediterranean long-term time-series. J. Plankton Res. **33**: 1163–1181. doi:10.1093/plankt/fbr017

MedECC. 2020. Climate and Environmental Change in the Mediterranean Basin – Current Situation and Risks for the Future. First Mediterranean Assessment Report [Cramer, W., Guiot, J., Marini, K. (eds)].

Mehrbach, C., C. H. Culberson, J. E. Hawley, and R. M. Pytkowicx. 1973. Measurement of the apparent dissociation constants of carbonic acid in seawater at atmospheric pressure. Limnol. Oceanogr. **18**: 897–908. doi:10.4319/lo.1973.18.6.0897

Mekkes, L., W. Renema, N. Bednaršek, S. R. Alin, R. A. Feely, J. Huisman, P. Roessingh, and K. T. C. A. Peijnenburg. 2021a. Pteropods make thinner shells in the upwelling region of the California Current Ecosystem. Sci. Rep. **11**: 1731. doi:10.1038/s41598-021-81131-9

Mekkes, L., G. Sepúlveda-Rodríguez, G. Bielkinaitė, and others. 2021b. Effects of Ocean Acidification on Calcification of the Sub-Antarctic Pteropod Limacina retroversa. Front. Mar. Sci. **8**.

Mercado, J. M., D. Cortes, A. Garcia, and T. Ramirez. 2007. Seasonal and inter-annual changes in the planktonic communities of the northwest Alboran Sea (Mediterranean Sea). Prog. Oceanogr. **74**: 273–293. doi:10.1016/j.pocean.2007.04.013

Mercado, J. M., T. Ramirez, D. Cortes, M. Sebastian, and M. Vargas-Yanez. 2005.

Seasonal and inter-annual variability of the phytoplankton communities in an upwelling area of the Alboran Sea (SW Mediterranean Sea). Sci. Mar. **69**: 451–465. doi:10.3989/scimar.2005.69n4451

Meyer, J., and U. Riebesell. 2015. Reviews and Syntheses: Responses of coccolithophores to ocean acidification: a meta-analysis. Biogeosciences **12**: 1671–1682. doi:10.5194/bg-12-1671-2015

Meyers, M. T., W. P. Cochlan, E. J. Carpenter, and W. J. Kimmerer. 2019. Effect of ocean acidification on the nutritional quality of marine phytoplankton for copepod reproduction F. Melzner [ed.]. PLoS One **14**: e0217047. doi:10.1371/journal.pone.0217047

Millot, C., and I. Taupier-Letage. 2012. Circulation in the Mediterranean Sea, p. 99–125. *In* Life in the Mediterranean Sea: A Look at Habitat Changes. Nova Science Publishers, Inc.

Milner, S., G. Langer, M. Grelaud, and P. Ziveri. 2016. Ocean warming modulates the effects of acidification on calcification and sinking. Limnol. Oceanogr. **61**: 1322–1336. doi:10.1002/lno.v61.4

Mitra, A., and K. J. Flynn. 2005. Predator–prey interactions: is 'ecological stoichiometry' sufficient when good food goes bad? J. Plankton Res. **27**: 393–399. doi:10.1093/plankt/fbi022

Mohan, R., K. Verma, L. P. Mergulhao, D. K. Sinha, S. Shanvas, and M. V. S. Guptha. 2006. Seasonal variation of pteropods from the Western Arabian Sea sediment trap. Geo-Marine Lett. **26**: 265–273. doi:10.1007/s00367-006-0035-1

Monteiro, F. M., L. T. Bach, C. Brownlee, and others. 2016. Why marine phytoplankton calcify. Sci. Adv. **2**: e1501822. doi:10.1126/sciadv.1501822

Morse, J. W., A. Mucci, and F. J. Millero. 1980. The solubility of calcite and aragonite in seawater of 35%. salinity at 25°C and atmospheric pressure. Geochim. Cosmochim. Acta **44**: 85–94. doi:10.1016/0016-7037(80)90178-7

Moscatello, S., C. Caroppo, E. Hajderi, and G. Belmonte. 2011. Space Distribution of Phyto- and Microzooplankton in the Vlora Bay (Southern Albania, Mediterranean Sea). J. Coast. Res. 80–94. doi:10.2112/SI_58_8

Moy, A. D., W. R. Howard, S. G. Bray, and T. W. Trull. 2009. Reduced calcification in modern Southern Ocean planktonic foraminifera. Nat. Geosci. **2**: 276–280. doi:10.1038/ngeo460

Moya, A., E. L. Howes, T. Lacoue-Labarthe, and others. 2016. Near-future pH

conditions severely impact calcification, metabolism and the nervous system in the pteropod *Heliconoides inflatus*. Glob. Chang. Biol. **22**: 3888–3900. doi:10.1111/gcb.13350

Mozetiĉ, P., S. F. Umani, B. Cataletto, and A. Malej. 1998. Seasonal and inter-annual plankton variability in the Gulf of Trieste (northern Adriatic). ICES J. Mar. Sci. **55**: 711–722. doi:10.1006/jmsc.1998.0396

Mucci, A., R. Canuel, and S. Zhong. 1989. The solubility of calcite and aragonite in sulfate-free seawater and the seeded growth kinetics and composition of the precipitates at 25°C. Chem. Geol. **74**: 309–320. doi:10.1016/0009-2541(89)90040-5

Müller, M. N., T. W. Trull, and G. M. Hallegraeff. 2017. Independence of nutrient limitation and carbon dioxide impacts on the Southern Ocean coccolithophore Emiliania huxleyi. ISME J. **11**: 1777–1787. doi:10.1038/ismej.2017.53

NASA OB.DAAC. 2018. NASA Goddard Space Flight Center, Ocean Ecology Laboratory, Ocean Biology Processing Group. Moderate-resolution Imaging Spectroradiometer (MODIS) Aqua Inherent Optical Properties Data.

Nejstgaard, J. C., I. Gismervik, and P. T. Solberg. 1997. Feeding and reproduction by Calanus finmarchicus, and microzooplankton grazing during mesocosm blooms of diatoms and the coccolithophore Emiliania huxleyi. Mar. Ecol. Prog. Ser. **147**: 197–217.

Nelder, J. A., and R. W. M. Wedderburn. 1972. Generalized Linear Models. J. R. Stat. Soc. Ser. A **135**: 370–384. doi:10.2307/2344614

Neri, F., T. Romagnoli, S. Accoroni, A. Campanelli, M. Marini, F. Grilli, and C. Totti. 2022. Phytoplankton and environmental drivers at a long-term offshore station in the northern Adriatic Sea (1988–2018). Cont. Shelf Res. **242**: 104746. doi:https://doi.org/10.1016/j.csr.2022.104746

Neukermans, G., L. Oziel, and M. Babin. 2018. Increased intrusion of warming Atlantic water leads to rapid expansion of temperate phytoplankton in the Arctic. Glob. Chang. Biol. **24**: 2545–2553. doi:https://doi.org/10.1111/gcb.14075

Nöel, M.-H., M. Kawachi, and I. Inouye. 2004. Induced dimorphic life cycle of a coccolithophorid, Calytrosphaera sphaeroidea (Prymnesiophyceae, Haptophyta). J. Phycol. **40**: 112–129. doi:https://doi.org/10.1046/j.1529-8817.2004.03053.x

O'Brien, C. J., M. Vogt, and N. Gruber. 2016. Global coccolithophore diversity: Drivers and future change. Prog. Oceanogr. **140**: 27–42.

doi:https://doi.org/10.1016/j.pocean.2015.10.003

Oakes, R. L., and J. A. Sessa. 2020. Determining how biotic and abiotic variables affect the shell condition and parameters of Heliconoides inflatus pteropods from a sediment trap in the Cariaco Basin. Biogeosciences **17**: 1975–1990. doi:10.5194/bg-17-1975-2020

Ofstad, S., K. Zamelczyk, K. Kimoto, M. Chierici, A. Fransson, and T. L. Rasmussen. 2021. Shell density of planktonic foraminifera and pteropod species Limacina helicina in the Barents Sea: Relation to ontogeny and water chemistry. PLoS One **16**: e0249178.

Oguz, T., D. Macias, J. Garcia-Lafuente, A. Pascual, and J. Tintore. 2014. Fueling Plankton Production by a Meandering Frontal Jet: A Case Study for the Alboran Sea (Western Mediterranean). PLoS One **9**: e111482.

Ohman, M. D., B. E. Lavaniegos, and A. W. Townsend. 2009. Multi-decadal variations in calcareous holozooplankton in the California Current System: Thecosome pteropods, heteropods, and foraminifera. Geophys. Res. Lett. **36**: L18608. doi:10.1029/2009GL039901

Oksanen, J., F. M. F. R. K. Guillaume Blanchet, P. Legendre, and others. 2019. vegan: Community Ecology Package.

Oviedo, A., P. Ziveri, M. Álvarez, and T. Tanhua. 2015. Is coccolithophore distribution in the Mediterranean Sea related to seawater carbonate chemistry? Ocean Sci. **11**: 13–32. doi:10.5194/os-11-13-2015

Pasqueron de Fommervault, O., A. Mangin, R. Serra, and others. 2015. Seasonal variability of nutrient concentrations in the Mediterranean Sea: Contribution of Bio-Argo floats. J. Geophys. Res. Ocean. **120**: 8528–8550. doi:10.1002/2015JC011103ï

Pasternak, A. F., A. V Drits, M. V Gopko, and M. V Flint. 2020. Influence of Environmental Factors on the Distribution of Pteropods Limacina helicina (Phipps, 1774) in Siberian Arctic Seas. Oceanology **60**: 490–500. doi:10.1134/S0001437020040177

Paul, A. J., and L. T. Bach. 2020. Universal response pattern of phytoplankton growth rates to increasing CO2. New Phytol. **228**: 1710–1716. doi:https://doi.org/10.1111/nph.16806

Paxinos, R., and J. G. Mitchell. 2000. A rapid Utermöhl method for estimating algal numbers. J. Plankton Res. **22**: 2255–2262. doi:10.1093/plankt/22.12.2255

Peijnenburg, K. T. C. A., A. W. Janssen, D. Wall-Palmer, E. Goetze, A. E. Maas, J. A. Todd, and F. Marlétaz. 2020. The origin and diversification of pteropods precede past perturbations in the Earth's carbon cycle. Proc. Natl. Acad. Sci. **117**: 25609 LP – 25617. doi:10.1073/pnas.1920918117

Pierrot, D., D. Wallace, E. Lewis, R. Wallace, and W. Wallace. 2011. MS Excel Program Developed for CO2 System Calculations.doi:10.3334/CDIAC/otg

Pinardi, N., M. Zavatarelli, M. Adani, and others. 2015. Mediterranean Sea large-scale low-frequency ocean variability and water mass formation rates from 1987 to 2007: A retrospective analysis. Prog. Oceanogr. **132**: 318–332. doi:https://doi.org/10.1016/j.pocean.2013.11.003

Pomar, L., P. Hallock, G. Mateu-Vicens, and J. I. Baceta. 2022. Why Do Bio-Carbonates Exist? J. Mar. Sci. Eng. **10**. doi:10.3390/jmse10111648

Pond, D. W., and R. P. Harris. 1996. The Lipid Composition of the Coccolithophore Emiliania Huxleyi and Its Possible Ecophysiological Significance. J. Mar. Biol. Assoc. United Kingdom **76**: 579–594. doi:DOI: 10.1017/S0025315400031295

Pörtner, H. O. 2008. Ecosystem effects of ocean acidification in times of ocean warming: A physiologist's view. Mar. Ecol. Prog. Ser. **373**: 203–217. doi:10.3354/meps07768

Poulos, S. E., P. G. Drakopoulos, and M. B. Collins. 1997. Seasonal variability in sea surface oceanographic conditions in the Aegean Sea (Eastern Mediterranean): an overview. J. Mar. Syst. **13**: 225–244. doi:https://doi.org/10.1016/S0924-7963(96)00113-3

Powley, H. R., M. D. Krom, and P. Van Cappellen. 2016. Circulation and oxygen cycling in the Mediterranean Sea: Sensitivity to future climate change. J. Geophys. Res. Ocean. **121**: 8230–8247. doi:https://doi.org/10.1002/2016JC012224

Prabhu, M., A. Chemodanov, R. Gottlieb, and others. 2019. Starch from the sea: The green macroalga Ulva ohnoi as a potential source for sustainable starch production in the marine biorefinery. Algal Res. **37**: 215–227. doi:https://doi.org/10.1016/j.algal.2018.11.007

Rampal, J. 1975. Les thécosomes (molluques pélagiques). Systématique et évolution - Écologies et biogéographie Mediterranéennes. Université Aix-Marseille.

Reid, F. M. H. 1980. Coccolithophorids of the North Pacific Central Gyre with Notes on Their Vertical and Seasonal Distribution. Micropaleontology **26**: 151–176. doi:10.2307/1485436

Reid, P. C., A. C. Fischer, E. Lewis-Brown, and others. 2009. Chapter 1 Impacts of the Oceans on Climate Change, p. 1–150. *In* Advances in Marine Biology. Academic Press.

Rekik, A., J. Elloumi, Z. Drira, S. Maalej, and H. Ayadi. 2017. Coupling of Phytoplankton and Ciliate Biomasses to Environmental Factors along the North Coast of Sfax (Tunisia, Eastern Mediterranean Sea). Water Resour. **44**: 849–863. doi:10.1134/S0097807817090019

Reygondeau, G., C. Guieu, F. Benedetti, J.-O. Irisson, S.-D. Ayata, S. Gasparini, and P. Koubbi. 2017. Biogeochemical regions of the Mediterranean Sea: An objective multidimensional and multivariate environmental approach. Prog. Oceanogr. **151**: 138–148. doi:https://doi.org/10.1016/j.pocean.2016.11.001

Riebesell, U., I. Zondervan, B. Rost, P. D. Tortell, and F. M. M. Morel. 2000. Reduced calcification of marine plankton in response to increased atmospheric CO2. Nature **407**: 364–367. doi:10.1038/35030078

Riegman, R., W. Stolte, A. A. M. Noordeloos, and D. Slezak. 2000. Nutrient uptake and alkaline phosphatase (ec 3:1:3:1) activity of emiliania huxleyi (prymnesiophyceae) during growth under n and p limitation in continuous cultures. J. Phycol. **36**: 87–96. doi:https://doi.org/10.1046/j.1529-8817.2000.99023.x

Ries, J. B. 2011. A physicochemical framework for interpreting the biological calcification response to CO2-induced ocean acidification. Geochim. Cosmochim. Acta **75**: 4053–4064. doi:https://doi.org/10.1016/j.gca.2011.04.025

Rigual-Hernández, A., T. Trull, S. Nodder, and others. 2020. Coccolithophore biodiversity controls carbonate export in the Southern Ocean. Biogeosciences **17**: 245–263. doi:10.5194/bg-17-245-2020

Roberts, D., W. R. Howard, J. L. Roberts, S. G. Bray, A. D. Moy, T. W. Trull, and R. R. Hopcroft. 2014. Diverse trends in shell weight of three Southern Ocean pteropod taxa collected with Polar Frontal Zone sediment traps from 1997 to 2007. Polar Biol. **37**: 1445–1458. doi:10.1007/s00300-014-1534-6

Robinson, A. R., and M. Golnaraghi. 1994. The Physical and Dynamical Oceanography of the Mediterranean Sea, p. 255–306. *In* Ocean Processes in Climate Dynamics: Global and Mediterranean Examples. Springer Netherlands.

Roger, L. M., A. J. Richardson, A. D. McKinnon, B. Knott, R. Matear, and C. Scadding. 2011. Comparison of the shell structure of two tropical Thecosomata (Creseis acicula and Diacavolinia longirostris) from 1963 to 2009: potential implications of

declining aragonite saturation. ICES J. Mar. Sci. **69**: 465–474. doi:10.1093/icesjms/fsr171

Rohling, E. J., R. Abu-Zied, J. S. L. Casford, A. Hayes, and B. Hoogakker. 2009. The Marine Environment: Present and Past, p. 33–67. *In* The Physical Geography of the Mediterranean.

Rosas-Navarro, A., G. Langer, and P. Ziveri. 2016. Temperature affects the morphology and calcification of Emiliania huxleyi strains. Biogeosciences **13**: 2913–2926. doi:10.5194/bg-13-2913-2016

Rossi, S., and J.-M. Gili. 2007. Short-time-scale variability of near-bottom seston composition during spring in a warm temperate sea. Hydrobiologia **575**: 373–388. doi:10.1007/s10750-006-0390-y

Rossi, S., E. Isla, M. Bosch-Belmar, and others. 2019. Changes of energy fluxes in marine animal forests of the Anthropocene: factors shaping the future seascape. ICES J. Mar. Sci. **76**: 2008–2019. doi:10.1093/icesjms/fsz147

Rossoll, D., R. Bermúdez, H. Hauss, K. G. Schulz, U. Riebesell, U. Sommer, and M. Winder. 2012. Ocean acidification-induced food quality deterioration constrains trophic transfer. PLoS One **7(4)**: e34737. doi:10.1371/journal.pone.0034737

Saavedra-Pellitero, M., K.-H. Baumann, J.-A. Flores, and R. Gersonde. 2014. Biogeographic distribution of living coccolithophores in the Pacific sector of the Southern Ocean. Mar. Micropaleontol. **109**: 1–20. doi:https://doi.org/10.1016/j.marmicro.2014.03.003

Sahin, M., and E. Eker-Develi. 2019. New Records of Haptophyte Species from the Northeastern Mediterranean Sea for Algal Flora of Turkey. TURKISH J. Fish. Aquat. Sci. **19**: 7–19. doi:10.4194/1303-2712-v19_1_02

Sailley, S., M. Vogt, S. Doney, and others. 2013. Comparing food web structures and dynamics across a suite of global marine ecosystem models. Ecol. Modell. **261**–**262**: 43–57. doi:10.1016/j.ecolmodel.2013.04.006

Sarà, G., M. Milanese, I. Prusina, and others. 2014. The impact of climate change on mediterranean intertidal communities: losses in coastal ecosystem integrity and services. Reg. Environ. Chang. **14**: 5–17. doi:10.1007/s10113-012-0360-z

Saracino, O., and F. Rubino. 2006. Phytoplankton composition and distribution along the Albanian coast, South Adriatic Sea. Nov. Hedwigia **83**: 253–266. doi:10.1127/0029-5035/2006/0083-0253

Sardou, J., M. Etienne, and V. Andersen. 1996. Seasonal abundance and vertical

distributions of macroplankton and micronekton in the Northwestern Mediterranean Sea. Oceanol. Acta **19**: 645–656.

Sarhan, T., J. Garcı́a Lafuente, M. Vargas, J. M. Vargas, and F. Plaza. 2000. Upwelling mechanisms in the northwestern Alboran Sea. J. Mar. Syst. **23**: 317–331. doi:https://doi.org/10.1016/S0924-7963(99)00068-8

Saugestad, A. H., and B. R. Heimdal. 2002. Light microscope studies on coccolithophorids from the western Mediterranean Sea, with notes on combination cells of Daktylethra pirus and Syracosphaera pulchra. Plant Biosyst. **136**: 3–27.

Schiebel, R., J. Waniek, M. Bork, and C. Hemleben. 2001. Planktic foraminiferal production stimulated by chlorophyll redistribution and entrainment of nutrients. Deep Sea Res. Part I Oceanogr. Res. Pap. **48**: 721–740. doi:10.1016/S0967-0637(00)00065-0

Schiebel, R., J. Waniek, A. Zeltner, and M. Alves. 2002. Impact of the Azores Front on the distribution of planktic foraminifers, shelled gastropods, and coccolithophorids. Deep Sea Res. Part II Top. Stud. Oceanogr. **49**: 4035–4050. doi:10.1016/S0967-0645(02)00141-8

Schlitzer, R. 2021. Ocean Data View.

Schlüter, L., K. T. Lohbeck, M. A. Gutowska, J. P. Gröger, U. Riebesell, and T. B. H. Reusch. 2014. Adaptation of a globally important coccolithophore to ocean warming and acidification. Nat. Clim. Chang. **4**: 1024–1030. doi:10.1038/nclimate2379

Schneider, A., D. W. R. Wallace, and A. Körtzinger. 2007. Alkalinity of the Mediterranean Sea. Geophys. Res. Lett. **34**: 1–5. doi:10.1029/2006GL028842

Seibel, B. A., and H. M. Dierssen. 2003. Cascading trophic impacts of reduced biomass in the Ross Sea, Antarctica: just the tip of the iceberg? Biol. Bull. **205**: 93–7. doi:10.2307/1543229

Seifert, M., B. Rost, S. Trimborn, and J. Hauck. 2020. Meta-analysis of multiple driver effects on marine phytoplankton highlights modulating role of pCO2. Glob. Chang. Biol. **26**: 6787–6804. doi:https://doi.org/10.1111/gcb.15341

Sett, S., L. T. Bach, K. G. Schulz, S. Koch-Klavsen, M. Lebrato, and U. Riebesell. 2014. Temperature modulates coccolithophorid sensitivity of growth, photosynthesis and calcification to increasing seawater pCO2. PLoS One **9(2)**: e88308. doi:10.1371/journal.pone.0088308

Shaltout, M., and A. Omstedt. 2014. Recent sea surface temperature trends and future

scenarios for the Mediterranean Sea. Oceanologia **56**: 411–443. doi:https://doi.org/10.5697/oc.56-3.411

Siokou-Frangou, I., U. Christaki, M. G. Mazzocchi, M. Montresor, M. R. d'Alcala, D. Vaque, and A. Zingone. 2010. Plankton in the open Mediterranean Sea: a review. BIOGEOSCIENCES **7**: 1543–1586. doi:10.5194/bg-7-1543-2010

Skampa, E., M. V Triantaphyllou, M. D. Dimiza, and others. 2019. Coupling plankton - sediment trap - surface sediment coccolithophore regime in the North Aegean Sea (NE Mediterranean). Mar. Micropaleontol. **152**. doi:10.1016/j.marmicro.2019.03.001

Skejic, S., J. Arapov, V. Kovacevic, and others. 2018. Coccolithophore diversity in open waters of the middle Adriatic Sea in pre- and post-winter periods. Mar. Micropaleontol. **143**: 30–45. doi:10.1016/j.marmicro.2018.07.006

Skjoldal, H. R., P. H. Wiebe, L. Postel, T. Knutsen, S. Kaartvedt, and D. D. Sameoto. 2013. Intercomparison of zooplankton (net) sampling systems: Results from the ICES/GLOBEC sea-going workshop. Prog. Oceanogr. **108**: 1–42. doi:https://doi.org/10.1016/j.pocean.2012.10.006

Socal, G., A. Boldrin, F. Bianchi, G. Civitarese, A. De Lazzari, S. Rabitti, C. Totti, and M. M. Turchetto. 1999. Nutrient, particulate matter and phytoplankton variability in the photic layer of the Otranto strait. J. Mar. Syst. **20**: 381–398. doi:10.1016/S0924-7963(98)00075-X

Somero, G. 2012. The Physiology of Global Change: Linking Patterns to Mechanisms. Ann. Rev. Mar. Sci. **4**: 39–61. doi:10.1146/annurev-marine-120710-100935

Sturdevant, M. V, J. A. Orsi, and E. A. Fergusson. 2012. Diets and Trophic Linkages of Epipelagic Fish Predators in Coastal Southeast Alaska during a Period of Warm and Cold Climate Years, 1997–2011. Mar. Coast. Fish. **4**: 526–545. doi:10.1080/19425120.2012.694838

Subhas, A. V, S. Dong, J. D. Naviaux, and others. 2022. Shallow Calcium Carbonate Cycling in the North Pacific Ocean. Global Biogeochem. Cycles **36**: e2022GB007388. doi:https://doi.org/10.1029/2022GB007388

Sunday, J. M., A. E. Bates, and N. K. Dulvy. 2012. Thermal tolerance and the global redistribution of animals. Nat. Clim. Chang. **2**: 686–690. doi:10.1038/nclimate1539

Šupraha, L., S. Bosak, Z. Ljubesic, G. Olujić, L. Horvat, and D. Viličić. 2011. The phytoplankton composition and spatial distribution in the north-eastern Adriatic

Channel in autumn 2008. Acta Adriat. **52**: 1–5113.

Supraha, L., Z. Ljubesic, H. Mihanovic, and J. Henderiks. 2016. Coccolithophore life-cycle dynamics in a coastal Mediterranean ecosystem: seasonality and species-specific patterns. J. Plankton Res. **38**: 1178–1193. doi:10.1093/plankt/fbw061

Tarling, G. A., J. B. L. Matthews, P. David, O. Guerin, and F. Buchholz. 2001. The swarm dynamics of northern krill (Meganyctiphanes norvegica) and pteropods (Cavolinia inflexa) during vertical migration in the Ligurian Sea observed by an acoustic Doppler current profiler. Deep. Res. Part I Oceanogr. Res. Pap. **48**: 1671–1686. doi:10.1016/S0967-0637(00)00105-9

Teruzzi, A., G. Bolzon, L. Feudale, and G. Cossarini. 2021. Deep chlorophyll maximum and nutricline in the Mediterranean Sea: emerging properties from a multi-platform assimilated biogeochemical model experiment. Biogeosciences **18**: 6147–6166. doi:10.5194/bg-18-6147-2021

Thabet, A. A., A. E. Maas, G. L. Lawson, and A. M. Tarrant. 2015. Life cycle and early development of the thecosomatous pteropod Limacina retroversa in the Gulf of Maine, including the effect of elevated CO2levels. Mar. Biol. **162**: 2235–2249. doi:10.1007/s00227-015-2754-1

Thibodeau, P. S., D. K. Steinberg, and A. E. Maas. 2020. Effects of temperature and food concentration on pteropod metabolism along the Western Antarctic Peninsula. J. Exp. Mar. Bio. Ecol. **530**–**531**: 151412. doi:https://doi.org/10.1016/j.jembe.2020.151412

Thibodeau, P. S., D. K. Steinberg, S. E. Stammerjohn, and C. Hauri. 2019. Environmental controls on pteropod biogeography along the Western Antarctic Peninsula. Limnol. Oceanogr. **64**: S240–S256. doi:10.1002/lno.11041

Totti, C., G. Civitarese, F. Acri, D. Barletta, G. Candelari, E. Paschini, and A. Solazzi. 2000. Seasonal variability of phytoplankton populations in the middle Adriatic sub-basin. J. Plankton Res. **22**: 1735–1756. doi:10.1093/plankt/22.9.1735

Totti, C., T. Romagnoli, S. Accoroni, A. Coluccelli, M. Pellegrini, A. Campanelli, F. Grilli, and M. Marini. 2019. Phytoplankton communities in the northwestern Adriatic Sea: Interdecadal variability over a 30-years period (1988–2016) and relationships with meteoclimatic drivers. J. Mar. Syst. **193**: 137–153. doi:https://doi.org/10.1016/j.jmarsys.2019.01.007

Trégouboff, G., and M. Rose. 1957. Manuel de Planctonologie Méditerranéenne, Centre national de la recherche scientifique, France.

Triantaphyllou, M. V, K. H. Baumann, B. T. Karatsolis, and others. 2018. Coccolithophore community response along a natural CO2 gradient off Methana (SW Saronikos Gulf, Greece, NE Mediterranean). PLoS One **13**. doi:10.1371/journal.pone.0200012

Turley, C. 2008. Impacts of changing ocean chemistry in a high-CO2 world. Mineral. Mag. **72**: 359–362. doi:DOI: 10.1180/minmag.2008.072.1.359

Uitz, J., D. Stramski, B. Gentili, F. D'Ortenzio, and H. Claustre. 2012. Estimates of phytoplankton class-specific and total primary production in the Mediterranean Sea from satellite ocean color observations. Global Biogeochem. Cycles **26**. doi:10.1029/2011gb004055

Utermöhl, H. 1931. Neue Wege in der quantitativen Erfassung des Plankton.(Mit besonderer Berücksichtigung des Ultraplanktons.). SIL Proceedings, 1922-2010 **5**: 567–596. doi:10.1080/03680770.1931.11898492

Utermöhl, H. 1958. Methods of collecting plankton for various purposes are discussed. SIL Commun. 1953-1996 **9**: 1–38. doi:10.1080/05384680.1958.11904091

Valavanidis, A., and T. Vlachogianni. 2013. Ecosystem and Biodiversity Hotspots in the Mediterranean Basin: Threats and Conservation Efforts. WEB-SITE Sci. Adv. Environ. Toxicol. Ecotoxicol.

Valencia-Vila, J., M. L. F. De Puelles, J. Jansa, and M. Varela. 2016. Phytoplankton composition in a neritic area of the Balearic Sea (Western Mediterranean). J. Mar. Biol. Assoc. United Kingdom **96**: 749–759. doi:10.1017/S0025315415001137

Vaquer-Sunyer, R., and C. M. Duarte. 2008. Thresholds of hypoxia for marine biodiversity. Proc. Natl. Acad. Sci. **105**: 15452–15457. doi:10.1073/pnas.0803833105

Varkitzi, I., S. Psarra, G. Assimakopoulou, A. Pavlidou, E. Krasakopoulou, D. Velaoras, E. Papathanassiou, and K. Pagou. 2020. Phytoplankton dynamics and bloom formation in the oligotrophic Eastern Mediterranean: Field studies in the Aegean, Levantine and Ionian seas. Deep Sea Res. Part II Top. Stud. Oceanogr. **171**: 104662. doi:https://doi.org/10.1016/j.dsr2.2019.104662

Vilicic, D., T. Djakovac, Z. Buric, and S. Bosak. 2009. Composition and annual cycle of phytoplankton assemblages in the northeastern Adriatic Sea. Bot. Mar. **52**: 291–305. doi:10.1515/BOT.2009.004

Viličić, D., M. Kuzmić, S. Bosak, T. Silovic, E. Hrustić, and Z. Ljubesic. 2009. Distribution of phytoplankton along the thermohaline gradient in the north-eastern

Adriatic channel; winter aspect. Oceanologia **51**: 495–513. doi:10.5697/oc.51-4.495

Viličić, D., T. Šilović, M. Kuzmić, H. Mihanović, S. Bosak, I. Tomažić, and G. Olujić. 2011. Phytoplankton distribution across the southeast Adriatic continental and shelf slope to the west of Albania (spring aspect). Environ. Monit. Assess. **177**: 593–607. doi:10.1007/s10661-010-1659-1

Viličić, D., S. Terzić, M. Ahel, Z. Burić, N. Jasprica, M. Carić, K. Caput Mihalić, and G. Olujić. 2008. Phytoplankton abundance and pigment biomarkers in the oligotrophic, eastern Adriatic estuary. Environ. Monit. Assess. **142**: 199–218. doi:10.1007/s10661-007-9920-y

de Vries, J. C., F. Monteiro, H. Andruleit, and others. 2020. Global SEM coccolithophore abundance compilation.doi:10.1594/PANGAEA.922933

de Vries, J., F. Monteiro, G. Wheeler, and others. 2021. Haplo-diplontic life cycle expands coccolithophore niche. Biogeosciences **18**: 1161–1184. doi:10.5194/bg-18-1161-2021

Wang, K., B. P. V Hunt, C. Liang, D. Pauly, and E. A. Pakhomov. 2017. Reassessment of the life cycle of the pteropod Limacina helicina from a high resolution interannual time series in the temperate North Pacific. ICES J. Mar. Sci. **74**: 1906–1920. doi:10.1093/icesjms/fsx014

Weinkauf, M. F. G., T. Moller, M. C. Koch, and M. Kučera. 2013. Calcification intensity in planktonic Foraminifera reflects ambient conditions irrespective of environmental stress. Biogeosciences **10**: 6639–6655. doi:10.5194/bg-10-6639-2013

Weldrick, C. K., R. Trebilco, D. M. Davies, and K. M. Swadling. 2019. Trophodynamics of Southern Ocean pteropods on the southern Kerguelen Plateau. Ecol. Evol. **9**: 8119–8132. doi:10.1002/ece3.5380

Wells, F. E. 1976. Growth rates of four species of euthecosomatous pteropods occurring off Barbados, West Indies. Nautilus (Philadelphia). **90**: 114–116.

Wells, F. E. J. 1975. Seasonal patterns of abundance and reproduction of euthecosomatous pteropods off Barbados West Indies. The Veliger **18**: 241–248.

White, M. M., J. D. Waller, L. C. Lubelczyk, D. T. Drapeau, B. C. Bowler, W. M. Balch, and D. M. Fields. 2018. Coccolith dissolution within copepod guts affects fecal pellet density and sinking rate. Sci. Rep. **8**: 9758. doi:10.1038/s41598-018-28073-x

Winter, A., B. Rost, H. Hilbrecht, and M. Elbrächter. 2002. Vertical and horizontal distribution of coccolithophores in the Caribbean Sea. Geo-Marine Lett. **22**: 150–161. doi:10.1007/s00367-002-0108-8

Woodworth, B. D., R. L. Mead, C. N. Nichols, and D. R. J. Kolling. 2015. Photosynthetic light reactions increase total lipid accumulation in carbon-supplemented batch cultures of Chlorella vulgaris. Bioresour. Technol. **179**: 159–164. doi:https://doi.org/10.1016/j.biortech.2014.11.098

Wormuth, J. H. 1981. Vertical distributions and diel migrations of Euthecosomata in the northwest Sargasso Sea. Deep Sea Res. Part A, Oceanogr. Res. Pap. **28**: 1493–1515. doi:10.1016/0198-0149(81)90094-7

Young, J., S. A. Davis, P. R. Bown, and S. Mann. 1999. Coccolith Ultrastructure and Biomineralisation. J. Struct. Biol. **126**: 195–215. doi:https://doi.org/10.1006/jsbi.1999.4132

Zamelczyk, K., A. Fransson, M. Chierici, E. Jones, J. Meilland, G. Anglada-Ortiz, and H. H. Lødemel. 2021. Distribution and Abundances of Planktic Foraminifera and Shelled Pteropods During the Polar Night in the Sea-Ice Covered Northern Barents Sea . Front. Mar. Sci. **8**.

Zarkogiannis, S. D., A. Antonarakou, A. Tripati, G. Kontakiotis, P. G. Mortyn, H. Drinia, and M. Greaves. 2019. Influence of surface ocean density on planktonic foraminifera calcification. Sci. Rep. **9**: 533. doi:10.1038/s41598-018-36935-7

Zavatarelli, M., F. Raicich, D. Bregant, A. Russo, and A. Artegiani. 1998. Climatological biogeochemical characteristics of the Adriatic Sea. J. Mar. Syst. **18**: 227–263. doi:https://doi.org/10.1016/S0924-7963(98)00014-1

Zervakis, V., D. Georgopoulos, A. P. Karageorgis, and A. Theocharis. 2004. On the response of the Aegean Sea to climatic variability: a review. Int. J. Climatol. **24**: 1845–1858. doi:https://doi.org/10.1002/joc.1108

Zingone, A., L. Dubroca, D. Iudicone, F. Margiotta, F. Corato, M. R. D'Alcala, V. Saggiomo, and D. Sarno. 2010. Coastal Phytoplankton Do Not Rest in Winter. Estuaries and Coasts **33**: 342–361. doi:10.1007/s12237-009-9157-9

Ziveri, P., B. de Bernardi, K.-H. Baumann, H. M. Stoll, and P. G. Mortyn. 2007. Sinking of coccolith carbonate and potential contribution to organic carbon ballasting in the deep ocean. Deep Sea Res. Part II Top. Stud. Oceanogr. **54**: 659–675. doi:10.1016/j.dsr2.2007.01.006

Ziveri, P., A. T. C. Broerse, J. E. van Hinte, P. Westbroek, and S. Honjo. 2000. The fate

of coccoliths at 48°N 21°W, Northeastern Atlantic. Deep Sea Res. Part II Top. Stud. Oceanogr. **47**: 1853–1875. doi:https://doi.org/10.1016/S0967-0645(00)00009-6

Ziveri, P., and M. Grelaud. 2015. Physical oceanography during Ángeles Alvariño cruise MedSeA2013, PANGAEA.

Ziveri, P., M. Passaro, A. Incarbona, M. Milazzo, R. Rodolfo-Metalpa, and J. M. Hall-Spencer. 2014. Decline in Coccolithophore Diversity and Impact on Coccolith Morphogenesis Along a Natural CO2 Gradient. Biol. Bull. **226**: 282–290. doi:10.1086/BBLv226n3p282

Zuur, A. F., E. N. Ieno, N. J. Walker, A. A. Saveliev, and G. M. Smith. 2009a. GLM and GAM for Count Data, p. 209–243. *In* Springer, New York, NY.

Zuur, A. F., E. N. Ieno, N. J. Walker, A. A. Saveliev, and G. M. Smith. 2009b. Meet the Exponential Family BT - Mixed effects models and extensions in ecology with R, p. 193–208. *In* A.F. Zuur, E.N. Ieno, N. Walker, A.A. Saveliev, and G.M. Smith [eds.]. Springer New York.

Supplementary Material – Chapter 2

Supplementary Introduction

Fig. S1. Major surface currents and gyres across the Mediterranean. Shaded regions indicate the formation of intermediate and deep water. From Rohling et al. (2009).

Supplementary Methods

Supplementary Results and Discussion

Fig S2. A Country affiliated with the first author, and **B** Country (or EU) of funding bodies for each study in the systematic review. The total number in Fig. **B** exceeds the number of studies included in the review as some articles have funding bodies from multiple countries/EU.

Fig S3. **A** Total, **B** heterococcolithophore, and **C** holococcolithophore abundance (L^{-1}) across the Mediterranean Sea year round, during winter, spring, summer, and autumn at different depth profiles: 0 – 25m, 25 – 50 m, 50 – 100m, and 100 – 215m. Maximum abundances for total and heterococcolithophores are capped at 200,000 coccolithophores L^{-1} as the majority of samples are within that range and higher abundances likely reflect coccolithophore blooms rather than trends in average abundance. Similarly, holococcolithophore maximum abundance in the Fig is capped at 40,000 which reflects the majority of abundances. Note that abundances indicated outside of the Mediterranean Sea, for instance in the Atlantic Ocean, are an artefact of the Data-Interpolating Variational Analysis (DIVA) gridding tool by ODV and do not reflect the data. White regions indicate an absence of data.

Fig. S4. Diversity (H') of the total coccolithophore community (total), heterococcolithophores (HET), and holococcolithophores (HOL) across the Mediterranean Sea at different depth profiles: 0 – 25m, 25 – 50 m, 50 – 100m, and 100 – 215m. White regions indicate an absence of data.

Table S1. Coccolithophore species identified using the dataset.

Table S2. Results of the Kruskal-Wallis test indicating significant differences diversity (H') using different types of microscopy. ILM = Inverted light microscopy; PLM = Polarised light microscopy; and SEM = Scanning electron microscopy.

Table S3. Results of the Kruskal-Wallis test indicating significant differences in hetero- (HET) and holo-coccolithophore (HOL) abundances in the eastern (East) and western (West) Mediterranean sub-basins.

Table S4. Results of the Kruskal-Wallis test indicating significant differences between Mediterranean Sea regions.

Table S5. Results of the Kruskal-Wallis test indicating significant differences in between Mediterranean-wide seasonal coccolithophore contribution (%) to phytoplankton communities.

Table S6. Results of the Kruskal-Wallis test indicating significant differences between microscopy methods at different depth brackets. ILM = Inverted light microscopy; PLM = Polarised light microscopy; and SEM = Scanning electron microscopy. The numbers after each microscopy code indicate the upper limit of a depth bracket: 25 = 0 – 25 m; 50 = 25 – 50 m; 100 = 50 – 100 m; and 215 = 100 – 215 m.

Table S7. Results of the Kruskal-Wallis test indicating significant the Eastern (E) and Western (W) Mediterranean subbasins at different depth brackets. The numbers after each microscopy code indicate the upper limit of a depth bracket: 25 = 0 – 25 m; 50 = 25 – 50 m; 100 = 50 – 100 m; and 215 = 100 – 215 m.

Table S8. Results of the Kruskal-Wallis test indicating significant differences between hetero- (HET) and holo-coccolithophore (HOL) abundances between the eastern (East) and western (West) Mediterranean sub-basins during different seasons.

Table S9. Results of the Kruskal-Wallis test indicating significant differences between hetero- (HET) and holo-coccolithophore (HOL) diversity between the eastern (East) and western (West) Mediterranean sub-basins during different seasons.

Table S10. Average Mediterranean-wide abundance (coccolithophores L^{-1}) of the most abundant 15 species. **Emiliania huxleyi* morphotype not specified.

Table S11. Average regional abundances and maximum abundances (coccolithophores L^{-1}) for the 10 most abundant species in each region. **Emiliania huxleyi* morphotype not specified.

Table S12. Relationship with environmental variables and total coccolithophore abundance outlined in 16 published articles.

Table S13. Relationship with environmental variables and holococcolithophore abundance outlined in seven published articles.

Table S14. Relationship with environmental variables and coccolithophore diversity outlined in two published articles.

Table S15. Relationship with environmental variables and *E. huxleyi* abundance outlined in five published articles.

Table S16. List of the 72 studies included in the systematic review.

Table S17. List of the 27 datasets included in the meta-analysis.

Supplementary Introduction

Oceanographic setting

The Mediterranean Sea is a temperate, semi-enclosed sea with an anti-estuarine circulation. It is connected to the Atlantic Ocean through the Strait of Gibraltar, where surface Atlantic waters enter, and through net evaporation, a west to east gradient of increasing sea surface temperature, salinity, and alkalinity occurs (Schneider et al. 2007; Rohling et al. 2009; Fedele et al. 2022). The eastern basin is separated from the western basin through the shallow Strait of Sicily and is considered ultra-oligotrophic (Krom et al. 1991), with a deep chlorophyll maxima (Teruzzi et al. 2021). The Mediterranean Sea is characterised by distinct biogeochemical regions that are largely differentiated by the basins' oceanographic setting, as well as differences in temperature, salinity, nutrients, and carbonate chemistry, which persist as biogeographical boundaries over time (Schneider et al. 2007; Rohling et al. 2009; Uitz et al. 2012; Dayan et al. 2015; Hassoun et al. 2015b; Pasqueron de Fommervault et al. 2015).

The Western Basin

The western basin is composed of three major seas – Alboran, Balearic, and Tyrrenhian. The Alboran Sea is a transitional region between the Atlantic Ocean and the Mediterranean Sea. The influx of Atlantic water through the Strait of Gibraltar results in two anticyclonic gyres, the Western and Eastern Alboran Gyres (Heburn and La Violette 1990; Fig. S1), which are characterised by high productivity (Mercado et al. 2005). This influx of seawater from the Atlantic drives nutrients from the ocean and western basin to the eastern ultra-oligotrophic basin (Garcia-Gorriz and Carr 1999; Sarhan et al. 2000). The Balearic Sea lies between the coast of Spain and the Balearic Islands. This region is comprised of two permanent frontal systems, the Catalan Front, which limits the exchange of coastal and open sea waters, and the Balearic Front, which is comprised of a strong temperature gradient that limits the mixing of Atlantic waters into central part of the Balearic Sea (Estrada and Margalef 1988; Font et al. 1988; Amores et al. 2013). Primary production in this region of the western basin is comparatively higher than other parts of the Mediterranean Sea due to different processes, including eutrophic input via

rivers and the frontal systems (Estrada and Salat 1989). The Tyrrhenian Sea is the deepest major basin in the Western Mediterranean and is connected to the Ligurian Sea to the north through the Corsica Channel, and to the Sardinia Chanel in the south (Astraldi and Gasparini 1994). The northern and central region of the Tyrrhenian Sea have year-round winds blowing east from the Strait of Bonifacio which enhance vertical motion in the sea, while the southern region is influenced by waters moving through the Strait of Sicily and the Sardinia Channel, which bring Levantine Intermediate Water (Astraldi and Gasparini 1994).

The Eastern Basin

The Ionian and Levantine Seas make up the main body of the eastern Mediterranean Basin (Fig. S1). The Ionian Sea is connected to the Strait of Sicily to the west, to the Adriatic Sea through the narrow and shallow Otranto Strait to the North (72 km wide and 780 m deep; (Cushman-Roisin et al. 2013), and to the Levantine Sea to the east. It is bounded by the north-west coast of Africa and the Gulf of Sidra to the south (Grandjacquet and Mascle 1978). The epipelagic waters of the Ionian Sea are made up of Atlantic water entering on the surface through the Strait of Sicily, and the denser and deeper Levantine Intermediate Water arriving through the Cretan passage to the east (Rohling et al. 2009). The Levantine Sea is the most eastern sea in the Mediterranean, characterised by high temperatures, ultra-oligotrophy, and high salinity. It is connected to the Red Sea through the artificial creation of the Suez Canal. Levantine Intermediate water is formed at the cyclonic Rhodes gyre, and the combination of the Asia Minor Current and small and mesoscale eddies direct the flow of water to the southern border of Crete and the Ionian Sea (Lascaratos and Nittis 1998). The majority of Atlantic Water in the Levantine Sea follows the coast of north Africa and forms a strong coastal jet near Libya (Alhammoud et al. 2005). The Nile is the major riverine output and source of nutrient input for the south-east section of the Levantine Sea.

Adriatic Sea

The Adriatic Sea is a body of water between the east coast of Italy, and the west coast of Slovenia, Croatia, Bosnia and Herzegovina, Montenegro, and Albania (Fig. S1). It is

made up of approximately 1300 islands. It is separated from the eastern Mediterranean sub-basin by the shallow Otronto Strait and has distinct biogeochemical properties from the eastern Mediterranean. It collects a large amount of freshwater from rivers, particularly the Po River (Cushman-Roisin et al. 2013), and is therefore characterised by higher productivity, and is cooler and less saline than the Eastern sub-basin (Zavatarelli et al. 1998). The Adriatic Sea declines in nutrients from the north, where the main river input is, to the south (Zavatarelli et al. 1998).

Aegean Sea

The Aegean Sea is an elongated embayment made up of many islands in the Eastern Mediterranean (Fig. S1). It is a region of intermittent dense water formation for the Eastern Mediterranean Sea (Zervakis et al. 2004) and circulation here is largely driven by wind stress, heat, salt fluxes, as well as river outflow (Kourafalou and Barbopoulos 2003). It is connected to the Marmara Sea through the Dardanelles Strait, and to the Black Sea through the Strait of Bosphorus. A major subdivision of the Aegean Sea is the Sea of Crete, which is located on its southern periphery and is bordered to the south by the Island of Crete. The Aegean Sea is a heterogenous body of water, and sea surface temperatures can vary from 8°C in winter in the northern region, to 26°C in summer in the southern region (Poulos et al. 1997). Salinity also varies from north to south, with lower salinities toward the north (31 psu) and near river mouths (<25 psu), and higher salinities near the major body of the eastern Mediterranean Sea (39 psu; Poulos et al., 1997).

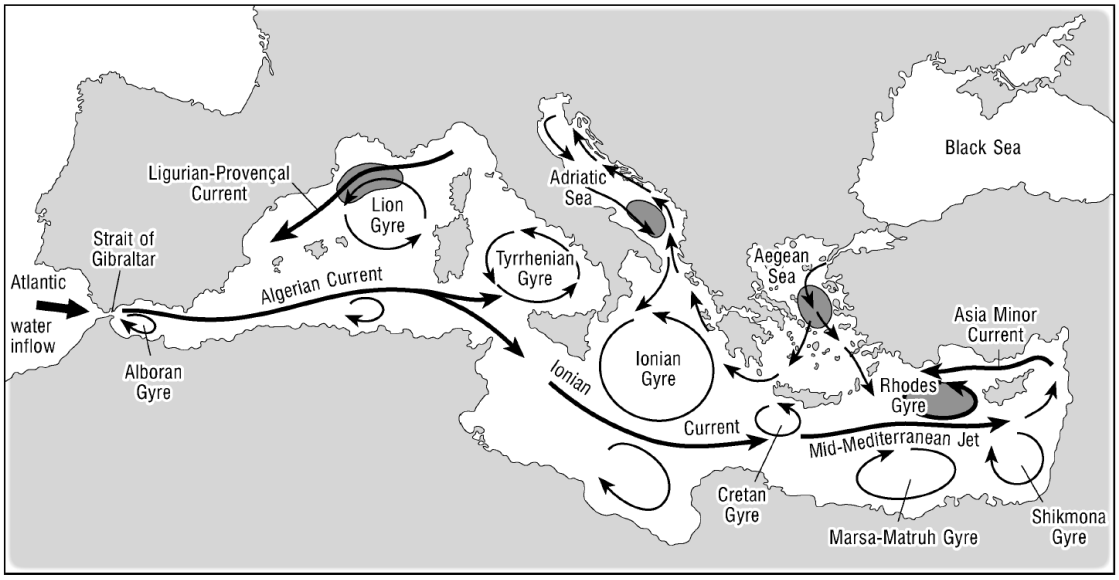

Fig. S1. Major surface currents and gyres across the Mediterranean. Shaded regions indicate the formation of intermediate and deep water. From Rohling et al. (2009).

Supplementary Methods

Using the position (latitude and longitude coordinates) included in the MA, abundance and composition estimates for several regions in the Mediterranean Sea could be made. To determine differences or patterns in depth distribution, average abundance was calculated within the following depth brackets (0 – 25 m, 25 – 50 m, 50 – 100 m, 100 – 215 m) for each individual sampling (not averaged if there was only one sample within the depth bracket). These are presented using maps created in Ocean Data View v3.1 (Supplementary Material). Seasonal abundance estimates were calculated, as were diversity estimates (Shannon's Diversity Index – H').

Supplementary Results and Discussion

First author affiliation and research funding

The first author affiliation of most studies included in the review are from Italy (23), followed by Croatia (12) and Greece (12; Fig. S2A). Most studies focus included here are based on the Adriatic and Aegean Seas, and as these countries border those seas, they are more highly represented. Spain has also published a comparable number of studies and

these focus mainly on the western basin (the Balearic and Alboran Seas). Articles whose first author is from countries that don't border the Mediterranean Sea including the Netherlands (Kleijne 1991; Knappertsbusch 1993) and Norway (Saugestad and Heimdal 2002) are not done in conjunction with any Mediterranean country. One article with a first author affiliation from Sweden (Supraha et al. 2016) was a collaborative project with a research group from Croatia.

Studies are generally funded by the country of the first author affiliation and many studies include EU funding as well (24 studies; Fig. S2B). Most studies receive funding from institutions from a single country (50), while others receive funding from either two (19 studies) or three (2) countries/funding bodies.

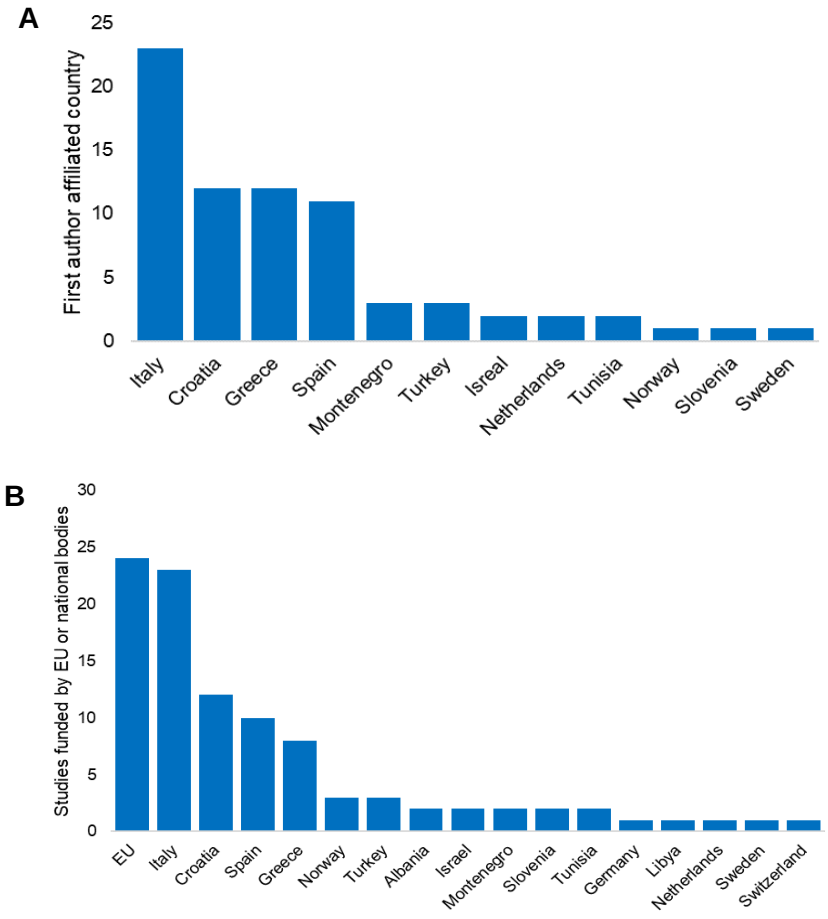

Fig S2. A Country affiliated with the first author, and **B** Country (or EU) of funding bodies for each study in the systematic review. The total number in Fig. **B** exceeds the number of studies included in the review as some articles have funding bodies from multiple countries/EU.

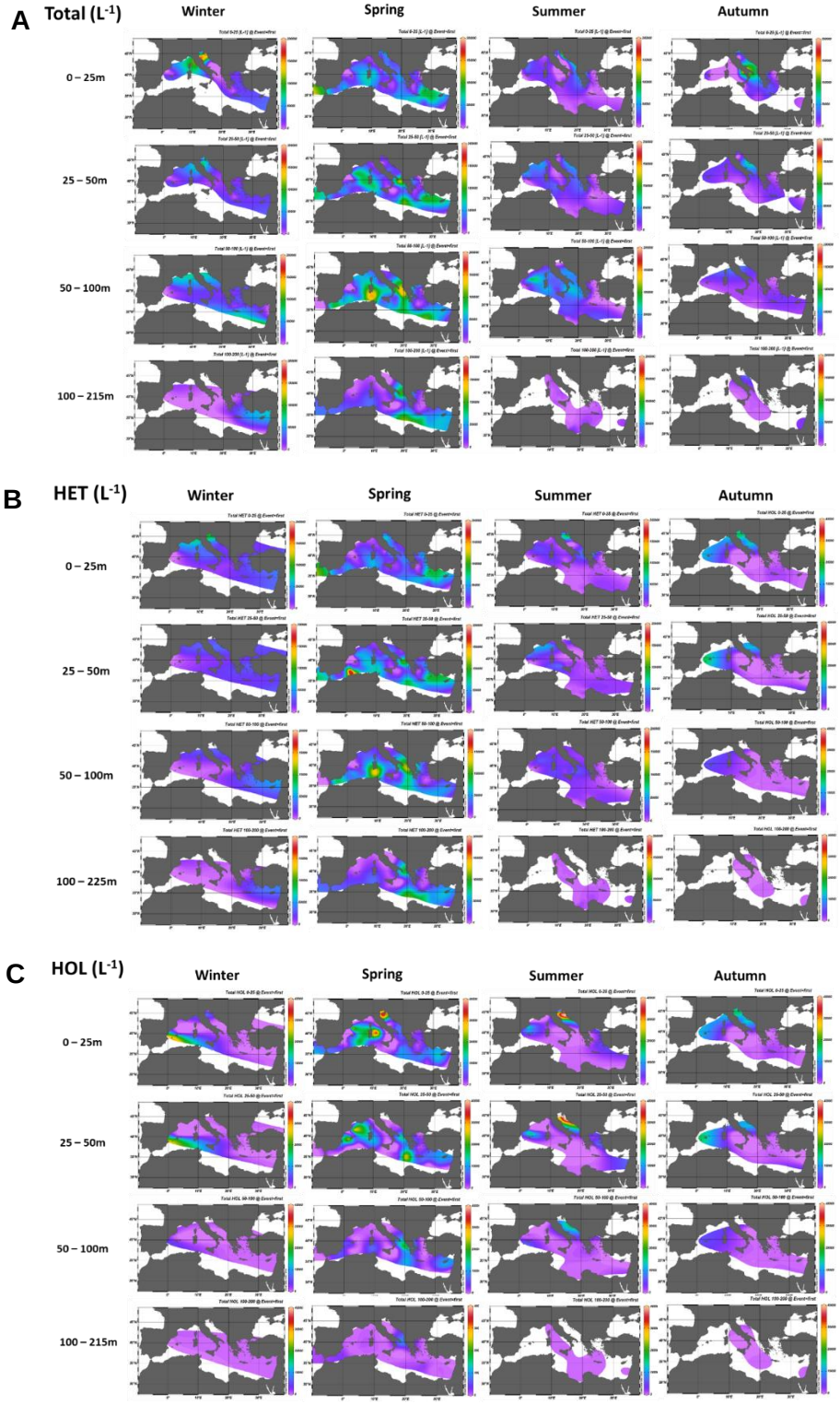

Fig S3. **A** Total, **B** heterococcolithophore, and **C** holococcolithophore abundance (L^{-1}) across the Mediterranean Sea year round, during winter, spring, summer, and autumn at different depth profiles: 0 – 25m, 25 – 50 m, 50 – 100m, and 100 – 215m. Maximum abundances for total and heterococcolithophores are capped at 200,000 coccolithophores L^{-1} as the majority of samples are within that range and higher abundances likely reflect coccolithophore blooms rather than trends in average abundance. Similarly, holococcolithophore maximum abundance in the Fig is capped at 40,000 which reflects the majority of abundances. Note that abundances indicated outside of the Mediterranean Sea, for instance in the Atlantic Ocean, are an artefact of the Data-Interpolating Variational Analysis (DIVA) gridding tool by ODV and do not reflect the data. White regions indicate an absence of data.

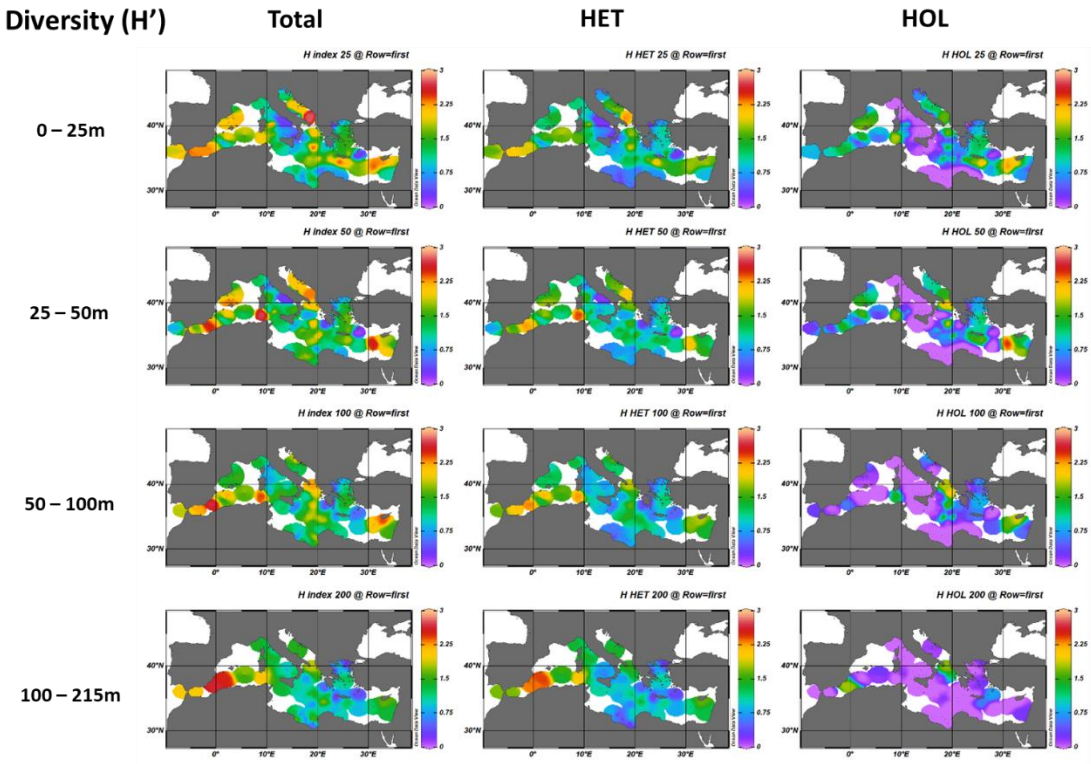

Fig. S4. Diversity (H') of the total coccolithophore community (total), heterococcolithophores (HET), and holococcolithophores (HOL) across the Mediterranean Sea at different depth profiles: 0 – 25m, 25 – 50 m, 50 – 100m, and 100 – 215m. White regions indicate an absence of data.

Table S1. Coccolithophore species identified using the dataset.

HETERCOCCOLITHOPHORES	HOLOCOCCOLITHOPHORE	COMBINATION	POLYCRATER
A. acanthifera	*A. quattrospina (HOL)*	*A. quattrospina (COMB)*	*A. gaudii (POL)*
A. acanthos	*A. robusta (HOL)*	*A. unicornis (COMB)*	*A. unicornis (POL)*
A. quattrospina	*A. gaudii (HOL)*	*C. mediterranea (HOL)*	*Canistrolithus sp. (POL)*
A. biscayensis	*A. lafourcadii (HOL)*	*R. xiphos (COMB)*	
A. robusta (Algirosphaera cf. robusta)	*A. periperforata (HOL)*	*S. arethusae (COMB)*	
A. cucullata	*A. origami (former Anthosphaera sp. Type ..)(HOL)*	*S. bannockii (COMB)*	
A. robusta	*C. leptoporus (HOL)*	*S. pulchra (COMB)*	
A. capulata	*C. leptoporus ssp. leptoporus (HOL)*	*S. strigilis (COMB)*	
A. extenta	*C. leptoporus ssp. quadriperforatus (HOL)*		
A. gaudii	*C. blokii (HOL)*		
A. ordinata	*C. concava (HOL)*		
A. quadrilatera	*C. multipora (HOL)*		
A. unicornis	*C. cialdii (HOL)*		
B. bigelowii	*C. sphaeroidea (HOL)*		
C. leptoporus	*C. pelagicus sp. braarudii (HOL)*		
C. leptoporus quadriperforatus	*Calyptrosphaera sphaeroidea HOL*		

C. brasiliensis	*Calyptrosphaera dentata HOL*		
C. corselli	*C. mediterranea (HOL hellenica type)*		
C. murrayi	*C. mediterranea (HOL gracillima type = Calyptr..)*		
C. rigidus	*C. mediterranea (HOL wettsteinii type)*		
C. caudatus	*Helicosphaera sp. (HOL catilliferus type)*		
C. dentata	*Helicosphaera sp. (HOL confusus type)*		
C. heimdalae	*Helicosphaera sp. (HOL dalmaticus type)*		
C. sphaeroidea	*Helicosphaera ponticuliferus HOL*		
Canistrolithus valliformis	*H. carteri (HOL)*		
C. cristatus	*H. carteri (HOL perforate)*		
C. cristatus HET nishidae type	*H. carteri (HOL solid)*		
C. cristatus CER cristatus type	*H. cornifera (HOL)*		
C. pelagicus	*H. cornifera (including H. spinosa) (HOL)*		
C. gracilis (Corisphaera cf. Gracilis)	*H. wallichii (HOL)*		
C. gracilis	*H. spinosa (HOL)*		
C. gracilis	*H. vercelli (HOL)*		
Corisphaera strigilis	*P. japonica (HOL)*		
C. tyrrheniensis	*P. aurisinae (HOL)*		
Calyptrolithina divergens	*S. apsteinii (HOL)*		
Calyptrosphaera heimdalae	*S. adenensis (HOL)*		
C. maxima	*S. quadridentate (HOL)*		
C. binodata [#7l]	*Sphaerocalyptra sp. (sp. 1 (from Cros and Fortuno (HOL)*		
C. mediterranea	*Sphaerocalyptra sp. (sp. 3 (from Cros and Fortuno) (HOL)*		
C. multipora	*Sphaerocalyptra sp. (sp. 6 (from Cros and Fortuno) (HOL)*		
Cyrtosphaera aculeata	*Syracolithus sp. (Type A) (HOL)*		
C. lecaliae	*S. amoena (HOL)*		
D. tubifera	*S. Anthos (HOL)*		
E. huxleyi	*S. arethusae (HOL)*		
E. huxleyi (Type B/C)	*S. bannockii (HOL)*		
F. profunda	*S. nana (HOL)*		
F. profunda var. elongata	*S. delicata (HOL)*		
F. profunda var. profunda	*S. halldalii (HOL)*		
F. profunda var rhinocera	*S. histrica (HOL)*		
F. pyramidosa	*S. marginiporata (HOL)*		
Flosculosphaera calceolariopsis	*S. molischii (HOL)*		
G. ericsonii	*S. molischii (HOL = Anthosphaera fragaria)*		
G. muellerae	*S. nana (HOL)*		
G. oceanica	*S. pulchra (HOL)*		
G. ornata	*S. pulchra (HOL oblonga type)*		
G. flabellatus	*S. pulchra (HOL pirus type)*		
Gliscolithus amitakareniae	*S. strigilis (HOL)*		
H. perplexus			

H. cornifera (Including H. spinosa)			
H. carteri			
H. hyalina			
H. pavimentum			
H. wallichii			
H. cornifera			
H. pienaarii			
H. kastriensis			
H. triarcha			
H. youngii			
H. roseola			
Kataspinifera baumannii			
M. adriaticus			
M. elegans			
Navilithus altivelum			
O. neapolitana			
O. fragilis			
O. formosus			
O. hydroideus			
O. minimus			
Pappomonas sp. (type 2)			
Pappomonas sp. (type 3)			
Pappomonas sp. (Type 5)			
Papposphaera sp. (Type 1)			
P. vandelii			
P. lepida			
P. galapagensis			
Pleurochrysis carterae			
P. margalefii			
P. japonica			
P. syracusana			
P. isselii			
P. poritectum (Poritectolithus cf. Poritectus)			
P. maximus			
Poricalyptra gaarderae			
R. parvula			
R. clavigera			
R. clavigera var stylifera			
R. clavigera var clavigera			
R. stylifera			
R. xiphos			
S. apsteinii			
S. adenensis (Sphaerocalyptra cf. Adenensis)			

S. dermitzakii			
S. bicorium			
S. porosa			
S. schilleri (Syracolithus cf. Schilleri)			
S. ampliora			
S. anthos			
S. arethusae			
S. azureaplaneta			
S. bannockii			
S. borealis			
S. anthos (Syracosphaera cf. Anthos)			
S. nana (Syracosphaera cf. Nana)			
S. tumularis (Syracosphaera cf. tumularis)			
S. corolla			
S. delicata			
S. dilatata			
S. epigrosa			
S. gaarderae			
S. halldalii			
S. halldalii (Syracosphaera halldalii + Syr..)			
S. hastata			
S. hirsuta			
S. histrica			
S. lamina			
S. leptolepis (Type L)			
S. marginiporata			
S. molischii			
S. molischii type 3 or 4			
S. nana			
S. nodosa			
S. noroitica			
S. orbiculus (including S. delicata)			
S. ossa			
S. ossa (Type 1)			
S. ossa (Type 2)			
S. pirus			
S. prolongata			
S. protrudens			
S. pulchra			
S. reniformis			
S. rotula			
S. squamosa (type K)			
S. strigilis			

S. tumularis			
T. adriatica			
T. latericioides			
T. heimii			
U. tenuis			
U. foliosa			
U. irregularis			
U. hulburtiana			
U. sibogae			
Umbilicosphaera sibogae var. foliosa			
V. cancellifer			
V. iaculifer			
Z. amoena			
Z. marsilii			

Table S2. Results of the Kruskal-Wallis test indicating significant differences diversity (H') using different types of microscopy. ILM = Inverted light microscopy; PLM = Polarised light microscopy; and SEM = Scanning electron microscopy.

Sample1-Sample2	Test Statistic	Std. Error	Std. Test Statistic	Sig.	Adj.Sig.
H ILM-H PLM	-743.267	33.618	-22.109	.000	.000
H ILM-H SEM	-1,115.303	33.308	-33.485	.000	.000
H PLM-H SEM	-372.036	35.450	-10.495	.000	.000

Each row tests the null hypothesis that the Sample 1 and Sample 2 distributions are the same.
Asymptotic significances (2-sided tests) are displayed. The significance level is .05.

Table S3. Results of the Kruskal-Wallis test indicating significant differences in hetero- (HET) and holo-coccolithophore (HOL) abundances in the eastern (East) and western (West) Mediterranean sub-basins.

Sample1-Sample2	Test Statistic	Std. Error	Std. Test Statistic	Sig.	Adj.Sig.
West HOL-East HOL	-255.903	46.614	-5.490	.000	.000
West HOL-East HET	-1,355.947	44.071	-30.768	.000	.000
West HOL-West HET	1,539.753	47.655	32.310	.000	.000
East HOL-East HET	1,100.043	42.943	25.617	.000	.000
East HOL-West HET	1,283.849	46.614	27.542	.000	.000
East HET-West HET	183.806	44.071	4.171	.000	.000

Each row tests the null hypothesis that the Sample 1 and Sample 2 distributions are the same.
Asymptotic significances (2-sided tests) are displayed. The significance level is .05.

Table S4. Results of the Kruskal-Wallis test indicating significant differences between Mediterranean Sea regions.

Sample1-Sample2	Test Statistic	Std. Error	Std. Test Statistic	Sig.	Adj.Sig.
Ionian-Aegean	-44.802	43.451	-1.031	.302	1.000
Ionian-Levantine	-146.590	58.666	-2.499	.012	.187
Ionian-Tyrrhenian	225.534	42.256	5.337	.000	.000
Ionian-Balearic	370.601	52.749	7.026	.000	.000
Ionian-Adriatic	-540.605	47.900	-11.286	.000	.000
Aegean-Levantine	101.788	49.615	2.052	.040	.603
Aegean-Tyrrhenian	180.732	28.382	6.368	.000	.000
Aegean-Balearic	325.799	42.455	7.674	.000	.000
Aegean-Adriatic	-495.802	36.255	-13.676	.000	.000
Levantine-Tyrrhenian	78.943	48.571	1.625	.104	1.000
Levantine-Balearic	224.010	57.931	3.867	.000	.002
Levantine-Adriatic	-394.014	53.554	-7.357	.000	.000
Tyrrhenian-Balearic	145.067	41.230	3.518	.000	.007
Tyrrhenian-Adriatic	-315.071	34.813	-9.050	.000	.000
Balearic-Adriatic	-170.004	46.998	-3.617	.000	.004

Each row tests the null hypothesis that the Sample 1 and Sample 2 distributions are the same.
Asymptotic significances (2-sided tests) are displayed. The significance level is .05.

Table S5. Results of the Kruskal-Wallis test indicating significant differences in between Mediterranean-wide seasonal coccolithophore contribution (%) to phytoplankton communities.

Sample1-Sample2	Test Statistic	Std. Error	Std. Test Statistic	Sig.	Adj.Sig.
Summer-Autumn	-2.981	14.475	-.206	.837	1.000
Summer-Winter	24.102	15.023	1.604	.109	.652
Summer-Spring	69.751	11.668	5.978	.000	.000
Autumn-Winter	21.121	14.772	1.430	.153	.917
Autumn-Spring	66.770	11.343	5.887	.000	.000
Winter-Spring	-45.648	12.034	-3.793	.000	.001

Each row tests the null hypothesis that the Sample 1 and Sample 2 distributions are the same.
Asymptotic significances (2-sided tests) are displayed. The significance level is .05.

Table S6. Results of the Kruskal-Wallis test indicating significant differences between microscopy methods at different depth brackets. ILM = Inverted light microscopy; PLM = Polarised light microscopy; and SEM = Scanning electron microscopy. The numbers after each microscopy code indicate the upper limit of a depth bracket: 25 = 0 – 25 m; 50 = 25 – 50 m; 100 = 50 – 100 m; and 215 = 100 – 215 m.

Sample1-Sample2	Test Statistic	Std. Error	Std. Test Statistic	Sig.	Adj.Sig.
ILM200-ILM100	46.090	52.869	.872	.383	1.000
ILM200-ILM50	105.088	50.476	2.082	.037	1.000
ILM200-ILM25	261.703	45.872	5.705	.000	.000
ILM200-PLM100	-386.286	60.836	-6.350	.000	.000
ILM200-SEM200	-393.985	81.824	-4.815	.000	.000
ILM200-PLM50	-433.747	52.536	-8.256	.000	.000
ILM200-PLM25	-529.576	42.231	-12.540	.000	.000
ILM200-SEM100	-568.345	50.745	-11.200	.000	.000
ILM200-SEM25	-622.704	43.682	-14.255	.000	.000
ILM200-PLM200	-658.848	81.824	-8.052	.000	.000
ILM200-SEM50	-678.532	48.361	-14.031	.000	.000
ILM100-ILM50	58.998	58.567	1.007	.314	1.000
ILM100-ILM25	215.613	54.648	3.946	.000	.005
ILM100-PLM100	-340.196	67.700	-5.025	.000	.000
ILM100-SEM200	-347.895	87.048	-3.997	.000	.004
ILM100-PLM50	-387.657	60.351	-6.423	.000	.000
ILM100-PLM25	-483.485	51.629	-9.365	.000	.000
ILM100-SEM100	-522.255	58.798	-8.882	.000	.000
ILM100-SEM25	-576.614	52.823	-10.916	.000	.000
ILM100-PLM200	-612.758	87.048	-7.039	.000	.000
ILM100-SEM50	-632.442	56.753	-11.144	.000	.000
PLM50-SEM100	-134.598	58.500	-2.301	.021	1.000
PLM50-SEM25	-188.957	52.490	-3.600	.000	.021
PLM50-PLM200	-225.101	86.847	-2.592	.010	.630
PLM50-SEM50	-244.785	56.444	-4.337	.000	.001
PLM25-SEM100	-38.769	49.453	-.784	.433	1.000
PLM25-SEM25	-93.128	42.174	-2.208	.027	1.000
PLM25-PLM200	-129.273	81.029	-1.595	.111	1.000
PLM25-SEM50	-148.956	47.003	-3.169	.002	.101
SEM100-SEM25	54.359	50.698	1.072	.284	1.000
SEM100-PLM200	90.503	85.775	1.055	.291	1.000
SEM100-SEM50	110.187	54.781	2.011	.044	1.000
SEM25-PLM200	36.145	81.795	.442	.659	1.000
SEM25-SEM50	-55.828	48.311	-1.156	.248	1.000

Sample1-Sample2	Test Statistic	Std. Error	Std. Test Statistic	Sig.	Adj.Sig.
ILM50-ILM25	156.615	52.337	2.992	.003	.183
ILM50-PLM100	-281.198	65.849	-4.270	.000	.001
ILM50-SEM200	-288.896	85.616	-3.374	.001	.049
ILM50-PLM50	-328.659	58.267	-5.641	.000	.000
ILM50-PLM25	-424.487	49.177	-8.632	.000	.000
ILM50-SEM100	-463.257	56.657	-8.176	.000	.000
ILM50-SEM25	-517.616	50.429	-10.264	.000	.000
ILM50-PLM200	-553.760	85.616	-6.468	.000	.000
ILM50-SEM50	-573.444	54.532	-10.516	.000	.000
ILM25-PLM100	-124.583	62.389	-1.997	.046	1.000
ILM25-SEM200	-132.282	82.985	-1.594	.111	1.000
ILM25-PLM50	-172.044	54.326	-3.167	.002	.102
ILM25-PLM25	-267.873	44.438	-6.028	.000	.000
ILM25-SEM100	-306.642	52.596	-5.830	.000	.000
ILM25-SEM25	-361.001	45.819	-7.879	.000	.000
ILM25-PLM200	-397.145	82.985	-4.786	.000	.000
ILM25-SEM50	-416.829	50.300	-8.287	.000	.000
PLM100-SEM200	-7.699	92.105	-.084	.933	1.000
PLM100-PLM50	47.461	67.440	.704	.482	1.000
PLM100-PLM25	143.290	59.763	2.398	.017	1.000
PLM100-SEM100	-182.059	66.055	-2.756	.006	.386
PLM100-SEM25	-236.418	60.797	-3.889	.000	.007
PLM100-PLM200	-272.563	92.105	-2.959	.003	.204
PLM100-SEM50	-292.246	64.241	-4.549	.000	.000
SEM200-PLM50	39.762	86.847	.458	.647	1.000
SEM200-PLM25	135.591	81.029	1.673	.094	1.000
SEM200-SEM100	174.360	85.775	2.033	.042	1.000
SEM200-SEM25	228.719	81.795	2.796	.005	.341
SEM200-PLM200	264.864	107.133	2.472	.013	.886
SEM200-SEM50	284.547	84.386	3.372	.001	.049
PLM50-PLM25	95.829	51.289	1.868	.062	1.000
PLM200-SEM50	-19.683	84.386	-.233	.816	1.000

Each row tests the null hypothesis that the Sample 1 and Sample 2 distributions are the same.
Asymptotic significances (2-sided tests) are displayed. The significance level is .05.

Table S7. Results of the Kruskal-Wallis test indicating significant the Eastern (E) and Western (W) Mediterranean subbasins at different depth brackets. The numbers after each microscopy code indicate the upper limit of a depth bracket: 25 = 0 – 25 m; 50 = 25 – 50 m; 100 = 50 – 100 m; and 215 = 100 – 215 m.

Sample1-Sample2	Test Statistic	Std. Error	Std. Test Statistic	Sig.	Adj.Sig.
200W-200E	89.787	79.690	1.127	.260	1.000
200W-100E	156.603	79.690	1.965	.049	1.000
200W-50E	197.249	76.462	2.580	.010	.277
200W-100W	320.737	80.006	4.009	.000	.002
200W-25E	322.723	74.755	4.317	.000	.000
200W-50W	386.746	78.352	4.936	.000	.000
200W-25W	506.452	74.951	6.757	.000	.000
200E-100E	66.816	50.851	1.314	.189	1.000
200E-50E	107.461	45.626	2.355	.019	.518
200E-100W	230.950	51.345	4.498	.000	.000
200E-25E	232.936	42.704	5.455	.000	.000
200E-50W	296.959	48.728	6.094	.000	.000
200E-25W	416.665	43.047	9.679	.000	.000
100E-50E	40.646	45.626	.891	.373	1.000
100E-100W	-164.134	51.345	-3.197	.001	.039
100E-25E	166.120	42.704	3.890	.000	.003
100E-50W	230.143	48.728	4.723	.000	.000
100E-25W	349.849	43.047	8.127	.000	.000
50E-100W	-123.489	46.176	-2.674	.007	.210
50E-25E	125.474	36.325	3.454	.001	.015
50E-50W	-189.497	43.247	-4.382	.000	.000
50E-25W	309.203	36.728	8.419	.000	.000
100W-25E	1.986	43.292	.046	.963	1.000
100W-50W	66.008	49.244	1.340	.180	1.000
100W-25W	185.715	43.630	4.257	.000	.001
25E-50W	-64.023	40.153	-1.594	.111	1.000
25E-25W	-183.729	33.028	-5.563	.000	.000
50W-25W	119.706	40.517	2.954	.003	.088

Each row tests the null hypothesis that the Sample 1 and Sample 2 distributions are the same.
Asymptotic significances (2-sided tests) are displayed. The significance level is .05.

Table S8. Results of the Kruskal-Wallis test indicating significant differences between hetero- (HET) and holo-coccolithophore (HOL) abundances between the eastern (East) and western (West) Mediterranean sub-basins during different seasons.

Sample1-Sample2	Test Statistic	Std. Error	Std. Test Statistic	Sig.	Adj.Sig.
East Autumn HOL-West Winter HOL	-64.259	94.640	-.679	.497	1.000
East Autumn HOL-East Winter HOL	419.133	76.344	5.490	.000	.000
East Autumn HOL-West Autumn HOL	-486.655	141.332	-3.443	.001	.069
East Autumn HOL-East Autumn HET	510.257	74.993	6.804	.000	.000
East Autumn HOL-East Summer HOL	531.714	63.665	8.352	.000	.000
East Autumn HOL-West Summer HOL	-650.569	86.142	-7.552	.000	.000
East Autumn HOL-East Spring HOL	769.016	70.950	10.839	.000	.000
East Autumn HOL-West Spring HOL	-794.569	112.121	-7.087	.000	.000
East Autumn HOL-East Summer HET	1,118.506	63.665	17.569	.000	.000
East Autumn HOL-West Summer HET	-1,463.907	86.142	-16.994	.000	.000
East Autumn HOL-East Winter HET	1,592.827	76.344	20.864	.000	.000
East Autumn HOL-West Winter HET	-1,652.698	94.640	-17.463	.000	.000
East Autumn HOL-East Spring HET	1,653.949	70.950	23.311	.000	.000
East Autumn HOL-West Autumn HET	-1,660.707	141.332	-11.750	.000	.000
East Autumn HOL-West Spring HET	-1,754.490	112.121	-15.648	.000	.000
West Winter HOL-East Winter HOL	354.874	95.714	3.708	.000	.025
West Winter HOL-West Autumn HOL	-422.396	152.668	-2.767	.006	.679
West Winter HOL-East Autumn HET	445.998	94.640	4.713	.000	.000
West Winter HOL-East Summer HOL	467.455	85.941	5.439	.000	.000
West Winter HOL-West Summer HOL	-586.310	103.698	-5.654	.000	.000
West Winter HOL-East Spring HOL	704.756	91.469	7.705	.000	.000
West Winter HOL-West Spring HOL	-730.309	126.111	-5.791	.000	.000
West Winter HOL-East Summer HET	1,054.247	85.941	12.267	.000	.000
West Winter HOL-West Summer HET	-1,399.648	103.698	-13.497	.000	.000
West Winter HOL-East Winter HET	1,528.568	95.714	15.970	.000	.000
West Winter HOL-West Winter HET	1,588.438	110.858	14.329	.000	.000
West Winter HOL-East Spring HET	1,589.689	91.469	17.379	.000	.000
West Winter HOL-West Autumn HET	-1,596.448	152.668	-10.457	.000	.000
West Winter HOL-West Spring HET	-1,690.231	126.111	-13.403	.000	.000
East Winter HOL-West Autumn HOL	-67.522	142.054	-.475	.635	1.000
East Winter HOL-East Autumn HET	-91.124	76.344	-1.194	.233	1.000
East Winter HOL-East Summer HOL	-112.581	65.251	-1.725	.084	1.000
East Winter HOL-West Summer HOL	-231.436	87.321	-2.650	.008	.965
East Winter HOL-East Spring HOL	-349.882	72.377	-4.834	.000	.000
East Winter HOL-West Spring HOL	-375.435	113.030	-3.322	.001	.107
East Winter HOL-East Summer HET	-699.373	65.251	-10.718	.000	.000
East Winter HOL-West Summer HET	-1,044.774	87.321	-11.965	.000	.000
East Winter HOL-East Winter HET	1,173.694	77.672	15.111	.000	.000
East Winter HOL-West Winter HET	-1,233.564	95.714	-12.888	.000	.000
East Winter HOL-East Spring HET	-1,234.815	72.377	-17.061	.000	.000
East Winter HOL-West Autumn HET	-1,241.574	142.054	-8.740	.000	.000
East Winter HOL-West Spring HET	-1,335.357	113.030	-11.814	.000	.000
West Autumn HOL-East Autumn HET	23.602	141.332	.167	.867	1.000
West Autumn HOL-East Summer HOL	45.059	135.661	.332	.740	1.000
West Autumn HOL-West Summer HOL	163.914	147.551	1.111	.267	1.000
West Autumn HOL-East Spring HOL	282.360	139.229	2.028	.043	1.000
West Autumn HOL-West Spring HOL	307.913	164.079	1.877	.061	1.000
West Autumn HOL-East Summer HET	631.851	135.661	4.658	.000	.000
West Autumn HOL-West Summer HET	977.252	147.551	6.623	.000	.000
West Autumn HOL-East Winter HET	1,106.172	142.054	7.787	.000	.000
West Autumn HOL-West Winter HET	1,166.042	152.668	7.638	.000	.000
West Autumn HOL-East Spring HET	1,167.293	139.229	8.384	.000	.000
West Autumn HOL-West Autumn HET	1,174.052	185.272	6.337	.000	.000
West Autumn HOL-West Spring HET	1,267.835	164.079	7.727	.000	.000
East Autumn HET-East Summer HOL	21.457	63.665	.337	.736	1.000
East Autumn HET-West Summer HOL	-140.312	86.142	-1.629	.103	1.000
East Autumn HET-East Spring HOL	258.759	70.950	3.647	.000	.032
East Autumn HET-West Spring HOL	-284.312	112.121	-2.536	.011	1.000
East Autumn HET-East Summer HET	608.249	63.665	9.554	.000	.000
East Autumn HET-West Summer HET	-953.650	86.142	-11.071	.000	.000
East Autumn HET-East Winter HET	1,082.570	76.344	14.180	.000	.000
East Autumn HET-West Winter HET	-1,142.440	94.640	-12.071	.000	.000
East Autumn HET-East Spring HET	1,143.692	70.950	16.120	.000	.000
East Autumn HET-West Autumn HET	-1,150.450	141.332	-8.140	.000	.000
East Autumn HET-West Spring HET	-1,244.233	112.121	-11.097	.000	.000
East Summer HOL-West Summer HOL	-118.855	76.483	-1.554	.120	1.000
East Summer HOL-East Spring HOL	237.301	58.849	4.032	.000	.007
East Summer HOL-West Spring HOL	-262.854	104.883	-2.506	.012	1.000
East Summer HOL-East Summer HET	586.792	49.824	11.777	.000	.000
East Summer HOL-West Summer HET	-932.193	76.483	-12.188	.000	.000
East Summer HOL-East Winter HET	1,061.113	65.251	16.262	.000	.000
East Summer HOL-West Winter HET	-1,120.983	85.941	-13.044	.000	.000
East Summer HOL-East Spring HET	1,122.234	58.849	19.070	.000	.000
East Summer HOL-West Autumn HET	-1,128.992	135.661	-8.322	.000	.000
East Summer HOL-West Spring HET	-1,222.776	104.883	-11.658	.000	.000
West Summer HOL-East Spring HOL	118.446	82.647	1.433	.152	1.000
West Summer HOL-West Spring HOL	143.999	119.866	1.201	.230	1.000
West Summer HOL-East Summer HET	467.937	76.483	6.118	.000	.000
West Summer HOL-West Summer HET	813.338	96.005	8.472	.000	.000
West Summer HOL-East Winter HET	942.258	87.321	10.791	.000	.000
West Summer HOL-West Winter HET	1,002.128	103.698	9.664	.000	.000
West Summer HOL-East Spring HET	1,003.379	82.647	12.141	.000	.000
West Summer HOL-West Autumn HET	-1,010.137	147.551	-6.846	.000	.000
West Summer HOL-West Spring HET	1,103.921	119.866	9.210	.000	.000

Sample1-Sample2	Test Statistic	Std. Error	Std. Test Statistic	Sig.	Adj.Sig.
East Winter HOL-East Spring HET	-1,234.815	72.377	-17.061	.000	.000
East Winter HOL-West Autumn HET	-1,241.574	142.054	-8.740	.000	.000
East Spring HOL-West Spring HOL	-25.553	109.459	-.233	.815	1.000
East Spring HOL-East Summer HET	-349.491	58.849	-5.939	.000	.000
East Spring HOL-West Summer HET	-694.892	82.647	-8.408	.000	.000
East Spring HOL-East Winter HET	823.812	72.377	11.382	.000	.000
East Spring HOL-West Winter HET	-883.682	91.469	-9.661	.000	.000
East Spring HOL-East Spring HET	884.933	66.663	13.275	.000	.000
East Spring HOL-West Autumn HET	-891.691	139.229	-6.404	.000	.000
East Spring HOL-West Spring HET	-985.475	109.459	-9.003	.000	.000
West Spring HOL-East Summer HET	323.938	104.883	3.089	.002	.241
West Spring HOL-West Summer HET	-669.339	119.866	-5.584	.000	.000
West Spring HOL-East Winter HET	798.259	113.030	7.062	.000	.000
West Spring HOL-West Winter HET	858.129	126.111	6.805	.000	.000
West Spring HOL-East Spring HET	859.380	109.459	7.851	.000	.000
West Spring HOL-West Autumn HET	-866.138	164.079	-5.279	.000	.000
West Spring HOL-West Spring HET	959.922	139.708	6.871	.000	.000
East Summer HET-West Summer HET	-345.401	76.483	-4.516	.000	.001

Each row tests the null hypothesis that the Sample 1 and Sample 2 distributions are the same.
Asymptotic significances (2-sided tests) are displayed. The significance level is .05.

Table S9. Results of the Kruskal-Wallis test indicating significant differences between hetero- (HET) and holo-coccolithophore (HOL) diversity between the eastern (East) and western (West) Mediterranean sub-basins during different seasons.

Sample1-Sample2	Test Statistic	Std. Error	Std. Test Statistic	Sig.	Adj.Sig.
West Winter HOL-East Autumn HOL	435.756	95.058	4.584	.000	.001
West Winter HOL-East Winter HOL	437.597	97.850	4.472	.000	.001
West Winter HOL-West Winter HET	466.667	113.332	4.118	.000	.005
West Winter HOL-West Autumn HOL	-509.759	156.075	-3.266	.001	.131
West Winter HOL-West Summer HOL	-714.301	106.012	-6.738	.000	.000
West Winter HOL-East Summer HOL	730.137	87.859	8.310	.000	.000
West Winter HOL-West Spring HOL	-737.912	128.926	-5.724	.000	.000
West Winter HOL-East Spring HOL	883.918	92.488	9.557	.000	.000
West Winter HOL-East Autumn HET	923.957	95.058	9.720	.000	.000
West Winter HOL-East Winter HET	1,069.691	97.850	10.932	.000	.000
West Winter HOL-East Summer HET	1,150.928	87.859	13.100	.000	.000
West Winter HOL-East Spring HET	1,240.422	93.511	13.265	.000	.000
West Winter HOL-West Summer HET	-1,426.519	106.012	-13.456	.000	.000
West Winter HOL-West Autumn HET	-1,606.362	156.075	-10.292	.000	.000
West Winter HOL-West Spring HET	-1,644.461	128.926	-12.755	.000	.000

Sample1-Sample2	Test Statistic	Std. Error	Std. Test Statistic	Sig.	Adj.Sig.
East Autumn HOL-East Winter HOL	1.841	75.938	.024	.981	1.000
East Autumn HOL-West Winter HET	-30.910	95.058	-.325	.745	1.000
East Autumn HOL-West Autumn HOL	-74.002	143.358	-.516	.606	1.000
East Autumn HOL-West Summer HOL	-278.545	86.201	-3.231	.001	.148
East Autumn HOL-East Summer HOL	294.381	62.540	4.707	.000	.000
East Autumn HOL-West Spring HOL	-302.155	113.198	-2.669	.008	.912
East Autumn HOL-East Spring HOL	448.162	68.891	6.505	.000	.000
East Autumn HOL-East Autumn HET	488.201	72.305	6.752	.000	.000
East Autumn HOL-East Winter HET	633.935	75.938	8.348	.000	.000
East Autumn HOL-East Summer HET	715.171	62.540	11.435	.000	.000
East Autumn HOL-East Spring HET	804.666	70.259	11.453	.000	.000
East Autumn HOL-West Summer HET	-990.762	86.201	-11.494	.000	.000
East Autumn HOL-West Autumn HET	-1,170.606	143.358	-8.166	.000	.000
East Autumn HOL-West Spring HET	-1,208.705	113.198	-10.678	.000	.000

Sample1-Sample2	Test Statistic	Std. Error	Std. Test Statistic	Sig.	Adj.Sig.
East Winter HOL-West Winter HET	-29.070	97.850	-.297	.766	1.000
East Winter HOL-West Autumn HOL	-72.162	145.224	-.497	.619	1.000
East Winter HOL-West Summer HOL	-276.704	89.270	-3.100	.002	.233
East Winter HOL-East Summer HOL	-292.540	66.707	-4.385	.000	.001
East Winter HOL-West Spring HOL	-300.315	115.553	-2.599	.009	1.000
East Winter HOL-East Spring HOL	-446.321	72.695	-6.140	.000	.000
East Winter HOL-East Autumn HET	-486.360	75.938	-6.405	.000	.000
East Winter HOL-East Winter HET	632.094	79.406	7.960	.000	.000
East Winter HOL-East Summer HET	-713.331	66.707	-10.693	.000	.000
East Winter HOL-East Spring HET	-802.825	73.993	-10.850	.000	.000
East Winter HOL-West Summer HET	-988.922	89.270	-11.078	.000	.000
East Winter HOL-West Autumn HET	-1,168.765	145.224	-8.048	.000	.000
East Winter HOL-West Spring HET	-1,206.864	115.553	-10.444	.000	.000
West Winter HET-West Autumn HOL	-43.092	156.075	-.276	.782	1.000
West Winter HET-West Summer HOL	-247.634	106.012	-2.336	.019	1.000
West Winter HET-East Summer HOL	263.470	87.859	2.999	.003	.325
West Winter HET-West Spring HOL	-271.245	128.926	-2.104	.035	1.000
West Winter HET-East Spring HOL	417.251	92.488	4.511	.000	.001
West Winter HET-East Autumn HET	457.291	95.058	4.811	.000	.000
West Winter HET-East Winter HET	603.024	97.850	6.163	.000	.000
West Winter HET-East Summer HET	684.261	87.859	7.788	.000	.000
West Winter HET-East Spring HET	773.755	93.511	8.274	.000	.000
West Winter HET-West Summer HET	-959.852	106.012	-9.054	.000	.000
West Winter HET-West Autumn HET	-1,139.695	156.075	-7.302	.000	.000
West Winter HET-West Spring HET	-1,177.794	128.926	-9.135	.000	.000
West Autumn HOL-West Summer HOL	204.542	150.844	1.356	.175	1.000
West Autumn HOL-East Summer HOL	220.379	138.689	1.589	.112	1.000
West Autumn HOL-West Spring HOL	228.153	167.742	1.360	.174	1.000
West Autumn HOL-East Spring HOL	374.159	141.666	2.641	.008	.992
West Autumn HOL-East Autumn HET	414.199	143.358	2.889	.004	.463
West Autumn HOL-East Winter HET	559.932	145.224	3.856	.000	.014
West Autumn HOL-East Summer HET	641.169	138.689	4.623	.000	.000
West Autumn HOL-East Spring HET	730.663	142.337	5.133	.000	.000
West Autumn HOL-West Summer HET	916.760	150.844	6.078	.000	.000
West Autumn HOL-West Autumn HET	1,096.603	189.407	5.790	.000	.000
West Autumn HOL-West Spring HET	1,134.702	167.742	6.765	.000	.000
West Summer HOL-East Summer HOL	15.836	78.191	.203	.839	1.000
West Summer HOL-West Spring HOL	23.611	122.541	.193	.847	1.000
West Summer HOL-East Spring HOL	169.617	83.357	2.035	.042	1.000
West Summer HOL-East Autumn HET	209.656	86.201	2.432	.015	1.000
West Summer HOL-East Winter HET	355.390	89.270	3.981	.000	.008
West Summer HOL-East Summer HET	436.627	78.191	5.584	.000	.000
West Summer HOL-East Spring HET	526.121	84.491	6.227	.000	.000
West Summer HOL-West Summer HET	712.218	98.148	7.257	.000	.000
West Summer HOL-West Autumn HET	-892.061	150.844	-5.914	.000	.000
West Summer HOL-West Spring HET	930.160	122.541	7.591	.000	.000
East Summer HOL-West Spring HOL	-7.775	107.224	-.073	.942	1.000
East Summer HOL-East Spring HOL	153.781	58.559	2.626	.009	1.000
East Summer HOL-East Autumn HET	-193.820	62.540	-3.099	.002	.233
East Summer HOL-East Winter HET	339.554	66.707	5.090	.000	.000
East Summer HOL-East Summer HET	420.791	50.936	8.261	.000	.000
East Summer HOL-East Spring HET	510.285	60.162	8.482	.000	.000
East Summer HOL-West Summer HET	-696.381	78.191	-8.906	.000	.000
East Summer HOL-West Autumn HET	-876.225	138.689	-6.318	.000	.000
East Summer HOL-West Spring HET	-914.324	107.224	-8.527	.000	.000
West Spring HOL-East Spring HOL	146.006	111.048	1.315	.189	1.000
West Spring HOL-East Autumn HET	186.046	113.198	1.644	.100	1.000
West Spring HOL-East Winter HET	331.779	115.553	2.871	.004	.491
West Spring HOL-East Summer HET	413.016	107.224	3.852	.000	.014
West Spring HOL-East Spring HET	502.510	111.902	4.491	.000	.001
West Spring HOL-West Summer HET	-688.607	122.541	-5.619	.000	.000
East Spring HOL-East Autumn HET	-40.039	68.891	-.581	.561	1.000
East Spring HOL-East Winter HET	185.773	72.695	2.556	.011	1.000
East Spring HOL-East Summer HET	-267.010	58.559	-4.560	.000	.001
East Spring HOL-East Spring HET	356.504	66.740	5.342	.000	.000
East Spring HOL-West Summer HET	-542.600	83.357	-6.509	.000	.000
East Spring HOL-West Autumn HET	-722.444	141.666	-5.100	.000	.000
East Spring HOL-West Spring HET	-760.543	111.048	-6.849	.000	.000
East Autumn HET-East Winter HET	145.734	75.938	1.919	.055	1.000

Each row tests the null hypothesis that the Sample 1 and Sample 2 distributions are the same.
Asymptotic significances (2-sided tests) are displayed. The significance level is .05.

Mediterranean Sea regions

Alboran Sea

Coccolithophores make between 13.1 – 19.5% of the phytoplankton community in the Alboran Sea (Mercado et al. 2007), however this differs by season, with a higher proportion during spring (Mercado et al. 2007). Spring also has the highest average coccolithophore abundance 86.97 x 10^3 L^{-1} (Mercado et al. 2007). The only season represented in the dataset for the Alboran Sea is spring, therefore inferences regarding other seasons are related solely to reported findings in the systematic review. *Emiliania huxleyi* is the most dominant species, which contributes an average of 41% to the coccolithophore community (Barcena et al. 2004), but can reach as high as ~60% (Barcena et al. 2004). High abundances of *E. huxleyi* in this region have been associated with a decrease in the abundance of diatoms (Mercado et al. 2007). *Gephyrocapsa oceanica* also has high abundances in the Alboran Sea (Mercado et al. 2007, Mercado et al. 2005, Barcena et al. 2004) and can contribute an average 27% to coccolithophore community (Barcena et al. 2004) and up to 73% (Barcena et al. 2004). *Florisphaera profunda* is also common and can contribute between 0 – 16% to the coccolithophore community (Barcena et al. 2004). The only data contributing to the MA from the Alboran Sea is from Oviedo et al. (2015), which indicates relatively high abundances and diversity during spring. This study also presents opposing depth diversity distribution for hetero and holococcolithophores, where holococcolithophore diversity is greater below 50 m and heterococcolithophore diversity is greatest between 50 – 100 m.

Balearic Sea

In the Balearic Sea coccolithophores have been shown to contribute to 14% of plankton diversity (Bouza and Aboal 2008) and can dominate the phytoplankton community during autumn due to increased abundance associated with high nutrient concentrations (Valencia-Vila et al. 2016). Additionally, offshore stations appear to be dominated by coccolithophores rather than diatoms (Estrada et al. 1999). Coccolithophore abundance was shown to be related to increasing stratification (Estrada et al. 1999), with the highest abundances in the upper 50 m of the water column (Vilicic et al. 2009).

The Balearic Sea is well represented in the MA, with six sets of data contributing to this region from D'Amario et al., (2017), Estrada et al., (1999), Oviedo et al., (2015), Valencia-Vila et al., (2016), Young et al., (2002) and the MAREDAT dataset which represents all seasons. Data on the contribution of coccolithophores to the phytoplankton community is limited (Oviedo et al. 2015; Valencia-Vila et al. 2016), and overall indicates a contribution of 29% from coccolithophores in this region. Data from the Balearic Sea is varied, with a large range of total abundances from 0 – 130 x 10^3 L^{-1} and an average of 9.4 x 10^3 L^{-1} (MA data). The most abundant species are *E. huxleyi* (average abundance 2.9 x 10^3), *Calyptrosphaera* species (1.8 x 10^3), *G. ericsonii* (0.46 x 10^3), *S. olischii* (0.36 x 10^3) and *H. carteri* (0.21 x 10^3; Fig. S11) Estrada et al. (1999) found high abundances for similar species including *E. huxleyi* (as also reported by Saugestad & Heimdal, 2002), as well as *H. carteri*, *Calcidiscus leptoporus,* and *U. sibage*. While high numbers of *E. huxleyi* have specifically been reported during winter (Valencia-Vila et al. 2016), the dataset here indicates relatively stable abundances of *E. huxleyi* throughout the year.

Tyrrhenian Sea

The Tyrrhenian Sea is most abundant during spring but generally has abundances below 5000 cells L^{-1} for the rest of the year (Fig. S3A). This region does not have high levels of species diversity however holococcolithophores contribute as much as 33% to species diversity (Saugestad and Heimdal 2002). Average species abundances range from 4.3 - 8.37 x 10^3 (Bonomo et al. 2014, 2017) which is distinctly lower than indicated in the MA (32.1 x 10^3). *Emiliania huxleyi* is recorded frequently as the most common species, with percentage contribution ranging from 37% (Bonomo et al. 2017) to 79% (Ziveri et al. 2014) in the literature, and 73% in the MA. Abundances of *E. huxleyi* have been shown to reach as high as 229 x 10^3 (October, 2014 – Bonomo et al. 2018). Other abundant species indicated in the literature include *Gephyrocapsa sp.* (13%; Bonomo et al. 2017), *Syracosphaera sp*. (Bonomo et al. 2017; 25% - Saugestad and Heimdal 2002), and *Rhabdosphaera xiphos* (9%; Bonomo et al. 2014), aligning well with the MA findings (Table S11).

The majority of studies from the Tyrrhenian Sea are coccolithophore studies (Fig. 4A). Of the two phytoplankton studies, one is based in a coastal region in the Gulf of Naples (Zingone et al. 2010). This is a long-term study that ran from 1985-2006, however very little detail is provided regarding the coccolithophore community, and only the most common species, *E. huxleyi*, is mentioned (Zingone et al. 2010). All coccolithophores studies are single point or two point surveys conducted during spring (Saugestad and Heimdal 2002; Bonomo et al. 2014, 2018a) and summer (Ziveri et al. 2014; Bonomo et al. 2017, 2021) except for one coastal study in autumn and winter (Bonomo et al. 2018a). Additionally, only one set of data included in the MA investigates the cooler months (February; Bonomo et al., 2018), limiting our knowledge of coccolithophore community dynamics during winter and autumn. *Emiliania huxleyi* is common throughout winter, and occasionally experienced blooms at the end of summer (Zingone et al. 2010). Coccolithophores were shown to be negatively correlated with temperature and positively correlated salinity (Zingone et al. 2010).

Ionian Sea

Coccolithophores sometimes form the majority of the phytoplankton assemblage (Malinverno et al. 2003), particularly in the photic zone in late autumn and early winter (Malinverno et al. 2003). *Emiliania huxleyi* has been noted as a dominant species of the phytoplankton community and can contribute 5-12% to the phytoplankton community in spring (1.7 - 3.9 x 10^3; Varkitzi et al. 2020) and 3-6% in summer (0.6-1.4 x 10^3; Varkitzi et al. 2020). *Emiliania huxleyi*, a cosmopolitan species, is likely abundant in the Ionian Sea due to the ocean like qualities of this region (Varkitzi et al. 2020).

Total coccolithophore abundances differ within the Ionian Sea, with higher abundances in the west compared to the east noted in Bonomo et al. (2021), while the opposite trend was noted in Malinverno et al. (2003). In the coccolithophore community, *E. huxleyi* is the most dominant coccolithophore species, making up approximately 80% of the assemblage (Malinverno et al. 2003) and nearly 100% of the assemblage at 200 m depth (Malinverno et al. 2003), correlating well with the MA.

Total maximum abundances were generally in the range of 20-30 x 10^3 (Malinverno et al. 2003; Bonomo et al. 2021), however abundances reached as high as 138 x 10^3 (MA). The next most abundant species as indicated by the literature is *F. profunda* (highest relative abundance in the MA - Fig. 9; Malinverno et al. 2003; Bonomo et al. 2021), which usually dominates assemblages at depth, peaking just below the thermocline (Malinverno et al. 2003).

Malinverno et al. (2003) noted a clear surface-depth decrease in abundance, however the dataset indicates an increase in abundance from 0 – 25m which is maintained until 200m depth (Fig. S3A). This may be related to the high abundances of the deep dwelling *F. profunda* in this region. The Ionian Sea is a comparatively diverse region from 0 – 150m, particularly in spring and summer (Fig. S4), and heterococcolithophores are more diverse than holococcolithophores (Fig. S4). Syracosphaera species are also common in this region, including the holococcolithophore *S. pulchra HOL* oblonga type (Table S11).

Adriatic Sea

The Adriatic Sea is the most highly studied region in the Mediterranean Sea and most of these studies focus on the whole phytoplankton community (Fig. 4A). Coccolithophores generally make up 1.3%-10.7% of the phytoplankton community in the Adriatic Sea (Cerino et al. 2017; Krivokapic et al. 2018), and the MA similarly indicates an average contribution of 4.25%, yet they can contribute up to 98.2% (including the long-term dataset). The winter phytoplankton community is sometimes dominated by coccolithophores (Godrijan et al. 2013), which is likely associated with the high abundances of *E. huxleyi*, which is more common in winter. In other cases, coccolithophores dominate the phytoplankton community in summer (Viličić et al. 2008) and have been shown to dominant phytoplankton assemblages at deep water stations (Viličić et al. 2011) and in certain regions of the Adriatic, such as the Adriatic channel (autumn 2008; Šupraha et al. 2011) or near the Po River, particularly during periods of low discharge (Burić et al. 2007).

The highest abundances are generally recorded during winter (e.g. 15 x 10^3 (Mozetiĉ et al. 1998; Viličić et al. 2008; Drakulović et al. 2017), and this aligns well with the long-

term dataset from the Adriatic as the highest abundance of 2029 x 10^3 also occurred during winter. Coccolithophore abundance can be higher in spring than in autumn (Saracino and Rubino 2006) and high abundances in the range of 1181 – 1136 x 10^3 have been reported during spring. Following the trend of the majority of the Mediterranean Sea (Fig. S4), diversity was highest in spring (also in Godrijan et al., 2018), followed by autumn. Holococcolithophore abundance tends to increase in spring (Cerino et al. 2017) and summer (Fig. S3C), indicating opposing temporal distribution to heterococcolithophores (Fig. S3B).

The Adriatic Sea has high winter abundances of *E. huxleyi*, which is recorded as the most common species (Table S11; Balestra et al., 2009; Bernardi Aubry et al., 2022; Caroppo et al., 1999; Cerino et al., 2017, 2019; Godrijan et al., 2013, 2018; Moscatello et al., 2011; Saracino & Rubino, 2006; Skejic et al., 2018; Supraha et al., 2016; Totti et al., 2000; Vilicic et al., 2009; Viličić et al., 2009) and can contribute as much as 88% to the coccolithophore community (Godrijan et al. 2013). *Emiliania huxleyi* is known to prefer cooler water and higher abundances are recorded in winter compared to summer or spring (Aubry and Acri 2004; Supraha et al. 2016; Cerino et al. 2017; Godrijan et al. 2018; Totti et al. 2019; Neri et al. 2022), when other species tend to dominate the community, such as Syracosphaera species (Supraha et al. 2016; Cerino et al. 2017; Totti et al. 2019). The MA similarly indicates that the most abundant season for *E. huxleyi* in the Adriatic Sea is winter, followed by spring (Table S11). *Florisphaera profunda* was noted the most common deep water species (Balestra et al. 2009) however the MA indicated that this was not a highly abundant species in the Adriatic Sea. Other common species in the Adriatic Sea include Rhabdosphaera species (Totti et al. 2000; Balestra et al. 2009; Skejic et al. 2018; Drakulović et al. 2021), Syracosphaera species (Supraha et al. 2016; Cerino et al. 2017; Drakulović et al. 2017, 2021; Godrijan et al. 2018; Skejic et al. 2018) and *Acanthoica quattrospina* (Supraha et al. 2016; Cerino et al. 2017), which is reflected well in the MA (Table S11).

Coccolithophore total abundance has been negatively associated with chlorophyll *a* concentrations (Mozetič et al. 1998), while holococcolithophore abundance has been positively correlated with temperature (Supraha et al. 2016). *Emiliania huxleyi* has been positively correlated with salinity and nutrients in the Adriatic Sea (Supraha et al. 2016; Godrijan et al. 2018; Krivokapic et al. 2018; Cerino et al. 2019; Neri et al. 2022) and

negatively correlated with temperature (Supraha et al. 2016; Cerino et al. 2017; Godrijan et al. 2018; Neri et al. 2022).

Aegean and Cretan Sea

Coccolithophores contribute between 2.2 – 55.2 % of the phytoplankton community in the Aegean Sea (Gotsis-Skretas et al. 1999; Mara et al. 2016; Varkitzi et al. 2020), and up to 61% during bloom events (Ignatiades et al. 1995), however this differs depending on the season. The MA indicates a much higher contribution of coccolithophores to the phytoplankton community, with an average of 55.9% contribution and up to 95.3%. Very high abundances have also been recorded in the Aegean Sea, which likely reflect the occurrence of blooms (396 x 10^3; Dimiza et al. 2016; Skampa et al. 2019). Several coccolithophore studies investigate seasonality (Dimiza et al. 2008, 2016, 2020), while spring and summer are the most investigated seasons for phytoplankton studies (Eker-Develi et al. 2006; Aktan 2011; Mara et al. 2016; Varkitzi et al. 2020). According to Gotsis-Skretas et al. (1999), in autumn, the phytoplankton assemblage consists of a large amount of coccolithophores (average 40.8%), followed by spring (22.7%), then winter (14.2%) and summer (19.2%; Gotsis-Skretas et al. 1999). The MA indicates that this region is not highly abundant (Fig. S3A), however it is highly diverse (Fig. S4), and this diversity increases during warmer months (Dimiza et al., 2016; Karatsolis et al., 2017).

Most phytoplankton studies from the Aegean Sea either do not report the individual species, or only mention highly abundant species such as *E. huxleyi* (Eker-Develi et al. 2006; Cerino et al. 2019). Gotsis-Skretas et al. (1999) reported *E. huxleyi*, as well as *Calyptrosphaera globosa* and Pontosphaera species as the most dominant components of the phytoplankton assemblage during autumn (Gotsis-Skretas et al. 1999). At large, coccolithophore studies indicate that *E. huxleyi* is the most abundant species, making up to 70-80% of the coccolithophore community (Dimiza et al. 2016; Triantaphyllou et al. 2018), with abundances reaching up to 274 x 10^3 (Karatsolis et al. 2017). *Emiliania huxleyi* was shown to be less abundant in summer (Dimiza et al. 2016; Karatsolis et al. 2017) and more dominant during late autumn-early spring (Dimiza et al., 2016; Skampa et al., 2019; Triantaphyllou et al., 2018). Other common species include *G. oceanica* which can occur in high abundances during late summer and autumn (up to 200 x 10^3),

and Syracosphaera species (Dimiza et al. 2016; Skampa et al. 2019). High concentrations of holococcoltihophore species represented 60-90% of the coccolithophore surface assemblages in early autumn in the south-west Aegean Sea (Triantaphyllou et al. 2018), however the MA indicates relatively low abundances of holococcolithophores, with peaks in spring and summer (Fig. S3C).

Coccolithophore community composition in the Aegean Sea has been shown to be related to temperature (Dimiza et al. 2008, 2016; Triantaphyllou et al. 2018), nutrients (Triantaphyllou et al. 2018) and pH (Triantaphyllou et al. 2018). *Emiliania huxleyi* abundances have been positively correlated with nitrate (Eker-Develi et al. 2006), however Varkitzi et al. (2020) showed that *E. huxleyi* can be more abundant in the ultra-oligotrophic northern Aegean Sea compared to the southern Aegean Sea.

Levantine Sea

There are four phytoplankton studies in the Levantine basin that incorporate coccolithophores and sampling was mostly confined to summer (Aktan 2011; Varkitzi et al. 2020). Coccolithophorse can make up to nearly 80% of the phytoplankton community in the deep chlorophyll maximum layer (Kimor et al. 1987), and *E. huxleyi* was shown to contribute 6-8% of the phytoplankton community, with abundances reaching 2.4 x 10^3 (Varkitzi et al. 2020). As many coccolithophore species, including the highly abundant *E. huxleyi*, increase in abundance during colder periods, we lack crucial data about coccolithophore abundances in this region, given that there is only one year-long study investigating seasonality.

Of the two coccolithophore studies in the Levantine Sea, one investigates new haptophyte species in the region (Sahin and Eker-Develi 2019). The other investigates seasonal coccolithophore patterns over a 12 month period (Keuter et al. 2022). Here, coccolithophore abundance increased during winter, however diversity decreased, and summer and autumn were the most diverse seasons (Sahin and Eker-Develi 2019). Coccolithophore abundance was highest at 100m during spring (50×10^3 L^{-1}), while the highest holococcoltihophore abundance was recorded during summer near the surface

(Sahin and Eker-Develi 2019). In the MA, abundances in the Levantine Sea are highest during spring, and this remains similar over all depth brackets (Fig. 3A).

Emiliania huxleyi was recorded as the most common species, while other common species include *F. profunda*, *A. robusta*, *U. irregularis*, *G oceanic*, *H. carteri*, *C. brasiliensis*, *S. ossa*, *U. tenuis*, and *R. clavigera* var. stylifera (Sahin and Eker-Develi 2019), correlating well with the dataset here (Table S11). When compared to cooler autumn and winter months, *E. huxleyi* abundance was greater at coastal stations versus open sea stations, and was also shown to be positively related to high nitrate concentrations (Eker-Develi et al. 2006). The MA indicates *E. huxleyi* abundances increased during autumn, which does not reflect the findings of Eker-Develi et al. (2006).

Other regions

Several Mediterranean Sea regions have conducted limited research regarding coccolithophores. The Ligurian Sea is understudied with respect to coccolithophores and is only included here in a study that investigated several regions (Bonomo et al. 2021). This region recorded high concentrations of *H. carteri* coupled with low concentrations of *E. huxleyi* during summer. A phytoplankton study conducted in the Gulf of Gabes includes very little data on coccolithophores, which it notes makes up only 1% of the phytoplankton community, and *E. huxleyi* is the only species mentioned (Rekik et al. 2017). A study in the Gulf of Tunis off the coast of Tunisia investigating the impact of fish farming on the phytoplankton community and water quality notes that coccolithophores appear in 32% of the samples collected over a year period, with a maximum abundance of 2800 cells L^{-1} (Challouf et al. 2017). One study in the Otranto Strait investigated nutrients and phytoplankton variability and noted *E. huxleyi* was the most common species (Socal et al. 1999). All studies bar the Ligurian study focus on the whole phytoplankton community and do not provide detailed information regarding coccolithophores.

The Strait of Sicily is a highly dynamic area in the Mediterranean Sea and has high abundances when compared to surrounding regions (Saugestad and Heimdal 2002) such as the Ionian and Tyrrhenian Sea, where abundances can reach a maximum of 520 x 10^3.

Emiliania huxleyi is the most common species with abundances reaching 60 x 10^3 (Bonomo et al. 2021).

Table S10. Average Mediterranean-wide abundance (coccolithophores L^{-1}) of the most abundant 15 species. **Emiliania huxleyi* morphotype not specified.

	Abundance (L^{-1})
E. huxleyi*	17071
S. halldalii	1536
R. clavigera	1219
S. pulchra	691
G. ericsonii	667
S. molischii	444
U. tenuis	441
R. xiphos	437
S. protrudens	436
S. arethusae (HOL)	427
A. quattrospina	415
P. vandelii	380
E. huxleyi (B/C)	359
S. histrica	357
C. gracilis	351

Table S11. Average regional abundances and maximum abundances (coccolithophores L^{-1}) for the 10 most abundant species in each region. **Emiliania huxleyi* morphotype not specified.

Alboran Sea		Balearic Sea		Tyrrhenian Sea		Ionian Sea		Levantine Sea		Adriatic Sea		Aegean Sea	
Species	**Avg.**	**Species**	**Avg.**	**Species**	**Avg.**	**Species**	**Avg.**	**Species**	**Avg.**	**Species**	**Avg.**	**Species**	**Avg.**
E. huxleyi*	23277	***E. huxleyi****	10165	***E. huxleyi****	23305	***E. huxleyi****	11644	***E. huxleyi****	13056	***E. huxleyi****	28116	***E. huxleyi****	9734
E. huxleyi (Type B/C)	22114	***G. ericsonii***	2596	***Gephyrocapsa sp.***	1150	***S. pulchra***	1222	***U. tenuis***	1365	***S. halldalii***	7086	***R. clavigera***	692
G. ericsonii	13939	***H. cornifera(HOL)***	1101	***S. pulchra***	536	***F. profunda***	1014	***S. protrudens***	771	***HOL others***	4509	***S. molischii***	292
G. oceanica	11876	***R. xiphos***	1082	***F. profunda***	458	***U. tenuis***	848	***R. clavigera***	647	***R. clavigera***	2694	***H. cornifera(HOL)***	202
C. gracilis	10162	***R. clavigera***	1063	***U. tenuis***	251	***S. protrudens***	829	***D. tubifera***	606	***A. quattrospina***	1698	***S. pulchra(HOL)***	189
G. muellerae	6922	***S. molischii***	1042	***R. xiphos***	200	***R. clavigera***	763	***P. vandelii***	471	***S. pulchra***	1267	***A. robusta(HOL)***	183
P. vandelii	6686	***U. tenuis***	979	***Calciosolenia sp.***	173	***P. vandelii***	479	***F. profunda***	437	***S. arethusae(HOL)***	1080	***S. pulchra***	173
S. arethusae(HOL)	3412	***S. bannockii(HOL)***	893	***C. gracilis***	81	***R. xiphos***	332	***S. pulchra***	409	***S. histrica(HOL)***	1020	***P. vandelii***	159
C. rigidus	3206	***H. carteri***	650	***R. clavigera***	78	***Syracosphaera sp.***	269	***U. sibogae***	340	***A. quattrospina(HOL)***	1008	***S. histrica(HOL)***	139
Corisphaera sp. Type A	2617	***S. arethusae(HOL)***	545	***H. carteri***	62	***S. pulchra (HOL oblonga type)***	257	***A. robusta***	319	***C. mediterranea(HOL)***	990	***U. tenuis***	131

Table S12. Relationship with environmental variables and total coccolithophore abundance outlined in 16 published articles.

Reference	Temp	Depth	Nutrients	NO_3	PO_4	SiO_4	pH	pCO_2	$CO^3{}_2$	Salinity	O_2
Neri et al. (2022)	Neg				Neg					Pos	
Skejić et al. (2021)	Pos	Pos		Pos							
Dimiza et al. (2020)	Pos			NE		NE	NE			NE	NE
Cerino et al. (2019)	NE			NE	Pos	Pos				NE	
Bonomo et al. (2018)			Neg								
Triantaphyllou et al. (2018)							Pos				
Skejic et al. (2018)		Neg		Neg	Neg		Pos				
Krivokapic et al. (2018)	Neg			Neg		Neg				Pos	
Godrijan et al. (2018)	NE			Pos		Pos				NE	
Rekik et al. (2017)											
Supraha et al. (2016)	Neg										
Oviedo et al. (2015)							Pos	Neg	Pos	Pos	
Vilicic et al. (2009)											
Balestra et al. (2009)	NE			NE	NE					NE	
Totti et al. (2000)				NE	NE	Neg				Neg	Pos
Knappertsbusch (1993)	NE									NE	
Positive	2	1	0	2	1	2	3	0	1	3	1
Negative	3	1	1	2	2	2	0	1	0	1	0
No effect	4	0	0	4	2	1	1	0	0	5	1

Table S13. Relationship with environmental variables and holococcolithophore abundance outlined in seven published articles.

Reference	Temp	Depth	NO_3	PO_4	pH	pCO_2	$CO^3{}_2$	Salinity	PAR
Bonomo et al. (2018)	Pos								
Triantaphyllou et al. (2018)					Neg				
Skejic et al. (2018)		Neg		Neg	Pos	Neg	Pos		Pos
D'Amario et al. (2017)	Pos		Neg	Neg	Neg			NE	
Supraha et al. (2016)	Pos							NE	
Oviedo et al. (2015)		Neg	Neg			Pos			
Kleijne (1990)	NE								
Positive	3	0	0	0	1	1	0	0	1
Negative	0	2	2	2	2	1	1	0	0
No effect	1	0	0	0	0	0	0	2	0

Table S14. Relationship with environmental variables and coccolithophore diversity outlined in two published articles.

Reference	Temp	Depth	PO_4	pH	CO^3_2	Salinity
Dimiza et al. (2020)	Neg	Neg	Neg			
Oviedo et al. (2015)				Neg	Neg	Neg
Positive	0	0	0	1	0	0
Negative	1	1	1	1	1	1
No effect	0	0	0	0	0	0

Table S15. Relationship with environmental variables and *E. huxleyi* abundance outlined in five published articles.

Reference	Temp	Depth	NO_3	PO_4	SiO_4	Salinity	O_2
Godrijan et al. (2018)	Neg		Pos			Pos	
Karatsolis et al. (2017)	Neg	NE	Pos	Pos		Pos	Pos
Godrijan et al. (2013)	Neg		Pos	Pos	NE	NE	
Balestra et al. (2009)	NE		NE	NE		NE	
Knappertsbusch (1993)	NE					NE	
Positive	**0**	**0**	**3**	**2**	**0**	**2**	**1**
Negative	**3**	**0**	**0**	**0**	**0**	**0**	**0**
No effect	**2**	**1**	**1**	**1**	**1**	**3**	**0**

Table S16. List of the 72 studies included in the systematic review.

1. Aktan, Y. 2011. Large-scale patterns in summer surface water phytoplankton (except picophytoplankton) in the Eastern Mediterranean. Estuar. Coast. Shelf Sci. **91**: 551–558. doi:10.1016/j.ecss.2010.12.010
2. Aubry, F. B., and F. Acri. 2004. Phytoplankton seasonality and exchange at the inlets of the Lagoon of Venice (July 2001–June 2002). J. Mar. Syst. **51**: 65–76. doi:https://doi.org/10.1016/j.jmarsys.2004.05.008
3. Aubry, F. B., F. Acri, S. Finotto, and A. Pugnetti. 2021. Phytoplankton Dynamics and Water Quality in the Venice Lagoon. Water **13**. doi:10.3390/w13192780
4. Aubry, F. B., F. Acri, M. Bastianini, S. Finotto, and A. Pugnetti. 2022. Differences and similarities in the phytoplankton communities of two coupled transitional and marine ecosystems (the Lagoon of Venice and the Gulf of Venice - Northern Adriatic Sea). Front. Mar. Sci. **9**.
5. Balestra, B., M. Marino, S. Monechi, C. Marano, and F. Locaiono. 2009. Coccolithophore communities in the Gulf of Manfredonia (Southern Adriatic Sea): data from water and surface sediments. Micropaleontology **54**: 377–396.
6. Barcena, M. A., J. A. Flores, F. J. Sierro, M. Perez-Folgado, J. Fabres, A.

Calafat, and M. Canals. 2004. Planktonic response to main oceanographic changes in the Alboran Sea (Western Mediterranean) as documented in sediment traps and surface sediments. Mar. Micropaleontol. **53**: 423–445. doi:10.1016/j.marmicro.2004.09.009

7. Bonomo, S., A. Cascella, I. Alberico, L. Ferraro, L. Giordano, F. Lirer, M. Vallefuoco, and E. Marsella. 2014. Coccolithophores from near the Volturno estuary (central Tyrrhenian Sea). Mar. Micropaleontol. **111**: 26–37. doi:10.1016/j.marmicro.2014.06.001
8. Bonomo, S., A. Cascella, I. Alberico, F. Lirer, M. Vallefuoco, E. Marsella, and L. Ferraro. 2018a. Living and thanatocoenosis coccolithophore communities in a neritic area of the central Tyrrhenian Sea. Mar. Micropaleontol. **142**: 67–91. doi:10.1016/j.marmicro.2018.06.003
9. Bonomo, S., M. Grelaud, A. Incarbona, and others. 2012. Living Coccolithophores from the Gulf of Sirte (Southern Mediterranean Sea) during the summer of 2008. Micropaleontology. **58**: 487–503.
10. Bonomo, S., F. Placenti, E. M. Quinci, A. Cuttitta, S. Genovese, S. Mazzola, and A. Bonanno. 2017. Living coccolithophores community from Southern Tyrrhenian Sea (Central Mediterranean - Summer 2009). Mar. Micropaleontol. **131**: 10–24. doi:10.1016/j.marmicro.2017.02.002
11. Bonomo, S., F. Placenti, S. Zgozi, and others. 2018b. Relationship between coccolithophores and the physical and chemical oceanography of eastern Libyan coastal waters. Hydrobiologia **821**: 215–234. doi:10.1007/s10750-017-3227-y
12. Bonomo, S., K. Schroeder, A. Cascella, I. Alberico, and F. Lirer. 2021. Living coccolithophore communities in the central Mediterranean Sea (Summer 2016): Relations between ecology and oceanography. Mar. Micropaleontol. **165**. doi:10.1016/j.marmicro.2021.101995
13. Bouza, N., and M. Aboal. 2008. Checklist of phytoplankton on the south coast of Murcia (SE Spain, SW Mediterranean Sea) V. Evangelista, L. Barsanti, A.M. Frassanito, V. Passarelli, and P. Gualtieri [eds.]. Algal Toxins Nature, Occur. Eff. Detect. 179–196. doi:10.1007/978-1-4020-8480-5_6
14. Burić, Z., I. Cetinić, D. Viličić, K. C. Mihalić, M. Carić, and G. Olujić. 2007. Spatial and temporal distribution of phytoplankton in a highly stratified estuary (Zrmanja, Adriatic Sea). Mar. Ecol. **28**: 169–177. doi:https://doi.org/10.1111/j.1439-0485.2007.00180.x
15. Buzancic, M., Ž. Ninčević Gladan, I. Marasović, G. Kušpilić, B. Grbec, and S. Matijevic. 2012. Population structure and abundance of phytoplankton in three bays on the eastern Adriatic coast: Šibenik Bay, Kaštela Bay and Mali Ston Bay. Acta Adriat: 413–435.
16. Cabrini, M., D. Fornasaro, G. Cossarini, M. Lipizer, and D. Virgilio. 2012. Phytoplankton temporal changes in a coastal northern Adriatic site during the last 25 years. Estuar. Coast. Shelf Sci. **115**: 113–124. doi:10.1016/j.ecss.2012.07.007
17. Caroppo, C., A. Fiocca, P. Sammarco, and G. Magazzu. 1999. Seasonal Variations of Nutrients and Phytoplankton in the Coastal SW Adriatic Sea (1995–1997). Bot. Mar. – Bot Mar. **42**: 389–400. doi:10.1515/BOT.1999.045

18. Carrada, G., E. Fresi, D. Marino, M. Modigh, and M. Ribera d'Alcala. 1981. Structural analysis of winter phytoplankton in the Gulf of Naples. J. Plankton Res. **3**. doi:10.1093/plankt/3.2.291
19. Cerino, F., D. Fornasaro, M. Kralj, M. Giani, and M. Cabrini. 2019. Phytoplankton temporal dynamics in the coastal waters of the north-eastern Adriatic Sea (Mediterranean Sea) from 2010 to 2017. Nat. Conserv. 343–372. doi:10.3897/natureconservation.34.30720
20. Cerino, F., E. Malinverno, D. Fornasaro, M. Kralj, and M. Cabrini. 2017. Coccolithophore diversity and dynamics at a coastal site in the Gulf of Trieste (northern Adriatic Sea). Estuar. Coast. Shelf Sci. **196**: 331–345. doi:10.1016/j.ecss.2017.07.013
21. Challouf, R., A. Hamza, M. Mahfoudhi, K. Ghozzi, and M. N. Bradai. 2017. Environmental assessment of the impact of cage fish farming on water quality and phytoplankton status in Monastir Bay (eastern coast of Tunisia). Aquac. Int. **25**: 2275–2292. doi:10.1007/s10499-017-0187-1
22. Cros, L. and J. M. Fortuno. 2002. Atlas of Northwestern Mediterranean coccolithophores. Sci. Mar. **66**: 5-+.
23. D'Amario, B., P. Ziveri, M. Grelaud, A. Oviedo, and M. Kralj. 2017. Coccolithophore haploid and diploid distribution patterns in the Mediterranean Sea: can a haplo-diploid life cycle be advantageous under climate change? J. Plankton Res. **39**: 781–794. doi:10.1093/plankt/fbx044
24. Dimiza, D., O. Koukousioura, I. Michailidis, V.-G. Dimou, V. Navrozidou, K. Aligizaki, and M. Seferlis. 2020. Seasonal living coccolithophore distribution in the enclosed coastal environments of the Thessaloniki Bay (Thermaikos Gulf, NW Aegean Sea). Rev. Micropaléontologie **69**: 100449. doi:https://doi.org/10.1016/j.revmic.2020.100449
25. Dimiza, M. D., M. V Triantaphyllou, and M. D. Dermitzakis. 2008. Seasonality and ecology of living coccolithophores in Eastern Mediterranean coastal environments (Andros Island, Middle Aegean Sea). Micropalontology **54**: 159–175.
26. Dimiza, M., M. V Triantaphyllou, E. Malinverno, S. Psarra, B. T. Karatsolis, P. Mara, A. Lagaria, and A. Gogou. 2016. The composition and distribution of living coccolithophores in the Aegean Sea (NE Mediterranean). Micropaleontology **61**: 521–540.
27. Drakulović, D., B. Pestorić, and A. Huter. 2021. Distribution of Phytoplankton in Montenegrin Open Waters BT - The Montenegrin Adriatic Coast: Marine Biology, p. 73–105. *In* A. Joksimović, M. Đurović, I.S. Zonn, A.G. Kostianoy, and A. V Semenov [eds.]. Springer International Publishing.
28. Drakulović, D., B. Pestorić, R. Kraus, S. Ljubimir, and S. Krivokapić. 2017. Phytoplankton Community and Trophic State in Boka Kotorska Bay BT - The Boka Kotorska Bay Environment, p. 169–201. *In* A. Joksimović, M. Djurović, A. V Semenov, I.S. Zonn, and A.G. Kostianoy [eds.]. Springer International Publishing.
29. Eker-Develi, E., A. E. Kideys, and S. Tugrul. 2006. Role of Saharan dust on phytoplankton dynamics in the northeastern Mediterranean. Mar. Ecol. Prog. Ser. **314**: 61–75. doi:10.3354/meps314061

30. Estrada, M., R. A. Varela, J. Salat, A. Cruzado, and E. Arias. 1999. Spatio-temporal variability of the winter phytoplankton distribution across the Catalan and North Balearic fronts (NW Mediterranean). J. Plankton Res. **21**: 1–20. doi:10.1093/plankt/21.1.1
31. Godrijan, J., D. Marić, I. Tomažić, R. Precali, and M. Pfannkuchen. 2013. Seasonal phytoplankton dynamics in the coastal waters of the north-eastern Adriatic Sea. J. Sea Res. **77**: 32–44. doi:https://doi.org/10.1016/j.seares.2012.09.009
32. Godrijan, J., J. R. Young, D. M. Pfannkuchen, R. Precali, and M. Pfannkuchen. 2018. Coastal zones as important habitats of coccolithophores: A study of species diversity, succession, and life-cycle phases. Limnol. Oceanogr. **63**: 1692–1710. doi:10.1002/lno.10801
33. Gotsis-Skretas, O., K. Pagou, M. Moraitou-Apostolopoulou, and L. Ignatiades. 1999. Seasonal horizontal and vertical variability in primary production and standing stocks of phytoplankton and zooplankton in the Cretan Sea and the Straits of the Cretan Arc (March 1994-Jannuary 1995). Prog. Oceanogr. **44**: 625–649. doi:10.1016/S0079-6611(99)00048-8
34. Ignatiades, L. 1979. The influence of water stability on the vertical structure of a phytoplankton community. Mar. Biol. **52**: 97–104. doi:10.1007/BF00390416
35. Ignatiades, L., D. Georgopoulos, and M. Karydis. 1995. Description of the phytoplankton community of the oligotrophic waters of the SE Aegean Sea (Mediterranean). Mar. Ecol. Publicazioni Della Stn. Cool. Di Napolo I **16**: 13–26. doi:10.1111/j.1439-0485.1995.tb00391.x
36. Ignatiades, L., O. Gotsis-Skretas, K. Pagou, and E. Krasakopoulou. 2009. Diversification of phytoplankton community structure and related parameters along a large-scale longitudinal east-west transect of the Mediterranean Sea. J. Plankton Res. **31**: 411–428. doi:10.1093/plankt/fbn124
37. Karatsolis, B. T., M. V Triantaphyllou, M. D. Dimiza, E. Malinverno, A. Lagaria, P. Mara, O. Archontikis, and S. Psarra. 2017. Coccolithophore assemblage response to Black Sea Water inflow into the North Aegean Sea (NE Mediterranean). Cont. Shelf Res. **149**: 138–150. doi:10.1016/j.csr.2016.12.005
38. Keuter, S., J. Silverman, M. D. Krom, and others. 2022. Seasonal patterns of coccolithophores in the ultra-oligotrophic South-East Levantine Basin, Eastern Mediterranean Sea. Mar. Micropaleontol. **175**: 102153. doi:https://doi.org/10.1016/j.marmicro.2022.102153
39. Kimor, B., T. Berman, and A. Schneller. 1987. Phytoplankton assemblages in the deep chlorophyll maximum layers off the Mediterranean coast of Israel. J. Plankton Res. **9**: 433–443. doi:10.1093/plankt/9.3.433
40. Kleijne, A. 1991. Holococcolithophorids from the Indian-Ocean, Red-Sea, Mediterranean-Sea and north-Atlantic Ocean. Mar. Micropaleontol. **17**: 1–76. doi:10.1016/0377-8398(91)90023-Y
41. Knappertsbusch, M. 1993. Geographic distribution of living and holocene coccolithophores in the Mediterranean Sea. Mar. Micropaleontol. **21**: 219–247. doi:10.1016/0377-8398(93)90016-Q

42. Krivokapic, S., S. Bosak, D. Vilicic, G. Kuspilic, D. Drakulovic, and B. Pestoric. 2018. Algal pigments distribution and phytoplankton group assemblages in coastal transitional environment - Boka Kotorska Bay (South eastern Adriatic Sea). ACTA Adriat. **59**: 35–50. doi:10.32582/aa.59.1.3
43. Malinverno, E., P. Ziveri, and C. Corselli. 2003. Coccolithophorid distribution in the Ionian Sea and its relationship to eastern Mediterranean circulation during late fall to early winter 1997. J. Geophys. Res. **108**. doi:10.1029/2002JC001346
44. Mara, P., S. Psarra, A. Tselepides, A. Eleftheriou, and N. Mihalopoulos. 2016. Influence of phytoplankton taxonomic proile on the distribution of total and dissolved dimethylated sulphur (DMSx) species in the North Aegean Sea (Eastern Mediterranean). Mediterr. Mar. Sci. **17**: 65–79.
45. Mercado, J. M., D. Cortes, A. Garcia, and T. Ramirez. 2007. Seasonal and inter-annual changes in the planktonic communities of the northwest Alboran Sea (Mediterranean Sea). Prog. Oceanogr. **74**: 273–293. doi:10.1016/j.pocean.2007.04.013
46. Mercado, J. M., T. Ramirez, D. Cortes, M. Sebastian, and M. Vargas-Yanez. 2005. Seasonal and inter-annual variability of the phytoplankton communities in an upwelling area of the Alboran Sea (SW Mediterranean Sea). Sci. Mar. **69**: 451–465. doi:10.3989/scimar.2005.69n4451
47. Moscatello, S., C. Caroppo, E. Hajderi, and G. Belmonte. 2011. Space Distribution of Phyto- and Microzooplankton in the Vlora Bay (Southern Albania, Mediterranean Sea). J. Coast. Res. 80–94. doi:10.2112/SI_58_8
48. Mozetiĉ, P., S. F. Umani, B. Cataletto, and A. Malej. 1998. Seasonal and inter-annual plankton variability in the Gulf of Trieste (northern Adriatic). ICES J. Mar. Sci. **55**: 711–722. doi:10.1006/jmsc.1998.0396
49. Neri, F., T. Romagnoli, S. Accoroni, A. Campanelli, M. Marini, F. Grilli, and C. Totti. 2022. Phytoplankton and environmental drivers at a long-term offshore station in the northern Adriatic Sea (1988–2018). Cont. Shelf Res. **242**: 104746. doi:https://doi.org/10.1016/j.csr.2022.104746
50. Oviedo, A., P. Ziveri, M. Álvarez, and T. Tanhua. 2015. Is coccolithophore distribution in the Mediterranean Sea related to seawater carbonate chemistry? Ocean Sci. **11**: 13–32. doi:10.5194/os-11-13-2015
51. Rekik, A., J. Elloumi, Z. Drira, S. Maalej, and H. Ayadi. 2017. Coupling of Phytoplankton and Ciliate Biomasses to Environmental Factors along the North Coast of Sfax (Tunisia, Eastern Mediterranean Sea). Water Resour. **44**: 849–863. doi:10.1134/S0097807817090019
52. Sahin, M., and E. Eker-Develi. 2019. New Records of Haptophyte Species from the Northeastern Mediterranean Sea for Algal Flora of Turkey. Turkish J. Fish. Aquat. Sci. **19**: 7–19. doi:10.4194/1303-2712-v19_1_02
53. Saracino, O., and F. Rubino. 2006. Phytoplankton composition and distribution along the Albanian coast, South Adriatic Sea. Nov. Hedwigia **83**: 253–266. doi:10.1127/0029-5035/2006/0083-0253
54. Saugestad, A. H., and B. R. Heimdal. 2002. Light microscope studies on coccolithophorids from the western Mediterranean Sea, with notes on combination cells of *Daktylethra pirus* and *Syracosphaera pulchra*. Plant

Biosyst. **136**: 3–27.

55. Skampa, E., M. V Triantaphyllou, M. D. Dimiza, and others. 2019. Coupling plankton - sediment trap - surface sediment coccolithophore regime in the North Aegean Sea (NE Mediterranean). Mar. Micropaleontol. **152**. doi:10.1016/j.marmicro.2019.03.001
56. Skejic, S., J. Arapov, M. Buzancic, Z. N. Gladan, A. Bakrac, M. Straka, and J. Mandic. 2021. First evidence of an intensive bloom of the coccolithophore *Syracosphaera halldalii* in a highly variable estuarine environment (Krka River, Adriatic sea). Mar. Ecol. Evol. Perspect. **42**. doi:10.1111/maec.12641
57. Skejic, S., J. Arapov, V. Kovacevic, and others. 2018. Coccolithophore diversity in open waters of the middle Adriatic Sea in pre- and post-winter periods. Mar. Micropaleontol. **143**: 30–45. doi:10.1016/j.marmicro.2018.07.006
58. Socal, G., A. Boldrin, F. Bianchi, G. Civitarese, A. De Lazzari, S. Rabitti, C. Totti, and M. M. Turchetto. 1999. Nutrient, particulate matter and phytoplankton variability in the photic layer of the Otranto strait. J. Mar. Syst. **20**: 381–398. doi:10.1016/S0924-7963(98)00075-X
59. Šupraha, L., S. Bosak, Z. Ljubesic, G. Olujić, L. Horvat, and D. Viličić. 2011. The phytoplankton composition and spatial distribution in the north-eastern Adriatic Channel in autumn 2008. Acta Adriat. **52**: 1–5113.
60. Šupraha, L., Z. Ljubesic, H. Mihanovic, and J. Henderiks. 2016. Coccolithophore life-cycle dynamics in a coastal Mediterranean ecosystem: seasonality and species-specific patterns. J. Plankton Res. **38**: 1178–1193. doi:10.1093/plankt/fbw061
61. Totti, C., G. Civitarese, F. Acri, D. Barletta, G. Candelari, E. Paschini, and A. Solazzi. 2000. Seasonal variability of phytoplankton populations in the middle Adriatic sub-basin. J. Plankton Res. **22**: 1735–1756. doi:10.1093/plankt/22.9.1735
62. Totti, C., T. Romagnoli, S. Accoroni, A. Coluccelli, M. Pellegrini, A. Campanelli, F. Grilli, and M. Marini. 2019. Phytoplankton communities in the northwestern Adriatic Sea: Interdecadal variability over a 30-years period (1988–2016) and relationships with meteoclimatic drivers. J. Mar. Syst. **193**: 137–153. doi:https://doi.org/10.1016/j.jmarsys.2019.01.007
63. Triantaphyllou, M. V, K. H. Baumann, B. T. Karatsolis, and others. 2018. Coccolithophore community response along a natural CO_2 gradient off Methana (SW Saronikos Gulf, Greece, NE Mediterranean). PLoS One **13**. doi:10.1371/journal.pone.0200012
64. Valencia-Vila, J., M. L. F. De Puelles, J. Jansa, and M. Varela. 2016. Phytoplankton composition in a neritic area of the Balearic Sea (Western Mediterranean). J. Mar. Biol. Assoc. United Kingdom **96**: 749–759. doi:10.1017/S0025315415001137
65. Varkitzi, I., S. Psarra, G. Assimakopoulou, A. Pavlidou, E. Krasakopoulou, D. Velaoras, E. Papathanassiou, and K. Pagou. 2020. Phytoplankton dynamics and bloom formation in the oligotrophic Eastern Mediterranean: Field studies in the Aegean, Levantine and Ionian seas. Deep Sea Res. Part II Top. Stud. Oceanogr. **171**: 104662. doi:https://doi.org/10.1016/j.dsr2.2019.104662

66. Viličić, D., S. Bosak, Z. Ljubesic, and K. Mihalić. 2007. Phytoplankton seasonality and composition along the coastal NE Adriatic Sea during the extremely low Po River discharge in 2006. Acta Bot. Croat. **66**.
67. Viličić, D., T. Djakovac, Z. Buric, and S. Bosak. 2009. Composition and annual cycle of phytoplankton assemblages in the northeastern Adriatic Sea. Bot. Mar. **52**: 291–305. doi:10.1515/BOT.2009.004
68. Viličić, D., M. Kuzmić, S. Bosak, T. Silovic, E. Hrustić, and Z. Ljubesic. 2009. Distribution of phytoplankton along the thermohaline gradient in the north-eastern Adriatic channel; winter aspect. Oceanologia **51**: 495–513. doi:10.5697/oc.51-4.495
69. Viličić, D., T. Šilović, M. Kuzmić, H. Mihanović, S. Bosak, I. Tomažić, and G. Olujić. 2011. Phytoplankton distribution across the southeast Adriatic continental and shelf slope to the west of Albania (spring aspect). Environ. Monit. Assess. **177**: 593–607. doi:10.1007/s10661-010-1659-1
70. Viličić, D., S. Terzić, M. Ahel, Z. Burić, N. Jasprica, M. Carić, K. Caput Mihalić, and G. Olujić. 2008. Phytoplankton abundance and pigment biomarkers in the oligotrophic, eastern Adriatic estuary. Environ. Monit. Assess. **142**: 199–218. doi:10.1007/s10661-007-9920-y
71. Zingone, A., L. Dubroca, D. Iudicone, F. Margiotta, F. Corato, M. R. D'Alcala, V. Saggiomo, and D. Sarno. 2010. Coastal Phytoplankton Do Not Rest in Winter. Estuaries and Coasts **33**: 342–361. doi:10.1007/s12237-009-9157-9
72. Ziveri, P., M. Passaro, A. Incarbona, M. Milazzo, R. Rodolfo-Metalpa, and J. M. Hall-Spencer. 2014. Decline in Coccolithophore Diversity and Impact on Coccolith Morphogenesis Along a Natural CO_2 Gradient. Biol. Bull. **226**: 282–290. doi:10.1086/BBLv226n3p282

Table S17. List of the 27 datasets included in the meta-analysis.

1. Bonomo, S., A. Cascella, I. Alberico, L. Ferraro, L. Giordano, F. Lirer, M. Vallefuoco, and E. Marsella. 2014. Coccolithophores from near the Volturno estuary (central Tyrrhenian Sea). Mar. Micropaleontol. **111**: 26–37. doi:10.1016/j.marmicro.2014.06.001
2. Bonomo, S., M. Grelaud, A. Incarbona, and others. 2012. Living Coccolithophores from the Gulf of Sirte (Southern Mediterranean Sea) during the summer of 2008. Micropaleontology **58**: 487–503.
3. Bonomo, S., F. Placenti, E. M. Quinci, A. Cuttitta, S. Genovese, S. Mazzola, and A. Bonanno. 2017. Living coccolithophores community from Southern Tyrrhenian Sea (Central Mediterranean - Summer 2009). Mar. Micropaleontol. **131**: 10–24. doi:10.1016/j.marmicro.2017.02.002
4. Bonomo, S., F. Placenti, S. Zgozi, and others. 2018. Relationship between coccolithophores and the physical and chemical oceanography of eastern Libyan coastal waters. Hydrobiologia **821**: 215–234. doi:10.1007/s10750-017-3227-y
5. Bonomo, S., K. Schroeder, A. Cascella, I. Alberico, and F. Lirer. 2021. Living coccolithophore communities in the central Mediterranean Sea

(Summer 2016): Relations between ecology and oceanography. Mar. Micropaleontol. **165**. doi:10.1016/j.marmicro.2021.101995

6. Cerino, F., E. Malinverno, D. Fornasaro, M. Kralj, and M. Cabrini. 2017. Coccolithophore diversity and dynamics at a coastal site in the Gulf of Trieste (northern Adriatic Sea). Estuar. Coast. Shelf Sci. **196**: 331–345. doi:10.1016/j.ecss.2017.07.013
7. Cros, L., and M. Estrada. 2013. Holo-heterococcolithophore life cycles: ecological implications. Mar. Ecol. Prog. Ser. **492**: 57–68. doi:10.3354/meps10473
8. D'Amario, B., P. Ziveri, M. Grelaud, A. Oviedo, and M. Kralj. 2017. Coccolithophore haploid and diploid distribution patterns in the Mediterranean Sea: can a haplo-diploid life cycle be advantageous under climate change? J. Plankton Res. **39**: 781–794. doi:10.1093/plankt/fbx044
9. Dimiza, D., O. Koukousioura, I. Michailidis, V.-G. Dimou, V. Navrozidou, K. Aligizaki, and M. Seferlis. 2020. Seasonal living coccolithophore distribution in the enclosed coastal environments of the Thessaloniki Bay (Thermaikos Gulf, NW Aegean Sea). Rev. Micropaléontologie **69**: 100449. doi:https://doi.org/10.1016/j.revmic.2020.100449
10. Dimiza, M. D., M. V Triantaphyllou, and M. D. Dermitzakis. 2008. Seasonality and ecology of living coccolithophores in Eastern Mediterranean coastal environments (Andros Island, Middle Aegean Sea). Micropalontology **54**: 159–175.
11. Dimiza, M., M. V Triantaphyllou, E. Malinverno, S. Psarra, B. T. Karatsolis, P. Mara, A. Lagaria, and A. Gogou. 2016. The composition and distribution of living coccolithophores in the Aegean Sea (NE Mediterranean). Micropaleontology **61**: 521–540.
12. Estrada, M., R. A. Varela, J. Salat, A. Cruzado, and E. Arias. 1999. Spatio-temporal variability of the winter phytoplankton distribution across the Catalan and North Balearic fronts (NW Mediterranean). J. Plankton Res. **21**: 1–20. doi:10.1093/plankt/21.1.1
13. Godrijan, J., J. R. Young, D. M. Pfannkuchen, R. Precali, and M. Pfannkuchen. 2018. Coastal zones as important habitats of coccolithophores: A study of species diversity, succession, and life-cycle phases. Limnol. Oceanogr. **63**: 1692–1710. doi:10.1002/lno.10801
14. Gotsis-Skretas, O., K. Pagou, M. Moraitou-Apostolopoulou, and L. Ignatiades. 1999. Seasonal horizontal and vertical variability in primary production and standing stocks of phytoplankton and zooplankton in the Cretan Sea and the Straits of the Cretan Arc (March 1994-Jannuary 1995). Prog. Oceanogr. **4**4: 625–649. doi:10.1016/S0079-6611(99)00048-8
15. Karatsolis, B. T., M. V Triantaphyllou, M. D. Dimiza, E. Malinverno, A. Lagaria, P. Mara, O. Archontikis, and S. Psarra. 2017. Coccolithophore assemblage response to Black Sea Water inflow into the North Aegean Sea (NE Mediterranean). Cont. Shelf Res. **149**: 138–150.

doi:10.1016/j.csr.2016.12.005

16. Keuter, S., J. Silverman, M. D. Krom, and others. 2022. Seasonal patterns of coccolithophores in the ultra-oligotrophic South-East Levantine Basin, Eastern Mediterranean Sea. Mar. Micropaleontol. **175**: 102153. doi:https://doi.org/10.1016/j.marmicro.2022.102153
17. Malinverno, E., P. Ziveri, and C. Corselli. 2003. Coccolithophorid distribution in the Ionian Sea and its relationship to eastern Mediterranean circulation during late fall to early winter 1997. J. Geophys. Res. **108**. doi:10.1029/2002JC001346
18. Neri, F., T. Romagnoli, S. Accoroni, A. Campanelli, M. Marini, F. Grilli, and C. Totti. 2022. Phytoplankton and environmental drivers at a long-term offshore station in the northern Adriatic Sea (1988–2018). Cont. Shelf Res. **242**: 104746. doi:https://doi.org/10.1016/j.csr.2022.104746
19. O'Brien, C. J. 2012. Global distributions of coccolithophores abundance and biomass - Gridded data product (NetCDF) - Contribution to the MAREDAT World Ocean Atlas of Plankton Functional Types.doi:10.1594/PANGAEA.785092
20. Oviedo, A., P. Ziveri, M. Álvarez, and T. Tanhua. 2015. Is coccolithophore distribution in the Mediterranean Sea related to seawater carbonate chemistry? Ocean Sci. **11**: 13–32. doi:10.5194/os-11-13-2015
21. Pagou, K., and G. Assimakopoulou. 2008. Microplankton abundance at bottle station SEPT-1999-K9. Hell. Cent. Mar. Res. Inst. Oceanogr. Greece. doi:10.1594/PANGAEA.688633
22. Skejic, S., J. Arapov, V. Kovacevic, and others. 2018. Coccolithophore diversity in open waters of the middle Adriatic Sea in pre- and post-winter periods. Mar. Micropaleontol. **143**: 30–45. doi:10.1016/j.marmicro.2018.07.006
23. Supraha, L., Z. Ljubesic, H. Mihanovic, and J. Henderiks. 2016. Coccolithophore life-cycle dynamics in a coastal Mediterranean ecosystem: seasonality and species-specific patterns. J. Plankton Res. **38**: 1178–1193. doi:10.1093/plankt/fbw061
24. Triantaphyllou, M. V, K. H. Baumann, B. T. Karatsolis, and others. 2018. Coccolithophore community response along a natural CO_2 gradient off Methana (SW Saronikos Gulf, Greece, NE Mediterranean). PLoS One **13**. doi:10.1371/journal.pone.0200012
25. Valencia-Vila, J., M. L. F. De Puelles, J. Jansa, and M. Varela. 2016. Phytoplankton composition in a neritic area of the Balearic Sea (Western Mediterranean). J. Mar. Biol. Assoc. United Kingdom **96**: 749–759. doi:10.1017/S0025315415001137
26. de Vries, J. C., F. Monteiro, H. Andruleit, and others. 2020. Global SEM coccolithophore abundance compilation.doi:10.1594/PANGAEA.922933
27. Ziveri, P., M. Passaro, A. Incarbona, M. Milazzo, R. Rodolfo-Metalpa, and J. M. Hall-Spencer. 2014. Decline in Coccolithophore Diversity and Impact on Coccolith Morphogenesis Along a Natural CO_2 Gradient. Biol. Bull. **226**: 282–290. doi:10.1086/BBLv226n3p282

Supplementary Material – Chapter 3

Table S1. Water chemistry parameters, total alkalinity (TA - µmol kg^{-1}) and pH were used to determine pCO_2, dissolved inorganic carbon (DIC - µmol kg^{-1}), pCO_2 (µatm), HCO_3^- (µmol kg^{-1}), CO_3^- (µmol kg^{-1}), and the saturation state of calcite (Ω calc) using CO2SYS. Salinity = 35. $pH_{adjusted}$ is the calculated pH adjusted to the target temperature (15°C or 20°C). SD indicates standard deviation.

Fig. S1. Target morphological distal shield (coccolith) features (distal shield length, distal shield width, inner circle diameter, tube width) measured from scanning electron images (Phenom G2 pro scanning electron microscope) using ImageJ.

Table S2. Estimated parameters from the generalized linear model for each response variable. : Lipids (pg $cell^{-1}$), POC (pg $cell^{-1}$), PIC (pg $cell^{-1}$), Chlorophyll *a* (pg $cell^{-1}$), growth rate (day^{-1}), Lipid production (pg $cell^{-1}$ day^{-1}), POC production (pg $cell^{-1}$ day^{-1}), PIC production (pg $cell^{-1}$ day^{-1}), Chlorophyll *a* production (pg $cell^{-1}$ day^{-1}), Production Potential - Lipids (ng), POC:N, PIC:N, PIC:POC, Lipid:POC (Cellular lipid content:Cellular POC content), coccosphere diameter (µm), coccolith distal shield length (µm), coccolith distal shield width (µm), inner circle diameter (µm), tube width (µm), collapsed coccosphere (%). Explanatory variables selected based on the model with the lowest Akaike Information Criterion score. Denotation: * $P \leq 0.05$; ** $P \leq 0.01$; † $P \leq 0.001$; β = coefficient; Ref. = reference category; n.s. = non-significant.

Table S1. Water chemistry parameters, total alkalinity (TA - µmol kg^{-1}) and pH were used to determine pCO_2, dissolved inorganic carbon (DIC - µmol kg^{-1}), pCO_2 (µatm), HCO_3^- (µmol kg^{-1}), CO_3^- (µmol kg^{-1}), and the saturation state of calcite (Ω calc) using CO2SYS. Salinity = 35. $pH_{adjusted}$ is the calculated pH adjusted to the target temperature (15°C or 20°C). SD indicates standard deviation.

Temp.	$pH_{Measured}$	pH SD	$pH_{Adjusted}$	TA	TA SD	DIC	pCO_2	HCO_3^-	CO_3	Ω_{calc}
15°C	8.27	0.007	8.43	2572.5	3.93	2072.0	149.4	1721.4	345.07	8.22
15°C	8.18	0.019	8.33	2467.3	2.86	2053.4	191.6	1763.8	282.49	6.73
15°C	8.07	0.001	8.23	2355.0	1.37	2023.0	248.0	1789.1	224.64	5.35
15°C	8.02	0.003	8.17	2307.8	0.55	2010.4	280.3	1799.0	200.91	4.79
15°C	7.91	0.003	8.06	2257.8	3.70	2024.6	374.4	1851.3	159.32	3.80
15°C	7.87	0.003	8.01	2214.9	6.84	2007.3	417.8	1849.3	142.46	3.40
15°C	7.77	0.005	7.92	2187.9	1.53	2024.0	534.0	1887.9	116.17	2.77
15°C	7.70	0.003	7.84	2170.1	2.03	2036.2	643.9	1913.3	98.94	2.36
15°C	7.53	0.001	7.66	2194.7	0.32	2121.1	1020.7	2013.9	69.15	1.65
20°C	8.36	0.007	8.44	2695.8	1.38	2099.4	145.9	1676.1	418.64	10.01
20°C	8.30	0.006	8.38	2529.3	0.11	2014.6	167.8	1654.6	354.62	8.48
20°C	8.22	0.008	8.29	2385.8	2.48	1953.1	202.5	1653.2	293.35	7.02
20°C	8.21	0.003	8.29	2250.5	0.04	1840.4	194.7	1561.8	272.28	6.51
20°C	8.11	0.005	8.19	2157.8	0.06	1823.3	250.9	1594.8	220.34	5.27
20°C	8.01	0.003	8.09	2101.2	1.05	1827.7	322.8	1636.8	180.43	4.32
20°C	7.89	0.001	7.97	2203.7	6.73	1983.5	472.6	1816.5	151.75	3.63
20°C	7.83	0.005	7.90	2155.0	0.07	1966.5	546.4	1817.4	131.40	3.14
20°C	7.67	0.005	7.74	2179.0	1.14	2055.1	846.8	1931.9	95.82	2.29

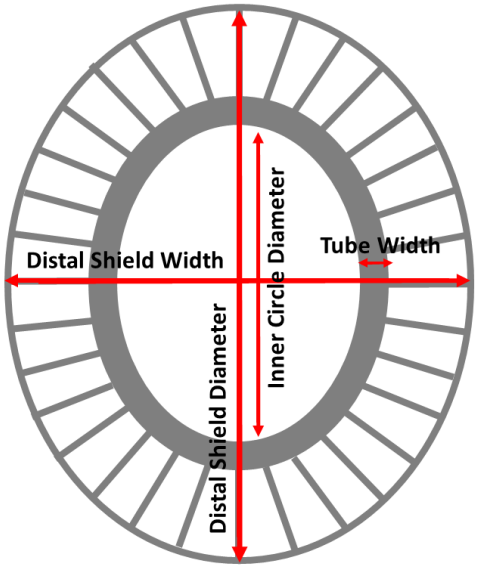

Fig. S1. Target morphological distal shield (coccolith) features (distal shield length, distal shield width, inner circle diameter, tube width) measured from scanning electron images (Phenom G2 pro scanning electron microscope) using ImageJ.

Table S2. Estimated parameters from the generalized linear model for each response variable. : Lipids (pg cell^{-1}), POC (pg cell^{-1}), PIC (pg cell^{-1}), Chlorophyll *a* (pg cell^{-1}), growth rate (day^{-1}), Lipid production (pg cell^{-1} day^{-1}), POC production (pg cell^{-1} day^{-1}), PIC production (pg cell^{-1} day^{-1}), Chlorophyll *a* production (pg cell^{-1} day^{-1}), Production Potential - Lipids (ng), POC:N, PIC:N, PIC:POC, Lipid:POC (Cellular lipid content:Cellular POC content), coccosphere diameter (µm), coccolith distal shield length (µm), coccolith distal shield width (µm), inner circle diameter (µm), tube width (µm), collapsed coccosphere (%). Explanatory variables selected based on the model with the lowest Akaike Information Criterion score. Denotation: * $P \leq 0.05$; ** $P \leq 0.01$; † $P \leq 0.001$; β = coefficient; Ref. = reference category; n.s. = non-significant.

	Explanatory variables	β	St. error	(95% lower CI)	(95% upper CI)	Sig.
Cellular quotas						
Lipids	**15°C**	-6.59	1.37	-9.27	-3.91	†
	20°C	Ref.				
	pH	11.16	5.17	1.03	21.28	*
	pH^2	-0.75	0.32	-1.38	-0.12	*
	15°C x pH	0.83	0.17	0.50	1.15	†
	20°C x pH	Ref.				
POC	**15°C**	-0.07	0.07	-0.21	0.07	n.s.
	20°C	Ref.				
	pH	37.12	11.59	14.42	59.83	**
	pH^2	-2.32	0.71	-3.71	-0.92	**
PIC	**15°C**	5.293	4.3496	-3.232	13.818	n.s.
	20°C	Ref.				
	pH	-2785.490	736.1466	-4228.311	-1342.669	†
	pH^2	353.355	91.8243	173.383	533.327	†
	pH^3	-14.925	3.8161	-22.405	-7.446	†
	15°C x pH	-.673	.5450	-1.742	.395	n.s.
	20°C x pH	Ref.				
Chlorophyll *a*	**15°C**	-10.10	2.51	-15.03	-5.18	†
	20°C	Ref.				
	pH	-1.23	0.29	-1.80	-0.67	†
	15°C x pH	1.20	0.30	0.60	1.79	†
	20°C x pH	Ref.				
Production rates						
Growth rate	**Constant**	-42.04	11.01	-63.63	-20.46	†
	15°C	3.27	0.71	1.88	4.66	†
	20°C	Ref.				
	pH	10.07	2.76	4.65	15.48	†
	pH^2	-0.60	0.17	-0.94	-0.26	†
	15°C x pH	-0.44	0.09	-0.62	-0.27	†
	20°C x pH	Ref.				
Lipid production	**15°C**	-0.21	0.05	-0.32	-0.11	†
	20°C	Ref.				
	pH	29.94	7.03	16.15	43.73	†
	pH^2	-1.89	0.44	-2.74	-1.03	†
POC production	**15°C**	4.84	3.02	-1.08	10.76	n.s.
	20°C	Ref.				
	pH	49.06	11.05	27.41	70.72	†
	pH^2	-3.03	0.68	-4.35	-1.70	†
	15°C x pH	-0.64	0.37	-1.37	0.08	n.s.
	20°C x pH	Ref.				
PIC production	**15°C**	8.90	4.16	0.75	17.05	*
	20°C	Ref.				
	pH	-2629.55	768.45	-4135.68	-1123.42	**
	pH^2	334.65	95.92	146.65	522.65	†
	pH^3	-14.18	3.99	-22.00	-6.36	†
	15°C x pH	-1.16	0.52	-2.18	-0.14	*

	20°C x pH	Ref.				
Chlorophyll *a* production	**15°C**	-0.75	0.06	-0.87	-0.64	†
	20°C	0[a]				
	pH	33.28	6.46	20.63	45.94	†
	pH²	-2.09	0.40	-2.88	-1.30	†
Production potential – Lipids	**15°C**	13.44	4.34	4.95	21.94	**
	20°C	Ref.				
	pH	59.95	16.63	27.35	92.54	†
	pH²	-3.65	1.04	-5.69	-1.61	†
	15°C x pH	-1.85	0.54	-2.91	-0.79	**
	20°C x pH	Ref.				
Carbon ratios						
POC:N	**15°C**	-2.60	0.69	-3.94	-1.25	†
	20°C	Ref.				
	pH	694.37	163.60	373.73	1015.01	†
	pH²	-86.05	20.38	-126.00	-46.10	†
	pH³	3.55	0.85	1.89	5.21	†
	15°C x pH	0.30	0.08	0.13	0.46	†
	20°C x pH	Ref.				
PIC:N	**15°C**	6.82	2.40	2.10	11.53	**
	20°C	Ref.				
	pH	0.34	0.17	0.00	0.68	n.s.
	15°C x pH	-0.86	0.30	-1.46	-0.27	**
	20°C x pH	Ref.				
PIC:POC	**pH**	-1901.39	575.67	-3029.68	-773.11	**
	pH²	239.71	72.03	98.53	380.89	**
	pH³	-10.06	3.00	-15.95	-4.18	**
Lipid:POC	**15°C**	0.29	0.04	0.21	0.36	†
	20°C	Ref.				
Morphological characteristics						
Coccosphere diameter	**15°C**	1.61	0.40	0.83	2.40	†
	20°C	Ref.				
	pH	7.19	1.73	3.79	10.59	†
	pH²	-0.44	0.11	-0.65	-0.23	†
	15°C x pH	-0.19	0.05	-0.29	-0.10	†
	20°C x pH	Ref.				
Distal shield length	**15°C**	0.06	0.01	0.04	0.09	†
	20°C	Ref.				
	pH	4.65	2.36	0.03	9.27	*
	pH²	-0.29	0.15	-0.57	0.00	*
Distal shield width	**15°C**	-1.24	0.46	-2.15	-0.34	**
	20°C	Ref.				
	pH	-0.05	0.05	-0.15	0.06	n.s.
	15°C x pH	0.17	0.06	0.05	0.28	**
	20°C x pH	Ref.				
Inner circle diameter	**No Significant Terms**					
Tube width	**Constant**	-2.88	.40	-3.67	-2.10	†
	pH	0.26	0.05	0.12	0.31	†
Collapsed coccospheres	**15°C**	6.57	3.81	-0.91	14.04	n.s.
	20°C	Ref.				
	pH	2195.85	887.47	456.45	3935.25	*
	pH²	-273.34	109.99	-488.92	-57.76	*
	pH³	11.33	4.54	2.43	20.24	*
	15°C x pH	-0.83	0.47	-1.75	0.08	n.s.
	20°C x pH	Ref.				

Appendix – Chapter 4

Table A1. Location and environmental parameters for each station of the cruise. All the parameters are averaged from 5 to 200 m depth. The table includes: Station code, Station name, day (day/month/year), location time (LT), latitude (Lat.), longitude (Long.), bottom depth (m), volume (m^3), temperature (Temp. °C), salinity (PSU), fluorescence (Fluor.), pH, aragonite saturation (Ω_{ar}), nitrate (NO_3), phosphate (PO_4), and oxygen (O_2). Ω_{ar} is a calculated parameter.

Table A2. Absolute (ind. m^{-3}), integrated abundance 0-200 m (ind. m^2), and relative abundance (%) of pteropods collected from BONGO nets. Western stations are 1-7a, 19-22 and Eastern stations are 9-'16-18'.

Table A3. Absolute (10 ind. m^{-3}) and relative abundance (%) of foraminifera (all species) collected from BONGO nets. Western stations are 1-7a, 19-22 and Eastern stations are 9-'16-18'. For data regarding individual species of foraminifera, please refer to Mallo et al. (2017).

Table A1. Location and environmental parameters for each station of the cruise. All the parameters are averaged from 5 to 200 m depth. The table includes: Station code, Station name, day (day/month/year), location time (LT), latitude (Lat.), longitude (Long.), bottom depth (m), volume (m^3), temperature (Temp. °C), salinity (PSU), fluorescence (Fluor.), pH, aragonite saturation (Ω_{ar}), nitrate (NO_3), phosphate (PO_4), and oxygen (O_2). Ω_{ar} is a calculated parameter.

Station name	Station	Day (dd/mm/yyyy)	Time (LT)	Latitude	Longitude	Bottom depth (m)	Volume (m^3)	Temp. (°C)	Salinity PSU	Fluor. (µg L^{-1})	pH	Ω_{ar} (µmol kg^{-1})	NO_3 (µmol L^{-1})	PO_4 (µmol L^{-1})	O_2 (µmol kg^{-1})
Atlantic	1	5/2/2013	00:03	36°03'	-6°64'	557	1016	16.39	36.19	0.36	8.06	2.70	1.92	0.13	226.03
Gibraltar	2	5/3/2013	12:47	35°95'	-5°56'	557	537	14.68	37.20	0.11	8.06	2.68	4.18	0.22	191.05
Alboran Sea	3	5/4/2013	20:55	36°12'	-4°19'	1337	1403	15.43	36.97	0.45	8.09	2.87	2.08	0.13	214.19
Southern Alguero-Balear	5	5/8/2013	10:44	38°52'	5°55'	2844	459	14.60	37.89	0.18	8.10	2.97	1.22	0.05	224.38
Strait of Sardinia	6	5/9/2013	20:34	38°27'	8°69'	2237	423	14.60	38.13	0.19	8.08	2.96	2.30	0.15	212.38
Strait of Sicily	7a	5/11/2013	00:20	37°04'	13°19'	469	447	15.40	38.09	0.23	8.09	3.07	1.35	0.06	216.91
Ionian Sea	9	5/12/2013	11:31	35°11'	18°29'	3775	425	16.64	38.75	0.13	8.12	3.44	0.41	0.02	227.67
Southern Crete	10	5/14/2013	14:40	33°81'	24°27'	1845	320	16.70	39.04	0.12	8.11	3.43	1.03	0.03	211.61
Eastern Basin	11	5/15/2013	13:01	33°50'	28°00'	2865	372	17.73	38.85	0.10	8.12	3.61	0.58	0.02	224.16
Nile Delta	12	5/17/2013	03:14	33°21'	32°00'	1648	364	18.18	39.06	0.15	8.11	3.56	0.50	0.03	225.32
Lebanon	13	5/17/2013	16:15	34°22'	33°23'	2043	397	17.80	38.96	0.16	8.11	3.53	0.40	0.03	222.81
Antikythera Strait	14	5/21/2013	6:06	35°70'	23°42'	619	334	16.90	39.06	0.12	8.13	3.57	0.37	0.03	229.53
Eastern Ionian Sea	15	5/21/2013	21:25	36°40'	20°81'	2897	391	16.52	39.05	0.15	8.12	3.40	1.08	0.04	228.12
Otranto Strait	16	5/24/2013	23:49	40°23'	18°84'	808	385	15.14	38.81	0.20	8.10	3.22	1.70	0.05	229.39
Adriatic Sea	17	5/23/2013	21:09	41°84'	17°25'	970	440	16.34	38.82	0.16	8.13	3.50	0.90	0.03	231.22
Between Otranto Strait and Central Ionian	16-18	5/25/2013	09:30	37°71'	18°52'	3069	426	16.15	38.88	0.14	8.11	3.40	1.97	0.06	216.01
Tyrrhenian Sea	19	5/27/2013	12:30	39°83'	12°52'	3165	391	15.05	38.29	0.18	8.12	3.21	1.60	0.07	212.45
Northern Alguero-Balear	20	5/29/2013	20:00	41°32'	5°67'	2561	356	14.08	38.39	0.36	8.14	3.24	4.01	0.20	208.91
Central Alguero-Balear	21	5/30/2013	10:30	40°07'	5°95'	2834	392	14.51	37.88	0.17	8.11	3.03	0.81	0.04	233.14
Catalano-Balear	22	5/31/2013	13:55	40°95'	3°32'	2275	339	14.62	38.39	0.25	8.13	3.23	3.55	0.17	210.47

Table A2. Absolute (ind. m^{-3}), integrated abundance 0-200 m (ind. m^2), and relative abundance (%) of pteropods collected from BONGO nets. Western stations are 1-7a, 19-22 and Eastern stations are 9-'16-18'.

Absolute abundance (individuals m^{-3})

Station name	Station	*H. inflata*	*L. trochiformis*	*L. bulimoides*	*Limacinidae sp.*	*C. inflexa*	*Cavoliniidae sp.*	*C. acicula*	*C. conica*	*S. subula*	*Creseidae sp.*	Total
Atlantic	1	0.049	0.010	0.038	0.002	0.022	0.000	0.037	0.049	0.010	0.002	0.219
Gibraltar	2	0.196	0.019	0.119	0.006	0.047	0.002	0.065	0.039	0.007	0.002	0.501
Alboran Sea	3	0.523	0.003	0.249	0.008	0.007	0.001	0.154	0.200	0.019	0.011	1.176
S. central W. Med.	5	0.031	0.007	0.026	0.002	0.020	0.002	0.052	0.305	0.015	0.004	0.464
Str. of Sardinia	6	0.026	0.000	0.092	0.007	0.000	0.000	0.007	0.028	0.002	0.002	0.165
Str. of Sicily	7a	0.018	0.056	0.013	0.002	0.022	0.002	0.000	0.000	0.000	0.000	0.114
S. of Ionian Sea	9	1.278	0.475	1.584	0.099	0.056	0.000	0.061	0.054	0.005	0.002	3.614
Off S. Crete	10	0.550	0.394	0.034	0.025	0.019	0.000	0.034	0.013	0.003	0.003	1.075
Eastern Basin	11	0.153	0.027	0.046	0.000	0.005	0.000	0.011	0.003	0.000	0.003	0.247
Off Nile delta	12	0.093	0.038	0.069	0.003	0.025	0.000	0.025	0.014	0.003	0.003	0.272
Off Lebanon	13	0.987	0.063	0.020	0.013	0.018	0.000	0.645	0.191	0.063	0.010	2.010
Antikythera Str.	14	1.677	1.428	1.162	0.042	0.009	0.000	0.072	0.057	0.000	0.000	4.446
E. Ionian Sea	15	0.488	0.327	0.504	0.041	1.440	0.000	0.552	0.601	0.036	0.013	4.003
Otranto Str.	16	0.818	2.353	1.894	0.002	0.016	0.000	0.036	0.034	0.000	0.000	0.270
Adriatic Sea	17	0.066	0.070	0.132	0.052	0.000	0.003	0.000	0.000	0.000	0.000	5.205
N. Ionian Sea	16-18	0.049	0.040	0.019	0.002	0.005	0.000	0.002	0.005	0.002	0.000	0.124
Tyrrhenian Sea	19	0.340	0.445	0.023	0.000	0.018	0.000	0.090	0.064	0.008	0.003	0.990
N-central W. Med.	20	0.000	0.000	0.000	0.000	0.000	0.000	0.000	0.000	0.000	0.000	0.000
Central W. Med.	21	0.120	0.138	0.041	0.000	0.000	0.000	0.102	0.077	0.000	0.003	0.480
Catalano-Balear	22	0.018	0.015	0.000	0.000	0.015	0.000	0.012	0.000	0.000	0.000	0.059
Avg. Western Stations	1-7a, 19-22	0.132	0.069	0.060	0.003	0.015	0.001	0.052	0.076	0.006	0.003	0.417
Avg. Eastern Stations	9-'16-18'	0.616	0.522	0.546	0.028	0.159	0.000	0.144	0.097	0.011	0.003	2.127
Avg. All Stations	1-22	0.374	0.295	0.303	0.015	0.087	0.000	0.098	0.087	0.009	0.003	1.272

Integrated abundance 0-200 m (individuals m^2)

	Station	*H. inflata*	*L. trochiformis*	*L. bulimoides*	*Limacinidae sp.*	*C. inflexa*	*Cavoliniidae sp.*	*C. acicula*	*C. conica*	*S. subula*	*Creseidae sp.*	Total
Atlantic	1	9.843	1.969	7.677	0.394	4.331	0.000	7.480	9.843	1.969	0.394	43.898
Gibraltar	2	39.106	3.724	23.836	1.117	9.311	0.372	13.035	7.821	1.490	0.372	100.186
Alboran Sea	3	104.633	0.570	49.893	1.568	1.426	0.143	30.791	40.057	3.849	2.281	235.210
S. central W. Med.	5	6.100	1.307	5.229	0.436	3.922	0.436	10.458	61.002	3.050	0.871	92.810
Str. of Sardinia	6	5.201	0.000	18.440	1.418	0.000	0.000	1.418	5.674	0.473	0.473	33.097
Str. of Sicily	7a	3.579	11.186	2.685	0.447	4.474	0.447	0.000	0.000	0.000	0.000	22.819
S. of Ionian Sea	9	255.529	95.059	316.706	19.765	11.294	0.000	12.235	10.824	0.941	0.471	722.824
Off S. Crete	10	110.000	78.750	6.875	5.000	3.750	0.000	6.875	2.500	0.625	0.625	215.000
Eastern Basin	11	30.645	5.376	9.140	0.000	1.075	0.000	2.151	0.538	0.000	0.538	49.462
Off Nile delta	12	18.681	7.692	13.736	0.549	4.945	0.000	4.945	2.747	0.549	0.549	54.396
Off Lebanon	13	197.481	12.594	4.030	2.519	3.526	0.000	128.967	38.287	12.594	2.015	402.015
Antikythera Str.	14	335.329	285.629	232.335	8.383	1.796	0.000	14.371	11.377	0.000	0.000	889.222
E. Ionian Sea	15	97.698	65.473	100.767	8.184	287.980	0.000	110.486	120.205	7.161	2.558	800.512
Otranto Str.	16	163.636	470.649	378.701	10.390	3.117	0.519	7.273	6.753	0.000	0.000	1041.039
Adriatic Sea	17	13.182	14.091	26.364	0.455	0.000	0.000	0.000	0.000	0.000	0.000	54.091
N. Ionian Sea	16-18	9.859	7.981	3.756	0.469	0.939	0.000	0.469	0.939	0.469	0.000	24.883
Tyrrhenian Sea	19	68.031	89.003	4.604	0.000	3.581	0.000	17.903	12.788	1.535	0.512	197.954
N-central W. Med.	20	0.000	0.000	0.000	0.000	0.000	0.000	0.000	0.000	0.000	0.000	0.000
Central W. Med.	21	23.980	27.551	8.163	0.000	0.000	0.000	20.408	15.306	0.000	0.510	95.918
Catalano-Balear	22	3.540	2.950	0.000	0.000	2.950	0.000	2.360	0.000	0.000	0.000	11.799
Western Stations	1-7a, 19-22	26.401	13.826	12.053	0.538	2.999	0.140	10.385	15.249	1.236	0.541	83.369
Eastern Stations	9-'16-18'	123.204	104.330	109.241	5.571	31.842	0.052	28.777	19.417	2.234	0.676	425.344
All Stations	1-22	74.803	59.078	60.647	3.055	17.421	0.096	19.581	17.333	1.735	0.608	254.357

Relative abundance (%)

	Station	*H. inflata*	*L. trochiformis*	*L. bulimoides*	*Limacinidae sp.*	*C. inflexa*	*Cavoliniidae sp.*	*C. acicula*	*C. conica*	*S. subula*	*Creseidae sp.*	Total
Atlantic	1	22.4	4.5	17.5	0.9	9.9	0.0	17.0	22.4	4.5	0.9	0.9
Gibraltar	2	39.0	3.7	23.8	1.1	9.3	0.4	13.0	7.8	1.5	0.4	2.0
Alboran Sea	3	44.5	0.2	21.2	0.7	0.6	0.1	13.1	17.0	1.6	1.0	4.6
S. central W. Med.	5	6.6	1.4	5.6	0.5	4.2	0.5	11.3	65.7	3.3	0.9	1.8

Str. of Sardinia	6	15.7	0.0	55.7	4.3	0.0	0.0	4.3	17.1	1.4	1.4	0.7
Str. of Sicily	7a	15.7	49.0	11.8	2.0	19.6	2.0	0.0	0.0	0.0	0.0	0.4
S. of Ionian Sea	9	35.4	13.2	43.8	2.7	1.6	0.0	1.7	1.5	0.1	0.1	14.2
Off S. Crete	10	51.2	36.6	3.2	2.3	1.7	0.0	3.2	1.2	0.3	0.3	4.2
Eastern Basin	11	62.0	10.9	18.5	0.0	2.2	0.0	4.3	1.1	0.0	1.1	1.0
Off Nile delta	12	34.3	14.1	25.3	1.0	9.1	0.0	9.1	5.1	1.0	1.0	1.1
Off Lebanon	13	49.1	3.1	1.0	0.6	0.9	0.0	32.1	9.5	3.1	0.5	7.9
Antikythera Str.	14	37.7	32.1	26.1	0.9	0.2	0.0	1.6	1.3	0.0	0.0	17.5
E. Ionian Sea	15	12.2	8.2	12.6	1.0	36.0	0.0	13.8	15.0	0.9	0.3	15.7
Otranto Str.	16	15.7	45.2	36.4	1.0	0.3	0.0	0.7	0.6	0.0	0.0	20.5
Adriatic Sea	17	24.4	26.1	48.7	0.8	0.0	0.0	0.0	0.0	0.0	0.0	1.1
N. Ionian Sea	16-18	39.6	32.1	15.1	1.9	3.8	0.0	1.9	3.8	1.9	0.0	0.5
Tyrrhenian Sea	19	34.4	45.0	2.3	0.0	1.8	0.0	9.0	6.5	0.8	0.3	3.9
N-central W. Med.	20	0.0	0.0	0.0	0.0	0.0	0.0	0.0	0.0	0.0	0.0	0.0
Central W. Med.	21	25.0	28.7	8.5	0.0	0.0	0.0	21.3	16.0	0.0	0.5	1.9
Catalano-Balear	22	30	25	0	0	25	0	20	0	0	0	0.2
Western Stations	1-7a, 19-22	31.7	16.6	14.5	0.6	3.6	0.2	12.5	18.3	1.5	0.6	16.4
Eastern Stations	9-'16-18'	29.0	24.5	25.7	1.3	7.5	0.0	6.8	4.6	0.5	0.2	83.6
All Stations	1-22	29.4	23.2	23.8	1.2	6.8	0.0	7.7	6.8	0.7	0.2	100

Table A3. Absolute (10 ind. m^{-3}) and relative abundance (%) of foraminifera (all species) collected from BONGO nets. Western stations are 1-7a, 19-22 and Eastern stations are 9-'16-18'. For data regarding individual species of foraminifera, please refer to Mallo et al. (2017).

Station name	Station	*Total abundance (10 ind. m^{-3})*	*Relative abundance (%)*
Atlantic	1	0.985	3.476
Gibraltar	2	5.120	18.070
Alboran Sea	3	4.141	14.614
S. central W. Med.	5	1.460	5.153
Str. of Sardinia	6	0.709	2.502
Str. of Sicily	7a	1.006	3.550
S. of Ionian Sea	9	0.683	2.410
Off S. Crete	10	3.003	10.598
Eastern Basin	11	0.753	2.657
Off Nile delta	12	0.439	1.549
Off Lebanon	13	1.689	5.961
Antikythera Str.	14	0.898	3.169
E. Ionian Sea	15	0.307	1.083
Otranto Str.	16	1.482	5.230
Adriatic Sea	17	0.114	0.402
N. Ionian Sea	16-18	0.258	0.911
Tyrrhenian Sea	19	3.607	12.730
N-central W. Med.	20	0.365	1.288
Central W. Med.	21	0.638	2.252
Catalano-Balear	22	0.678	2.393
Avg. Western Stations	1-7a, 19-22	1.871	66.028
Avg. Eastern Stations	9-'16-18'	0.963	33.972
Avg. All Stations	1-22	1.417	100.000

Supplementary Material – Chapter 4

Table S1. Maximum, average, and percentage of total abundance of pteropods within the Mediterranean. This dataset was created from the dataset used in Bednaršek et al. (2012). A link to the dataset and a list of datasets used in this study can be found at the end of this document.

Fig. S1. A Abundance of pteropods (expressed as ind. M^{-3}) in the Mediterranean Sea from the dataset in Bednaršek et al. (2012) only including sites where pteropods have been collected below and above 200 m; **B** Location of stations within the Mediterranean Sea where data were collected above and below 200 m water depth. Unfortunately, there are a paucity of datasets in the western Mediterranean that we can utilise to differentiate the depth distribution of pteropods above and below 200 m (Bednaršek et al. [2012]; see Figure 1 from this document, © depth 200-500 m and (d) below 500m for the Western Mediterranean).

Table S2. ANOVA table using night/day as the dependent variable against total and species abundances.

Figure S2. Pearson's Correlation matrix showing the correlation between several environmental variables. Labels – NO_3 (NO3), PO_4 (PO4), fluorescence (Fluores), 234emperatura, salinity, pH, O_2 (O2), and Ω_{ar} (Aragonite).

Datasets used in Table S3

Table S1. Maximum, average, and percentage of total abundance of pteropods within the Mediterranean. This dataset was created from the dataset used in Bednaršek et al. (2012). A link to the dataset and a list of datasets used in this study can be found at the end of this document.

Depth range (m)	Max abundance (ind. M^{-3})	Number of observations	Avg. abundance (ind. M^{-3})	% Abundance (ind. M^{-3})
0-200	26.67	455	0.98	93.37
201-850	19	502	0.07	6.63

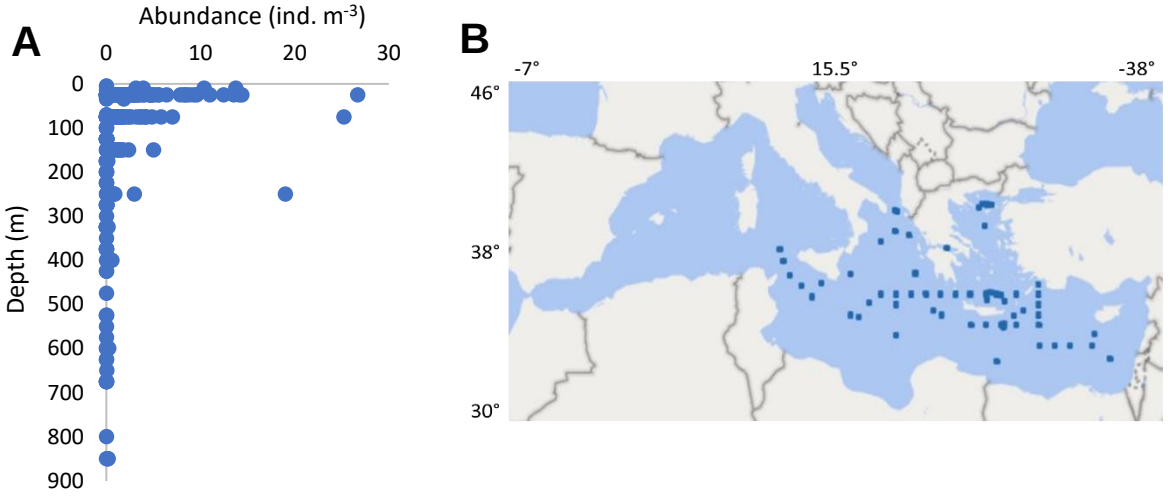

Fig. S1. A Abundance of pteropods (expressed as ind. m^{-3}) in the Mediterranean Sea from the dataset in Bednaršek et al. (2012) only including sites where pteropods have been collected below and above 200 m; **B** Location of stations within the Mediterranean Sea where data were collected above and below 200 m water depth. Unfortunately, there are a paucity of datasets in the western Mediterranean that we can utilise to differentiate the depth distribution of pteropods above and below 200 m (Bednaršek et al. [2012]; see Figure 1 from this document, (c) depth 200-500 m and (d) below 500m for the Western Mediterranean).

Table S2. ANOVA table using night/day as the dependent variable against total and species abundances.

		Sum of Squares	df	Mean Square	F	Sig.
total abundance	Between Groups	1.988	1	1.988	.713	.409
	Within Groups	50.182	18	2.788		
	Total	52.170	19			
H. inflatus	Between Groups	.000	1	.000	.000	.987
	Within Groups	4.317	18	.240		
	Total	4.317	19			
L. trochiformis	Between Groups	.354	1	.354	1.029	.324
	Within Groups	6.198	18	.344		
	Total	6.552	19			
L. bulimoides	Between Groups	.251	1	.251	.789	.386
	Within Groups	5.726	18	.318		
	Total	5.977	19			
C. acicula	Between Groups	.002	1	.002	.056	.816
	Within Groups	.590	18	.033		
	Total	.592	19			
C. conica	Between Groups	.003	1	.003	.121	.732
	Within Groups	.400	18	.022		
	Total	.403	19			

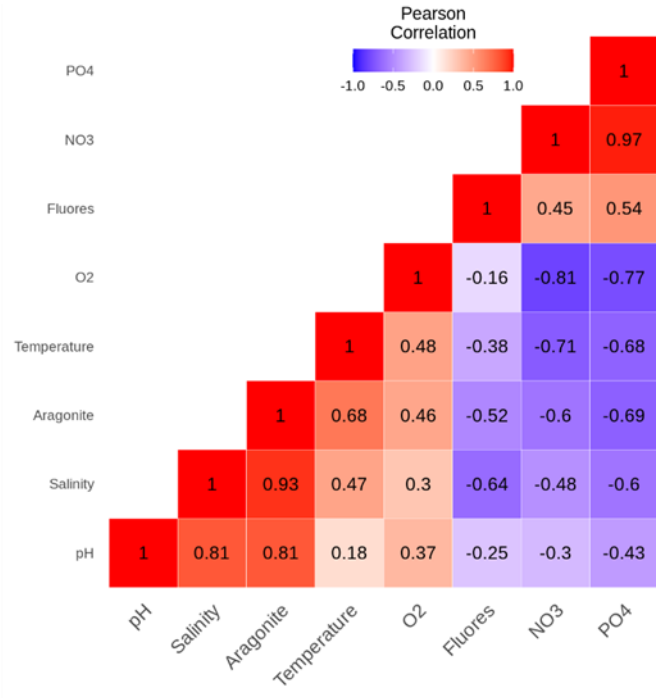

Fig. S2. Pearson's Correlation matrix showing the correlation between several environmental variables. Labels - NO_3 (NO3), PO_4 (PO4), fluorescence (Fluores), temperature, salinity, pH, O_2 (O2), and Ω_{ar} (Aragonite).

Datasets used in Table S3

From Bednaršek, Nina & Možina, J & Vogt, Meike & O'Brien, Colleen & Tarling, Geraint. (2012). The global distribution of pteropods and their contribution to carbonate and carbon biomass in the modern ocean. Earth System Science Data. 4. 167-186. 10.5194/essd-4-167-2012.

Downloaded from Bednaršek, Nina; Mozina, Jasna; Vogt, Meike; O'Brien, Colleen J; Tarling, Geraint A (2012): Global distributions of pteropods (Gymnosomata, Thecosomata, Pseudothecosomata) abundance and biomass - Gridded data product (NetCDF) - Contribution to the MAREDAT World Ocean Atlas of Plankton Functional Types. PANGAEA, https://doi.org/10.1594/PANGAEA.777387

1. Koppelmann, Rolf; Weikert, Horst (2008): Plankton abundance of mocness net M44/4_D-MOC216. doi:10.1594/PANGAEA.249974
2. Koppelmann, Rolf; Weikert, Horst (2008): Plankton abundance of mocness net M44/4_D-MOC220. doi:10.1594/PANGAEA.249975
3. Koppelmann, Rolf; Weikert, Horst (2008): Plankton abundance of mocness net M44/4_D-MOC242. doi:10.1594/PANGAEA.249977
4. Koppelmann, Rolf; Weikert, Horst (2008): Plankton abundance of mocness net M44/4_D-MOC249. doi:10.1594/PANGAEA.249978
5. Koppelmann, Rolf; Weikert, Horst (2008): Plankton abundance of mocness net M44/4_D-MOC268. doi:10.1594/PANGAEA.81995
6. Koppelmann, Rolf; Weikert, Horst (2008): Plankton abundance of mocness net M44/4_D-MOC273. doi:10.1594/PANGAEA.81998
7. Koppelmann, Rolf; Weikert, Horst (2008): Plankton abundance of mocness net M44/4_D-MOC280. doi:10.1594/PANGAEA.81999
8. Koppelmann, Rolf; Weikert, Horst (2008): Plankton abundance of mocness net M44/4_D-MOC281. doi:10.1594/PANGAEA.249979
9. Koppelmann, Rolf; Weikert, Horst (2008): Plankton abundance of mocness net M44/4_D-MOC293. doi:10.1594/PANGAEA.249980

10. Koppelmann, Rolf; Weikert, Horst (2008): Plankton abundance of mocness net M44/4_D-MOC304. doi:10.1594/PANGAEA.249982
11. Mazzocchi, Maria Grazia (2008): Mesozooplankton abundance and species composition in the Ionian Sea in April-May 1992. Part 2. Stazione Zoologica Anton Dohrn, doi:10.1594/PANGAEA.703258
12. Mazzocchi, Maria Grazia (2008): Mesozooplankton abundance and species composition in the Ionian Sea in April-May 1999. Stazione Zoologica Anton Dohrn, doi:10.1594/PANGAEA.703201
13. Mazzocchi, Maria Grazia (2008): Mesozooplankton abundance and species composition in the Levantine Sea in November 1991. Stazione Zoologica Anton Dohrn, doi:10.1594/PANGAEA.703972
14. Mazzocchi, Maria Grazia (2008): Mesozooplankton abundance and species composition in the Sicily Channel in October 1991. Part 2. Stazione Zoologica Anton Dohrn, doi:10.1594/PANGAEA.703256
15. Ramfos, A. and Isari, S. and Rastaman, N., Mesozooplankton abundance in water of the Ionian Sea (March 2000), Department of Biology, University of Patras, 2008.
16. Siokou-Frangou, Ioanna et al. (2008): Mesozooplankton abundance in waters of the Aegean Sea at Station O91-GN3619910270126804wp3. Hellenic Center of Marine Research, Institut of Oceanography, Greece, doi:10.1594/PANGAEA.692018
17. Siokou-Frangou, Ioanna et al. (2008): Mesozooplankton abundance in waters of the Aegean Sea at Station O91-GN3619910270126811wp3. Hellenic Center of Marine Research, Institut of Oceanography, Greece, doi:10.1594/PANGAEA.692019
18. Siokou-Frangou, Ioanna; Christou, Epaminondas; Giannakourou, Antonia; Zoulias, Theodoros (2008): Mesozooplankton abundance and biomass in surface waters of the Aegean Sea in spring 1997. Station MARCH-1997-GN36199704601MSB01wp2. Hellenic Center of Marine Research, Institut of Oceanography, Greece, doi:10.1594/PANGAEA.688659
19. Siokou-Frangou, Ioanna; Christou, Epaminondas; Giannakourou, Antonia; Zoulias, Theodoros (2008): Mesozooplankton abundance and biomass in surface waters of the Aegean Sea in spring 1997. Station MARCH-1997-GN36199704601MSB02wp2.

Hellenic Center of Marine Research, Institut of Oceanography, Greece, doi:10.1594/PANGAEA.688664

20. Siokou-Frangou, Ioanna; Christou, Epaminondas; Giannakourou, Antonia; Zoulias, Theodoros (2008): Mesozooplankton abundance and biomass in surface waters of the Aegean Sea in spring 1997. Station MARCH-1997-GN36199704601MSB06wp2. Hellenic Center of Marine Research, Institut of Oceanography, Greece, doi:10.1594/PANGAEA.688665
21. Siokou-Frangou, Ioanna; Christou, Epaminondas; Giannakourou, Antonia; Zoulias, Theodoros (2008): Mesozooplankton abundance and biomass in surface waters of the Aegean Sea in spring 1997. Station MARCH-1997-GN36199704601MSB07wp2. Hellenic Center of Marine Research, Institut of Oceanography, Greece, doi:10.1594/PANGAEA.688666
22. Siokou-Frangou, Ioanna; Christou, Epaminondas; Giannakourou, Antonia; Zoulias, Theodoros (2008): Mesozooplankton abundance and biomass in surface waters of the Aegean Sea in spring 1997. Station MARCH-1997-GN36199704603MNB01wp2. Hellenic Center of Marine Research, Institut of Oceanography, Greece, doi:10.1594/PANGAEA.688667
23. Siokou-Frangou, Ioanna; Christou, Epaminondas; Giannakourou, Antonia; Zoulias, Theodoros (2008): Mesozooplankton abundance and biomass in surface waters of the Aegean Sea in spring 1997. Station MARCH-1997-GN36199704603MNB02wp2. Hellenic Center of Marine Research, Institut of Oceanography, Greece, doi:10.1594/PANGAEA.688734
24. Siokou-Frangou, Ioanna; Christou, Epaminondas; Giannakourou, Antonia; Zoulias, Theodoros (2008): Mesozooplankton abundance and biomass in surface waters of the Aegean Sea in spring 1997. Station MARCH-1997-GN36199704603MNB03wp2. Hellenic Center of Marine Research, Institut of Oceanography, Greece, doi:10.1594/PANGAEA.688735
25. Siokou-Frangou, Ioanna; Christou, Epaminondas; Giannakourou, Antonia; Zoulias, Theodoros (2008): Mesozooplankton abundance and biomass in surface waters of the Aegean Sea in spring 1997. Station MARCH-1997-GN36199704603MNB05wp2.

Hellenic Center of Marine Research, Institut of Oceanography, Greece, doi:10.1594/PANGAEA.688737

26. Siokou-Frangou, Ioanna; Christou, Epaminondas; Giannakourou, Antonia; Zoulias, Theodoros (2008): Mesozooplankton abundance and biomass in surface waters of the Aegean Sea in spring 1997. Station MARCH-1997-GN36199704603MNB07wp2. Hellenic Center of Marine Research, Institut of Oceanography, Greece, doi:10.1594/PANGAEA.688739
27. Siokou-Frangou, Ioanna; Christou, Epaminondas; Rastaman, Nina (2008): Mesozooplankton abundance in waters of the Aegean Sea at Station A92-GN3619920270226404wp2. Hellenic Center of Marine Research, Institut of Oceanography, Greece, doi:10.1594/PANGAEA.693561
28. Siokou-Frangou, Ioanna; Christou, Epaminondas; Rastaman, Nina (2008): Mesozooplankton abundance in waters of the Aegean Sea at Station A92-GN3619920270226605wp2. Hellenic Center of Marine Research, Institut of Oceanography, Greece, doi:10.1594/PANGAEA.693563
29. Siokou-Frangou, Ioanna; Christou, Epaminondas; Rastaman, Nina (2008): Mesozooplankton abundance in waters of the Aegean Sea at Station A92-GN3619920270226704wp2. Hellenic Center of Marine Research, Institut of Oceanography, Greece, doi:10.1594/PANGAEA.693564
30. Siokou-Frangou, Ioanna; Christou, Epaminondas; Rastaman, Nina (2008): Mesozooplankton abundance in waters of the Levantine Sea at Station A92-GN3619920270224502wp2. Hellenic Center of Marine Research, Institut of Oceanography, Greece, doi:10.1594/PANGAEA.693555
31. Siokou-Frangou, Ioanna; Christou, Epaminondas; Rastaman, Nina (2008): Mesozooplankton abundance in waters of the Levantine Sea at Station A92-GN3619920270224603wp2. Hellenic Center of Marine Research, Institut of Oceanography, Greece, doi:10.1594/PANGAEA.693556
32. Siokou-Frangou, Ioanna; Christou, Epaminondas; Rastaman, Nina (2008): Mesozooplankton abundance in waters of the Levantine Sea at Station A92-GN3619920270225810wp2. Hellenic Center of Marine Research, Institut of Oceanography, Greece, doi:10.1594/PANGAEA.693559

33. Siokou-Frangou, Ioanna; Christou, Epaminondas; Rastaman, Nina (2008): Mesozooplankton abundance in waters of the Levantine Sea at Station A92-GN3619920270226804wp2. Hellenic Center of Marine Research, Institut of Oceanography, Greece, doi:10.1594/PANGAEA.693565
34. Siokou-Frangou, Ioanna; Christou, Epaminondas; Rastaman, Nina (2008): Mesozooplankton abundance in waters of the Levantine Sea at Station A92-GN3619920270226811wp2. Hellenic Center of Marine Research, Institut of Oceanography, Greece, doi:10.1594/PANGAEA.693566
35. Siokou-Frangou, Ioanna; Christou, Epaminondas; Zervoudaki, Soultana; Zoulias, Theodoros (2008): Mesozooplankton abundance and biomass in waters of the Aegean Sea in September 1997. Station SEPT-1997-GN36199704605MSB01wp2. Hellenic Center of Marine Research, Institut of Oceanography, Greece, doi:10.1594/PANGAEA.690849
36. Siokou-Frangou, Ioanna; Christou, Epaminondas; Zervoudaki, Soultana; Zoulias, Theodoros (2008): Mesozooplankton abundance and biomass in waters of the Aegean Sea in September 1997. Station SEPT-1997-GN36199704605MSB02wp2. Hellenic Center of Marine Research, Institut of Oceanography, Greece, doi:10.1594/PANGAEA.690850
37. Siokou-Frangou, Ioanna; Christou, Epaminondas; Zervoudaki, Soultana; Zoulias, Theodoros (2008): Mesozooplankton abundance and biomass in waters of the Aegean Sea in September 1997. Station SEPT-1997-GN36199704605MSB03wp2. Hellenic Center of Marine Research, Institut of Oceanography, Greece, doi:10.1594/PANGAEA.690851
38. Siokou-Frangou, Ioanna; Christou, Epaminondas; Zervoudaki, Soultana; Zoulias, Theodoros (2008): Mesozooplankton abundance and biomass in waters of the Aegean Sea in September 1997. Station SEPT-1997-GN36199704605MSB06wp2. Hellenic Center of Marine Research, Institut of Oceanography, Greece, doi:10.1594/PANGAEA.690852
39. Siokou-Frangou, Ioanna; Christou, Epaminondas; Zervoudaki, Soultana; Zoulias, Theodoros (2008): Mesozooplankton abundance and biomass in waters of the Aegean Sea in September 1997. Station SEPT-1997-GN36199704605MSB07wp2. Hellenic

Center of Marine Research, Institut of Oceanography, Greece, doi:10.1594/PANGAEA.690853

40. Siokou-Frangou, Ioanna; Christou, Epaminondas; Zervoudaki, Soultana; Zoulias, Theodoros (2008): Mesozooplankton abundance and biomass in waters of the Aegean Sea in September 1997. Station SEPT-1997-GN36199704606MNB01wp2. Hellenic Center of Marine Research, Institut of Oceanography, Greece, doi:10.1594/PANGAEA.690813
41. Siokou-Frangou, Ioanna; Christou, Epaminondas; Zervoudaki, Soultana; Zoulias, Theodoros (2008): Mesozooplankton abundance and biomass in waters of the Aegean Sea in September 1997. Station SEPT-1997-GN36199704606MNB02wp2. Hellenic Center of Marine Research, Institut of Oceanography, Greece, doi:10.1594/PANGAEA.690814
42. Siokou-Frangou, Ioanna; Christou, Epaminondas; Zervoudaki, Soultana; Zoulias, Theodoros (2008): Mesozooplankton abundance and biomass in waters of the Aegean Sea in September 1997. Station SEPT-1997-GN36199704606MNB03wp2. Hellenic Center of Marine Research, Institut of Oceanography, Greece, doi:10.1594/PANGAEA.690815
43. Siokou-Frangou, Ioanna; Christou, Epaminondas; Zervoudaki, Soultana; Zoulias, Theodoros (2008): Mesozooplankton abundance and biomass in waters of the Aegean Sea in September 1997. Station SEPT-1997-GN36199704606MNB05wp2. Hellenic Center of Marine Research, Institut of Oceanography, Greece, doi:10.1594/PANGAEA.690817
44. Siokou-Frangou, Ioanna; Christou, Epaminondas; Zervoudaki, Soultana; Zoulias, Theodoros (2008): Mesozooplankton abundance and biomass in waters of the Aegean Sea in September 1997. Station SEPT-1997-GN36199704606MNB07wp2. Hellenic Center of Marine Research, Institut of Oceanography, Greece, doi:10.1594/PANGAEA.690820
45. Siokou-Frangou, Ioanna; Christou, et al. (2008): Mesozooplankton abundance in waters of the Aegean Sea at Station O91-GN3619910270125307wp3. Hellenic Center of Marine Research, Institut of Oceanography, Greece, doi:10.1594/PANGAEA.691996

46. Siokou-Frangou, Ioanna; et al. (2008): Mesozooplankton abundance in waters of the Aegean Sea at Station O91-GN3619910270126404wp3. Hellenic Center of Marine Research, Institut of Oceanography, Greece, doi:10.1594/PANGAEA.692014
47. Siokou-Frangou, Ioanna; et al. (2008): Mesozooplankton abundance in waters of the Aegean Sea at Station O91-GN3619910270126502wp3. Hellenic Center of Marine Research, Institut of Oceanography, Greece, doi:10.1594/PANGAEA.692015
48. Siokou-Frangou, Ioanna; et al. (2008): Mesozooplankton abundance in waters of the Aegean Sea at Station O91-GN3619910270126605wp3B. Hellenic Center of Marine Research, Institut of Oceanography, Greece, doi:10.1594/PANGAEA.692016
49. Siokou-Frangou, Ioanna; et al. (2008): Mesozooplankton abundance in waters of the Aegean Sea at Station O91-GN3619910270126704wp3. Hellenic Center of Marine Research, Institut of Oceanography, Greece, doi:10.1594/PANGAEA.692017
50. Siokou-Frangou, Ioanna; et al. (2008): Mesozooplankton abundance in waters of the Ionian Sea at Station O91-GN3619910270124303wp3. Hellenic Center of Marine Research, Institut of Oceanography, Greece, doi:10.1594/PANGAEA.692870
51. Siokou-Frangou, Ioanna; et al. (2008): Mesozooplankton abundance in waters of the Ionian Sea at Station O91-GN3619910270124405wp3. Hellenic Center of Marine Research, Institut of Oceanography, Greece, doi:10.1594/PANGAEA.692871
52. Siokou-Frangou, Ioanna; et al. (2008): Mesozooplankton abundance in waters of the Ionian Sea at Station O91-GN3619910270124502wp3. Hellenic Center of Marine Research, Institut of Oceanography, Greece, doi:10.1594/PANGAEA.692872
53. Siokou-Frangou, Ioanna; et al. (2008): Mesozooplankton abundance in waters of the Ionian Sea at Station O91-GN3619910270124702wp3. Hellenic Center of Marine Research, Institut of Oceanography, Greece, doi:10.1594/PANGAEA.692874
54. Siokou-Frangou, Ioanna; et al. (2008): Mesozooplankton abundance in waters of the Ionian Sea at Station O91-GN3619910270124830wp3. Hellenic Center of Marine Research, Institut of Oceanography, Greece, doi:10.1594/PANGAEA.692875
55. Siokou-Frangou, Ioanna; et al. (2008): Mesozooplankton abundance in waters of the Ionian Sea at Station O91-GN3619910270125202wp3. Hellenic Center of Marine Research, Institut of Oceanography, Greece, doi:10.1594/PANGAEA.692876

56. Siokou-Frangou, Ioanna; et al. (2008): Mesozooplankton abundance in waters of the Ionian Sea at Station O91-GN3619910270125810wp3. Hellenic Center of Marine Research, Institut of Oceanography, Greece, doi:10.1594/PANGAEA.692877
57. Siokou-Frangou, Ioanna; et al. (2008): Mesozooplankton abundance in waters of the Ionian Sea at Station O91-GN3619910270125817wp3. Hellenic Center of Marine Research, Institut of Oceanography, Greece, doi:10.1594/PANGAEA.692878
58. Siokou-Frangou, Ioanna; et al. (2008): Mesozooplankton abundance in waters of the Ionian Sea at Station O91-GN3619910270126002wp3. Hellenic Center of Marine Research, Institut of Oceanography, Greece, doi:10.1594/PANGAEA.692240
59. Siokou-Frangou, Ioanna; et al. (2008): Mesozooplankton abundance in waters of the Ionian Sea at Station O91-GN3619910270126102wp3B, doi:10.1594/PANGAEA.692241
60. Siokou-Frangou, Ioanna; et al. (2008): Mesozooplankton abundance in waters of the Ionian Sea at Station O91-GN3619910270126203wp3., doi:10.1594/PANGAEA.692868
61. Siokou-Frangou, Ioanna; et al. (2008): Mesozooplankton abundance in waters of the Ionian Sea at Station O91-GN3619910270136903wp3. Hellenic Center of Marine Research, Institut of Oceanography, Greece, doi:10.1594/PANGAEA.692869
62. Siokou-Frangou, Ioanna; et al.(2008): Mesozooplankton abundance in waters of the Ionian Sea at Station O91-GN3619910270124603wp3. Hellenic Center of Marine Research, Institut of Oceanography, Greece, doi:10.1594/PANGAEA.692873
63. Siokou-Frangou, Ioanna; Zervoudaki, Soultana; Christou, Epaminondas; Zoulias, Theodoros (2008): Mesozooplankton abundance in water of the Aegean Sea at Station MAY-1997-MNB2wp2. Hellenic Center of Marine Research, Institut of Oceanography, Greece, doi:10.1594/PANGAEA.695140
64. Siokou-Frangou, Ioanna; Zervoudaki, Soultana; Christou, Epaminondas; Zoulias, Theodoros (2008): Mesozooplankton abundance in water of the Aegean Sea at Station MAY-1997-MNB5wp2. Hellenic Center of Marine Research, Institut of Oceanography, Greece, doi:10.1594/PANGAEA.695144
65. Siokou-Frangou, Ioanna; Zervoudaki, Soultana; Christou, Epaminondas; Zoulias, Theodoros (2008): Mesozooplankton abundance in water of the Aegean Sea at

Station MAY-1997-MNB7wp2. Hellenic Center of Marine Research, Institut of Oceanography, Greece, doi:10.1594/PANGAEA.695146

66. Zervoudaki, Soultana; Christou, Epaminondas; Siokou-Frangou, Ioanna; Zoulias, Theodoros (2008): Mesozooplankton abundance in water of the Aegean Sea at Station SEPT-1998-MNB5wp2. Hellenic Center of Marine Research, Institut of Oceanography, Greece, doi:10.1594/PANGAEA.695158
67. Zervoudaki, Soultana; Christou, Epaminondas; Siokou-Frangou, Ioanna; Zoulias, Theodoros (2008): Mesozooplankton abundance in water of the Ionian Sea at Station SEPT-2000-IKO3wp2. Hellenic Center of Marine Research, Institut of Oceanography, Greece, doi:10.1594/PANGAEA.695161
68. Zervoudaki, Soultana; Christou, Epaminondas; Siokou-Frangou, Ioanna; Zoulias, Theodoros (2008): Mesozooplankton abundance in water of the Ionian Sea at Station SEPT-2000-IRI47wp2. Hellenic Center of Marine Research, Institut of Oceanography, Greece, doi:10.1594/PANGAEA.695186
69. Zervoudaki, Soultana; Siokou-Frangou, Ioanna; Christou, Epaminondas; Zoulias, Theodoros (2008): Mesozooplankton abundance in water of the Aegean Sea at Station JUNE-1998-MNB2wp2. Hellenic Center of Marine Research, Institut of Oceanography, Greece, doi:10.1594/PANGAEA.695102
70. Zervoudaki, Soultana; Siokou-Frangou, Ioanna; Christou, Epaminondas; Zoulias, Theodoros (2008): Mesozooplankton abundance in water of the Aegean Sea in June 1998. Hellenic Center of Marine Research, Institut of Oceanography, Greece, doi:10.1594/PANGAEA.695104
71. Koppelmann, Rolf; Weikert, Horst (2008): Plankton abundance of mocness net M44/4_D-MOC216. doi:10.1594/PANGAEA.249974
72. Koppelmann, Rolf; Weikert, Horst (2008): Plankton abundance of mocness net M44/4_D-MOC220. doi:10.1594/PANGAEA.249975
73. Koppelmann, Rolf; Weikert, Horst (2008): Plankton abundance of mocness net M44/4_D-MOC242. doi:10.1594/PANGAEA.249977
74. Koppelmann, Rolf; Weikert, Horst (2008): Plankton abundance of mocness net M44/4_D-MOC249. doi:10.1594/PANGAEA.249978

75. Koppelmann, Rolf; Weikert, Horst (2008): Plankton abundance of mocness net M44/4_D-MOC268. doi:10.1594/PANGAEA.81995
76. Koppelmann, Rolf; Weikert, Horst (2008): Plankton abundance of mocness net M44/4_D-MOC273. doi:10.1594/PANGAEA.81998
77. Koppelmann, Rolf; Weikert, Horst (2008): Plankton abundance of mocness net M44/4_D-MOC280. doi:10.1594/PANGAEA.81999
78. Koppelmann, Rolf; Weikert, Horst (2008): Plankton abundance of mocness net M44/4_D-MOC281. doi:10.1594/PANGAEA.249979
79. Koppelmann, Rolf; Weikert, Horst (2008): Plankton abundance of mocness net M44/4_D-MOC293. doi:10.1594/PANGAEA.249980
80. Koppelmann, Rolf; Weikert, Horst (2008): Plankton abundance of mocness net M44/4_D-MOC304. doi:10.1594/PANGAEA.249982
81. Mazzocchi, Maria Grazia (2008): Mesozooplankton abundance and species composition in the Ionian Sea in April-May 1992. Part 2. Stazione Zoologica Anton Dohrn, doi:10.1594/PANGAEA.703258
82. Mazzocchi, Maria Grazia (2008): Mesozooplankton abundance and species composition in the Ionian Sea in April-May 1999. Stazione Zoologica Anton Dohrn, doi:10.1594/PANGAEA.703201
83. Mazzocchi, Maria Grazia (2008): Mesozooplankton abundance and species composition in the Levantine Sea in November 1991. Stazione Zoologica Anton Dohrn, doi:10.1594/PANGAEA.703972
84. Mazzocchi, Maria Grazia (2008): Mesozooplankton abundance and species composition in the Sicily Channel in October 1991. Part 2. Stazione Zoologica Anton Dohrn, doi:10.1594/PANGAEA.703256
85. Ramfos, A. and Isari, S. and Rastaman, N., Mesozooplankton abundance in water of the Ionian Sea (March 2000), Department of Biology, University of Patras, 2008.
86. Siokou-Frangou, Ioanna et al. (2008): Mesozooplankton abundance in waters of the Aegean Sea at Station O91-GN3619910270126804wp3. Hellenic Center of Marine Research, Institut of Oceanography, Greece, doi:10.1594/PANGAEA.692018

87. Siokou-Frangou, Ioanna et al. (2008): Mesozooplankton abundance in waters of the Aegean Sea at Station O91-GN3619910270126811wp3. Hellenic Center of Marine Research, Institut of Oceanography, Greece, doi:10.1594/PANGAEA.692019
88. Siokou-Frangou, Ioanna; Christou, Epaminondas; Rastaman, Nina (2008): Mesozooplankton abundance in waters of the Aegean Sea at Station A92-GN3619920270226404wp2. Hellenic Center of Marine Research, Institut of Oceanography, Greece, doi:10.1594/PANGAEA.693561
89. Siokou-Frangou, Ioanna; Christou, Epaminondas; Rastaman, Nina (2008): Mesozooplankton abundance in waters of the Aegean Sea at Station A92-GN3619920270226605wp2. Hellenic Center of Marine Research, Institut of Oceanography, Greece, doi:10.1594/PANGAEA.693563
90. Siokou-Frangou, Ioanna; Christou, Epaminondas; Rastaman, Nina (2008): Mesozooplankton abundance in waters of the Aegean Sea at Station A92-GN3619920270226704wp2. Hellenic Center of Marine Research, Institut of Oceanography, Greece, doi:10.1594/PANGAEA.693564
91. Siokou-Frangou, Ioanna; Christou, Epaminondas; Rastaman, Nina (2008): Mesozooplankton abundance in waters of the Levantine Sea at Station A92-GN3619920270224502wp2. Hellenic Center of Marine Research, Institut of Oceanography, Greece, doi:10.1594/PANGAEA.693555
92. Siokou-Frangou, Ioanna; Christou, Epaminondas; Rastaman, Nina (2008): Mesozooplankton abundance in waters of the Levantine Sea at Station A92-GN3619920270224603wp2. Hellenic Center of Marine Research, Institut of Oceanography, Greece, doi:10.1594/PANGAEA.693556
93. Siokou-Frangou, Ioanna; Christou, Epaminondas; Rastaman, Nina (2008): Mesozooplankton abundance in waters of the Levantine Sea at Station A92-GN3619920270225810wp2. Hellenic Center of Marine Research, Institut of Oceanography, Greece, doi:10.1594/PANGAEA.693559
94. Siokou-Frangou, Ioanna; Christou, Epaminondas; Rastaman, Nina (2008): Mesozooplankton abundance in waters of the Levantine Sea at Station A92-GN3619920270226804wp2. Hellenic Center of Marine Research, Institut of Oceanography, Greece, doi:10.1594/PANGAEA.693565

95. Siokou-Frangou, Ioanna; Christou, Epaminondas; Rastaman, Nina (2008): Mesozooplankton abundance in waters of the Levantine Sea at Station A92-GN3619920270226811wp2. Hellenic Center of Marine Research, Institut of Oceanography, Greece, doi:10.1594/PANGAEA.693566
96. Siokou-Frangou, Ioanna; Christou, Epaminondas; Zervoudaki, Soultana; Zoulias, Theodoros (2008): Mesozooplankton abundance and biomass in waters of the Aegean Sea in September 1997. Station SEPT-1997-GN36199704605MSB01wp2. Hellenic Center of Marine Research, Institut of Oceanography, Greece, doi:10.1594/PANGAEA.690849
97. Siokou-Frangou, Ioanna; Christou, Epaminondas; Zervoudaki, Soultana; Zoulias, Theodoros (2008): Mesozooplankton abundance and biomass in waters of the Aegean Sea in September 1997. Station SEPT-1997-GN36199704605MSB02wp2. Hellenic Center of Marine Research, Institut of Oceanography, Greece, doi:10.1594/PANGAEA.690850
98. Siokou-Frangou, Ioanna; Christou, Epaminondas; Zervoudaki, Soultana; Zoulias, Theodoros (2008): Mesozooplankton abundance and biomass in waters of the Aegean Sea in September 1997. Station SEPT-1997-GN36199704605MSB03wp2. Hellenic Center of Marine Research, Institut of Oceanography, Greece, doi:10.1594/PANGAEA.690851
99. Siokou-Frangou, Ioanna; Christou, Epaminondas; Zervoudaki, Soultana; Zoulias, Theodoros (2008): Mesozooplankton abundance and biomass in waters of the Aegean Sea in September 1997. Station SEPT-1997-GN36199704605MSB06wp2. Hellenic Center of Marine Research, Institut of Oceanography, Greece, doi:10.1594/PANGAEA.690852
100. Siokou-Frangou, Ioanna; Christou, Epaminondas; Zervoudaki, Soultana; Zoulias, Theodoros (2008): Mesozooplankton abundance and biomass in waters of the Aegean Sea in September 1997. Station SEPT-1997-GN36199704605MSB07wp2. Hellenic Center of Marine Research, Institut of Oceanography, Greece, doi:10.1594/PANGAEA.690853
101. Siokou-Frangou, Ioanna; Christou, Epaminondas; Zervoudaki, Soultana; Zoulias, Theodoros (2008): Mesozooplankton abundance and biomass in waters of

the Aegean Sea in September 1997. Station SEPT-1997-GN36199704606MNB01wp2. Hellenic Center of Marine Research, Institut of Oceanography, Greece, doi:10.1594/PANGAEA.690813

102. Siokou-Frangou, Ioanna; Christou, Epaminondas; Zervoudaki, Soultana; Zoulias, Theodoros (2008): Mesozooplankton abundance and biomass in waters of the Aegean Sea in September 1997. Station SEPT-1997-GN36199704606MNB02wp2. Hellenic Center of Marine Research, Institut of Oceanography, Greece, doi:10.1594/PANGAEA.690814

103. Siokou-Frangou, Ioanna; Christou, Epaminondas; Zervoudaki, Soultana; Zoulias, Theodoros (2008): Mesozooplankton abundance and biomass in waters of the Aegean Sea in September 1997. Station SEPT-1997-GN36199704606MNB03wp2. Hellenic Center of Marine Research, Institut of Oceanography, Greece, doi:10.1594/PANGAEA.690815

104. Siokou-Frangou, Ioanna; Christou, Epaminondas; Zervoudaki, Soultana; Zoulias, Theodoros (2008): Mesozooplankton abundance and biomass in waters of the Aegean Sea in September 1997. Station SEPT-1997-GN36199704606MNB05wp2. Hellenic Center of Marine Research, Institut of Oceanography, Greece, doi:10.1594/PANGAEA.690817

105. Siokou-Frangou, Ioanna; Christou, Epaminondas; Zervoudaki, Soultana; Zoulias, Theodoros (2008): Mesozooplankton abundance and biomass in waters of the Aegean Sea in September 1997. Station SEPT-1997-GN36199704606MNB07wp2. Hellenic Center of Marine Research, Institut of Oceanography, Greece, doi:10.1594/PANGAEA.690820

106. Siokou-Frangou, Ioanna; Christou, et al. (2008): Mesozooplankton abundance in waters of the Aegean Sea at Station O91-GN3619910270125307wp3. Hellenic Center of Marine Research, Institut of Oceanography, Greece, doi:10.1594/PANGAEA.691996

107. Siokou-Frangou, Ioanna; et al. (2008): Mesozooplankton abundance in waters of the Aegean Sea at Station O91-GN3619910270126404wp3. Hellenic Center of Marine Research, Institut of Oceanography, Greece, doi:10.1594/PANGAEA.692014

108. Siokou-Frangou, Ioanna; et al. (2008): Mesozooplankton abundance in waters of the Aegean Sea at Station O91-GN3619910270126502wp3. Hellenic Center of Marine Research, Institut of Oceanography, Greece, doi:10.1594/PANGAEA.692015

109. Siokou-Frangou, Ioanna; et al. (2008): Mesozooplankton abundance in waters of the Aegean Sea at Station O91-GN3619910270126605wp3B. Hellenic Center of Marine Research, Institut of Oceanography, Greece, doi:10.1594/PANGAEA.692016

110. Siokou-Frangou, Ioanna; et al. (2008): Mesozooplankton abundance in waters of the Aegean Sea at Station O91-GN3619910270126704wp3. Hellenic Center of Marine Research, Institut of Oceanography, Greece, doi:10.1594/PANGAEA.692017

111. Siokou-Frangou, Ioanna; et al. (2008): Mesozooplankton abundance in waters of the Ionian Sea at Station O91-GN3619910270124303wp3. Hellenic Center of Marine Research, Institut of Oceanography, Greece, doi:10.1594/PANGAEA.692870

112. Siokou-Frangou, Ioanna; et al. (2008): Mesozooplankton abundance in waters of the Ionian Sea at Station O91-GN3619910270124405wp3. Hellenic Center of Marine Research, Institut of Oceanography, Greece, doi:10.1594/PANGAEA.692871

113. Siokou-Frangou, Ioanna; et al. (2008): Mesozooplankton abundance in waters of the Ionian Sea at Station O91-GN3619910270124502wp3. Hellenic Center of Marine Research, Institut of Oceanography, Greece, doi:10.1594/PANGAEA.692872

114. Siokou-Frangou, Ioanna; et al. (2008): Mesozooplankton abundance in waters of the Ionian Sea at Station O91-GN3619910270124702wp3. Hellenic Center of Marine Research, Institut of Oceanography, Greece, doi:10.1594/PANGAEA.692874

115. Siokou-Frangou, Ioanna; et al. (2008): Mesozooplankton abundance in waters of the Ionian Sea at Station O91-GN3619910270124830wp3. Hellenic Center of

Marine Research, Institut of Oceanography, Greece, doi:10.1594/PANGAEA.692875

116. Siokou-Frangou, Ioanna; et al. (2008): Mesozooplankton abundance in waters of the Ionian Sea at Station O91-GN3619910270125202wp3. Hellenic Center of Marine Research, Institut of Oceanography, Greece, doi:10.1594/PANGAEA.692876

117. Siokou-Frangou, Ioanna; et al. (2008): Mesozooplankton abundance in waters of the Ionian Sea at Station O91-GN3619910270125810wp3. Hellenic Center of Marine Research, Institut of Oceanography, Greece, doi:10.1594/PANGAEA.692877

118. Siokou-Frangou, Ioanna; et al. (2008): Mesozooplankton abundance in waters of the Ionian Sea at Station O91-GN3619910270125817wp3. Hellenic Center of Marine Research, Institut of Oceanography, Greece, doi:10.1594/PANGAEA.692878

119. Siokou-Frangou, Ioanna; et al. (2008): Mesozooplankton abundance in waters of the Ionian Sea at Station O91-GN3619910270126002wp3. Hellenic Center of Marine Research, Institut of Oceanography, Greece, doi:10.1594/PANGAEA.692240

120. Siokou-Frangou, Ioanna; et al. (2008): Mesozooplankton abundance in waters of the Ionian Sea at Station O91-GN3619910270126102wp3B, doi:10.1594/PANGAEA.692241

121. Siokou-Frangou, Ioanna; et al. (2008): Mesozooplankton abundance in waters of the Ionian Sea at Station O91-GN3619910270126203wp3., doi:10.1594/PANGAEA.692868

122. Siokou-Frangou, Ioanna; et al. (2008): Mesozooplankton abundance in waters of the Ionian Sea at Station O91-GN3619910270136903wp3. Hellenic Center of Marine Research, Institut of Oceanography, Greece, doi:10.1594/PANGAEA.692869

123. Siokou-Frangou, Ioanna; et al.(2008): Mesozooplankton abundance in waters of the Ionian Sea at Station O91-GN3619910270124603wp3. Hellenic Center of

Marine Research, Institut of Oceanography, Greece, doi:10.1594/PANGAEA.692873

124. Siokou-Frangou, Ioanna; Zervoudaki, Soultana; Christou, Epaminondas; Zoulias, Theodoros (2008): Mesozooplankton abundance in water of the Aegean Sea at Station MAY-1997-MNB2wp2. Hellenic Center of Marine Research, Institut of Oceanography, Greece, doi:10.1594/PANGAEA.695140

125. Siokou-Frangou, Ioanna; Zervoudaki, Soultana; Christou, Epaminondas; Zoulias, Theodoros (2008): Mesozooplankton abundance in water of the Aegean Sea at Station MAY-1997-MNB7wp2. Hellenic Center of Marine Research, Institut of Oceanography, Greece, doi:10.1594/PANGAEA.695146

126. Zervoudaki, Soultana; Christou, Epaminondas; Siokou-Frangou, Ioanna; Zoulias, Theodoros (2008): Mesozooplankton abundance in water of the Aegean Sea at Station SEPT-1998-MNB5wp2. Hellenic Center of Marine Research, Institut of Oceanography, Greece, doi:10.1594/PANGAEA.695158

127. Zervoudaki, Soultana; Christou, Epaminondas; Siokou-Frangou, Ioanna; Zoulias, Theodoros (2008): Mesozooplankton abundance in water of the Ionian Sea at Station SEPT-2000-IKO3wp2. Hellenic Center of Marine Research, Institut of Oceanography, Greece, doi:10.1594/PANGAEA.695161

128. Zervoudaki, Soultana; Christou, Epaminondas; Siokou-Frangou, Ioanna; Zoulias, Theodoros (2008): Mesozooplankton abundance in water of the Ionian Sea at Station SEPT-2000-IRI47wp2. Hellenic Center of Marine Research, Institut of Oceanography, Greece, doi:10.1594/PANGAEA.695186

Supplementary Material – Chapter 5

Table S1. Location and environmental parameters for each station of the cruise. All the parameters are averaged from 5 to 200 m depth. LT is location time. The parameter Ω_{ar} is calculated. Values with an * are from station 18.

Table S2. Abundance (m^{-2}), shell length (µm), diameter (µm), mass (µg), size normalised mass (SNM) and SNM_{sc} (for size class 525 – 575 µm) data for *H. inflatus* at for individual stations, including the Gibraltar Area, the Western Mediterranean, the Eastern Mediterranean and the entire Mediterranean Sea.

Fig. S1. Box plot of the shell mass of *H. inflatus* in the **A** first leg of the MedSEA 2013 cruise from the Atlantic to Lebanon and **B** the second leg of the cruise from the Antikythera Strait to the Catalona-Balear region in the western Mediterranean. The X indicates the mean. The dots indicate outliers calculated from the interquartile range.

Fig. S2. Box plot of the shell length of *H. inflatus* in the **A** first leg of the MedSEA 2013 cruise from the Atlantic to Lebanon and **B** the second leg of the cruise from the Antikythera Strait to the Catalona-Balear region in the western Mediterranean. The X indicates the mean. The dots indicate outliers calculated from the interquartile range.

Fig. S3. Box plot of the shell diameter of *H. inflatus* in the **A** first leg of the MedSEA 2013 cruise from the Atlantic to Lebanon and **B** the second leg of the cruise from the Antikythera Strait to the Catalona-Balear region in the western Mediterranean. The X indicates the mean. The points indicate outliers calculated using the interquartile range.

Fig. S4. Box plot of the size normalised mass (SNM) of *H. inflatus* in the **A** first leg of the MedSEA 2013 cruise from the Atlantic to Lebanon and **B** the second leg of the cruise from the Antikythera Strait to the Catalona-Balear region in the western Mediterranean. The X indicates the mean. The dots indicate outliers calculated from the interquartile range.

Fig. S5. Each station superimposed over a map dividing the Mediterranean Sea divided into 12 biogeochemical epipelagic regions based on *in situ* data – temperature, salinity, chlorophyll *a* concentration, NO_2 concentration, NO_3 concentration, PO_4 concentration, SiO_4 concentration, dissolved oxygen concentration, pH, bathymetry, particular organic flux, euphotic depth, thermocline intensity, thermocline depth, mixed layer depth, and wind speed. Figure modified from Regondeau et al. (2017).

Table S1. Location and environmental parameters for each station of the cruise. All the parameters are averaged from 5 to 200 m depth. LT is location time. The parameter Ω_{ar} is calculated. Values with an * are from station 18.

Station code	Station name	Day (dd/mm/yyyy)	Time (LT)	Latitude	Longitude	Bottom depth (m)	Volume (m^3)	Temperature (℃)	Salinity PSU	Fluorescense (µg L^1)	pH	Ω_{ar}	NO_3	PO_4	O_2	pCO_2
1	Atlantic	5/2/2013	00:03	36°03'	-6°64'	557	1016	16.39	36.19	0.36	8.06	2.70	1.92	0.13	226.03	393.96
2	Gibraltar	5/3/2013	12:47	35°95'	-5°56'	557	537	14.68	37.20	0.11	8.06	2.68	4.18	0.22	191.05	407.19
3	Alboran Sea	5/4/2013	20:55	36°12'	-4°19'	1337	1403	15.43	36.97	0.45	8.09	2.87	2.08	0.13	214.19	369.09
5	Southern Alguero-Balear	5/8/2013	10:44	38°52'	5°55'	2844	459	14.60	37.89	0.18	8.10	2.97	1.22	0.05	224.38	368.25
6	Strait of Sardine	5/9/2013	20:34	38°27'	8°69'	2237	423	14.60	38.13	0.19	8.08	2.96	2.30	0.15	212.38	389.51
7a	Strait of Sicily	5/11/2013	00:20	37°04'	13°19'	469	447	15.40	38.09	0.23	8.09	3.07	1.35	0.06	216.91	375.76
9	Ionian Sea	5/12/2013	11:31	35°11'	18°29'	3775	425	16.64	38.75	0.13	8.12	3.44	0.41	0.02	227.67	354.28
10	Southern Crete	5/14/2013	14:40	33°81'	24°27'	1845	320	16.70	39.04	0.12	8.11	3.43	1.03	0.03	211.61	368.15
11	Eastern Basin	5/15/2013	13:01	33°50'	28°00'	2865	372	17.73	38.85	0.10	8.12	3.61	0.58	0.02	224.16	361.25
12	Nile Delta	5/17/2013	03:14	33°21'	32°00'	1648	364	18.18	39.06	0.15	8.11	3.56	0.50	0.03	225.32	369.06
13	Lebanon	5/17/2013	16:15	34°22'	33°23'	2043	397	17.80	38.96	0.16	8.11	3.53	0.40	0.03	222.81	370.02
14	Antikythera Strait	5/21/2013	6:06	35°70'	23°42'	619	334	16.90	39.06	0.12	8.13	3.57	0.37	0.03	229.53	347.83
15	Eastern Ionian Sea	5/21/2013	21:25	36°40'	20°81'	2897	391	16.52	39.05	0.15	8.12	3.40	1.08	0.04	228.12	352.18
17	Adriatic Sea	5/23/2013	21:09	41°84'	17°25'	970	440	16.34	38.82	0.16	8.13	3.50	0.90	0.03	231.22	348.93
16	Otranto Strait	5/24/2013	23:49	40°23'	18°84'	808	385	15.14	38.81	0.20	8.10	3.22	1.70	0.05	229.39	379.20
16-18	North Ionian Sea	5/25/2013	09:30	37°71'	18°52'	3069	426	16.15*	38.88*	0.14*	8.11 *	3.40 *	1.97 *	0.06 *	216.01 *	359.78 *
19	Tyrrhenian Sea	5/27/2013	12:30	39°83'	12°52'	3165	391	15.05	38.29	0.18	8.12	3.21	1.60	0.07	212.45	354.12
20	Northern Alguero-Balear	5/29/2013	20:00	41°32'	5°67'	2561	356	14.08	38.39	0.36	8.14	3.24	4.01	0.20	208.91	343.27
21	Central Alguero-Balear	5/30/2013	10:30	40°07'	5°95'	2834	392	14.51	37.88	0.17	8.11	3.03	0.81	0.04	233.14	362.91
22	Catalano-Balear	5/31/2013	13:55	40°95'	3°32'	2275	339	14.62	38.39	0.25	8.13	3.23	3.55	0.17	210.47	348.79

Table S2. Abundance (m^{-2}), shell length (µm), diameter (µm), mass (µg), size normalised mass (SNM) and SNM_{sc} (for size class 525 – 575 µm) data for *H. inflatus* at for individual stations, including the Gibraltar Area, the Western Mediterranean, the Eastern Mediterranean and the entire Mediterranean Sea.

Station	Station	*Abundance (no. $^{-2}$)*	*Length (µm)*	*Diameter (µm)*	*Mass (µg)*	*SNM*	*SNM_{sc}*
Atlantic	1	43.90	520.8	520.8	16.6	0.0312	0.0331
Gibraltar	2	100.19	546.9	546.9	18.5	0.0332	0.0327
Alboran Sea	3	235.21	534.3	534.3	17.4	0.0320	0.0336
Southern Alguero-Balear	5	92.81	496.1	496.1	14.6	0.0291	0.0329
Strait of Sardine	6	33.10	550.4	550.4	18.3	0.0331	0.0333
Strait of Sicily	7a	22.82	545.0	545.0	18.0	0.0328	0.0340
Ionian Sea	9	722.82	538.3	538.3	19.2	0.0353	0.0342
Southern Crete	10	215.00	540.5	540.5	18.9	0.0343	0.0336
Eastern Basin	11	49.46	541.2	541.2	18.8	0.0343	0.0326
Nile Delta	12	54.40	532.1	532.1	18.2	0.0338	0.0374
Lebanon	13	402.02	548.5	548.5	19.6	0.0353	0.0347
Antikythera Strait	14	889.22	535.7	535.7	18.6	0.0341	0.0336
Eastern Ionian Sea	15	800.51	534.3	534.3	18.4	0.0340	0.0347
Otranto Strait	17	54.09	532.1	532.1	18.3	0.0339	0.0361
Adriatic Sea	16	1041.04	540.0	540.0	18.6	0.0340	0.0354
North Ionian Sea	16-18	24.88	563.1	563.1	20.5	0.0360	0.0352
Tyrrhenian Sea	19	197.95	543.0	543.0	18.0	0.0328	0.0358
Northern Alguero-Balear	21	95.92	534.1	534.1	17.4	0.0321	0.0350
Central Alguero-Balear	22	11.80	594.8	594.8	22.1	0.0369	0.0350
Gibraltar Area	1-3	126.43	534.0	534.0	17.5	0.0322	0.0333
Western Stations	5-7a, 19-22	75.73	543.9	543.9	18.1	0.0324	0.0339
Eastern Stations	9-'16-18'	425.34	540.6	540.6	18.9	0.0345	0.0355
All Stations		267.74	540.6	540.6	18.4	0.0336	0.0349

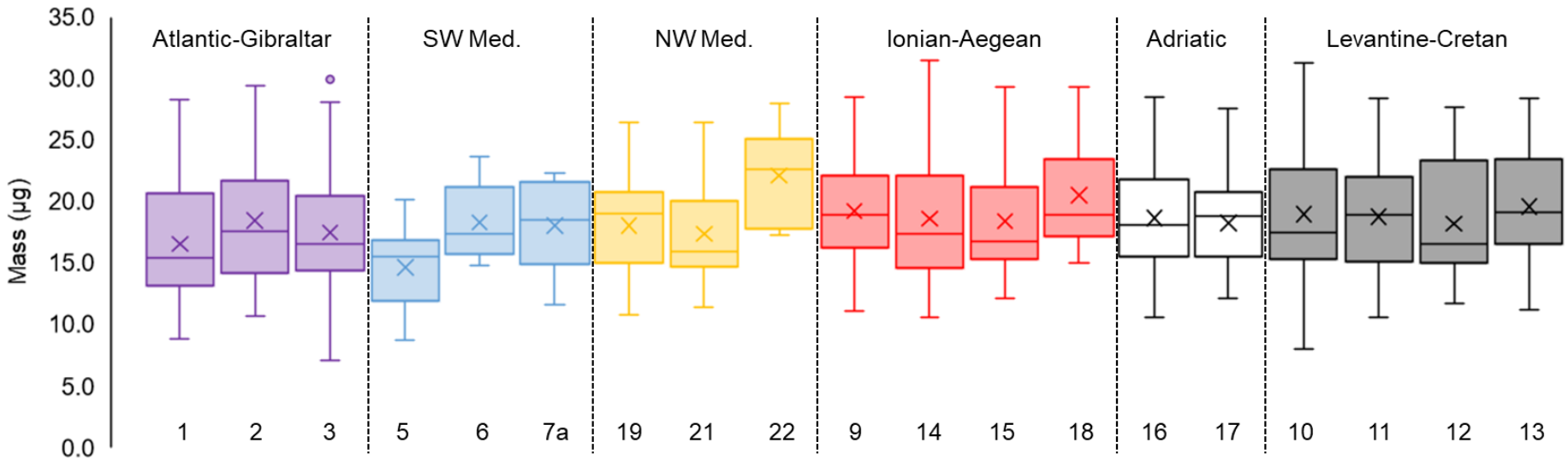

Fig. S1. Box plot of the shell mass of *H. inflatus* at each station of the MedSeA 2013 cruise. Each number indicates the associated sampling station (Table S1). Stations are grouped by biogeochemical region. The X indicates the mean. The dots indicate outliers calculated from the interquartile range. The number of samples from each station can be found in Table S2.

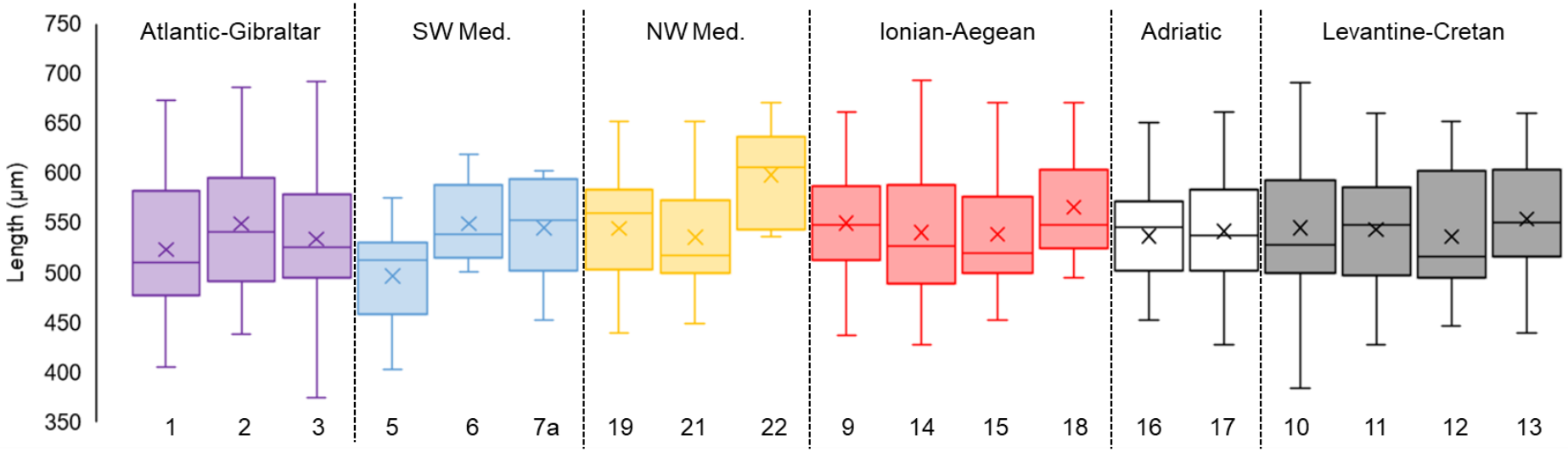

Fig. S2. Box plot of the shell length of *H. inflatus* at each station of the MedSeA 2013 cruise. Each number indicates the associated sampling station (Table S1). Stations are grouped by biogeochemical region. The X indicates the mean. The dots indicate outliers calculated from the interquartile range. The number of samples from each station can be found in Table S2.

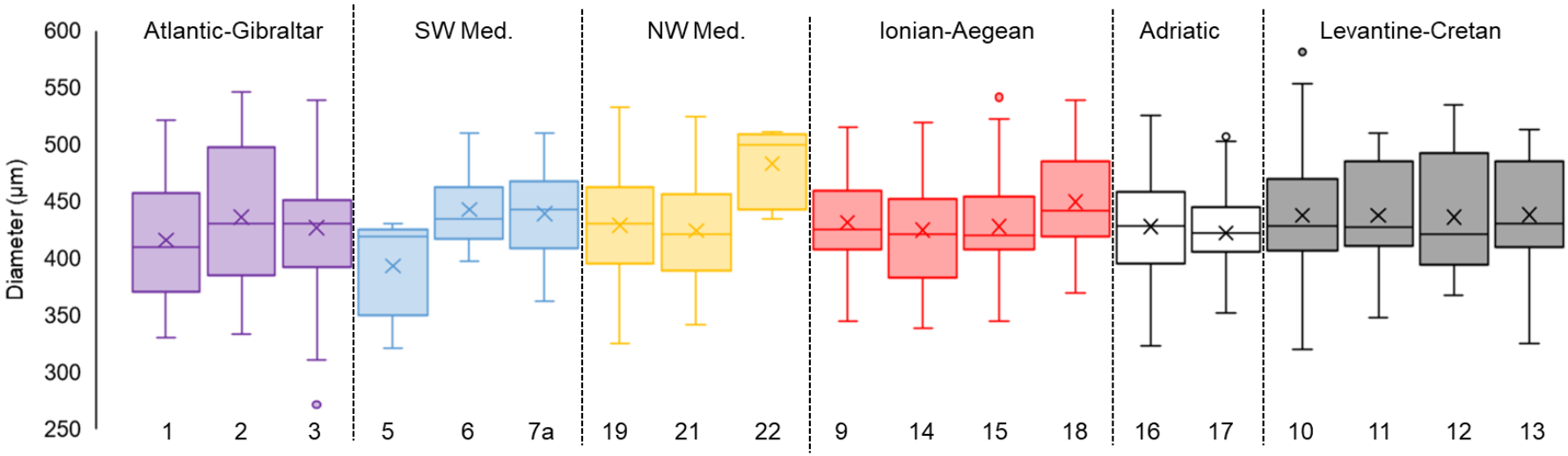

Figure S3. Box plot of the shell diameter of *H. inflatus* at each station of the MedSeA 2013 cruise. Each number indicates the associated sampling station (Table S1). Stations are grouped by biogeochemical region. The X indicates the mean. The dots indicate outliers calculated from the interquartile range. The number of samples from each station can be found in Table S2.

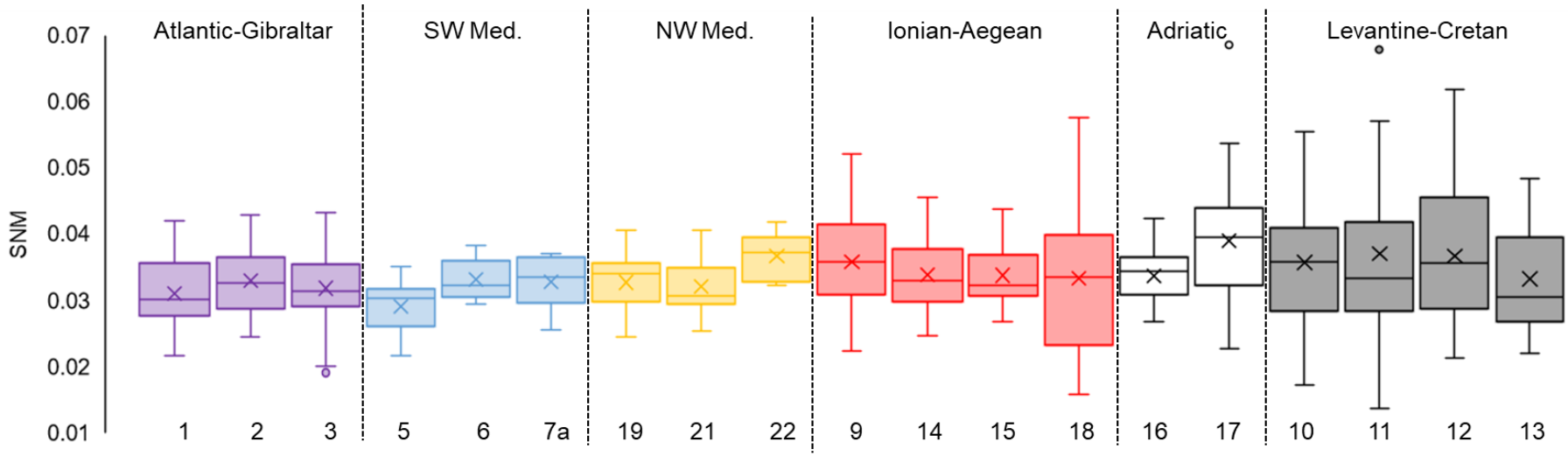

Figure S4. Box plot of the size normalised mass (SNM) of *H. inflatus* at each station of the MedSeA 2013 cruise. Each number indicates the associated sampling station (Table S1). Stations are grouped by biogeochemical region. The X indicates the mean. The dots indicate outliers calculated from the interquartile range. The number of samples from each station can be found in Table S2.

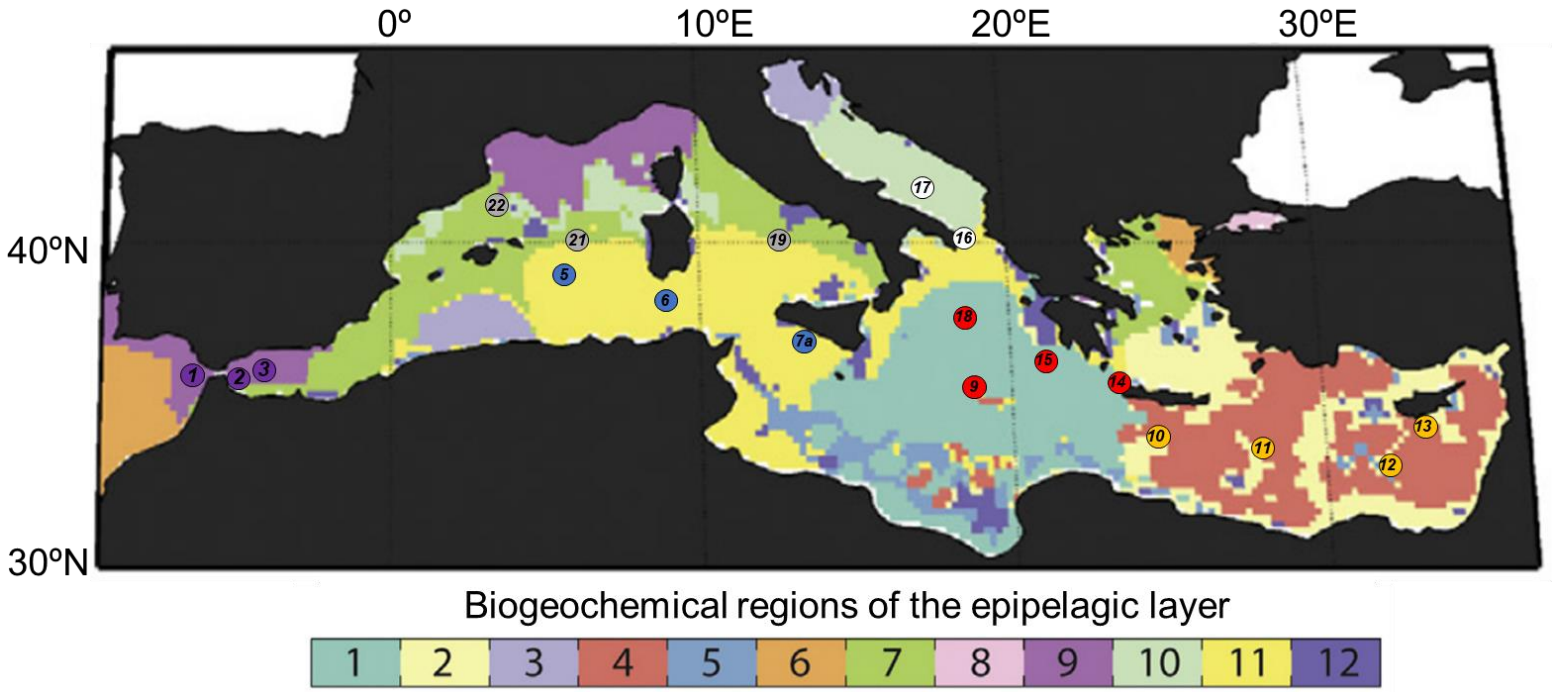

Figure S5. Each station superimposed over a map dividing the Mediterranean Sea divided into 12 biogeochemical epipelagic regions based on *in situ* data – temperature, salinity, chlorophyll *a* concentration, NO_2 concentration, NO_3 concentration, PO_4 concentration, SiO_4 concentration, dissolved oxygen concentration, pH, bathymetry, particular organic flux, euphotic depth, thermocline intensity, thermocline depth, mixed layer depth, and wind speed. Figure modified from Regondeau et al. (2017).